$P2X_7$ ACTIVATION OF NON-PRIMED MYELOID CELLS PROMOTES THE SHEDDING OF STIMULATORY MATERIALS WITHIN MICROVESICLES

by

Louis Michael Thomas

B.S., University of Maryland, College Park, 2005

Submitted to the Graduate Faculty of

University of Pittsburgh School of Medicine in partial fulfillment

of the requirements for the degree of

Doctor of Philosophy

University of Pittsburgh

2011

UNIVERSITY OF PITTSBURGH

SCHOOL OF MEDICINE

This dissertation was presented

by

Louis Michael Thomas

It was defended on

February 2nd, 2011

and approved by

Robert J. Binder, Ph.D., Assistant Professor, Department of Immunology

Lawrence P. Kane, Ph.D., Associate Professor, Department of Immunology

Simon C. Watkins, Ph.D., Professor, Department of Cell Biology and Physiology

Ora A. Weisz, Ph.D., Professor, Department of Cell Biology and Physiology & the Renal-Electrolyte Division of the Department of Medicine

Dissertation Advisor: Russell D. Salter, Ph.D., Professor, Department of Immunology

$P2X_7$ ACTIVATION OF NON-PRIMED MYELOID CELLS PROMOTES THE SHEDDING OF STIMULATORY MATERIALS WITHIN MICROVESICLES

Louis Michael Thomas

University of Pittsburgh, 2011

There is an increasing need to understand how inflammation is initiated by endogenous factors in the absence of infection. Various diseases such as atherosclerosis and arthritis are shaped by endogenous mediators. In situations such as transplant or trauma where there is extensive amount of tissue damage, endogenous factors can be released to influence inflammation. The modes of activation in which immune cells liberate endogenous factors for incurring immune responses remain elusive.

Adenosine triphosphate (ATP) activation of the puringeric receptor $P2X_7$ has been implicated in several immune responses. $P2X_7$ promotes the shedding of microvesicles (MV) and the secretion of inflammatory mediators. I hypothesized that $P2X_7$-induced MV containing some of these inflammatory mediators would promote the activation of innate immune cells such as macrophages.

Using murine bone marrow derived macrophages as a model for macrophage function, I describe that harvested $P2X_7$-induced MV from myeloid cells promote macrophage activation including pro-inflammatory cytokine secretion and co-stimulatory ligand upregulation. Phospholipids from $P2X_7$-induced MV are partially responsible for the observed macrophage activation. Isolated phospholipids from $P2X_7$-induced MV activate TLR4.

Secondly, I describe mature cathepsin D release into $P2X_7$-induced MV from myeloid cells. $P2X_7$-induced MV from myeloid cells contain both intermediate and mature forms of cathepsin D. Furthermore, $P2X_7$ stimulation of myeloid cells promotes the peripheral displacement of cathepsin D and dynamin. Dynasore, a selective and potent dynamin inhibitor, significantly reduced the secretion of mature but not intermediate cathepsin D.

Lastly, I describe a novel morphological alteration following $P2X_7$ activation of myeloid cells. ATP stimulates *de novo* filopodia production. These filopodia are the result of actin polymerization, Rho kinases, and phospholipases. Furthermore, $P2X_7$ promotes the re-localization of lipids and actin-based machinery to the periphery of ATP treated cells.

Collectively, these results demonstrate that $P2X_7$-induced MV possess stimulatory cargo including phospholipids that can activate macrophages and cathepsins that are potentially capable of degrading extracellular matrix components. This data would suggest a provocative role for $P2X_7$-induced MV and actin-based processes in promoting sterile disease.

TABLE OF CONTENTS

LIST OF FIGURES

LIST OF TABLES

PREFACE

The University of Pittsburgh afforded me many resources to succeed as a graduate student during my studies. In particular, the collaborative environment of Pitt facilitated open sharing of ideas, techniques, and resources. Without the help of faculty, staff, and fellow graduate students, I certainly would not have accomplished as much as I did during my time at Pitt.

Before I acknowledge my friends and colleagues at Pitt, I would like to thank the University of Maryland, College Park, where I completed my undergraduate studies. I owe a large debt of gratitude to my undergraduate advisors Sherri Dennis from the Food and Drug Administration, and Norman Hansen from Maryland's Department of Chemistry and Biochemistry. Dr. Dennis initially exposed me to the professional side of science by allowing me to attend conventions and to meet great scientists. Dr. Hansen provided my first exposure to conducting and designing experiments. Furthermore, he taught me to be confident in my ideas.

While I have several people at Pitt to thank, I would first like to acknowledge my mentor Russ Salter, who enabled me to pursue several of my research ideas during graduate school. Russ ensured that I was in a position to not only focus on several of my research interests, but to achieve success in investigating them. I am very grateful for his guidance, support, and collaboration. I also appreciate his willingness to review my abstracts and presentations, as well as his guidance during the writing of my thesis and my first-author manuscript.

Along with Russ, all of the other Salter lab members were instrumental in my success as a graduate student. I have special thanks to offer to both past and present members. Jessica Chu,

in particular, not only helped to optimize protocols but to cultivate ideas in my research. Her help was invaluable, especially in preparing for my comprehensive exam and, for lectures at scientific conferences. I also want to thank other members of the lab for their thoughtful feedback and expertise, namely, from Michelle Heid, Peter Keyel, Sarita Singh, and Cheng Sun.

I am also thankful to the Department of Immunology, the Center for Biologic Imaging, and the Graduate School Office. I would not have gone far without proper direction and training from them. I am very thankful for the Department of Immunology especially Olja Finn for equipping students like me with training grants. My gratitude is sent out to the administration in both the Immunology Department and the Graduate Office for keeping me organized.

My committee members have been invaluable in offering me advice and reagents over the course of my graduate training; I am very thankful for their assistance. I appreciate their patience and willingness to hear out my ideas. I also value how welcomed I felt when interacting with their labs. In fact, it may be fair to say that I am an honorary Binder lab member.

Last but most important to acknowledge, I am grateful for the support of my friends and family. I am thankful for fellow graduate students from our program, who created an environment that supported good research and the enjoyment of science. Brian Janelsins in particular was good at keeping me on time and for thoughtful discussions concerning science. Katy Deljoui provided a ton of morale support and I am very grateful for her friendship. My family has always been there for me and helped me to reach all of my aspirations, namely, Dad, Mom, Brandon, and Janelle. Finally, I want to acknowledge Laura Kropp. Laura is not only good at helping me with scientific experimentation and writing but she taught me how to be a better and much more complete person.

1.0 INTRODUCTION

Inflammation is highly relevant in the study of life and disease. It has been described since the start of recorded history and it is reported in the earliest of scientific publications. Our definition of inflammation has expanded beyond the cardinal features of redness and swelling as inflammation is now understood to be indicative for how efficient immune responses are mounted. Furthermore, this has led to a vast and complex understanding of cells and their interplay with various molecules. There is increasing awareness that inflammation is not just initiated by foreign materials but it can also be initiated by endogenously derived materials. “Sterile inflammation” results from endogenous materials acting on immune cells in the absence of infection; these endogenous materials are called “endogenous danger signals”. An objective for our lab is to establish how endogenous danger signals are generated, how they are disseminated, and how they act to promote inflammation. The following sections aim to provide the background of what is currently known and being hypothesized for inflammation. In particular, the following sections will discuss how various endogenous danger signals promote sterile inflammation or how endogenous danger signals act in complex with foreign materials to promote pathogenesis and ultimately disease.

1.1 INNATE IMMUNE RESPONSES

Immunity is a unifying term used to describe a physiological response that is engaged at least in part by immune cells (e.g., T cells, B cells, macrophages, etc.) to elicit inflammation or immunosuppression. Immune cells are the primary mediators for immunity but there is an increasing understanding that they are not the only mediators, as epithelial and fibroblasts, among other non-immune cells, can influence inflammation or immunosuppression (1). Secreted soluble factors such as cytokines or membrane-bound materials such as integrins can dictate immune responses.

Inflammation is described by a variety of phenotypes on several levels. On a larger scale, an inflammatory response results in increased swelling, heat, pain, and redness; this process was detailed by Celsus, a physician from the first century (2). This is in part due to an influx of immune cells such as monocytes and neutrophils from blood to sites of inflammation. These immune cells, among several other immune cells, employ secreted and membrane-bound factors that alter cellular and tissue composition. This alteration may be beneficial when dealing with situations such as infections, whereby this influx of immune cells controls pathogen load, while also promoting the development of subsequent immune responses.

In contrast to inflammation is immunosuppression whereby there is a calming down response to negate inflammation. Immunosuppression is recognized through several mechanisms. Once thought to be passive, it is actually a very active process by cells (e.g., T regulatory cells) that recognizes normal/healthy self versus compromised self (3). Immunosuppression in this manner can also be programmed subsequent to inflammation to

promote activities such as wound healing (4). Explanations of innate immune mechanisms that modulate inflammation will be discussed at length throughout this introduction.

1.1.1 Innate versus adaptive immunity

Innate and adaptive immune cells respond to stimuli in different ways (5). Thus the ways that they affect immunity are different. Adaptive immunity is an immunological response against very specific recognizable molecular epitopes (e.g., major histocompatibility complex plus peptide on antigen presenting cells) and the initial response promotes the development of a "memory" response whereby subsequent encounter(s) with the same specific recognized epitope typically results in faster and stronger immunity. Usually it is thought that adaptive immune responses are developed slowly over time (e.g., on the order of several days to months). In contrast to adaptive immunity, innate immunity is an immunological response against conserved recognizable molecular patterns (e.g., pathogen associated molecular patterns) and it does not maintain a "memory" response for subsequent encounters with the same specific recognized pattern. Innate immune responses develop faster than adaptive responses (e.g., on the order of minutes to hours).

Innate immune cells can "prime" and coordinate the type of adaptive immune response that occurs in a given situation. This coordination is in part due to specific intrinsic abilities that various immune cells have and where they are located at various times during the injury or insult. The following introduction will elaborate on the types of immune cells, how immune cell function, and some of the stimuli that alter their function.

1.1.2 Innate immune cells

Innate immune cells comprise of a diverse group of cells originating from hematopoietic stem cell precursors (5). Some members of the innate immune cell family includes mononuclear myeloid precursor derived cells such as subsets of monocytes, macrophages and dendritic cells, mononuclear lymphoid precursor derived cells such as subsets of NK cells, and polymorphonuclear cells such as neutrophils. Their functions can be quite different but together they can help promote a quicker response in situations of insult or injury.

One function following injury or infection is for these innate immune cells to produce cytokines and chemokines. Tissue resident macrophages are usually thought of as the first and largest producers of these inflammatory mediators (6). The most common mediators include cytokines such IL-1β, IL-6, TNF-α, which promote inflammation through the ligation of receptors on a variety of cell types; thus in this way they are described as inflammatory cytokines. For instance, TNF-α can ligate TNF receptor inducing the recipient cell's apoptotic death; this may be beneficial for the control of pathogen load in the case of an infected cell. Depending on the stimuli found at the site of insult, specific cytokines can influence the ensuing immune response(s). Secreted chemokines are important for the recruitment of other types of immune cells – both of the innate and adaptive arms. For instance, CCL3 and CCL4 are potent in recruiting primed T cells from lymph nodes (described below) whereas IL-8 is very potent for circulating neutrophil and monocyte recruitment from the blood (7). Once these cells are recruited, they can also respond to inflammatory cytokines and release inflammatory content including other inflammatory cytokines or materials that result in inflammation. Chemokines can

also result in signal transduction for the release of these materials such as inflammatory granules (including secretory lysosomes) from neutrophils.

Several innate immune cells function as phagocytic cells – in other words, they are endowed with intrinsic capabilities to engulf and internalize relatively larger sized materials (e.g., materials that are one micron or larger in diameter) (6). Phagocytes include cell types such as macrophages, dendritic cells and neutrophils. Their specific functions, localizations, and responses to stimuli may vary but as phagocytes, these cells are able to engulf and internalize materials such as bacteria for their clearance. In addition to phagocytic activities during infection, innate immune cells can produce factors that promote the innate immune response or the development of adaptive immune responses.

Antigen presentation allows innate immune cells to promote adaptive immune response development. Some phagocytic cells can also act as professional antigen presenting cells (APC) (6). In the process of infection macrophages and in particular dendritic cells process proteins and lipids in unique compartmentalized ways such that they can engage the adaptive immune response; this process is called antigen presentation. Antigen presentation can occur in a variety of ways and the compartmentalization of proteins and lipids processing can vary. Most notably, antigen presentation occurs with specifically sized peptides associated within proteins called major histocompatibility complexes (MHC). MHC come in different types – most notably class I and class II for the presentation of peptides. The types of peptides, as well as where and how they are modified, are different between MHC class I and MHC class II. Typically, endogenous proteins/peptides found within cells are targeted for degradation within proteasomes then trafficked to the endoplasmic retriculum for processing and loading onto MHC class I molecules

(8). Exogenous proteins/peptides or self proteins that are endocytosed are typically targeted for degradation within acidified late endosomes to be loaded onto MHC class II molecules (9). The loading of these peptides onto MHC enable the stable expression of these MHC on the plasma membrane. Once there, MHC in context of peptides can initiate signal transduction pathways through specific T cell receptors expressed by T cells.

Dendritic cells are thought to be the primary cell type for effective antigen presentation to initiate primary immune responses (10). Dendritic cells can not only efficiently handle peptides for antigen presentation but they are also more likely than macrophages to migrate from sites of insult towards lymph nodes. Lymph nodes provide an environment conducive for activating naïve T cells, which have not previously encountered presented antigen outside of the thymus. Dendritic cells are matured by stimuli such as pathogen associated molecular patterns (PAMPs), which activate pattern recognition receptors (PRRs) expressed by dendritic cells. Following their maturation, dendritic cells migrate towards increasing concentration gradients of CCL19, a chemokine secreted within lymph nodes (11). CCL19 binds to CCR7 found on mature dendritic cells, which initiates signal transduction pathways that enables this specific migration. Dendritic cells approach lymph nodes from peripheral tissues and engage with various cell types, including lymph node-resident dendritic cells and naïve T cells. Migratory dendritic cells can transfer intact protein antigens (cross-presentation) (12) or MHC plus peptides (semi-direct presentation) (13) to lymph node resident dendritic cells. In this manner, the lymph node resident dendritic cells can engage naïve T cells in the lymph node and result in their induction of signal transduction pathways for activation (i.e., priming). Migratory dendritic cells are also able to prime naïve T cells (14). Primed T cells initially proliferate then migrate away from lymph nodes

to peripheral sites of insult. For instance, expression of CCR5 sensitizes certain subsets of T cells to high concentrations of CCL3 and CCL4 secreted by innate immune cells at sites of insult (15).

1.1.3 Pathogen Associated Molecular Patterns versus Damage Associated Molecular Patterns

For the initial recognition response to mount immunity, immune cells need to be properly licensed. The specific mechanisms in which this coordination occurs is still a work in progress but there are two main hypotheses put forward. These two hypotheses include:

1) the recognition of self versus non-self (16) and

2) the recognition of healthy self versus non-healthy self (17)

While these two hypotheses are generally put forward, they do not fully answer how innate immune cells are engaged. There are different types of mounted immune responses to infection versus endogenous materials that promote diseases in the absence of infection (18). For the recognition of dying cells, there are “find me” or “eat me” signals that have completely different roles than what the two hypotheses provide (19, 20). Instead of promoting pro-inflammatory situations, endogenous factors released during cell death can also dampen immune responses to allow the repair of tissue (21). Furthermore, it is increasingly understood that certain endogenous factors may synergize with foreign materials to induce immune responses (22).

The self versus non-self hypothesis is supported by observations that immune cells become activated in response to infection whereas immune cells can be quiescent in the absence of infection. Pathogens such as bacteria or viruses contain novel repeating molecular patterns or foreign materials that are not normally found within the host organism (5). Most innate immune

cells possess a battery of receptors and ways of recognizing the presence of pathogen originated materials. Together these pathogen originated materials are called Pathogen Associated Molecular Patterns (PAMPs). The receptors that can be ligated by these PAMPs and elicit downstream signal transduction are called Pattern Recognition Receptors (PRRs). PRRs are expressed by many types of innate immune cells. An example of PAMPs and PRRs would be flagellin activation of Toll-Like Receptor 5 (TLR5) (23). Flagellin is a protein found on bacterial flagella and TLR5 is expressed by CD11c+ intestinal lamina propria dendritic cells (24). TLRs can be differentially expressed among several types of cells; for instance, TLR5 is not expressed by conventional mouse dendritic cells or bone marrow derived macrophages (25). In the context of infection, flagellin proteins ligate TLR5 expressed on dendritic cells to activate transcription factors such as nuclear factor κ-light-chain-enhancer of activated B cells (NF-κB) (26). These transcription factors result in the transcription of novel response elements and the eventual translation of inflammatory mediators such as pro-inflammatory cytokines and chemokines.

There are many different PAMPs, and the recognition of PAMPs is achieved through a diversity of plasma membrane-bound and intracellular PRRs (5). Toll-like receptors (TLRs) can be found on the plasma membrane or within endosomes (27). A listing of TLRs and their respective PAMPs are provided in Table 1. In addition to TLRs, there are other types of PRRs. These include the nucleotide-binding oligomerization domain-containing protein (NOD)-like receptors (NLRs) (28) and retinoic acid-inducible gene 1 protein (RIG)-I-like receptors (RLRs) (29), which are included in Table 2 with their respective PAMPs.

Table 1: Toll-like receptors (TLRs), ligands, cellular expression and localization. DC, dendritic cell; DN, double negative for CD4+ and CD8+; pDC, plasmacytoid dendritic cell; mΦ, macrophage; nΦ, neutrophil; NK, natural killer; T reg, T regulatory cell. Data compiled from (23, 27, 30, 31)

TLR	Primary Physiological Ligand	Generalized Immune Cell Type Expression	Cellular Localization
TLR1/2	Triacylated lipoproteins from Gram-negative bacteria & mycoplasma	Mouse: CD4+ DC, CD8+ DC, DN DC, pDC, monocyte, mΦ, nΦ Human: monocyte, mDC, pDC, T cells, B cells, mΦ, nΦ	Plasma membrane
TLR2/6	Diacylated lipopeptides from Gram-positive bacteria & mycoplasma	Mouse: CD4+ DC, CD8+ DC, DN DC, pDC, T cells, T reg, B cells, monocyte, mΦ, nΦ, NK cells Human: monocyte, mDC, T cells, mΦ, nΦ, NK cells	Plasma membrane
TLR3	Double-stranded RNA	Mouse: CD8+ DC, DN DC, T cells Human: mDC, NK cells	Endosomes
TLR4	Lipopolysaccharide	Mouse: CD4+ DC, CD8+ DC, DN DC, pDC, T reg, mΦ, monocytes, nΦ, NK cells Human: monocytes, T cells, mΦ, nΦ, NK cells	Plasma membrane & endosomes
TLR5	Flagellin	Mouse: CD4+ DC, DN DC, pDC, T reg, nΦ Human: monocytes, mDC, nΦ, NK cells	Plasma membrane
TLR7	Single-stranded RNA	Mouse: CD4+ DC, DN DC, pDC, B cells, mΦ Human: monocytes, mDC, pDC, B cells, mΦ	Endosomes
TLR8	Single-stranded RNA	Mouse: CD4+ DC, CD8+ DC, DN DC, pDC, T reg Human: monocytes, mDC	Endosomes
TLR9	Unmethylated 2'deoxyribo(cytidine-phosphate-guanosine)	Mouse: CD4+ DC, CD8+ DC, DN DC, pDC, T cells, mΦ, B cells Human: pDC, T cells, B cells	Endosomes
TLR10	Unknown; involved in recognition of TLR2 ligands?	Human: mDC, pDC, B cells	Plasma membrane
TLR11	Uropathogenic bacterial components; profilin-like molecule derived *T. gondii*	None reported	Endosomes

Table 2: Cytosolic pattern recognition receptors (PRRs), ligands and cellular expression. DC, dendritic cell; mΦ, macrophage; nΦ, neutrophil; NK, natural killer. Data compiled from (23, 27, 30, 31)

PRR	Primary Physiological Ligand	Generalized Immune Cell Type Expression
NOD1	Diaminopimelic acid-containing muropeptide from Gram-negative bacteria	Broad expression across immune cells
NOD2	Muramyl dipeptide	Monocytes, DC, nΦ
NLRP1	Muramyl dipeptide	Monocytes, mΦ, DC
NLRP3	Various stimuli	Monocytes, mΦ, DC, nΦ
NLRC4	Flagellin	Monocytes, mΦ, DC
NAIP5	Flagellin	MΦ, DC
AIM2	Double-stranded DNA	MΦ, DC
MDA5	Double-stranded RNA	Monocytes, mΦ, nΦ, NK cells
RIG-I	Double-stranded RNA	Monocytes, mΦ, DC, nΦ, NK cells

The type of signal transduction that occurs downstream from PRRs can also greatly vary between PRRs to elicit different responses. Some TLRs require adaptor molecules such as MyD88 or TRIF to elicit signal transduction (27); the type of accessory molecule required is different for specific TLRs. Some TLRs modulate transcription factors more effectively than others such as by modulating the function of NF-κB, activator protein-1 (AP-1), or interferon regulatory factors (IRF) (e.g., IRF-3) (32). These transcription factors influence the type of cytokines that will be produced. For instance, IRF-3 is a prominent transcription factor for Type I interferon transcription rather than NF-κB (32). Many of these induced pathways are elicited with specificity for the type of insult. For instance, double stranded RNA, a product of many viruses, is found within endosomes during certain viral infections, and can activate TLR3 for IRF-3 activity (32). Type I interferons directly interfere with virus propagation through ligation of receptors to elicit signal transduction for viral clearance (33).

Some PRRs do not directly induce the production and secretion of pro-inflammatory cytokines. In some instances, they promote the conversion of an inactive cytokine to become an inflammatory cytokine. This is the case for certain NLRs (e.g., NLRP1 and NLRP3), whereby the product of another PRR, such as IL-1β and IL-18, is actually sequestered in a zymogen state within cells (28). In this case, pro-IL-1β and pro-IL-18 are inactive and are not secreted from these non-NLR (but PAMP-activated) innate immune cells. Pro-IL-1β and pro-IL-18 (among other substrates) can be cleaved through the activity of caspase-1, which is activated through a multi-protein platform called the inflammasome (34). This complex includes a specific NLR protein (e.g., NLRP3) and linker domains (CARD domains found on the NLR protein or ASC that bind in pyrin domains found on some NLRs like NLRP3) to caspase-1. Multiple molecules of caspase-1 then oligomerize, which promotes the cleavage of various substrates, including pro-IL-1β and pro-IL-18, to mature IL-1β and IL-18, respectively. Through pathways that are not fully understood, mature IL-1β and IL-18 are rapidly released as soluble mediators of inflammation.

In addition to PAMPs, there are Damage Associated Molecular Patterns (DAMPs) (35). At sites of injury or infection, normally sequestered cellular content is either passively or actively released from cells that have compromised plasma membrane. In order for the released cellular content to be classified as a DAMP, the extracellular expression of these released materials should be minor in non-compromised individuals and the released material should modulate inflammation. For instance, intracellular adenosine triphosphate (ATP) is held within cells at a high concentration (>3 mM) ATP but upon cellular damage, ATP is lost out to the

extracellular space resulting in a gradient of ATP surrounding damaged cells (36). The danger hypothesis is strengthened through observations that inflammation can occur in the absence of infection such as situations of trauma or diseases such as arthritis or atherosclerosis; instead of foreign materials, it is appreciated that several endogenous factors promote inflammation in these instances (18).

Innate immune cells possess a variety of receptors that can recognize various DAMPs (32). In the case of ATP, these receptors are called purinergic receptors (37), ATP binding receptors that will be discussed at length in the following section. Many DAMPs are reported to act through PRRs that can also be activated by PAMPs. For instance, High Mobility Group Box 1 (HMGB1) is reported to activate TLR2 and TLR4 (38), in addition to activating TLR9 through endocytosis into endosomes by the non-PRR Receptor for Advanced Glycosylation End products (RAGE) (39). A list of known DAMPs with their receptors is shown in Table 3.

Table 3: DAMPs and their activating receptors. ECM, extracellular matrix. Data compiled from (22, 32) unless indicated.

DAMP	Physiological Source/Description	Reported Receptor(s)
Biglycan	ECM proteoglycan found in bone, cartilage, and tendons	TLR2, TLR4
Extra domain A of fibronectin	Cellular fibronectin produced in response to tissue injury	TLR4
Heparan sulfates	ECM proteoglycan layered over endothelial cells; released upon tissue damage	TLR4
Hyaluronic acid	Glycosaminoglycan that is a primary component of ECM	TLR2, TLR4
Surfactant protein A	Protein component of pulmonary surfactant	TLR4
Tenascin-C	ECM glycoprotein upregulated in inflammation	TLR4
Versican	ECM proteoglycan upregulated in tumors	TLR2
Fibrinogen	Soluble plasma glycoprotein	TLR4
Heat shock proteins	Intracellular compartments	TLR2, TLR4 (Disputed)
Formyl-peptides	From mitochondria of necrotic cells	FPR1 (40)
S100A8 and S100A9	Abundant cytoplasmic proteins of phagocytes	TLR4, RAGE
HMGB1 alone or in complex with self DNA or RNA	Non-histone DNA-binding protein from nuclei of necrotic cells	TLR2, TLR4, TLR7, TLR9, RAGE
Chromatin-DNA/RNA & ribonucleoprotein complexes	Nuclei of necrotic cells	TLR7, TLR9
Oxidized low-density lipoprotein (OxLDL)	Atherosclerotic lesions	TLR4/6 heterodimer (41)
Advanced glycation end-product of low density lipoprotein (AGE-LDL)	Derived from oxidized low-density lipoprotein	TLR4, RAGE
Oxidized palmitoyl-arachidonyl-phosphatidyl-choline (OxPAPC)	Derived from oxidized low-density lipoprotein	TLR4
Serum amyloid A	Apolipoproteins associated with high-density lipoprotein	TLR2, TLR4
β-amyloid	Alzheimer's disease	TLR4/6 heterodimer
Cardiac myosin	Abundant protein in the heart	TLR2, TLR8
Angiotensin II	Oligopeptide found in blood	TLR4
β-defensin 2	Secreted from neutrophils	TLR4
LL37 + self DNA or RNA	Secreted from neutrophils	TLR7, TLR9
ATP	Sequestered purine within cells	NLRP3 (via $P2X_7$)
Self double-stranded DNA	Released from nuclei of necrotic cells	AIM2
Uric acid crystals; cholesterol crystals	Breakdown of purine nucleotides formed during gout disease; developed during atherogenesis	NLRP3 (via phagocytosis)

In addition to the promiscuity of PRR for PAMPs and DAMPs, DAMPs can coordinate with PAMPs to elicit inflammation. This is especially evident with the inflammasome whereby PAMP induced activation (e.g., TLR activity) results in pro-IL-1β and inflammasome expression then DAMP induced activation (e.g., ATP ligation of the $P2X_7$ purinergic receptor) results in pro-IL-1β cleavage through inflammasome assembly (42). It is becoming more apparent that DAMPs may serve as an adjuvant to PAMPs in eliciting more efficient innate immune responses (22).

Although not often described as being DAMPs, various host-derived materials such as certain types of lipids can modulate immunity (6). Prominent among lipid ligands are eicosanoids such as prostaglandin E_2, which can enhance inflammation among other activities (43). Oxidized low density lipoprotein built up in atherosclerotic lesions during the progression of atherosclerosis has agonistic activities through TLR4/6 heterodimer (41). Phospholipids such as phosphatidylinositols and sphingomylein also have demonstrated NF-κB activity although their route of activation is not revealed (44). The primary stimulatory and immunosuppressive lipids are included in Table 4.

Table 4: Lipids in immunological responses. Data compiled from (45-47).

Lipids/fatty acids	Synthesizing Enzyme(s)	Activating Receptor(s)	Activities
Arachidonic acid (AA)	Phospholipase C (PLC) or phospholipase A_2 (PLA_2)	NA	Precursor fatty acid in eicosanoid synthesis
Prostaglandins	Cyclooxygenase pathways from arachidonic acid	DP_{1-2}, EP_{1-4}, FP, IP_{1-2}, TP	PGE_2 and PGI_2 are pro-inflammatory; PGJ_2 and $PGA_{1/2}$ are anti-inflammatory
Leukotrienes	5-lipoxygenase activity from arachidonic acid for LTA_4; LTA_4 is converted by other enzymes to the other forms	GPCR and PPAR groups	Histamine production; LTB_4 and LTC_4 are pro-inflammatory
Lipoxins	15-lipoxygenase from arachidonic acid	Cysteinyl leukotriene receptor type 1	Antagonist to several leukotrienes
Phosphatidic acid (PA)	Phospholipase D (PLD) activity from phosphatidylcholine or diacylglycerol kinase phosphorylation of diacylglycerol	NA	Precursor lipid for conversion to other forms; incorporates into membranes for curvature
Lysophos-phatidic acid (LPA)	Phospholipase A_2 (PLA_2) from phosphatidic acid	Lysophosphatidic acid receptor 1, 3	G protein-coupled receptor activity for proliferation, migration, and survival
Diacylglycerol (DAG)	Lipid phosphate phosphohydrolase activity from phosphatidic acid; cleavage product from phospholipase C	Transient Receptor Potential Canonical cation channel (TRPC3/6/7)	Precursor lipid for conversion to other forms; activates protein kinase C, TRPC3/6/7 cation channels
Lysophos-phatidylcholine (LPC)	Phospholipase A_2 from phosphatidylcholine	G2A	G protein-coupled receptor activity to downregulate T cell responsiveness
Ceramide	Ceramide is produced by dihydroceramide desaturase.	NA	Precursor lipid for conversion to other forms; stabilizes lipid rafts for signal transduction; pro-apoptotic
Sphingomyelin	Sphingomyelinase activity from ceramide	NA	Precursor lipid for conversion to other forms – primarily ceramide and sphingosine 1-phosphate
Sphingosine 1-phosphate (S1P)	Ceramidase conversion from ceramide to sphingosine then sphingosine kinase to S1P	$S1P_1$-$S1P_5$	G protein-coupled receptor activity to promote survival
Sphingosyl-phosphoryl-choline (SPC)	Sphingomyelinase conversion from ceramide to sphingomyelin then sphingomyelin deacylase to SPC	OGR1	G protein-coupled receptor activity for immunosuppression
Oxidized phospholipids with *sn-2* acyl group	Oxidation processes of phospholipids; found in oxidized low density lipoprotein (LDL) or minimally modified LDL	CD36, PPAR-γ, or TLR4/6 hetrodimer	Phagocytosis; macrophage activation; immunosuppression

1.1.4 Toll-Like Receptor signaling pathways

TLRs are a set of receptors that can differentially respond to specific PAMPs and DAMPs via signal transduction pathways to activate gene transcription (32). Typical transcription factors include NF-κB, mitogen-activated protein kinase (MAPK)-induced AP-1, and IRFs (e.g., IRF-3, IRF-5 IRF-7). These transcription factors can be fine-tuned to transcribe different gene response elements. NF-κB can homodimerize or heterodimerize between 5 different subunits. The type of NF-κB dimerization dictates which gene response elements are activated for the expression of co-stimulatory ligands, cytokines, pro-survival factors, among other materials (26).

TLR signaling pathways are modulated in several ways. The basic signal transduction elicited by a ligand involves cross-linking of a given TLR with the same TLR (homodimer) or with another TLR (heterodimer) (48). Sometimes the interaction of a PAMP with its respective TLR is mediated through accessory proteins. For TLR4 signaling, the ligand lipopolysaccharide (LPS) binds to the accessory molecules CD14 and LPS binding protein (49). The sensitivity of TLR4 is modulated by MD2, which enables enhanced cross-linking. Most PAMP ligand recognition is mediated by the leucine-rich repeat domains of TLRs.

The localization of a TLR can affect the type of accessory molecules that it encounters and the resulting downstream signal transduction (50). As mentioned, some TLRs are expressed at the plasma membrane whereas others are contained within endosomes. Sometimes the location places the TLR within reach of other essential macromolecules that enable its activity. For instance, once TLR9 is ligated by unmethylated CpG DNA (commonly derived from certain bacteria and viruses) within endolysosomes its activation occurs after cleavage by

endolysosomal proteases (51). TLR7 activity often requires autophagic processes to deliver its ligand of ssRNA (commonly associated with certain viruses that replicate in cytosol) to endolysosomes as well (52). TLR4 is also differentially modulated by its localization (32). At the plasma membrane, TLR4 interacts through its intracellular TIR domain with accessory signaling molecules MyD88 and TIRAP, which signal an early phase activation of NF-κB for pro-inflammatory cytokine production. After clathrin/dynamin-dependent endocytosis into endosomes, the TIR domain of TLR4 then interacts with the accessory molecules TRIF and TRAM, where they signal a late phase activation of NF-κB and IRF3 for pro-inflammatory cytokines and type I interferons, respectively.

The specific accessory molecules that associate with the TIR domains of various TLRs dictate the type of downstream cytokines that are produced (32). Most TLRs employ MyD88 as an accessory molecule, which recruits other molecules called IL-1 receptor associated kinases (IRAK-1, -2, -4, and –M). IRAK-4 initiates downstream activity for NF-κB and MAPK-mediated transcription pathways whereas IRAK-1 and IRAK-2 sustain signaling for robust transcription. IRAK activates the E3 ligase TRAF6, which mediates polyubiquitination and binding and activation of TAK1 and NEMO. TAK1 then phosphorylates IKKαβ, which phosphorylates IκB for proteasome-mediated degradation to activate NF-κB. Additionally, TAK1 initiates MAPK pathways Erk1/2, p38, and Jnk for AP-1 activity. There is also a MyD88-independent activation pathway that is dependent upon TRIF, which can activate TAK1 through different accessory proteins but yet activate the same downstream signaling pathways – NF-κB and MAPK. Unlike MyD88, TRIF can also activate IRF3 activity for Type I Interferon-β transcription, through TRAF3 activation of TBK1-IKKi phosphorylation. These pathways are illustrated in Figure 1-1.

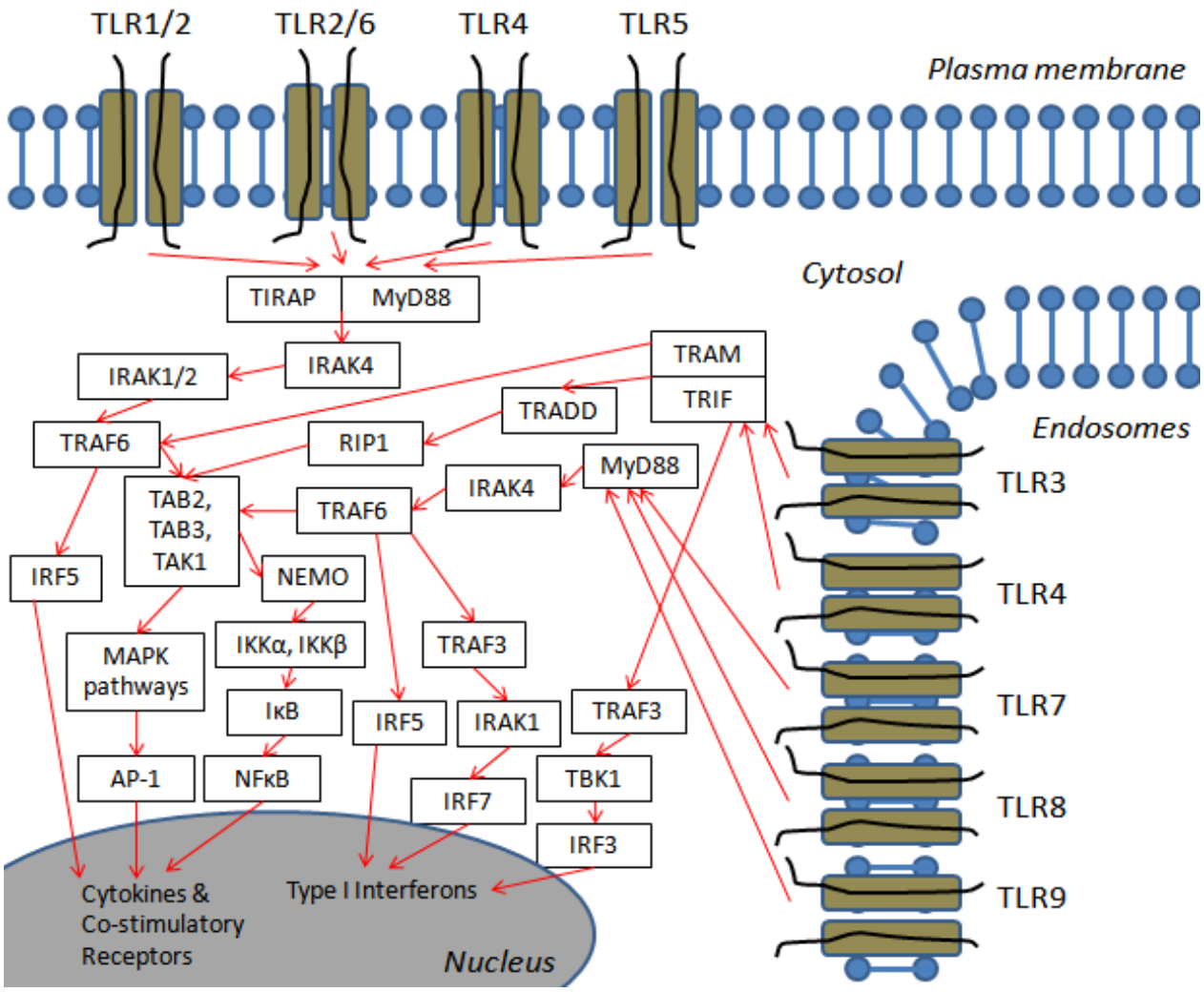

Figure 1-1: TLR induced signaling pathways.

TLR are found on the plasma membrane or within endosomes. Upon engagement with specific ligands, a given TLR can interact with adaptor proteins such as TIRAP/MyD88, TRIF/TRAM, or MyD88 alone. These adaptor proteins connect with signal transduction pathways for protein phosphorylation or ubiquitination. Ultimately, these signals converge for transcription factor activation (e.g., AP-1 or NF-κB) for pro-inflammatory cytokine production and upregulation of co-stimulatory ligands or for the production of type I interferons (e.g., IRF3 or IRF7).

MAPK signaling can be activated through a variety of upstream pathways (53), for example through the activities of protein kinase A (PKA) and protein kinase C (PKC). PKA is activated through elevated intracellular levels of cyclic adenosine monophosphate (cAMP), generated by adenylate cyclase (54). PKC is activated by at least two different stimuli, depending on the specific PKC isoform (55). Conventional PKC isoforms are activated by elevated intracellular levels of calcium and diacylglycerol (DAG), whereas novel PKC isoforms are activated by DAG, but not calcium. As kinases, PKA and PKC can lead to the phosphorylation of several signaling intermediate pathways that tie into MAPK pathways among other signaling pathways to elicit biological responses. For instance, PKC can influence guanine exchange factors (GEFs) (e.g., RasGEF SOS) to activate small G proteins (e.g., Ras) to lead to its downstream activities with MEK1/2, which can modulate activities for p38, Erk1/2, and Jnk MAPK pathways. PKA can be activated by various G proteins (especially Gs-mediated cAMP generation) but they can also activate 14-3-3, which can then associate with c-Raf family members to engage MAPK pathways.

There is an established connection between TLRs and other various stimuli that regulate NF-κB and MAPK pathways. For instance, TNF-α is a cytokine that is commonly added as a reagent to dendritic cell maturation cocktails in addition to Poly I:C, a TLR3 agonist, for better dendritic cell maturation (56). Direct PKA activation of dendritic cells alone, however, can also elicit ample levels of maturation (57). Various isoforms of PKC have been demonstrated to modulate TLR function. PKCδ binds to TLR2 and TLR4 adaptors TIRAP/Mal (co-factors of MyD88) to influence p38 MAPK and NF-κB (58). PKCα/β enhances nuclear translocation of NF-κB in TLR2 and TLR4 stimulated neutrophils, and also enhances IKKα/β activation as well as phosphorylation of the p65 subunit of NF-κB (59). PKCϵ phosphorylates TRIF following

TLR4-induced activation of macrophages (60). In some instances, LPS-induced NF-κB requires PKCζ (61, 62). Hyaluronan signaling through TLR2 with macrophages also requires PKCζ (63). Finally, PKCα modulate NF-κB activation in several immune cell types including T cells (64), monocytes (65), and neutrophils (66).

Deficiencies in TLR signaling can seriously impact the clearance of pathogens and protection from their subsequent pathogenesis; however, at the same time, TLR recognition of DAMPs can have also pathological consequences. DNA-chromatin complexes and ribonucleoprotein complexes released from dying cells mediate TLR7- and TLR9-dependent development of systemic autoimmune diseases such as systemic lupus erythematosus (67). HMGB1 acts in a similar capacity, where it is thought that HMGB1 or other DNA binding proteins may protect released self DNA and allow its entry to endocytic compartments (68). HMGB1 itself can bind to TLR4 for its activation (69). HMGB1 is acknowledged to promote septic shock and ischemic reperfusion through TLR2, TLR3, TLR4, and TLR9 (70). Host derived β-amyloid and oxidized phospholipids act in a TLR4/TLR6 heterodimeric dependent manner for the potential of non-pathogenic disease progression of Alzheimer's disease and atherosclerosis respectively; it is thought that TLR4 and TLR6 heterodimerize through cooperative activities of the scavenger receptor CD36 (41). Injury and cellular damage to the lungs liberate hyaluronic acid cleavage products that promote inflammation for eventual wound healing through TLR2 and TLR4 dependent mechanisms (71).

1.1.5 NOD-Like Receptor signaling pathways

In contrast to TLRs, NLRs are strictly intracellular cytosolic receptors (28). NLRs function as oligomerization platforms for the recruitment and coupling of several proteins through common binding domains such as caspase activation and recruitment domains (CARD). This recruitment can result in several different activities, depending on the NLR and its binding partners. NOD1 and NOD2 recognize various bacterial cell wall components, leading to RIP2 activation of the IKK complex and NF-κB transcription.

In contrast to NOD1 and NOD2, most of the other NLRs activate caspase-1 (42). NLRP1 is activated by muramyl dipeptide (72) or anthrax lethal toxin in collaboration with NOD2 (73). NLRC4 and NAIP5 are activated by the specific flagellin of *Salmonella typhimurium* (74) and *Shigella flexneri* (75), and *Legionella pneumophila* (76), respectively. AIM2 is activated by double stranded DNA (77). NLRP3 is activated by several stimuli without apparent molecular specificity; it appears to occur downstream of materials that inflict membrane damage. Examples include pore forming agents like certain bacterial toxins or ATP activation of large-pore formation by $P2X_7$ (78), materials that are hard to phagocytose such as uric acid crystals (79) or cholesterol crystals (80), or materials that promote potassium efflux such as the potassium ionophore nigericin or maitotoxin (78). Stability of lysosomes (81), activation of cathepsin B (81, 82), and reactive oxygen species (83-85) can also contribute to NLRP3 activation. Regardless of the initial stimuli and the ensuing pathways, the hallmark of these particular NLRs is the activation of caspase-1 through their respective inflammasome platforms for the processing of pro-IL-1β and pro-IL-18 to their biologically active, mature, forms. These pathways are depicted in Figure 1-2.

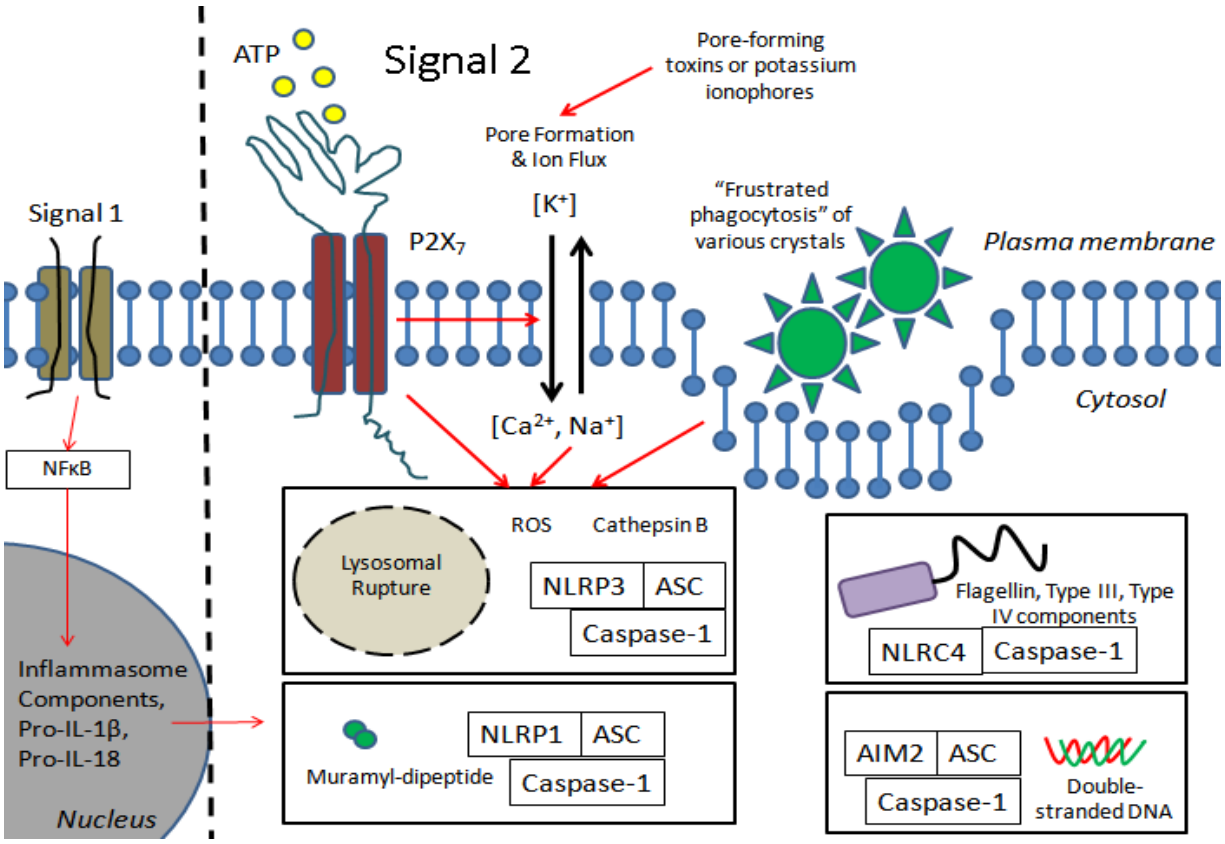

Figure 1-2: Inflammasome activation pathways.

Activation of the inflammasome requires two distinct and sequential signals: a "signal 1" prerequisite of NF-κB induction (e.g., by TLR ligands) and a "signal 2", which is promoted by a variety of stimuli depending on the type of NLR-inflammasome protein (i.e., NLRP3, AIM2, NLRP1, or NLRC4). NLRP3 is activated by several materials including ATP activation of P2X7/Pannexin-1, pore-forming toxins, and the "frustrated phagocytosis" of various crystals. NLRP3 activation can also require potassium efflux, cathepsin B activity, reactive oxygen species (ROS), or lysosomal damage. AIM2 is activated by cytosolic recognition of double-stranded DNA. NLRP1 is activated by muramyl-dipeptide. NLRC4 is activated by certain types of flagellin and/or Type III or Type IV secretion components. NLRP3, AIM2, and NLRP1 act with ASC to activate caspase-1 for caspase-1 cleavage. NLRC4 is ASC-independent. Ultimately, these inflammasome platforms result in the caspase-1 dependent cleavage of immature zymogen forms of IL-1β and IL-18 to their mature biologically active forms.

NLRP3 contributes to both infectious and non-infectious disease. Even though TLRs such as TLR7 and various RLRs recognize viral components, they are dispensable in terms of promoting CD8+ T cell cytolytic responses against influenza A viruses, whereas NLRP3 is indispensable; this is in large part due to its capacities to promote IL-1β (83, 86, 87). Mutations in NLRP3 promote familial cold autoinflammatory syndrome, Muckle-Wells syndrome, and chronic infantile neurological, cutaneous and articular syndrome (88); these autosomal diseases are the result in overactive NLRP3 and IL-1β production (89). Other activators of NLRP3 include silica crystals and asbestos (90), which can promote silicosis- and asbestosis-induced pulmonary fibrosis, respectively, in a NLRP3-dependent manner.

1.1.6 Macrophage activation

Macrophages and dendritic cells, among other cell types, can be stimulated by various PAMPs and DAMPs. The responses to these stimuli are often called activation or maturation for macrophages and dendritic cells respectively. Macrophage activation is characterized in a few distinctive ways (91). Often the types of activation are loosely correlated to polarized CD4+ T cell helper subtypes including Th1, Th2, and T regulatory polarized T helper cells. Without extensive elaboration that is beyond the scope of this dissertation, CD4+ T cells can be polarized to become cytolytic-assisting Th1 T cells, promoters of antibody class-switching (Th2 T cells), pro-inflammatory Th17 T cells, or immunosuppressive T regulatory cells (Treg). This list now includes even more than these four helper subtypes. Macrophage activation was previously divided into two groups – classically activated macrophages (M1), which helps to promote the

cytolytic response by Th1 T cells, and alternatively activated macrophages (M2), which promote the class-switching capabilities of Th2 T cells (92). This area is still in a state of flux, given the ongoing developments in the T cell polarization field; thus macrophage activation was recently reclassified to include the following subtypes (91):

1) Classically activated macrophages
2) Regulatory macrophages
3) Wound-healing macrophages

These different macrophage activation states and some key polarizing molecules are diagramed in Figure 1-3.

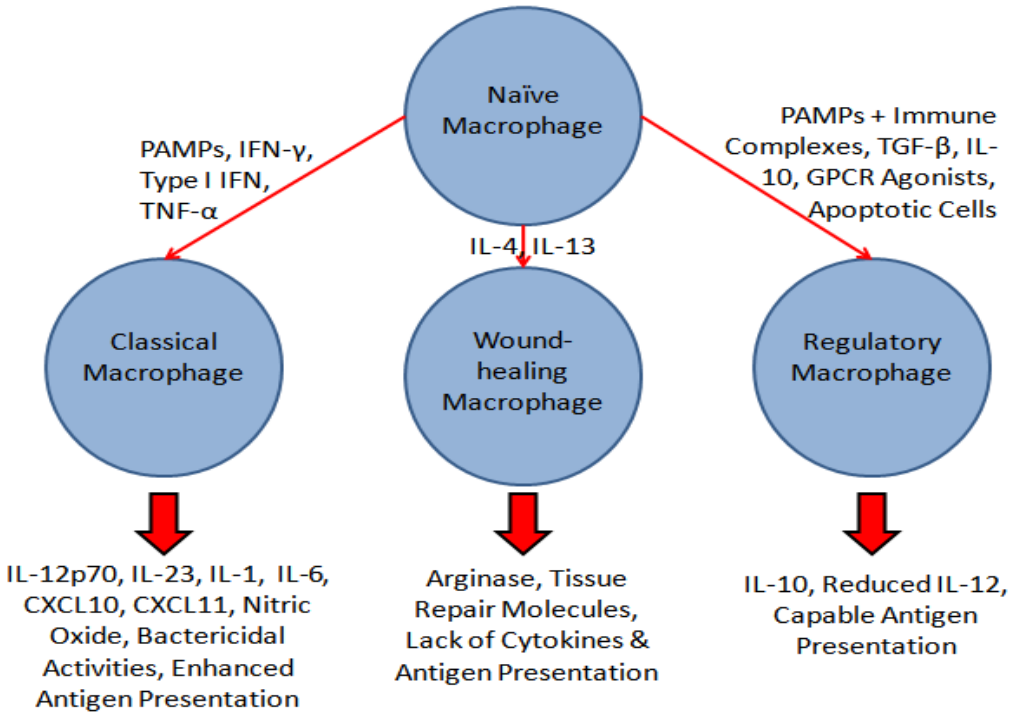

Figure 1-3: Macrophage activation.

Macrophages can differentiate into several types. PAMPs, IFN-γ, type I interferons, and/or TNF-α can act together or alone to polarize macrophages to the classical phenotype. Classically activated macrophages secrete several pro-inflammatory cytokines and perform bactericidal activities and antigen presentation. IL-4 or IL-13 can promote wound healing macrophage polarization. Wound healing macrophages promote arginase activity for generating tissue repair molecules while decreasing cytokines secretion and antigen presentation. PAMPs plus immune complexes (e.g., antibodies bound to their specific epitopes), immunosuppressive stimuli (e.g., TGF-β, IL-10, apoptotic cells), or other stimuli for GPCR activation can promote regulatory macrophage polarization. Regulatory macrophages secrete a higher ratio of IL-10 to IL-12 while still exhibiting capable antigen presentation abilities including the upregulation of co-stimulatory ligands. These polarized forms can be very plastic, especially in the context of disease development. For instance regulatory macrophages can be diverted from regulatory macrophages to wound healing macrophages by activities or factors produced by Th2 polarized helper T cells.

Classically activated macrophages promote cytolytic activities. At first, it was found that IFN-γ and TNF-α promote macrophage activity for pro-inflammatory cytokines secretion (e.g., IL-6 and IL-1) (93) and polarizing cytokine secretion (e.g., IL-12p70 and IL-23) (94, 95); however, it is now appreciated that Type I interferons and/or certain PAMPs, through TLRs, can perform some of the same activities (96). PAMPs alone can induce classical activation especially when their ligation results in Type I intereferon and TNF-α production; this could most readily come about if the PAMP activates NF-κB and IRF3, such as for TLR3 and TLR4 agonists. Classically activated macrophages also secrete chemokines such as CXCL10 and CXCL11 that attract NK and T cells to sites of insult (97). In addition to cytokines or chemokines, classically activated macrophages can induce superoxide anion production and iNOS for pro-inflammatory NO (98) which, together with other processes induced by Type I and Type II interferons, can generate efficient microbicidal and anti-viral activities.

Several cell types can promote the generation of classically activated macrophages. Early responders to infection, such as NK cells and NKT cells, can secrete prodigious amounts of IFN-γ (99). This can additionally be aided and sustained at later times by recruited Th1 T cells, which can release IFN-γ at sites of insult. In the absence of being directly activated by PAMPs, tissue resident macrophages can receive TNF-α from PAMP-activated APC. Together IFN-γ and TNF-α greatly promote classical activation (93). Classically activated macrophages can further promote Th1 polarization of CD4+ T cells and cytolytic activities of CD8+ T cells, through the production of IL-12 (95).

It is also possible that classically activated macrophages could help promote Th17 polarization of naïve CD4+ T cells, since these macrophages produce large amounts of IL-1, IL-

6, and IL-23, which can promote Th17 polarization (94). Additionally, whereas classically activated macrophages are important mediators of host defense, they can also elicit immunopathologies such as rheumatoid arthritis (100) and inflammatory bowel disease (101), which have been described as Th17-mediated pathologies (102, 103).

In addition to the secretion of polarizing cytokines, classically activated macrophages are also capable of antigen presentation to T cells. Classically activated macrophages exhibit enhanced antigen processing and antigen presentation machinery for both MHC class I and MHC class II antigen pathways (104). For MHC class I presentation, proteasome activity is enhanced, transporter associated with antigen processing (TAP, a molecule used for the transport of antigen from the proteasome to the ER) is upregulated, and various MHC class I chaperone molecules (such as calnexin and calreticulin) among others are also upregulated. For MHC class II, the over-all level of expressed MHC class II at the cell surface is enhanced, in part due to IFN-γ-inducible activation of MHC class II transactivator (CIITA), a transcriptional co-activator of MHC class II expression. For both presentation pathways, classically activated macrophages also display elevated levels of co-stimulatory ligands, such as CD80 and CD86, that aid to enhance and sustain MHC/peptide mediated signaling through antigen cognate T cell receptors found on T cells.

Regulatory macrophages and wound-healing macrophages are more recently identified macrophage subsets (91). Before regulatory and wound-healing macrophages were identified, activated macrophages without classical activation phenotype were classified as alternatively activated macrophages (92). We now know that wound-healing macrophages display different

phenotypes than regulatory macrophages; however they can share similar phenotypes and these subsets of macrophages are very plastic from one type of differentiation to another (105).

Regulatory macrophages are mostly defined by their ability to promote immunosuppression. Regulatory macrophages display elevated production of IL-10 and reduced production of IL-12, although there can still be some production of pro-inflammatory cytokines (106). Even in the presence of pro-inflammatory cytokines, IL-10 is very immunosuppressive and is sufficient to decrease both the secretion of IL-12 and the efficacy of pro-inflammatory cytokines (107). Phagocytosis of apoptotic cells/bodies helps to promote TGF-β secretion and is thought to aid in regulatory macrophage differentiation (108). Prostaglandins (109), adenosine (110), dopamine (111), histamine (112), and sphingosine-1-phosphate (113), among several other host derived materials that deviate T helper responses away from Th1 polarization, can also promote different forms of regulatory macrophages. Tumor-associated macrophages display similar characteristics to regulatory macrophages, suggesting that tumor microenvironments may also promote regulatory macrophage differentiation (114).

TLR activation of regulatory macrophages can elicit responses that are different from wound-healing macrophages or classically activated macrophages. In addition to increasing IL-10 secretion, TLR ligation of regulatory macrophages can result in efficient naïve T cell activation. Regulatory macrophages can display high levels of co-stimulatory ligands including CD80, CD86, and LIGHT, which can enhance T cell receptor stimulation (115). Thus, in this manner, regulatory macrophages may serve as efficient APC – perhaps mostly for the induction of T regulatory cells.

Wound-healing macrophages are typically generated with the help of Th2 T cells with the purpose to act in tissue repair (115). A major factor for their differentiation is IL-4 (116), which is produced in large part by granulocytes (polymorphonuclear innate immune cells, including basophils and mast cells, which are involved in type I hypersensitivity immune responses) and Th2 T helper cells (117). IL-4 promotes activity of arginase, which converts arginine to ornithine, a precursor of the extracellular matrix components collagen and polyamines (118). Wound-healing macrophages appear to be dispensable for host-defense, as they are unable to clear various infections and do not control pathologies generated by several types of organisms including parasites (119). Wound-healing macrophages are also poor APCs, as they fail to upregulate co-stimulatory ligands or antigen presentation machinery (115). In terms of phenotype, wound-healing macrophages are most readily identified and separated from other types of macrophages by their expression of molecules involved in tissue repair, such as YM-1, RELM-α, and Factor XIII-A (120). The markers for and functions of wound-healing macrophages, classically activated macrophages, and regulatory macrophages are listed in Table 5.

Table 5: Types of polarized macrophages. PAMPs: pathogen associated molecular patterns. GPCR: G-protein coupled receptors. Data taken from (91).

Type of Macrophage	Inducers	Markers	Functions/Characteristics
Classical Macrophage	PAMPs, IFN-γ, Type I interferons, TNF-α	IL-12p70, nitric oxide, CCL15, CCL20, CXCL9, CXCL10, CXCL11	Bactericidal activities, enhanced antigen presentation
Wound-healing Macrophage	IL-4, IL-13	Arginase, tissue repair molecules, CCL18, YM1, RELMα, CCL17, IL-27Rα, IGF1, CCL22, DCIR, stabilin 1, Factor XIII-A	Wound-healing activities, lack of cytokines and antigen presentation
Regulatory Macrophage	PAMPs + Immune complexes, TGF-β, IL-10, GPCR agonists, apoptotic cells	IL-10, SPHK1, LIGHT, CCL1	Immunosuppression

The type of macrophage activation state can be fairly plastic, especially between regulatory macrophages and wound-healing macrophages. This is very apparent given that regulatory macrophages secrete large amounts of IL-10 (115). Secreted IL-10 can induce Th2 CD4+ T helper cells to produce IL-4 and IL-13 (121), which can act back on macrophages to promote their differentiation to wound-healing macrophages.

The plasticity between wound-healing or regulatory macrophages and classical macrophages can result in various immunopathologies. The exact role of macrophages throughout tumor progression is a bit ambiguous (i.e., whether they promote or help to resolve cancer), but it is clear that the macrophage resident populations display more of a classically activated phenotype during early settings of neoplasia whereas over time macrophages switch to a more regulatory phenotype (122). Regulatory macrophages are thought to play a role in inhibiting adaptive immune responses to neo-antigens and to promote angiogenesis.

There is some evidence that the switch from wound-healing/regulatory macrophages to classically activated macrophages can promote diseases such as atherosclerosis and diabetes. Normally within healthy individuals, macrophages associated with adipose tissue are generally anti-inflammatory (123). This immunosuppression is mediated by PPAR-γ, a transcriptional regulator of several different factors including arginase and a factor found in wound-healing macrophages (124). In contrast, macrophages within adipose tissue of obese individuals are highly inflammatory and produce pro-inflammatory cytokines, similar to those made by classically activated macrophages, that interfere with insulin signaling in adipocytes for type-2 diabetes progression (125). It is generally thought that the elevated amount of necrotic cell death found in adipose tissue of obese individuals dictates whether factors are released to promote classically activated macrophages versus wound-healing activated macrophages (126). In general it is acknowledged that necrotic cell death can be inflammatory, whereas apoptotic cell death is neutral or in some circumstances is immunosuppressive (127).

In the case of atherosclerosis, atherosclerotic lesions can develop along blood vessels that are susceptible to lipid accumulation (128). Macrophages are gradually attracted to these lipid accumulations and form necrotic cell cores that are sites of inflammation including the presence of pro-inflammatory cytokines characteristic of classically activated macrophages (129). The exact mechanism for how this progression from wound-healing/regulatory macrophages to classically activated macrophages is initiated is a bit unclear, although various factors such as oxidized phospholipids, extracellular matrix fragments, and cellular debris found within atherosclerotic plagues have an ability to promote this turnover (101).

1.2 PURINERGIC RECEPTORS AND THEIR SIGNAL TRANSDUCTION PATHWAYS

A variety of purines, including ATP, adenosine disphosphate (ADP), adenosine, and uridine triphosphate (UTP) can activate a set of receptors that are expressed at the plasma membrane of several types of cells (130). Purinergic receptors contain extracellular binding pockets for purines. Once engaged extracellularly with their specific purine ligand (some purinergic receptors display greater affinity for certain purines), purinergic receptors undergo conformational change to elicit specific signal transduction pathways.

Purinergic receptors are divided into two subtypes – P1 and P2 receptors (130). P1 receptors have greater specificity for adenosine and inosine and do not bind ATP, ADP, or UTP. P1 receptors are G protein coupled receptors (GPCRs); thus when bound by their ligand, they induce the activation of various G proteins including differential activation of Gs, Gq, or Gi depending on the type of P1 receptor. P2 receptors have greater specificity for binding ATP, ADP, UTP, uridine-diphosphate (UDP), and UDP-glucose. P2 receptors are further divided into P2X and P2Y receptors. P2X receptors act as ligand-gated ion channels that allow for the influx and efflux of different ions. P2X receptors often act as homotrimers and heterotrimers. ATP is the primary physiological ligand for P2X receptors. P2Y receptors act as GPCRs for the activation of Gs, Gq, or Gi. A full listing of all of the known purinergic receptors, their primary physiological ligands and their respective EC_{50} values, and their immunological functions are within Table 6.

Table 6: Purinergic receptors, ligands, and functions. DC, dendritic cell; mΦ, macrophage; nΦ, neutrophil; NK, natural killer; PGE_2, prostaglandin E_2; ROS, reactive oxygen species; RNS, reactive nitrogen species; VEGF, vascular endothelial growth factor. Unless otherwise mentioned, data is taken from (37).

Purinergic Receptor	Physiological Ligand & Immune Cell Expression	Immunological Function
A_1	Adenosine (EC_{50}: 0.18-0.53 µM) Inosine (EC_{50}: 290 µM) Expressed by nΦ, monocytes, mΦ, DC, NK cells	NΦ: Enhances adherence to endothelium; induces chemotaxis; enhances phagocytosis; enhances ROS MΦ: Enhances phagocytosis; enhances ROS NK cells: Enhances cell-mediated cytotoxicity
A_{2A}	Adenosine (EC_{50}: 0.56-0.95 µM Inosine (EC_{50}: 50 µM) Expressed by nΦ, monocytes, mΦ, DC, T cells, B cells	NΦ: Inhibits adherence to endothelium; inhibits ROS; may be involved in adenosine-mediated inhibition of degranulation; enhances COX-2 and prostaglandin E2 expression; delays onset of apoptosis Monocytes: Inhibits adherence to endothelium MΦ: Inhibits NF-κB binding to DNA; increases IL-10 secretion; syngerize with TLR ligands to enhance VEGF expression but inhibits TNF-α and IL-12; promotes wound-healing and angiogenesis; decreases ROS DC: Inhibits TNF-α and IL-12 following maturation T cells: Attenuates activation and cytotoxicity
A_{2B}	Adenosine (EC_{50}: 16.2-64.1 µM) Expressed by nΦ, monocytes, mΦ, DC, T cells	NΦ: Inhibits adherence to endothelium; inhibits the release of VEGF Monocytes: Inhibits adherence to endothelium; enhances IL-10 MΦ: Enhances IL-10; decreases NOS T cells: Attenuates activation; inhibit NF-κB signaling
A_3	Adenosine (EC_{50}: 0.18-0.53 µM) Inosine (EC_{50}: 0.03-2.5 µM) Expressed by nΦ, monocytes, mΦ, DC, T cells	NΦ: Inhibits degranulation; promotes chemotaxis (131) MΦ: Inhibits LPS-induced CCL3 and NF-κB; decreases RNS T cells: Attenuates adherence of cytolytic T cells to tumor targets and cytolytic functions
$P2X_1$	ATP (EC_{50}: 0.05-1 µM) Expressed by nΦ, monocytes, mΦ, DC, T cells, NK cells	NΦ: Promotes chemotaxis (132) T cells: Promotes activation (133)
$P2X_2$	ATP (EC_{50}: 1-30 µM) No reported expression	No reported function

Table 6 (continued)		
$P2X_3$	ATP (EC_{50}: 0.3-1 μM) No reported expression	No reported function
$P2X_4$	ATP (EC_{50}: 1-10 μM) Expressed by nΦ, monocytes, mΦ, DC, T cells, NK cells	MΦ: Promotes PGE_2 (134) and IL-1β secretion (135) Microglial cells: Promotes chemotaxis (136) T cells: Promotes activation (133)
$P2X_5$	ATP (EC_{50}: 1-10 μM) Expressed by nΦ, monocytes, mΦ, DC, T cells	No reported function
$P2X_6$	ATP (EC_{50}: 1-12 μM) No reported expression	No reported function
$P2X_7$	ATP (EC_{50}: 100-780 μM) Expressed by nΦ, monocytes, mΦ, DC, T cells, B cells, NK cells	NΦ: Enhance adherence to endothelium; promote priming for ROS Monocytes: Promote NF-κB; induce shedding of L-selectin; promotes IL-1β, IL-18, IL-1α, and arachidonic acid secretion; upregulates COX-2; induces cell death MΦ: Promotes NF-κB; promotes IL-1β, IL-18, IL-1α, and arachidonic acid secretion; upregulates COX-2; regulates phagocytosis; enhances lysosomal enzyme secretion enhances RNS and ROS; induces cell death DC: Induces maturation; promotes IL-1β, IL-18, IL-1α secretion; induces cell death T cells: Induces shedding of L-selection; induces proliferation; induces cell death of regulatory T cells; enhances activity of AP-1 and NF-κB B cells: Induces proliferation
$P2Y_1$	ADP (EC_{50}: 8 μM) Expressed by nΦ, monocytes, mΦ, DC, T cells	No reported function
$P2Y_2$	UTP (EC_{50}: 0.14 μM) = ATP (EC_{50}: 0.23 μM) Expressed by nΦ, monocytes, mΦ, DC, T cells, eosinophils	NΦ: Promotes chemotaxis (131); enhances degranulation; promotes priming for ROS Monocytes: Enhances adherence to endothelium; promotes CCL20 (137) and IL-8 (138) secretion; promotes apoptotic cell clearance (139) MΦ: Enhances IL-6 and CCL2 (140) secretion; increases phagocytosis; promotes chemotaxis (141); promotes apoptotic cell clearance (139) DC: Promotes CCL20 secretion (137); promotes chemotaxis (142) Eosinophils: Promotes chemotaxis (142); promotes accumulation in lungs (143); promotes cytokine release (144)

Table 6 (continued)		
$P2Y_4$	UTP (EC_{50}: 2.5-2.6 μM) >> ATP, UDP Expressed by nΦ, monocytes, mΦ, DC, T cells	No reported function
$P2Y_6$	UDP (EC_{50}: 0.3 μM) >> UTP (EC_{50}: 6 μM) Expressed by nΦ, monocytes, mΦ, DC, T cells, microglial cells	Monocytes: Enhances CXCL8, IL-8 (138) and TNF-α secretion MΦ: Enhances NF-κB; enhances PGE_2 secretion Dendritic cells: Enhances CXCL8 secretion Microglial cells: Enhances phagocytosis (145)
$P2Y_{11}$	ATP (EC_{50}: 17 μM) Expressed by nΦ, monocytes, mΦ, DC, T cells, B cells	DC: Induces maturation; enhances chemotaxis; inhibits IL-12 and IL-27 secretion; induces IL-23, thrombospondin-1 (146) and indoleamine 2, 3-dioxygenase (146) secretion B cells: Promotes activation
$P2Y_{12}$	ADP (EC_{50}: 0.07 μM) Expressed by monocytes, mΦ, T cells, microglial cells, mast cells	MΦ: Promotes chemotaxis Microglial cells: Promotes chemotaxis (136) Mast cells: Promotes chemokine and prostaglandin D2 secretion
$P2Y_{13}$	ADP (EC_{50}: 0.06 μM) > ATP (EC_{50}: 0.26 μM) Expressed by monocytes, DC, T cells	No reported function
$P2Y_{14}$	UDP-glucose (EC_{50}: 0.1-0.5 μM) Expressed by nΦ, DC, T cells	No reported function

Purinergic receptors are expressed by virtually every cell type, including immune cells (37), although the subset of receptors expressed can be different between various cells. Thus purines can differentially regulate cellular function. Varying the concentration of particular extracellular purines can also differentially regulate cellular function, as each purinergic receptor has its own EC_{50} and preferred purinergic ligand. Many cell types also express plasma membrane-localized ectoapyrases such as CD39 and CD73; ectoapyrases can decrease the local

concentration of purines such as ATP by hydrolyzing ATP to adenosine monophosphate and adenosine, thus regulating purinergic receptor activation.

Purines can be released from cells passively (147). Cellular damage can result in compromised plasma membranes, which can allow for the passive release of intracellular content including purines. Purines such as ATP are normally harbored within cells at high concentrations, and once released can act in high local concentrations close to cells (148).

Purine release can also be actively induced. For instance, the activation of TLRs on myeloid cells can result in ATP release (149, 150). The activation of certain purinergic receptors such as $P2X_7$ or associated hemichannels such as pannexin 1 can result in ATP release as well (151). It is recently appreciated that upon cell death induced by UV light or Fas ligation, pannexin-1, an ion hemichannel capable of promoting large pore formation (i.e., promote membrane break-down to allow the entry of dyes such propidium iodide), is responsible for appreciable amounts of ATP and UTP release (152). From this study, UV or Fas activated caspase-3 and caspase-7 cleaved pannexin-1 to make it functional, to induce large pore formation that resulted in the release of purines.

Proteins and lipids are modified through purinergic signaling. In particular, $P2X_7$ initiates several of these modifications. Following PAMP stimulation of macrophages, activation of $P2X_7$ results in caspase-1 through the NLRP3 inflammasome (78). Cleavage by caspase-1 results in the non-conventional secretion of several proteins including pro-inflammatory cytokines IL-1β, IL-1α, IL-18, and fibroblast growth factor-2 (153). $P2X_7$ activation can also result in the release of other proteins such as HMGB1 (154), which may involve the inflammasome. $P2X_7$ activation can also stimulate various phospholipases (calcium dependent phospholipase A_2 [$cPLA_2$] (155),

calcium independent phospholipase A_2 [$iPLA_2$] (155), phospholipase D [PLD] (156)) that result in the cleavage of different lipid substrates such as phosphoinositols (PI) and phosphatidylcholine (PC). $P2X_7$ also promotes "phosphatidylserine (PS)-flip" (157) whereby the topology of PS is switched from associating with the cytosolic side of the plasma membrane to being exposed extracellularly by plasma membrane associated floppases.

Purinergic signaling has been studied in a variety of fields including neurology, hematology, osteology, and immunology (130). Purinergic receptors greatly influence neuropathic and inflammatory pain, platelet aggregation, bone generation, among several other functions. Several of the cells involved in these processes express multiple purinergic receptors.

Purinergic signaling can greatly modulate immune responses (37). In the context of ATP, there is a generalized spectrum of responses, where lower doses of ATP promote immunosuppression, and higher doses of ATP can promote inflammation (158). In this manner, the dose of ATP determines which purinergic receptor gets activated and thus which differential signal transduction pathways are initiated for various functions. It is also appreciated that ATP and UTP can serve as chemotactic agents to recruit myeloid-derived cells (139). The diversity and distribution of all of the known purinergic receptors in immune cells is listed in Table 6.

1.2.1 $P2X_7$-induced inflammation

Compared to the other purinergic receptors, $P2X_7$ could be argued to be the greatest inducer of inflammation. $P2X_7$ can promote pro-inflammatory cytokine and protease release from cells, and promote inflammatory forms of cell death, among several other inflammatory activities. $P2X_7$ is

expressed by several types of immune cells (37) (as noted in Table 6), and thus has global impacts on immunity. Additionally, $P2X_7$ expression is upregulated on classically activated macrophages, compared with other types of activated macrophages (159).

$P2X_7$ initiates NLRP3 inflammasome activity of PAMP activated macrophages and monocytes, which results in the generation and release of biologically active forms of the inflammatory cytokines IL-1β and IL-18 (78). The NLRP3 inflammasome is physiologically relevant given its role in protection against infections such as influenza A (83), and its hyperactivation in autoinflammatory diseases such as familial cold autoinflammatory syndrome and Muckle-Wells syndrome (89). ATP and $P2X_7$ themselves are highly physiologically relevant in terms of the inflammasome. Mutations of $P2X_7$ that decrease its function or $P2X_7$-deficient mice display decreased levels of IL-1β (160). Release of IL-1β is a crucial determining factor for neutrophil adherence at, and eventual recruitment to, sites of necrotic cell damage (40) and for the development of type IV hypersensitivity immune responses (161), both of which require ATP, $P2X_7$, NLRP3, and IL-1β. In the context of cancer, ATP released during chemotherapy can activate NLRP3 in a $P2X_7$-dependent manner in dendritic cells and the resulting IL-1β is required for the development of cytolytic CD8+ T cell cellular immunity (162). In the absence of chemotherapy induced ATP release, NLRP3 promotes tumor development through myeloid derived suppressor cell recruitment to tumors (163).

As a consequence of $P2X_7$ over-stimulation, cells can succumb to cell death. The context of $P2X_7$ engagement often dictates which form of cell death occurs; however, the form of cell death can be ambiguous. For instance, in the case of PAMP primed and inflammasome activated macrophages, it has been proposed that $P2X_7$ induces a caspase-1 mediated cell death called

pyroptosis (164). Alternatively, without the need for PAMP priming, T regulatory cells, which highly express $P2X_7$, readily undergo cell death in the presence of $P2X_7$ ligands (165); while not highly characterized in the aforementioned study, a closer look at $P2X_7$-induced lymphocyte cell death concluded that it was neither apoptosis nor necrosis, but rather a type of cell death that displays phenotypes of both (166). In the context of a live mycobacterial infection, THP-1 monocyte cell line undergoes autophagy in response to $P2X_7$ to induce bactericidal activities (167); while not discussed in this study, autophagy can disallow cell death or it can induce type II/autophagic cell death (168).

$P2X_7$ activation of macrophages promotes bactericidal activities. Most studies have dealt with mycobacteria as their bacterial load is readily controlled by $P2X_7$-activated macrophages (169). Mycobacteria normally reside within endosomes of phagocytes. Upon $P2X_7$ stimulation, macrophages undergo a process of endosome fusion with lysosomes, which then allows for the clearance of internalized mycobacteria (170). This process is mediated by phospholipase D (PLD) as $P2X_7$ induces PLD-mediated phagosome-lysosome fusion (170, 171). $P2X_7$-induced apoptosis of macrophages that had taken up mycobacteria has also been suggested as a mechanism for $P2X_7$-related bactericidal activities (172). Additionally, individuals carrying deleterious polymorphisms of $P2X_7$ are more susceptible to mycobacterial infection as their macrophages display decreased killing capacities (173). Furthermore, $P2X_7$ regulates phagocytosis (174).

$P2X_7$ promotes PLD to act as a strong regulator of lipid signaling that can exacerbate inflammation (as mentioned above). PLD exists in two isoforms: PLD1 and PLD2. The exact localization of these isoforms is disputed, but it is largely reported that PLD1 is found in the

Golgi apparatus, whereas PLD2 is localized at the plasma membrane (175). However, in response to stimuli, PLD1 can be active at the plasma membrane. For instance, PLD1 remobilizes to the plasma membrane to promote secretory granule exocytosis (176), which is a potential outcome of $P2X_7$ stimulation (177). PLD hydrolyzes PC to choline and phosphatidic acid (PA) (178), which directly contribute to cell signaling or be converted to other lipids. PA is localized at the plasma membrane and due to its ability to apply negative curvature of the plasma membrane, PA can promote differential recruitment of materials to the plasma membrane (178). Additionally, PA can directly bind to proteins such as phosphatidylinositol 4-phosphate 5-kinase, PKCε, and PLCβ (179). As a signaling intermediate, PA can be converted through further hydrolysis by $cPLA_2$ or $iPLA_2$ to lysophosphatidic acid (LPA) or to diacylglycerol (DAG) by lipid phosphate phosphohydrolases (180). LPA is cleaved off into the extracellular space, where it can bind to receptors found on the cell surface on numerous cell types. The hydrophobicity of DAG keeps it at the plasma membrane where it can promote the recruitment and activation of molecules like PKC (181). DAG can be converted to PC, PS, phosphatidylglycerol (PG), phosphatidylethanolamine (PE), and phosphatidylinositol (PI). Additionally, DAG can also be converted to arachidonic acid (AA), which serves a substrate for generation of eicosanoids (including prostaglandins and leukotrienes). Notably, LPA, AA, prostaglandins, and leukotrienes promote inflammation (182) and are products of ATP ligation of $P2X_7$ (183). $P2X_7$-induced alterations of lipids are illustrated in Figure 1-4.

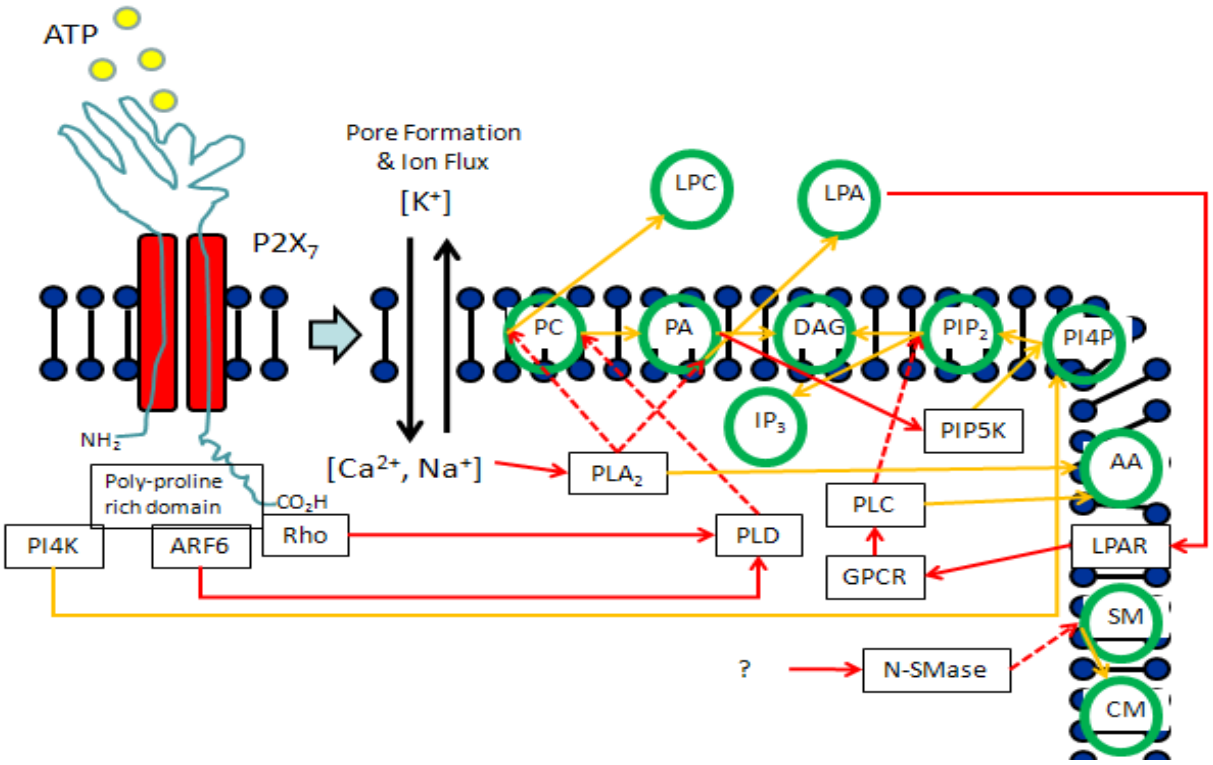

Figure 1-4: $P2X_7$ lipid signaling pathways.

ATP engagement of $P2X_7$ initiates the generation and modification of lipids. The carboxy-terminus of $P2X_7$ has several protein domains including a poly-proline-rich sequence that can recruit proteins with SH3 domains such as ADP-ribosylation factor 6 (ARF6), Rho family GTPases, and phosphatidylinositol 4-kinase (PI4K). PI4K generates phosphatidylinositol 4-phosphate (PI4P) from phosphatidylinositol (PI). ARF6 and Rho may activate phospholipase D (PLD) to produce phosphatidic acid (PA) from phosphatidylcholine (PC). PA can activate phosphatidylinositol 4-phosphate 5-kinase (PIP5K) to make phosphatidylinositol 4, 5-bisphosphate (PIP_2) from PI4P. Ion fluxes induce phospholipase A_2 (PLA_2) to produce lysophosphatidic acid (LPA) from PA, lysophosphatidylcholine (LPC) from phosphatidylcholine (PC), or aracidonic acid (AA). $P2X_7$ can also activate phospholipase C (PLC) via LPA activation of the GPCR receptor LPA receptor (LPAR); PLC induced cleavage of PIP_2 or lipid phosphate phosphohydrolase (LPP) conversion of PA can generate diacylglycerol (DAG). PLC also produces inositol trisphosphate (IP_3) and AA. $P2X_7$ can also activate neutral sphingomyelinase (N-SMase) for ceramide (CM) generation from sphingomyelin (SM). Solid red lines indicate activation. Dashed red lines indicate cleavage. Solid orange lines indicate lipid conversion. Question marks (?) indicate unknown causes.

$P2X_7$ biology has relevance for several inflammatory diseases. Arthritis is an inflammatory disease of the joint. Macrophages from rheumatoid arthritis patients display elevated inflammatory responses to ATP (perhaps due to hyperactive $P2X_7$ polymorphisms) compared to healthy individuals (184). Additionally, collagen-induced arthritis is significantly decreased in $P2X_7$ knock-out mice (185). Independent of the inflammasome and pro-inflammatory cytokines like IL-1β, $P2X_7$ activation results in the release of several proteases called cathepsins from macrophages (186); in an *in vitro* model of the extracellular matrix, these cathepsins were able to degrade collagen, an activity relevant to arthritis. ATP acting on $P2X_7$ on APCs can initiate the priming of naïve T cells for graft versus host disease (187). Alzheimer's disease is a neurological inflammatory disease potentiated by β-amyloid, which is able to induce ATP release from microglial cells (188). Alzheimer's progression is dependent upon $P2X_7$ (189). Atherosclerosis is another relevant $P2X_7$ influenced disease, as $P2X_7$ promotes the shedding of small lipid bilayer microparticles from dendritic cells that have coagulation properties (190); coagulation is one of the early steps towards generating the thrombogenicity of atherosclerotic plaques. Lastly, among several other examples of $P2X_7$ involvement in inflammatory diseases, abrogation of $P2X_7$ and ATP ameliorates the experimental autoimmune encephalomyelitis model of multiple sclerosis (191), a chronic degenerative disease of the central nervous system.

1.3 SECRETED LYSOSOME-RELATED ORGANELLES

The intracellular trafficking of cells dictates cellular survival and their potential to function in unique roles. Intracellular trafficking is also tightly linked to organelle biogenesis and the exocytosis of materials from cells. This section aims to detail the calcium-induced secretory granule (SG) activities of immune cells, highlighting the unique activity of secreting lysosome-related organelles (LRO) (i.e., secretory lysosomes).

Certain immune cells can traffic proteins within SG to several unique compartments and have various modes for their secretion from the trans-Golgi network (TGN) (192). SG are secreted through regulated pathways. The biogenesis of SG start from the TGN as immature granules (IG), following a specific initiating stimulus. The mechanism by which certain proteins are retained in IG is unclear (193). Sorting signals may direct proteins whereas IG form from the TGN. Alternatively, proteins that are not ultimately retained for matured SG may be lost from IG following IG formation from the TGN. SG are then able to be secreted to the plasma membrane, where their contents are released to the extracellular environment.

LRO are an unique type of SG for immune cells including cytolytic lymphocytes, antigen presenting cells, mast cells, and neutrophils (194). LRO are different from conventional SG in terms of biogenesis. The biogenesis of LRO involves a constitutive secretion step from the TGN to the plasma membrane. From the plasma membrane, immature LRO are recycled from the plasma membrane to early endosomes and eventually to multi-vesicular bodies (MVB). Unlike conventional lysosomes, which primarily serve for the degradation of macromolecules, LRO

fuse with the plasma membrane, allowing for the dispersion of their contents into the localized extracellular space.

The contents of LRO are similar to conventional lysosomes in their expression of hydrolases, cathepsins, and lysosome markers (e.g., Lamp-2) (194). Conventional lysosomes and LRO recruit similar proteins through shared lysosomal sorting signals (195). Some of these materials localize due to common dileucine (e.g., tyrosinase) or tyrosine-based signals on these sorted proteins but there are some non-common motifs. For instance, FasL, a common factor found within LRO generated from NK cells and cytolytic T cells to induce cell death of targeted cells, is instead localized to LRO due to polyproline-rich domains sandwiched between di-arginine and di-lysine residues (196). The non-conventional localization is not only amino acid-based; N-linked and O-linked glycosylation regulate LRO localization of TNF-α (197) and Syt I (198) respectively.

Conventional SG and LRO traffic to the plasma membrane in some conserved ways. Upon stimulation, microtubule based processes promote the migration of SG to the plasma membrane (194). This initial phase of migration through microtubules is calcium-independent but it can depend on protein tyrosine kinases Syk and Fyn (199) or the coat-adaptor complex AP-3 (200); Syk and Fyn may modulate microtubule nucleation, whereas the exact mechanism for AP-3 is a bit unclear. Rab GTPases, including Rab27a and Rab27b, connect with cell-type specific adaptors to transition SG from microtubules to the plasma membrane (201); this may occur by aiding in the tethering of SG to the plasma membrane to actin nucleation processes.

The fusion of SG to the plasma membrane involves SNAREs and synaptotagmins (Syts) (194). SNAREs include vesicle SNAREs (v-SNAREs) and target membrane SNAREs (t-

SNAREs). V-SNAREs include VAMP proteins. V-SNAREs are found on SG and they “zipper” into t-SNAREs at the plasma membrane to form trans-membrane complexes. T-SNAREs include syntaxins and SNAP-25 proteins, and the type of SNARE used for a given cell’s LRO exocytosis is cell-type specific. There are several different subsets of SG that possess different combinations of SNAREs (202); for example, one such combination commonly found in mast cells is VAMP-8 (v-SNARE) and SNAP-23 (t-SNARE) (203). Syts are also involved in efficient fusion of SG to the plasma membrane (194). Syts have an N-terminal domain, an intermediate transmembrane domain, and cytosolic tails that include C2 domains. C2A and C2B domains act via calcium-dependent and calcium-independent mechanisms to promote protein-protein interactions involved in membrane fusion. C2A enables Syt binding to phospholipids and syntaxins. C2B enables Syt binding to inositol polyphosphates and phosphoinositide polyphosphates ligands. Some common Syts are Syt I, Syt II, and Syt IV. Syt I potentiates LRO exocytosis in a calcium-dependent manner whereas Syt II retards its exocytosis. Syt II also in effect negatively regulates MHC class II surface expression. Syt VII is described as a calcium regulatory protein for promoting LRO exocytosis. Following fusion, NSF allows the disassocation of the SNAREs for efficient exocytosis.

There are numerous triggers for LRO exocytosis, but all are regulated through common mechanisms. For cytolytic lymphocytes, this would include calcium-driven pathways resulting from receptor engagement (194). For instance, TCR stimulation of cytolytic T cells with sufficient co-stimulation results in remobilization of their microtubule organizing centers (MTOC) and provides recruitment of their lytic granules towards a target cell. NK cells engage in strong LRO exocytosis upon antibody Fc-portion recognition by CD16. In a general sense for macrophages, LRO exocytosis is potentiated by stimuli that promote PKC and elevate lysosomal

pH (204). Such stimuli include zymosan, monensin, methylamine, and nigericin among others. ATP ligation of $P2X_7$ provokes LRO exocytosis from myeloid cells (177), mast cells (205), and rat submandibular glands (206).

LRO exocytosis is highly relevant in the field of immunology. Cytolytic responses are dependent upon LRO exocytosis for their function. Genetic diseases that display characteristic defects in LRO exocytosis include Chediak-Higashi syndrome, Hermansky-Pudlak syndrome 1, 2, and 3, and Griscelli's syndrome (207); individuals with these diseases display defects in cell-mediated immune responses. Cathepsins released from LRO also have significant roles in promoting inflammation (208). Cathepsins are a family of proteases including cysteine proteases (cathepsins B, C, F, H, K, L1, L2, O, S, W, and Z), serine proteases (cathepsins A and G), and aspartyl proteases (cathepsins D and E). Released cathepsins have notable roles in cancer, especially in context of substrate cleavage in the extracellular matrix (e.g., laminin and fibronectin), which promotes tumor metastasis (209). Extracellular cathepsins also have roles in exacerbating other inflammatory diseases such as arthritis, Alzheimer's, and stroke.

1.4 MICROVESICLES

Many cell types release to the extracellular space small membraneous vesicles called microvesicles (MV) (210). MV comprise membrane vesicles that are typically sized between either 100-1000 nm or 30-150 nm in diameter. MV are also derived from a variety of cellular sources including from the plasma membrane or from internal compartments. The material that MV contain depends on the cell of origin, the cellular compartment that they originate, and the stimuli that promotes their generation.

Among the best described MV are exosomes (210). Exosomes are 30-150 nm diameter in size lipid bilayer vesicles derived from MVB. Exosomes are thus among the types of MV that are derived from internal cellular sources. MVB are a class of organelles involved in endosome maturation that typically results in the transport of materials to lysosomes; however, some cell types can instead deliver these materials at times to the plasma membrane. Often, exosomes are generated constitutively from healthy cells; however, exosomes can be released by stimuli such as ATP, via $P2X_7$ expressed on myeloid cells (211). Some of the cell types that are efficient producers of exosomes include B cells and dendritic cells, although the spectrum ranges to non-immune cells such as platelets, tumor cells, and epithelial cells among several others. Markers of exosomes can vary depending on the cell type of origin, but exosomes can be identified with expression of ESCRT machinery proteins (e.g., Alix and TSG101) and tetraspanin proteins (e.g., CD81 and CD9) (212). Classical markers also include MHC class II and Lamp-2, although these are not uniquely expressed by exosomes. The materials within exosomes (i.e., their cargo) include several different types of proteins, lipids, DNA, and RNA (including microRNA).

Exosomes originate from MVB (212), which consist of several intraluminal invaginations that eventually bud off to form intraluminal vesicles (ILV). These invaginations have been shown to contain non-specific cytoplasmic proteins (through passive engulfment), ESCRT (endosomal sorting complexes required for transport) machinery and related proteins, co-sorting lipids (often through GPI [glycosylphosphatidylinositol] anchors) and protein (often through tetraspanins or other chaperones). Since they are unique exosome markers, it is generally thought that Alix and TSG101 serve significant roles in preferentially loading materials into these ILV (213). GPI anchors have been implicated in part because exosomes are enriched with dense lipid-raft microdomains and associated proteins such as tetraspanins (214).

Exosomes are generated and eventually secreted from MVB that deviate away from fusing with lysosomes (212). MVB can be trafficked to fuse with lysosomes (for cargo degradation), recycle their material back to the cytosol, or fuse with the plasma membrane for exosome release. How MVB engage in directed migration to the plasma membrane is not fully understood. Several analogies have been made to secretory lysosomes. Rab11 has been implicated in efficient exosome secretion (215); however, it is not fully understood whether it acts primarily in the exosome biogenesis phase to generate ILVs or to differentially present cargo, such as lipids, that better facilitate membrane fusion events. Once at the plasma membrane though, it is believed that MVB fuse with the plasma membrane, similar to secretory lysosomes, through the activities of SNARE proteins and synaptotagmins (216). At present time, the most convincing evidence for SNARE involvement is indirect; exosome secretion is sensitive to inhibition of calcium-driven pathways and it is known that SNARE proteins and synaptotagmin family membranes are modulated in part by calcium.

There are a variety of non-exosome MV. Several of these MV are derived from the plasma membrane but some types are derived from intracellular compartments that are not MVB (210). MV derived from the plasma membrane include “plasma-membrane derived MV”, which are typically 100-1000 nm in diameter, and microparticles (aka ectosomes), which are typically 30-150 nm in diameter. Smaller sized (30-150 nm in diameter) MV can also be shed from non-MVB compartments such as endosomes that are released through the plasma membrane to the extracellular space. The phenotypic markers for different types of MV are mostly revealed according to their origin (e.g., plasma derived MV express plasma membrane markers); however, there are not uniquely identified markers that are only expressed by these MV as is the case with exosomes.

Plasma-membrane derived MV are often induced through stimuli that promote calcium-driven pathways (210). Notable examples include $P2X_7$ stimulation of myeloid cells and neutrophils (217), thrombin-receptor activation of platelets (218), and TLR4 ligation on dendritic cells (219). The lipid topology at the plasma membrane is primarily governed by membrane pumps called flippase (cytofacial-directed), floppase (exofacial-directed), and scramblase (bi-directional), which are localized within lipid rafts domains in the plasma membrane (220). Heightened levels of intracellular calcium can result in the inhibition of flippase, which results in phosphatidylserine exposure on the outer-leaflet of the plasma membrane. Calcium promotes floppase and scramblase. While floppase and scramblase are not specific for particular lipids, they randomize lipid distribution and promote membrane asymmetry. It is speculated that this loss of membrane asymmetry is required for the shedding plasma membrane-derived MV (221). It is observed downstream of $P2X_7$ stimulation (157). Additional calcium-dependent effectors

reported to be required for plasma membrane-derived MV include calpain (222), calcium-dependent and potassium channels (for potassium efflux) (223).

MV can interact with various cell types through a variety of mechanisms. Due to the presence of adhesion molecules including tetraspanins, exosomes can directly bind to surface receptors found on several cells (212). For instance, exosomes expressing ICAM-1 can engage LFA-1 expressing CD8+ DC and activated T cells (224). Phosphatidylserine found on both exosomes and plasma-membrane derived MV is recognized by TIM1 and TIM4 found on Th2 skewed T cells and phagocytes, respectively (225). Following this receptor engagement, the exact following mechanisms are a bit unclear. Some suggest that MV may fuse with the plasma membrane of the recipient cell (219). There is also evidence of receptor mediated endocytosis, where MV are trafficked into endosomes or, in the case of larger MV, the uptake can be mediated by phagocytosis (212). Regardless of how the MV are handled after initial receptor interactions, MV materials can remain on the plasma membrane, enter into the cytosol, or reach late endosomes where they can affect the recipient cell's behavior.

MV have several mechanisms to initiate immune responses (212). Most are related to the type of cargo that they carry or express outwardly from their membrane. These mechanisms can also either be direct (i.e., the MV can express materials that directly bind to target cells to initiate a response) or indirect (i.e., MV-contained cargo is further manipulated by some cell type that takes up the MV and in turn that cell initiates a target cells for a response). For instance, MV can outwardly express NK cell activating and inhibitory receptor ligands that can modulate NK cell function (226, 227). Myeloid cell activation (228), myeloid cell immunosuppression (229), and myeloid cell activation indifference (230) are also possible from various MV settings. Cellular

modulation may be imparted not only through outwardly expressed ligands or receptors but also possibly through other proteins, lipids, and nucleic acids including microRNAs (210). Various mechanisms for MV-induced immune cell modulation are detailed in Table 7.

Table 7: MV-induced modulation of immune cells. Data are compiled from (210) unless indicated.

MV Type and Source	Inducer	Cargo or Induced Modulating Factor	Modulated Immune Cell	Immunological Function
Tumor-derived MV	Constitutive	Tumor-derived antigens	Professional antigen presenting cells, antigen-specific T cells	Adaptive immune responses against tumors
	Constitutive	CD95L and galectin-9	T cells	Apoptosis
	Constitutive	TGF-β	Regulatory T cells	Activation for immunosuppression
	Constitutive	TGF-β	Cytolytic T cells and NK cells	Impaired activation (decreased cytotoxicity)
	Constitutive	TGF-β	Myeloid cells	Generation of myeloid-derived suppressor cells
	Constitutive	Phosphatidylserine	Macrophages	Immunosuppression via TGF-β secretion (231)
	Heat shock stress response	HSP70	NK cells	NK cell activation
	Heat shock stress response	HSP70	Macrophages	TNF-α secretion
	Constitutive	HSP72	Myeloid-derived suppressor cells	Activation for immunosuppression (232)
	Constitutive	NKG2D	NK cells	NK cell inhibition
	Constitutive	Surface determinants, mRNA	Monocytes	Release of cytokines
Dendritic cell-derived MV	Constitutive	Peptides + MHC	Antigen specific CD8+ or CD4+ T cells	T cell activation
	Heat shock stress response	BAT3	NK cells	NK cell activation

Table 7 (continued)				
	Constitutive	UL16, MICA, MICB	NK cells	NK cell activation
	Constitutive	IL-15Rα	NK cells	NK cell activation
	Constitutive	TNF-α	Epithelial cells	Release of pro-inflammatory factors (233)
T cell derived MV	Activation	CD95L	T cells	Apoptosis (activation induced cell death)
	Constitutive	CD95L	DC	Apoptosis (234)
	HIV infection	Nef	CD4+ T cells	Apoptosis (235)
Neutrophil derived MV	Activation	Phosphatidylserine	Macrophages, DC	Immunosuppression (reduced cytokines)
Macrophage derived MV	$P2X_7$ activation	Phospholipids	Macrophages	Induction of pro-inflammatory cytokines & co-stimulatory markers (236)
	$P2X_7$ activation and mycobacterial infection	MHC class II + mycobacterium peptide antigen epitope	Antigen-specific CD4+ T cells	T cell activation (237)
Platelet-derived MV	Thrombin-induced activation	CD154	B cells	B cell activation
	Thrombin-induced activation	CD154	Monocytes	Release of cytokines
	Thrombin-induced activation	Phosphatidylserine	Phagocytes	Induction of phagocytosis
Reticulocyte-derived MV	Maturation to erythrocytes	Galectin-5	Macrophages	Induction of phagocytosis (238)
Fibroblast-derived MV	Constitutive	Membrane-bound TNF	T cells	Resistance to apoptosis by activation induced cell death
Placenta-derived MV	Constitutive	NKG2D	NK cells	Inhibition of NK cell activation
Leishmania-derived MV	“Infection-like stressors”	Leishmania components	Macrophages	Release of IL-8 (239)

The activities of MV-derived materials can promote either inflammation or immunosuppression (210). As mentioned, MV can promote immune cell activation or

inactivation, but some of these measures are achieved less directly. For instance, MV can regulate the survival of cells that they engage – either promoting survival or more often inducing apoptosis. FasL can be expressed on MV shed from dendritic cells, which could engage Fas on T cells to induce their apoptosis (240). Conversely, TNF-α on MV from fibroblasts of rheumatoid arthritis individuals interferes with activated T cell-induced apoptosis (241).

MV notably promote antigen-specific responses in both direct and indirect manners. For the direct response, MV have been shown to outwardly express MHC class I and II plus antigenic peptides to activate CD8+ and CD4+ T cells, respectively (242). In addition to MV alone activating T cells for an antigen-specific response, antigen presenting cells such as dendritic cells can capture MHC+peptide containing MV such that the MHC+peptide from the MV is transferred onto the plasma membrane of the recipient dendritic cell; these transferred intact MHC+peptides can then engage T cells for their activation (12). As MV can be derived from MVB (e.g., exosomes), which contain a large supply of MHC class II (212), MV can increase the recipient dendritic cells antigenic machinery for increased levels of MHC. Exosomes may also increase dendritic cell plasma membrane levels of co-stimulatory ligands to enhance antigen-specific responses from T cells (12). This process of receiving transferred MHC+peptides has been termed semi-direct presentation or “cross-dressing” (243). For the indirect response, dendritic cells can endocytose/phagocytose exosomes. In this manner, dendritic cells can process antigens from exosomes and place them within the dendritic cell’s endogenous MHC molecules to activate both CD8+ and CD4+ T cells through antigen cross-presentation and antigen presentation, respectively (244).

1.4.1 $P2X_7$ as an instigator of shed microvesicles from myeloid cells

$P2X_7$ has been reported to promote the shedding of plasma membrane derived MV and exosomes from myeloid cells (211, 217, 245). $P2X_7$ directly binds to several components of actin-related machinery, which can result in topological and compositional changes of the plasma membrane (246). Though the mechanism has yet to be elucidated, $P2X_7$-driven calcium pathways rapidly promote MV shedding from the plasma membrane (217). The mechanisms of MV induced shedding is unclear, given that $P2X_7$ also promotes membrane blebbing, which some have suggested to be the source of shed MV (217), whereas others have refuted the notion (211, 247).

$P2X_7$-induced MV from TLR-primed myeloid cells contain mature IL-1β (211, 217, 245, 247); however, the exact type, source, and content of these MV are disputed (248). It was originally reported that mature IL-1β is secreted within larger 1 μm diameter MV shed from the plasma membrane (217). The Dubyak group noted that larger sized plasma membrane MV, derived in response to $P2X_7$ stimulation of TLR-primed macrophages, do not require NLRP3 inflammasome activation, and likely do not contain IL-1β (211, 246). Instead, IL-1β is released in exosomes. For exosome exocytosis, NLRP3, but not caspase-1, is required. $P2X_7$-induced MV are shed from both TLR-primed and non-primed cells (246, 249); however, the biological activities of these MV have not been evaluated. It is speculated though that $P2X_7$-induced MV released from dendritic cells may have thrombotic activities (regardless of initial PAMP-priming), as these MV contain membrane-bound tissue factor, a blood coagulant factor relevant for diseases such as atherosclerosis (250).

1.5 MISSION STATEMENT FOR THESIS WORK

Inflammation is a complex biological process. Inflammation occurs not just through the recognition of foreign particles but it is also can occur in response to endogenously derived materials. In addition, inflammation is not strictly driven by soluble mediators. While significant progress has been made towards identifying several inflammatory mediators and their activating receptors, there are details left unresolved. Sterile inflammation is an emerging area in immunology and its interplay with chronic diseases such as atherosclerosis and arthritis is becoming increasingly important as disease incidence is rising.

Damaged cells promote high local concentrations of ATP that can activate purinergic receptors for modulating inflammation. At higher concentrations, ATP promotes inflammation. From PAMP-activated or pro-inflammatory cytokine stimulated myeloid cells, ATP ligation of $P2X_7$ engages NLRP3 inflammation for IL-1β and IL-18 release. IL-1β in particular has immense activities for inflammation from a vast diversity of cells (due to wide-spread expression of IL-1 receptor). Thus ATP, NLRP3, and $P2X_7$ have several roles in promoting inflammatory diseases. $P2X_7$ also has inflammatory roles outside of the NLRP3 inflammasome including the release of stimulatory lipids and the extracellular matrix-degrading cathepsins.

Because of the relevance of $P2X_7$ in inflammation, our lab has sought to further understand its mechanisms including potential inflammasome independent activities that might promote inflammation. It has been noted for several years that $P2X_7$ promotes MV shedding; in most studies, it is suggested that MV shedding serves as a mechanism for IL-1β secretion from inflammasome-activated myeloid cells. At the same time, PAMP or pro-inflammatory cytokine

priming of myeloid cells is not a necessary component for efficient MV shedding, prompting me to hypothesize that MV, in the absence of cytokine cargo, have the capability to activate macrophages for pro-inflammatory cytokine release and upregulation of antigenic machinery (e.g., upregulation of surface expression of co-stimulatory markers and MHC class II). To test this hypothesis, I generated $P2X_7$-induced MV and evaluated macrophage activation (as described above) paying close attention to uncovering activation signal transduction pathways and potential novel stimulatory materials from harvested MV. I also hypothesized that $P2X_7$ promotes the redistribution stimulatory materials, including cathepsins, through actin-dependent mechanisms, including possibly tying into how MV are shed from cells. To test this hypothesis, I characterized various MV populations and visually assessed global cytoskeletal alterations in response to $P2X_7$ stimulation for the ability to stimulate macrophage activation and/or to remobilize stimulatory materials.

2.0 ACTIVATION OF MACROPHAGE BY $P2X_7$-INDUCED MICROVESICLES FROM MYELOID CELLS IS MEDIATED BY PHOSPHOLIPIDS AND IS PARTIALLY DEPENDENT ON TLR4

2.1 AUTHORS AND THEIR CONTRIBUTIONS

This study was published in the *Journal of Immunology* in the September 15th issue, vol. 185, pp. 3740-3749. Copyright permission to reprint the published study was obtained from the *Journal of Immunology*. *Copyright 2010. The American Association of Immunologists, Inc.* Some additional unpublished data was added for Figure 2-6, Figure 2-12, and Figure 2-13; there is an expanded *Materials and Methods* to explain the procedures for these experiments. L. Michael Thomas (Graduate Program in Immunology, University of Pittsburgh School of Medicine, Pittsburgh, PA) designed and performed the experiments and prepared the manuscript; his funding was supported by an NIH training grant T32CA082084. Russell D. Salter (Department of Immunology, University of Pittsburgh School of Medicine) designed the scope of the study and prepared and edited the manuscript; his funding was supported by NIH funds R01AI072083 and P01CA073743. Dewayne H. Falkner received acknowledgement for his assistance in using the BD Biosciences FACSAria. Judong Lee and Sudesh Pawaria assisted in using a luminometer. Michelle E. Heid, Jessica Chu, Peter A. Keyel, and Chengqun Sun provided helpful discussions and cell culture assistance. Judson M. Englert provided helpful discussions and reagents. Laura E. Kropp provided critical reading of the manuscript. Lastly, various contributors provided reagents including murine bone marrow and cell lines, which are discussed and acknowledged within the *Materials and Methods*.

2.2 ABSTRACT

ATP-mediated activation of the purinergic receptor $P2X_7$ elicits morphological changes and pro-inflammatory responses in macrophages. These changes include rapid shedding of microvesicles (MV), and the non-conventional secretion of cytokines, such as IL-1β and IL-18 following priming. In this study, I demonstrate the activation potential of $P2X_7$-induced MV isolated from non-primed murine macrophages. Co-treatment of non-primed macrophages with ATP and calcium ionophore induced a rapid release of MV that were predominantly 0.5-1 μm in size. Exposure of primary murine bone marrow-derived macrophages to these MV resulted in co-stimulatory ligand upregulation and TNF-α secretion. Cell homogenates or supernatants cleared of MV did not activate macrophages. MV-mediated activation was p38 MAPK and NF-κB-dependent, and partially dependent on TLR4 activity, but was high-mobility group box 1 independent. Biochemical fractionation of the MV demonstrated that the phospholipid fraction, not the protein fraction, mediated macrophage activation through a TLR4 dependent process. $P2X_7$ activation is known to induce calcium independent phospholipase A_2, calcium dependent phospholipase A_2, and phospholipase D activities, but inhibition of these enzymes did not inhibit MV generation or shedding. However, blocking phospholipase D activity resulted in release of MV incapable of activating recipient macrophages. These data demonstrate a novel mechanism of macrophage activation resulting from exposure to MV from non-primed macrophages, and identifies phospholipids in these MV as the biologically active component. I suggest that phospholipids delivered by MV may be mediators of sterile inflammation in a number of diseases.

2.3 INTRODUCTION

Released microvesicles (MV) mediate intercellular communication between multiple cell types, and affect cytokine secretion, inflammatory processes, and tumor progression (251). MV can be released from intracellular storage sites or shed directly from the cell surface. Release of plasma membrane-derived MV is typically regulated by intracellular Ca^{2+} mediated processes (245, 252), or by protein kinase B (253) or protein kinase C (254, 255), and may involve engagement of a number of cell type specific receptors. Shedding typically involves a budding process, in which surface blebs selectively accumulate cellular constituents that are then packaged into MV. In contrast, MV derived from inside cells include secretory lysosomes (256-258), characterized by expression of lysosomal proteases, and exosomes (210, 251), which are stored in multivesicular bodies before being released by an active exocytic process.

In macrophages and other myeloid cells, engagement of $P2X_7$ purinergic receptors triggers the release of MV derived from both inside the cell (211, 257, 259) and from the plasma membrane (190, 217, 245, 252, 260). Secretion of IL-1β mediated by $P2X_7$ was suggested to occur through the release of cell surface derived MV many years ago (217), but the content of these MV is still unclear. A more recent study suggests that the majority of IL-1β containing MV may be exosomes, as opposed to larger shedding vesicles (211). Members of the IL-1 family (IL-1α, IL-1β, and IL-18) are stored as inactive precursors and their release after processing can be MV-mediated (211, 217, 245, 252), but this does not exclude other mechanisms of secretion (164, 261, 262). In any case, rapid secretion of mature IL-1β requires the Nod-like receptor family, pyrin domain containing 3 (NLRP3) inflammasome, which recruits caspase-1, allowing

cleavage of the pro-form of the cytokine to its bioactive form (34). Some exosomes from macrophages contain MHC class II and their exocytosis requires the NLRP3 inflammasome despite being caspase-1 independent (259). Less clear is the requirement for NLRP3 in controlling the $P2X_7$-dependent release of secretory lysosomes (257) although their exocytosis from human monocytes is caspase-1 independent.

Macrophages and other cells of the phagocytic lineage bind and internalize MV from various sources, with diverse effects on their function (210). Human monocytes binding tumor-derived MV become activated, expressing increased HLA-DR, reactive oxygen species, and TNF-α through a CD44-dependent mechanism (263). In another study, human tumor-derived MV promoted differentiation of CD14+ myeloid cells, resulting in an $HLA\text{-}DR^{low}$ phenotype. These cells also lacked CD80 and CD86 expression, and secreted TNF-β, TGF-β, and IL-6, with suppressive effects on T cell proliferation (264). Less is known about the potential immune stimulatory effects that macrophage-derived $P2X_7$-induced MV may exert, which could involve IL-1β.

To address this question, I induced MV shedding from non-primed mouse primary macrophages or cell lines through $P2X_7$ activation, and tested purified MV for their ability to activate bone marrow derived macrophages (BMDM). I found that MV were able to activate BMDM in a partially TLR4-dependent manner and that the stimulatory component within the MV was found within phospholipid fractions. MV derived phospholipids activated macrophage through TLR4. Furthermore, MV induced activation is independent of observed loaded cargo such as IL-1β, TNF-α, and high-mobility group box 1 (HMGB1).

2.4 MATERIALS AND METHODS

Cell culture and reagents - J774A.1 (TIB-67™; American Type Culture Collection, Manassas, VA), a murine macrophage-like cell line, and D2SC-1, a murine splenic derived immature dendritic cell (DC) line (a gift from L. Kane, University of Pittsburgh) were maintained in DMEM (Mediatech, Manassas, VA) supplemented with 10% FBS (Gemini Bio-Products; West Sacramento, CA), 1% additional L-glutamine (Lonza, Basel, Switzerland), and 1% penicillin and streptomycin (Lonza) (hereafter called DMEM complete). FSDC, a murine fetal skin derived immature DC line (a gift from Paula Ricciardi-Castagnoli, Singapore Immunology Network, Singapore), and THP-1, a human monocyte cell line (American Type Culture Collection), were maintained in IMDM (Lonza) supplemented with 10% FBS, 1% additional L-glutamine, and 1% penicillin and streptomycin (hereafter called IMDM complete). For experiments, THP-1 cells were treated with 20 μM PMA for 2 d to differentiate them to become more macrophage-like. RAW264.7 murine macrophage cell line transfected with NF-κB reporter plasmid pNF-κB-MetLuc Vector (BD Clontech, Mountain View, CA) encoding inducible *Metridia* luciferase protein expression and secretion was a gift from R. Binder (University of Pittsburgh) and was maintained in DMEM complete supplemented with 500 μg/ml G418. Murine bone marrow derived macrophages (BMDM) were derived from C57BL/6 bone marrow (gift from L. Borghesi, University of Pittsburgh) and were differentiated with L-cell supplemented media as described previously (265). $TLR4^{-/-}$ mouse bone marrow (266) was a gift from R. O'Doherty (University of Pittsburgh). $RAGE^{-/-}$ mouse bone marrow (267) was a gift from T. Oury (University of Pittsburgh). All knock-out mouse bone marrow described were of the C57BL/6 background.

Other reagents include AACOCF3 (Cayman Chemical, Ann Arbor, MI), ATP (Thermo Fisher Scientific; Waltham, MA), A23187 (Sigma-Aldrich, St. Louis, MO), A 438079 (Tocris Bioscience, Ellisville, MO), A 740003 (Tocris Bioscience), brefeldin A (Sigma-Aldrich), SB203580 (EMD Chemicals, Gibbstown, NJ), BATPA/AM (EMD Chemicals), bromoenol lactone (BEL; Enzo Life Sciences, Farmingdale, NY), bisindolylmaleimide I HCl (BIM; EMD Chemicals), Ki16425 (Cayman Chemical), MDL-12330A (Enzo Life Sciences), H-89 2HCl (EMD Chemicals), CAY10593 (Enzo Life Sciences), CAY10594 (Enzo Life Sciences), bromoenol lactone (BEL; Enzo Life Sciences), LPS from *Escherichia coli* 026:B6 (Sigma-Aldrich), poly(I:C) (Sigma-Aldrich), synthetic monophosphoryl lipid A (MPLA; InvivoGen, San Diego, CA), Pam_3CSK_4 (InvivoGen), *Limulus* amebocyte lysate QCL-1000 (Lonza; used according to manufacturer's protocol to assess endotoxin levels), and soluble RAGE (267) was a gift from T. Oury.

Yo-Pro-1 uptake by cells - To measure $P2X_7$-induced large pore formation, 1 x 10^6 J774A.1 were treated with or without 100 µM A 740003 for 15 min before exposure to ATP and were then stained with 5 µM Yo-Pro-1 (Invitrogen, Carlsbad, CA) on ice. Cells were kept on ice until flow cytometric analysis using FITC settings, which are similar to manufacturer's protocols for the dye. Flow cytometry was performed with a BD Biosciences LSR II and results were analyzed using FlowJo software (Tree Star, Inc., Ashland, OR).

MV generation and harvest - J774A.1 and other myeloid cell types were plated in T225 cm^2 flasks in duplicate per treatment. Where indicated cells were labeled with biotin using EZ-Link Sulfo-NHS-SS-Biotin reagent (Thermo Scientific) for 30 min using the protocols supplied by the manufacturers. Cells were washed twice with PBS before adding inhibitors in serum-free

DMEM with no additions. Cells were then treated with 3 mM ATP and 10 μM A23187 in a final volume of 20 ml serum-free DMEM with no additions for 30 min at 37°C. Supernatant was harvested and centrifuged at 309.1 x *g* for 10 min at 4°C to remove cells and larger debris. MV were collected by centrifugation at 100,000 x *g* ultracentrifugation for 1 h at 4°C. The pellet material from the 100,000 x *g* ultracentrifugation was resuspended in 500 μl of PBS. MV were disrupted with 10 passes through a 27 gauge needle. Bradford assay (Thermo Fisher Scientific) was used to determine the protein concentration with each MV fraction according to manufacturer's specifications. MV were either used immediately or stored at -20°C for later use.

For biochemical fractionation of MV, proteins and lipids were separated through the Bligh and Dyer method of protein/lipid extraction with 1:2 of chloroform and methanol (268). The protein fraction was harvested at the biphasic interphase and reconstituted in PBS. The lipid fraction was either dried by speed vacuum centrifugation or further separated through a lipid polarity extraction technique (269). Lipid extract was passed through a silicic acid (Sigma-Aldrich) column (1 mg silicic acid per 1 μl vol lipid extract). The pass through was collected as a sample. Bed layer volumes of chloroform, acetone, and then methanol were passed in sequential and separate fashion to elute off potential neutral lipids, glycolipids/sulpholipids, and phospholipids respectively. Samples were harvested from each elute, dried with speed vacuum centrifugation, and stored at -20°C.

Generating cell homogenate - Ten million J774A.1 were washed twice in PBS, pelleted and resuspended in homogenization buffer (100 mM KCl, 25 mM NaCl, 2 mM $MgSO_4$, 12 mM sodium-citrate, 10 mM glucose, 25 mM HEPES [N-2-hydroxyehylpiperazine-N'-2-ethanesulfonic acid], 5 mM ATP, 0.35% BSA [pH 7.0]) supplemented with protease inhibitor

mixture (Sigma-Aldrich). Cells were lysed through four cycles of freeze-thawing and homogenized with 30 strokes within a tight-fitting dounce homogenizer. The homogenate was then ultracentrifugated at 100,000 x *g* for 1 h at 4°C. Resulting pellets were resuspended in 500 µl PBS, and then homogenized with 10 passes through a 27 gauge needle. Samples were used immediately or stored at -20°C.

Measuring activation of treated BMDM - BMDM (wild-type [WT] or knock-out derived where indicated) were harvested following differentiation and plated at 1 x 10^6 cells/ml in IMDM complete (unless described differently) in petri dishes. Inhibitors where indicated were applied for at least 30 min prior to exposure to MV or other compounds, and were maintained throughout the experiment. Supernatants were tested for TNF-α ELISA (eBioscience, San Diego, CA), IL-12p70 ELISA (eBioscience), or IL-23 ELISA (eBioscience) according to manufacturers' protocols.

For flow cytometry studies to determine viability and expression of activation markers, cells were blocked with 1.5% normal goat serum diluted in 0.1% BSA in PBS for 20 min then stained with allophycocyanin anti-CD80 (BD Biosciences, San Jose, CA), PE anti-CD83 (BD Biosciences), FITC anti-CD86 (BD Biosciences), allophycocyanin anti-CD86 (BD Biosciences), or PE anti-I-A^b (BD Biosciences) Abs for 40 min. Cells were stained with 1 µg/ml DAPI (Sigma-Aldrich) viability dye. Flow cytometry was performed with a BD Biosciences LSR II and results analyzed using FlowJo software. MFI and population percentages of FITC, PE, and/or allophycocyanin were calculated for DAPI negative cell populations (i.e., living cells), which were >85% of the total cell population for all results and treatments shown in this work.

RAW264.7 NF-κB reporter assay - RAW264.7 macrophages stably transfected with pNF-κB-MetLuc Vector (BD Clontech) under G418 selection were plated as 1 x 10^6 cells/ml of DMEM complete for each treatment. Supernatant following treatment was centrifuged at 10,000 x *g* for 10 min and was then stored at -20°C until used to assay for luciferase activity according to manufacturer's protocol (BD Clontech). Luminescence readings from each sample were read with an Orion microplate luminometer (Berthold Detection Systems, Huntsville, AL) in duplicate and the average was taken using Simplicity version 2.1 software (Berthold Detection Systems). Average readings and SEM were calculated according to the ratio of fold change over non-treated cells at each respective time point of the time course.

Western blotting - For whole-cell culture supernatant studies, 2 x 10^6 J774A.1 were plated in 1 ml of DMEM complete with or without 1 μg/ml of LPS for 4 h. Cells were washed once with serum-free DMEM with no additions, and treated with or without 3 mM ATP and 10 μM A23187 for 30 min. Supernatants were centrifugated at 10,000 x *g* for 30 s and proteins were precipitated through a TCA/cholic acid procedure (265) before loading onto a 9% SDS-PAGE gel. SDS-PAGE and protein transfer to 0.45-μm polyvinylidene difluoride transfer membrane were performed as previously described (265).

For Western blot analysis of whole-cell lysates for phosphorylated and total p38 expression, 1 x 10^6 BMDM were plated with or without 1 μg/ml LPS or 25 μg protein equivalents/ml J774A.1 derived MV for 2, 10, 30, or 60 min. Following the time course, cells were washed once with PBS and then given 100 μl of 1% Triton X-100 lysis buffer in the presence of protease inhibition mixture (Sigma-Aldrich) and phosphatase inhibition (Sigma-

Aldrich) for 15 min on ice. Lysates were collected and centrifuged at 10,000 x *g* for 10 min at 4°C before addition of sample buffer and loading onto 11% SDS-PAGE gels.

Western blot was performed using the SNAP-ID according to manufacturer's procedures (Millipore, Billerica, MA). Abs for Western blotting included 0.5 µg/ml mouse anti-HMGB1 Ab (Abcam, Cambridge, MA), 0.1 µg/ml rabbit anti-phospho-p38 (Thr^{180}/Try^{182} epitope) (Millipore), 1:2,000 diluted rabbit anti-p38 (Poly6224; BioLegend, San Diego, CA), 1/1666.7 diluted HRP-conjugated goat anti-mouse IgG (Santa Cruz Biotechnology; Santa Cruz, CA), and 1/1666.7 diluted HRP-conjugated donkey anti-rabbit IgG (BioLegend). Signals were developed using Western blotting luminol reagent (Santa Cruz Biotechnology). Imaging was performed with KODAK Image Station 4000MM and its accompanying KODAK MI SE Software Informer (Carestream Molecular Imaging, New Haven, CT). In some instances, the membrane was stripped for Western blot reprobing with Restore Western blot stripping buffer (Thermo Fisher Scientific), according to manufacturer's protocols.

Biotinylation and Cy5 labeling of MV and uptake by BMDM - MV were labeled with biotin or Cy5 using EZ-Link Sulfo-NHS-SS-Biotin reagent (Thermo Scientific) or monoreactive Cy5 dye (GE Healthcare, Piscataway, NJ), respectively for 1 h in the 500 µl PBS reconstitution using the protocols supplied by the manufacturers. An additional wash with PBS followed by ultracentrifugation at 100,000 x *g* for 1 h at 4°C was used to remove non-conjugated biotin or Cy5 reagent. Sizing of MV was performed with BD Biosciences FACSAria with various sized YG beads (Polysciences, Warrington, PA).

For assessing MV association with recipient BMDM, 1 x 10^6 BMDM were plated on 12-mm poly(d-lysine)-coated coverslips in petri dishes. Cells were allowed to adhere for at least 4 h.

Indicated amounts of Cy5-labeled or biotinylated MV were given to the BMDM for varying times. Cells not associated to the coverslips were harvested and processed for FACS analysis of CD86 and biotin/Cy5 label. For some experiments, coverslip associated cells were further stained with 5-chloromethylfluorescein diacetate (CMFDA) as a cytoplasmic counterstain (Invitrogen) and LysoTracker Red to label lysosomal compartments (Invitrogen), according to manufacturer's protocols. Coverslips were then washed, 2% paraformaldehyde (PFA) fixed, then permeabilized and blocked with 0.5% saponin, 1.5% normal goat serum, and 1% BSA in PBS for 30 min. Alexa647 conjugated streptavidin (Invitrogen) and FITC-anti-CD86 (BD Biosciences) were used at 1/100 dilution for 1 h to visualize biotin and CD86 expression respectively. After successive washes, the coverslips were stained for nuclei with 1 µg/ml DAPI and then mounted with gelvatol. Confocal microscopy images were taken with an Olympus Fluoview 1000 (Inverted) and accompanying software (Olympus America Inc., Center Valley, PA). Laser excitations and emissions were performed sequentially for DAPI, Cy5/Alexa647, LysoTracker Red, and FITC/CMFDA and background noise was minimized. Differential interference contrast microscopy images for each field of view were also taken. Final images were then directly exported to Adobe Photoshop CS2 (Adobe, San Jose, CA).

Liposomes – Artificial liposomes mixtures were generated as follows: Control liposomes (Con. Lipo) with 20% cholesterol (chol.) (Sigma-Aldrich), 10% phosphatidylserine (PS) (Cat.# 840032C; Avanti Polar Lipids, Alabaster, AL), 35% phosphatidylcholine (PC) (Cat.# 840051C; Avanti Polar Lipids), and 35% phosphatidyletholamine (PE) (Cat.# 84118C; Avanti Polar Lipids); lysophosphatidylcholine (LPC)-loaded liposomes (LPC-Lipo) with 20% chol., 10% PS, 22.5% PC, 22.5% PE, and 25% LPC (Cat.# 855476P; Avanti Polar Lipids); phosphatidic acid (PA)-loaded liposomes with 20% chol., 10% PS, 22.5% PC, 22.5% PE, and 25% PA (Cat.#

P3591; Sigma-Aldrich); 1-palmitoyl-2-oleoyl-*sn*-glycero-3-phosphocholine (POPC)-loaded liposomes with 20% chol., 10% PS, 22.5% PC, 22.5% PE, and 25% POPC (Cat.# 850457P; Avanti Polar Lipids). Lipid formulations were prepared in chloroform, dried under nitrogen gas, then resuspended in PBS for 4 mg lipids/ml. Liposomes were kept at 37°C for 1 h then freeze/thawed five times. Liposososomes were stored at -80°C until used in applications.

Determining the amount of protein within non-surface-derived MV and depleting surface-derived MV – 500 µl streptavidin-coated magnetic 1 µM sized beads (Invitrogen) were washed and handled according to manufacturer's protocol. Harvested MV from biotinylated J774A.1 were quantified for their protein content by Bradford assay. For each separation, 75 µg protein equivalents were added to the washed beads within 100 µl PBS for 30 min. The negative fraction following application of a magnet was removed and quantified for its protein content by Bradford assay.

Statistical analyses - Unpaired Student's *t* test or one-way ANOVA analyses were performed using Graph Pad Prism (GraphPad Software, La Jolla, CA). Values of *p* were calculated where indicated, and for all statistical studies $p<0.05$ was considered as significant.

2.5 RESULTS

2.5.1 $P2X_7$-induced MV drive *de novo* TNF-α secretion and upregulate co-stimulatory ligand surface expression in macrophages

J774A.1, a murine macrophage cell line that expresses $P2X_7$ (249) was used to produce MV in response to ATP plus calcium ionophore. Whereas 3 mM ATP alone was sufficient for generating detectable levels of MV, the addition of 10 μM calcium ionophore A23187 produced greater quantities of MV as judged by Bradford assay of collected material (data not shown). A23187 alone did not induce MV release. These results suggested that MV release is $P2X_7$ dependent, and enhanced by A23187. To test this, J774A.1 cells were treated with $P2X_7$ inhibitor A 740003 or A 438079 prior to generating MV. To confirm that the inhibitors blocked $P2X_7$ activity, I measured Yo-Pro-1 uptake, a common measure of $P2X_7$-induced pore formation (270). Whereas treatment with 3 mM ATP alone was sufficient to induce Yo-Pro-1 uptake, co-treatment with 10 μM A23187 and 3 mM ATP greatly increased the signal (Figure 2-1*A*). Furthermore, Yo-Pro-1 uptake by cells exposed either to 3 mM ATP or to 3 mM ATP plus 10 μM A23187 was blocked by pretreatment with A 740003 inhibitor. Both $P2X_7$ inhibitors either completely abolished or significantly decreased MV shedding, as determined through protein concentration determination by Bradford assay (Figure 2-1*B*). These results demonstrate that MV shedding induced by ATP is dependent on $P2X_7$ activity, as others have shown (211, 245, 252, 259).

MV isolated from culture supernatants by ultracentrifugation were analyzed by flow cytometry and range in size from 0.5 to 1 μm (Figure 2-2). These sizes were confirmed by

electron microscopy (data not shown). The 0.5 to 1 µm size is consistent with plasma membrane derived MV and not exosomes or apoptotic blebs (246).

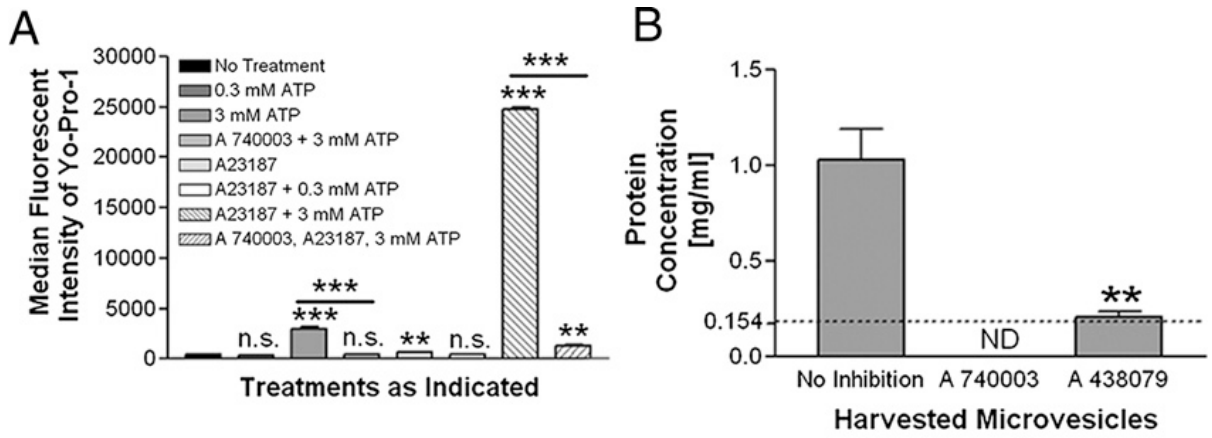

Figure 2-1: P2X$_7$ induces MV shedding.

A, J774A.1 were treated with or without 100 µM A 740003 and then given further indicated treatment for 30 min. Cells were analyzed for Yo-Pro-1 association by flow cytometry. The histogram indicates median fluorescent intensities means ± SEM of n = 3. Statistical comparisons are made to non-treated J774A.1, except where indicated with the inclusion bars. B, J774A.1 were treated with or without 100 µM A 740003 or 10 µM A 438079 for 15 min prior to MV generation. Harvested MV were quantified for their protein concentration by Bradford assay. The histogram indicates protein concentration means ± SEM of n = 3. Statistical comparisons are made to MV harvested from non-drug-treated J774A.1. ND indicates that the protein concentration was lower than the lower limit of detection, which is marked with the dotted line. ** $p<0.01$; *** $p<0.001$; n.s., not significant.

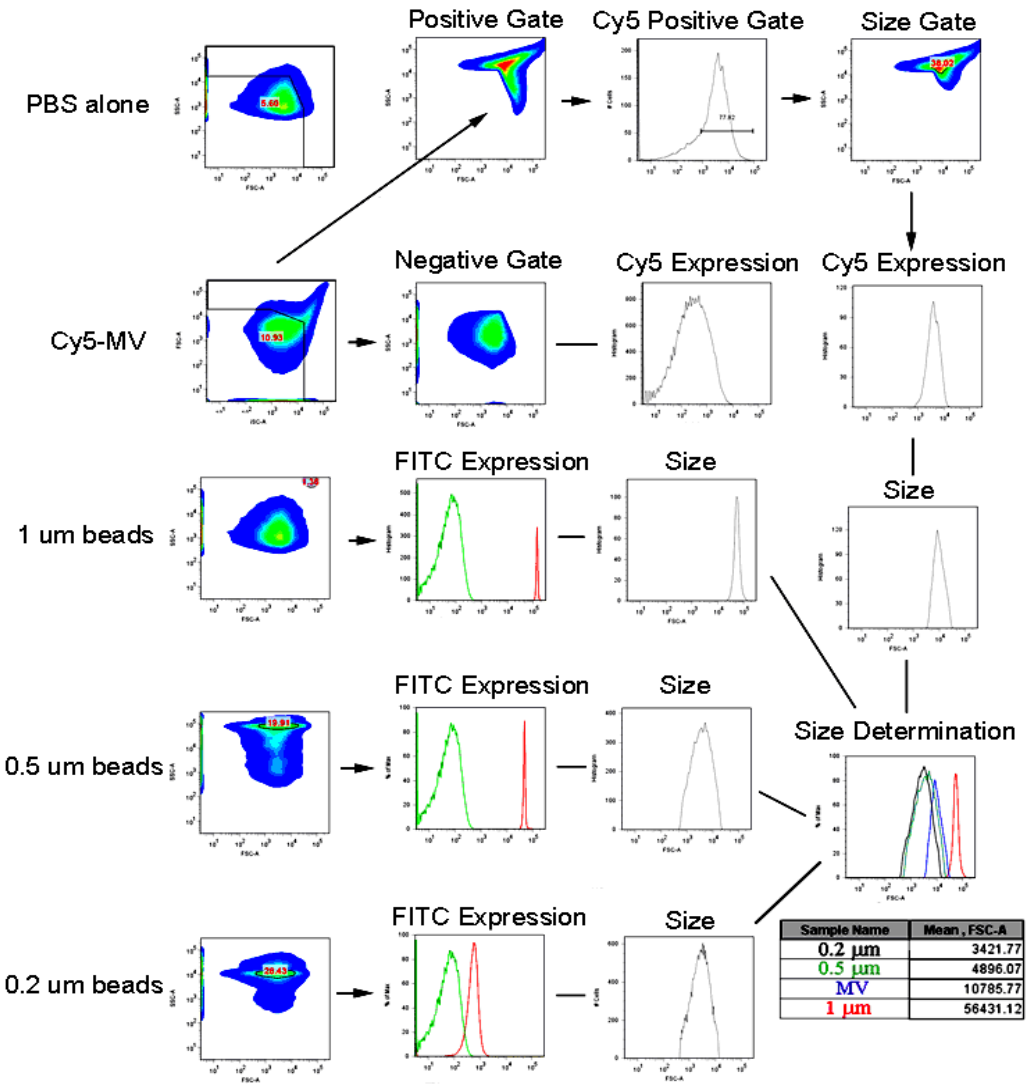

Figure 2-2: MV range in size between 0.5-1 µm.

Under "Size Determination", Cy5-labeled MV (*blue*) were analyzed for forward scatter (FSC-A) via FACS. 0.2 (*black*), 0.5 (*green*), and 1 µm (*red*) sized YG fluorescent beads were included to estimate MV size under the size determination diagram. Mean forward scatter for each are indicated in the adjacent table. MV and bead signals were gated based on fluorescence and size. For "FITC Expression" histograms, green curve indicates a negative control population whereas the red curve indicates the identified population mentioned. Forward scatter is representative of 3 different Cy5-labeled MV preparations.

To study the effect of MV on macrophage function, purified MV were incubated with BMDM for 18 h and supernatants were analyzed by ELISA for TNF-α. MV induced TNF-α secretion in a dose-dependent fashion, with the highest dose of MV (75 μg protein equivalents) stimulating more TNF-α secretion than LPS (Figure 2-3*A* and *B*). Importantly, an equivalent amount of cell homogenate from J774A.1 cells did not induce TNF-α secretion at significant levels. MV-depleted ultracentrifugation supernatant from MV preparations also did not induce TNF-α at significant levels.

Next I examined the effects of MV on co-stimulatory ligand CD86 expression. CD86 surface expression was upregulated in a dose-dependent fashion following exposure to MV (Figure 2-3*C*). Importantly, cell homogenates and MV-depleted supernatants did not increase CD86 levels compared to non-treated control BMDM (Figure 2-3*C*). To exclude the possibility that CD86 upregulation reflected a passive uptake of the protein from MV, BMDM were pre-treated with brefeldin A (BFA). This significantly diminished CD86 upregulation induced by MV, suggesting that the observed increase of CD86 was due to transport of endogenously synthesized CD86 to the cell surface (Figure 2-3*D*). Similar results of CD86 upregulation were also observed for BMDM treated with MV generated from BMDM, human monocyte cell line THP-1, the murine splenic dendritic cell line D2SC-1, and the murine fetal skin derived dendritic cell line FSDC (Figure 2-3*E*).

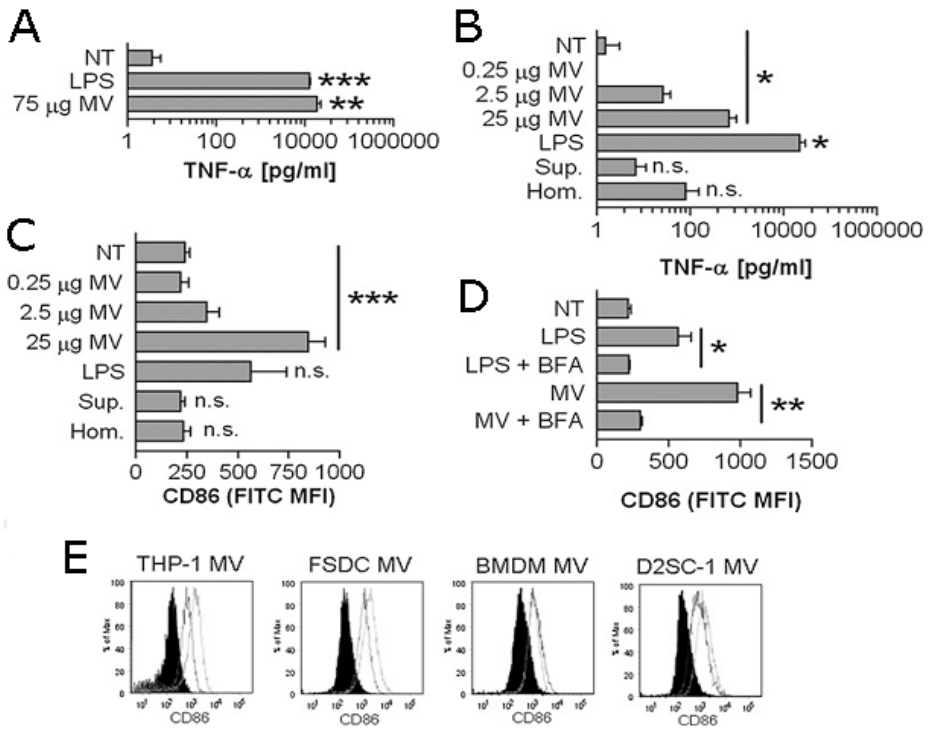

Figure 2-3: P2X$_7$-induced MV promote TNF-α secretion and upregulation of CD86.

A, BMDM were treated with 1 μg/ml LPS or 75 μg protein equivalents of MV, or were left non-treated for 18 h. The histogram indicates TNF-α means ± SEM of n = 3. The statistical comparison is made to non-treated BMDM. B, BMDM were treated with 0.25, 2.5, or 25 μg protein equivalents of MV; 25 μg protein equivalents of cell homogenate; the volume equivalent of 25 μg protein equivalent from ultracentrifugate following generation of MV pellets; or 1 μg/ml LPS; or were left non-treated for 18 h. The histogram indicates TNF-α means ± SEM of n = 3. The statistical comparison is made to non-treated BMDM. C, BMDM from B were analyzed for surface CD86 MFI means ± SEM of n = 3. The statistical comparison is made to non-treated BMDM. D, BMDM were treated with 1 μg/ml LPS or 25 μg protein equivalents of MV, or were left non-treated with or without 10 μg/ml brefeldin A for 18 h. The histogram indicates surface CD86 MFI means ± SEM of n = 3. E, MV harvested from PMA-differentiated THP-1, FSDC, BMDM, or D2SC-1 (25 μg protein equivalents) were incubated with 1 x 10^6 BMDM for 18 h. CD86 expression induced by MV from each indicated cell (solid line) is compared with CD86 expression induced by an equivalent amount of J774A.1 MV (dotted line) and with non-treated BMDM (black filled). Each flow cytometry histogram is representative of n = 2. *p<0.05; **p<0.01; ***p<0.001. BFA, brefeldin A; Hom., homogenate; n.s., not significant; NT, non-treated; Sup., supernatant.

Exposure of cells to MV also upregulated the expression of other markers of activation, specifically CD80, CD83, and I-A^b (Figure 2-4*A*). I next characterized the potential for MV to elicit the production of cytokines known to have roles in polarizing Th1 and Th17 responses. In contrast to TNF-α, however, no increase in IL-12p70 or IL-23 was observed following MV treatment (Figure 2-4*B*). These data demonstrate that P2X$_7$-induced MV can activate macrophages through a stimulatory activity that is not present in equivalent amounts of homogenates of the cells from which the MV derive.

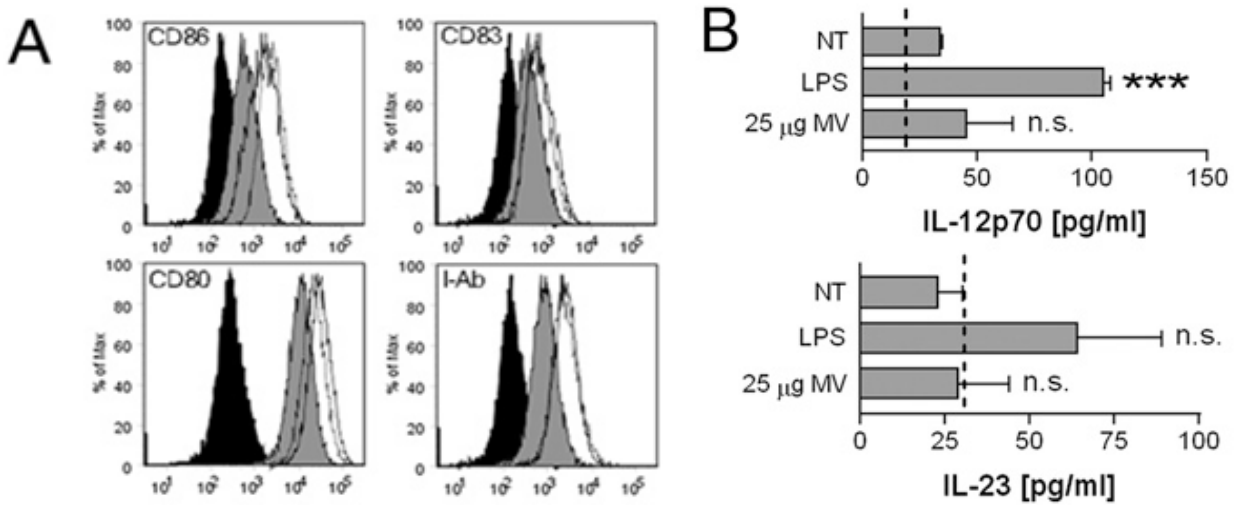

Figure 2-4: MV upregulate multiple activation markers, but do not induce IL-12p70 or IL-23 secretion.

A, BMDM were treated with 1 μg/ml LPS (solid line) or 25 μg protein equivalents of MV (dotted line), or were left non-treated (gray filled) for 18 h. Cells were analyzed for CD80, CD83, and CD86 or I-Ab surface expression. Isotype control is shown filled in black. Data are representative of multiple experiments. B, BMDM were treated with 1 μg/ml LPS or 25 μg protein equivalents of MV, or were left non-treated for 18 h. The histogram indicates IL-12p70 or IL-23 means ± SEM of $n = 3$. The statistical comparison is made to non-treated BMDM. The dotted line indicates the bottom limit of detection for each respective ELISA. ***$p<0.001$; n.s., not significant; NT, non-treated.

2.5.2 MV bind to BMDM and are largely retained at the plasma membrane before inducing TNF-α secretion and CD86 upregulation

To examine their interaction with BMDM, MV were first biotinylated. After washing and repelleting, biotinylated MV were incubated for varying times with BMDM. Alexa647-labeled streptavidin was then added to visualize the interaction. When added to BMDM, MV bound to the cell surface within 30 min, with little increase seen after that (Figure 2-5*A*, 2-5*B*). In contrast, CD86 expression increased steadily, reaching an observed maximum at 18 h. Similar kinetics were seen with TNF-α secretion (Figure 2-5*C*). Confocal microscopy demonstrated that CD86 and MV were not colocalized at the cell surface. By 4 h some MV congregated within lysosomes, whereas most of the MV remained at the plasma membrane (Figure 2-5*D*).

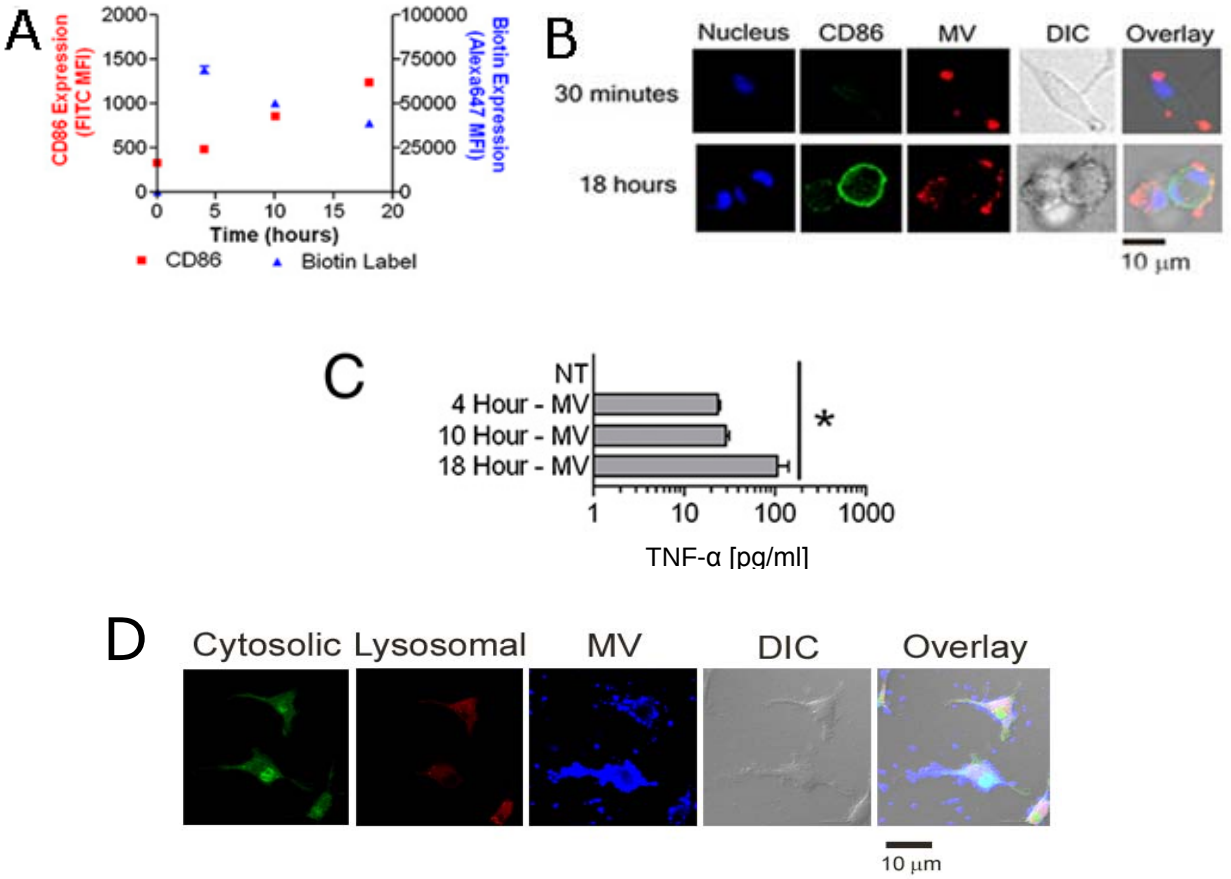

Figure 2-5: Differential kinetics of TNF-α and CD86 expression relative to surface binding of MV to BMDM.

A, 5 x 10^5 BMDM were left untreated or treated with 75 µg protein equivalents of MV for 4, 10, or 18 h. The histogram indicates means ± SEM of TNF-α released into the supernatant of n = 3. B, BMDM were left untreated or exposed to 25 µg biotinylated MV for 4, 10, or 18 h. Surface CD86 and biotin MFI changes over time are shown. The histogram indicates MFI means ± SEM of *n* = 3. C, BMDM were incubated with 25 µg biotinylated MV for 0.5 or 18 h. Cells were analyzed for nucleus (blue), CD86 (green), and biotin (red), and expression by confocal microscopy. Differential interference contrast image is also shown. Overlay of three fluorescent signals and differential interference contrast is shown in the *far right image* on the panel. Images are representative of 10 random fields of view from two separate experiments. Scale bar, 10 µm. *p<0.05. DIC, differential interference contrast; NT, non-treated. D, Cytosolic dye CMFDA label (*green*) and lysosomal dye LysoTrackerRed (*red*) labeled BMDM were incubated with 50 µg of biotinylated MV for 4 h. Cell-associated biotin is in (*blue*). Overlay of three fluorescent signals with a DIC image is shown in the panel on the far right. Bar = 10 µm.

2.5.3 MV-induced activation is partially TLR4-dependent and is independent of MyD88

Damaged cells can release a number of mediators (such as damage associated molecular patterns) that can activate immune cells through TLR engagement. In particular, HMGB1 (38), hyaluronic acid (271) and S100A8/S100A9 complex (272), among others, bind TLR4 for cellular activation. To examine whether MV also act through a TLR4-dependent pathway, BMDM were generated from WT and $TLR4^{-/-}$ mice. TNF-α induction by MV was reduced in $TLR4^{-/-}$ BMDM, which produced 35-81% less TNF-α than WT BMDM; however, the decrease was not statistically significant (Figure 2-6*A*). $TLR4^{-/-}$ BMDM were significantly impaired in CD86 upregulation when treated with MV with WT BMDM (Figure 2-6*B*). In contrast, CD86 upregulation induced by the TLR4 agonist monophosphoryl lipid A (MPLA) was completely dependent on TLR4, whereas poly(I:C) stimulation was TLR4-independent, as expected. These data suggest that MV contain a stimulatory component that activates BMDM via TLR4, but that additional means of activation that are not dependent on TLR4 may also be present.

MyD88 and TRIF are the primary adaptor proteins downstream of TLR signaling. TLR4 pathways initiate both MyD88 and TRIF pathways. Thus macrophages derived from $MyD88^{-/-}$ mice were treated with MV, Pam_3CSK_4, or poly(I:C). Pam_3CSK_4, a TLR2 and MyD88-dependent agonist, was able to upregulate the secretion of TNF-α (Figure 2-7*A*) and IL-6 (Figure 2-7*B*) from WT, but not $MyD88^{-/-}$ BMDM, and failed to upregulate CD86 on either WT or $MyD88^{-/-}$ BMDM. Poly(I:C), a TLR3 and MyD88-independent agonist, and MV were able to upregulate TNF-α (Figure 2-7*A*), IL-6 (Figure 2-7*B*), and CD86 (Figure 2-7*C*) from WT and $MyD88^{-/-}$ BMDM; $MyD88^{-/-}$ BMDM express more basal CD86 than WT. These results would

suggest that MV-induced activation shares similar signal transduction pathways to poly(I:C), including acting through MyD88-independent mechanisms.

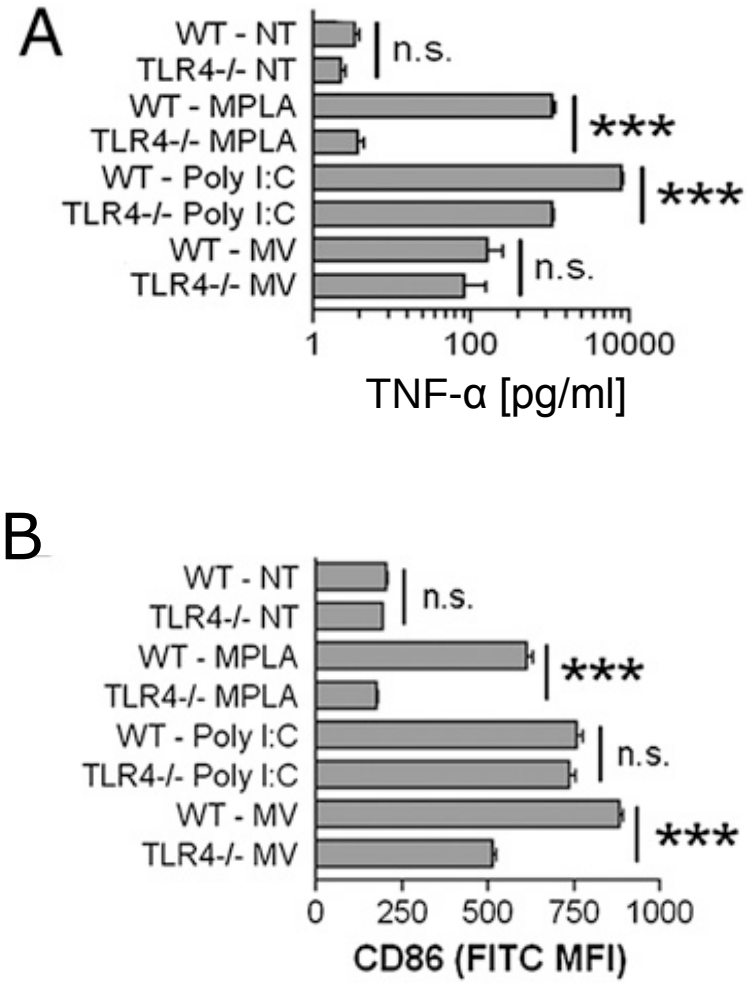

Figure 2-6: Partial TLR4 dependence of MV-induced BMDM activation.

A, 5 x 10^5 WT or $TLR4^{-/-}$ BMDM were treated with 10 µg/ml poly(I:C), 5 µg/ml MPLA, or 75 µg protein equivalents of MV, or were left untreated for 18 h. The histogram indicates TNF-α means ± SEM of $n = 3$. B, WT or $TLR4^{-/-}$ BMDM were treated with 10 µg/ml poly(I:C), 5 µg/ml MPLA, or 25 µg protein equivalents of MV, or were left untreated for 18 h. Surface CD86 MFI means ± SEM of $n = 3$ are shown. ***$p<0.001$. n.s., not significant; NT, non-treated.

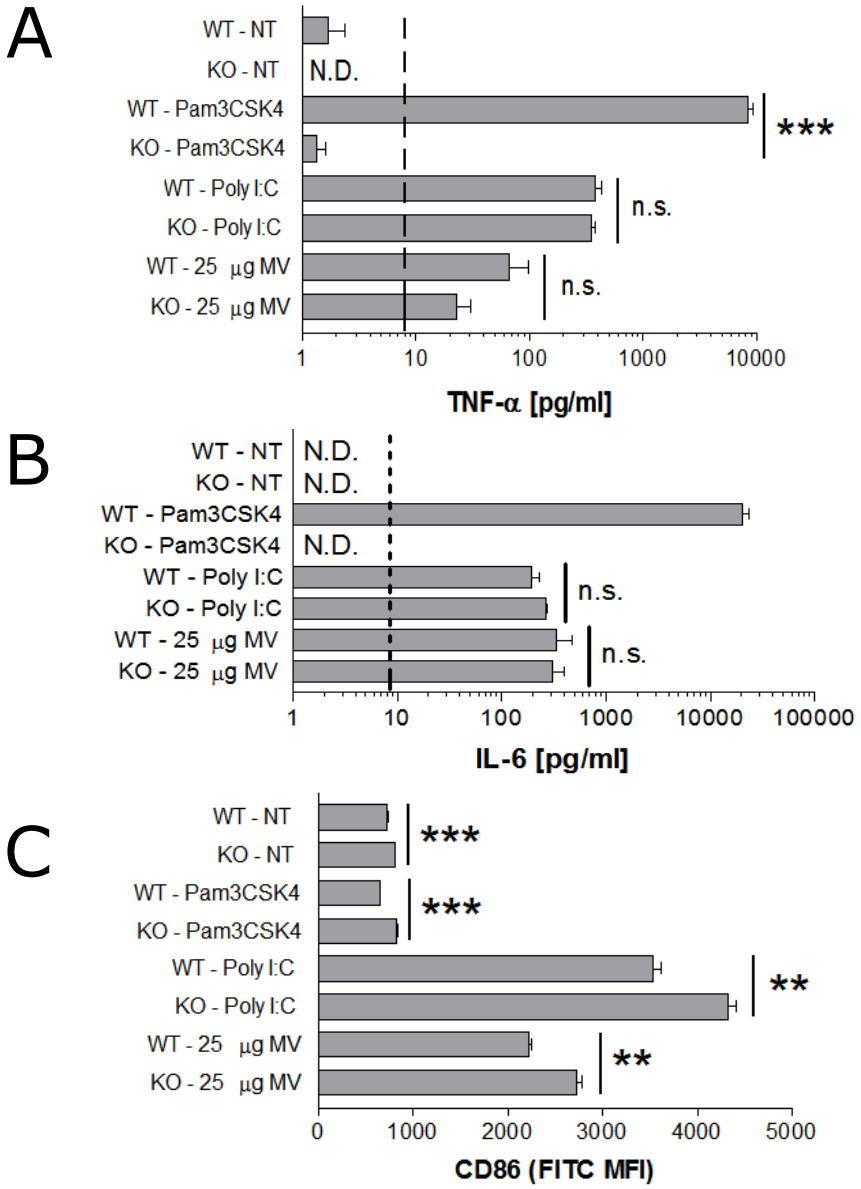

Figure 2-7: MyD88 is not required for TNF-α, IL-6, or CD86 production in response to MV.

BMDM were non-treated or treated with 10 µg/ml Pam_3CSK_4, 10 µg/ml poly(I:C), or 25 µg/ml MV for 18 h. Supernatants were evaluated for TNF-α (A) or IL-6 (B). The histogram indicates TNF-α or IL-6 means ± SEM of *n* = 3. The dotted line indicates the lower limit of detection for the assay. C, BMDM were evaluated for surface expression of CD86. Surface CD86 MFI means ± SEM of *n* = 3 are shown. $^{**}p<0.01$; $^{***}p<0.001$. n.s., not significant; N.D., none detected; NT, non-treated; KO, $MyD88^{-/-}$. Dashed line indicates the lower limit of detection for the assay.

2.5.4 MV-induced activation is independent of HMGB1 and RAGE

Given the partial TLR4 response from macrophage derived MV, HMGB1 could mediate MV-induced activation. HMGB1 can activate monocytes and macrophages (273) through TLR2, TLR4, and RAGE (38). Also, HMGB1 can be released from activated monocytes and macrophage (274) or necrotic cells (275) and is expressed within secretory lysosomes that are released from monocytes following stimulation with ATP (154). Furthermore, unlike hyaluronic acid and S100A8/S100A9 complexes, which require prior priming through agents like IFN-γ or LPS for their expression (276-278), HMGB1 can be passively released through cellular damage without the need for priming (279). Indeed, HMGB1 was detected in the supernatants of ATP/A23187-treated J774A.1 cells and also in purified MV, but not in supernatants from untreated or LPS-treated cells (Figure 2-8*A*, *B*). LPS treatment before exposure to ATP/A23187 increased secretion of HMGB1 (Figure 2-8*A*).

In addition to TLR4, HMGB1 can act through RAGE. To assess whether MV-induced activation requires RAGE, BMDM from RAGE-deficient mice were generated. I determined that there were no significant differences in TNF-α release between MV-treated WT and $RAGE^{-/-}$ BMDM (Figure 2-8*C*) following stimulation with either LPS or MV. To determine more broadly whether HMGB1 is a stimulatory agent in MV-induced activation, BMDM were incubated with MV in the presence of soluble RAGE, which should block the binding of HMGB1 to all of its potential receptors. Soluble RAGE did not diminish MV-mediated TNF-α release (Figure 2-8*C*). Additionally, there were no significant differences in CD86 upregulation between WT and $RAGE^{-/-}$ BMDM, demonstrating that RAGE does not participate in MV-induced activation (Figure 2-8*D*). Furthermore, soluble RAGE did not block MV-induced CD86 upregulation even

at high concentrations, suggesting that HMGB1 does not mediate the effects of MV (Figure 2-8*E*).

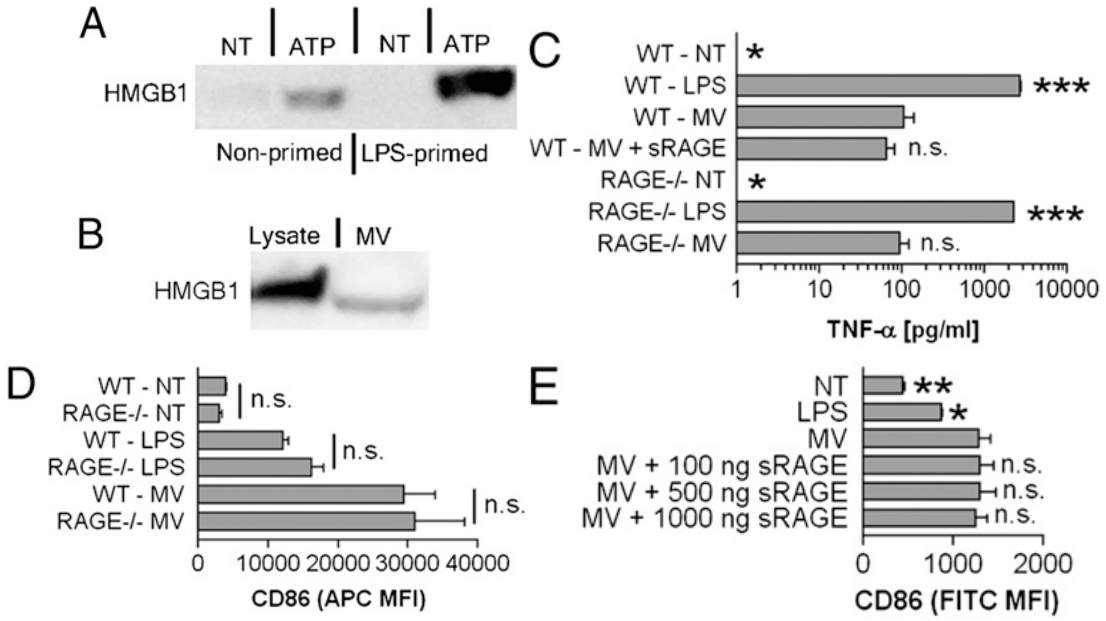

Figure 2-8: MV contain HMGB1, but CD86 upregulation is HMGB1 independent.

A, J774A.1 cells were primed with 1 µg/ml LPS or left unprimed for 4 h, and were treated with 3 mM ATP and 10 µM A23187 for 30 min or untreated. Supernatants were analyzed for HMGB1 by Western blot. Data are representative of repeat experiments. B, 25 µg protein equivalents from a reference lysate or 25 µg protein equivalents of MV were compared for HMGB1 expression via Western blot. C, 5 x 10^5 WT or $RAGE^{-/-}$ BMDM were treated with 1 µg/ml LPS or 75 µg protein equivalents of MV with or without 30-min preincubation with 1 µg/ml soluble RAGE, or were left non-treated for 18 h. The histogram shows TNF-α means ± SEM of n = 3. Statistical comparison is to WT BMDM treated with 25 µg MV. D, WT or $RAGE^{-/-}$ BMDM were treated with 1 µg/ml LPS or 25 µg protein equivalents of MV, or were untreated for 18 h. The histogram indicates surface CD86 MFI means ± SEM of n = 3. E, 25 µg protein equivalents of MV were pretreated with 100, 500, or 1000 ng/ml soluble RAGE for 30 min prior to addition to BMDM. NT, LPS, and 25 µg protein equivalents of MV were included. Surface CD86 MFI ± SEM of n = 3 are shown. The statistical comparison is to 25 µg MV-alone. *p<0.05; **p<0.01; ***p<0.001. n.s., not significant; NT, non-treated.

2.5.5 Characterizing MV-induced signaling pathways

NF-κB and p38 MAPK activation pathways are commonly initiated through TLR engagement (27). Indeed, in BMDM, p38 phosphorylation was induced within minutes of exposure to MV, and then declined over time, similar to the response to LPS (Figure 2-9*A*). To address whether p38 MAPK blockade was sufficient to diminish MV mediated CD86 upregulation, BMDM were pre-incubated with a titration of the p38 inhibitor SB203580 before exposure to MV. In the presence of the drug, CD86 upregulation was strongly inhibited, supporting a role for p38 MAPK in MV-mediated activation (Figure 2-9*B*). In contrast, LPS-induced CD86 expression actually increased in the presence of 1 and 10 μM inhibitor, with significant inhibition only observed at 50 μM, suggesting differences in the two signaling pathways (data not shown).

I also tested whether MV were able to activate NF-κB, using a RAW264.7 reporter cell line (Figure 2-9*C*). The kinetics of the response induced by MV were similar to LPS, with activation evident after 4 and 18 h but not after 1 h. The magnitude of the response was less with MV than with LPS however, and declined by 18 h post-treatment.

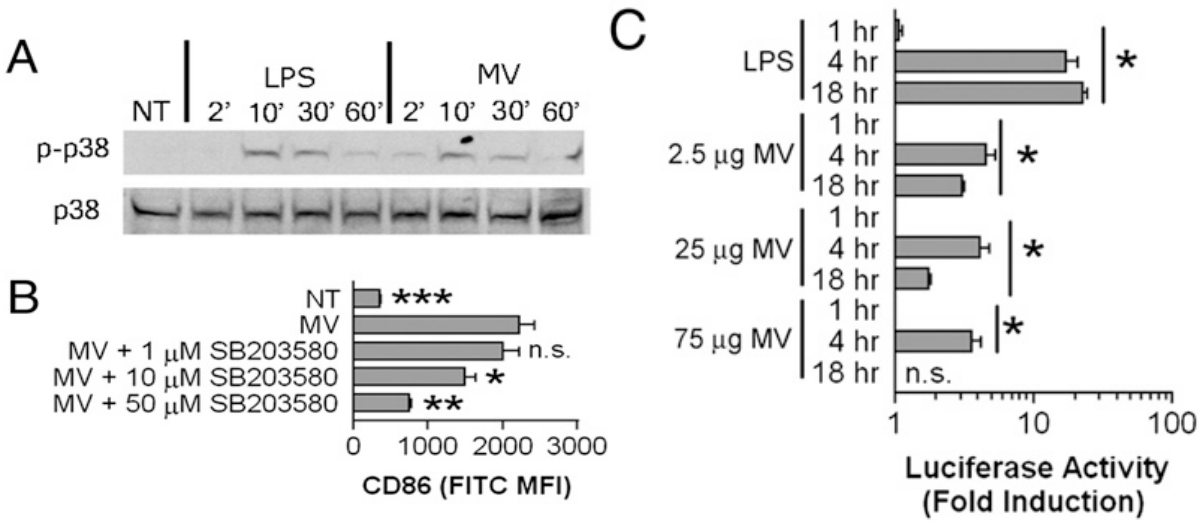

Figure 2-9: MV activate p38 MAPK and NF-κB pathways.

A, BMDM were left non-treated or were treated with 1 μg/ml LPS or 25 μg protein equivalents of MV for 2, 10, 30, or 60 min. Expression of phosphorylated p38 (p-p38) and total p38 (p38) was evaluated via Western blot. Data are representative of repeat experiments. B, BMDM were treated with 25 μg protein equivalents of MV with or without additional treatment of the phosphorylated p38 inhibitor SB203580 at either 1, 10, or 50 μM, or were left non-treated for 18 h. The histogram indicates surface CD86 MFI means ± SEM of $n = 3$. The statistical comparison is made to 25 μg MV-alone–treated BMDM. C, RAW264.7 macrophages expressing luciferase under control of a NF-κB promoter were treated with 1 μg/ml LPS or 2.5, 25, or 75 μg protein equivalents of MV for 1, 4, or 18 h. The fold change over non-treated cells is shown. The histogram indicates fold change means ± SEM of $n = 3$. The statistical comparison is made to the 1-h fold change value for each respective treatment. *$p<0.05$; **$p<0.01$; ***$p<0.001$; n.s., not significant; NT, non-treated.

Protein kinase A (PKA) and protein kinase C (PKC) can both influence p38 and NF-κB in immune cells (27). PKC is modulated by intracellular calcium and/or diacylglycerol (55) whereas PKA is cAMP-controlled (54). To indirectly inhibit calcium sensitive isoforms of PKC, BMDM were treated with 30 μM BAPTA/AM to chelate intracellular calcium. Treatment did

not impair CD86 upregulation in response to MV or LPS (Figure 2-10*A*). Direct PKC inhibition, through use of 50 µM Bisindolylmaleimide I HCl (BIM), significantly decreased MV mediated CD86 upregulation (Figure 2-10*B*). In contrast, PKC inhibition enhanced LPS-mediated CD86 upregulation. MDL-12330A was used to inhibit adenylate cyclase, which generates cAMP, resulting in a significant decrease in expression from MV, but not LPS, treated BMDM (Figure 2-10*C*). Inhibition of PKA using 10 µM H-89 HCl also resulted in a significant decrease (Figure 2-10*D*). These results support the idea that MV mediated activation requires PKA and PKC pathways, which is in contrast to the activation response induced by LPS.

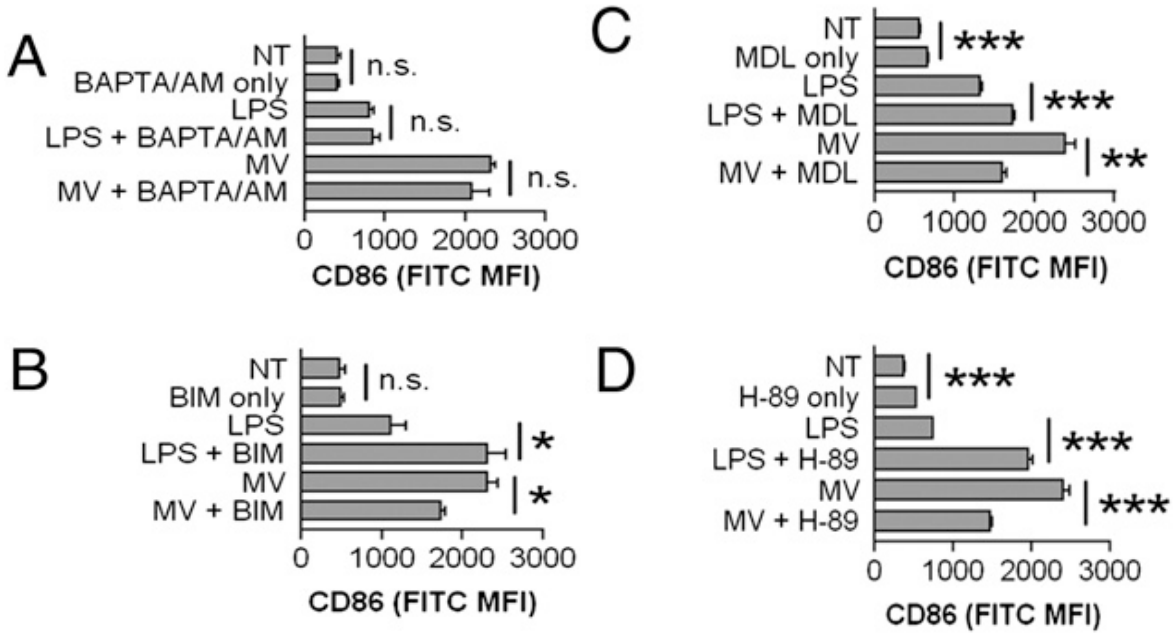

Figure 2-10: CD86 upregulation is cAMP, PKA, and PKC dependent, but Ca^{2+} independent.

BMDM were left non-treated or treated with 1 µg/ml LPS or 25 µg MV with or without additional treatment of 10 µM intracellular calcium chelator BAPTA/AM in A, 50 µM PKC inhibitor BIM in B, 10 µM adenylate cyclase inhibitor MDL-12330A in C, or 10 µM PKA inhibitor H-89 in D, for 18 h. Surface CD86 MFI ± SEM of $n = 3$ are shown. *$p<0.05$; **$p<0.01$; ***$p<0.001$. n.s., not significant; NT, non-treated.

2.5.6 The stimulatory activity from MV consists of one or more phospholipids

To characterize the stimulatory agent(s) from MV, biochemical fractionation was used to separate lipids and proteins as described in *Materials and Methods*. Only the lipid fraction, but not the protein fraction, significantly activated BMDM, as measured by CD86 upregulation (Figure 2-11*A*). Lipids were further separated according to polarity. The phospholipid fraction provided significant upregulation of CD86 as compared to non-treated control. Only minimal activity was recovered from the flow-through, the neutral lipids fraction, or the glycolipid/sulpholipid fraction (Figure 2-11*B*). Mock elution from the column for a phospholipid fraction also did not recover any stimulatory material, demonstrating that the columns themselves did not contain contaminants that could activate BMDM.

To test the TLR4 dependence of the phospholipid-containing fraction of MV, $TLR4^{-/-}$ or WT BMDM were given equal amounts of phospholipid fraction. In agreement with the partial TLR4 dependence for MV mediated activation described in Figure 2-6, the phospholipid fraction from MV had a significant difference in activation between the $TLR4^{-/-}$ and WT BMDM. Additionally, phospholipid fraction activation of $TLR4^{-/-}$ BMDM did not significantly differ from non-treated BMDM. This at least partially confirms that the TLR4 agonist from the MV came in the form of a phospholipid.

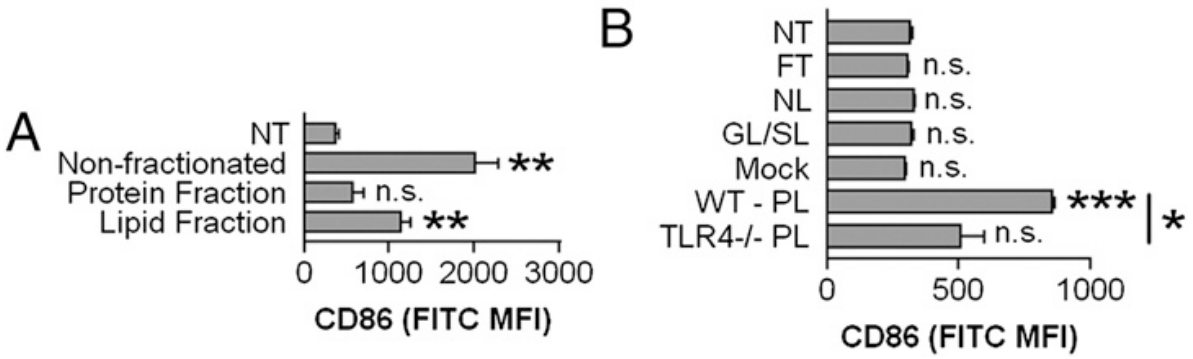

Figure 2-11: The phospholipid but not protein fraction from MV activates BMDM.

A, Lipids and protein were isolated from 25 µg protein equivalents of MV and applied to BMDM for 18 h. No treatment and non-fractionated 25 µg protein equivalents of MV were included as controls. Surface CD86 MFI means ± SEM of n = 3 are shown. The statistical comparison is made to non-treated BMDM. B, Total lipid fractions from 225 µg protein equivalents of MV were isolated and were further fractionated as follows: column flow-through, neutral lipids, glycolipids and sulpholipids, and phospholipids. Mock methanol elution of the column without any loaded material was included as a control. Fractions were incubated with BMDM for 18 h. Non-treated BMDM and incubation of the phospholipid fraction with TLR4$^{-/-}$ BMDM are also shown. Surface CD86 MFI means ± SEM of n = 3 are shown. The statistical comparison is made to non-treated BMDM, except where indicated. *p<0.05; **p<0.01; ***p<0.001. FT, column flow-through; GL/SL, glycolipid and sulpholipid; NL, neutral lipid; n.s., not significant; NT, non-treated; PL, phospholipid.

2.5.7 Lipid-modifying enzymes play a role in generating MV capable of activating BMDM

The above results led me to hypothesize that purinergic receptor activation in MV producer cells exposed to ATP might generate stimulatory phospholipids that are packaged into MV. This could explain why MV activated BMDM more strongly than the equivalent amount of cell lysate, as described earlier. $P2X_7$ activation, which is required for generating ATP-induced MV, can activate lipid-modifying enzymes such as calcium-independent phospholipase A_2 ($iPLA_2$) (155),

phospholipase D (PLD) (156), and calcium dependent phospholipase A_2 ($cPLA_2$) (155). To test whether PLD, $iPLA_2$, or $cPLA_2$ were required to generate stimulatory MV, producer cells were treated with either PLD inhibitors (50 μM CAY10593 for PLD1 and 50 μM CAY10594 for PLD2), $iPLA_2$ inhibitor (10 μM bromoenol lactone [BEL]), or $cPLA_2$ inhibitor (10 μM AACOCF3) prior to, and during, ATP/A23187-elicited MV induction. When equivalent amounts of these MV populations were applied to recipient BMDM, MV from PLD1- and PLD2-inhibited J774A.1 producer cells were unable to stimulate CD86 upregulation (Figure 2-12*A*). PLD inhibitors did not directly impact MV-mediated CD86 upregulation of recipient BMDM, as inclusion of MV from PLD1- and PLD2-inhibited J774A.1 with MV from mock treated J774A.1 did not result in any significant differences from BMDM treatment with MV from mock treated J774A.1 (Figure 2-12*B*). Furthermore, MV from mock or from PLD1- or PLD2-inhibited cells did not decrease phosphatidic acid levels of treated J774A.1, relative to non-treated J774A.1 (data not shown). By contrast, inhibition of $iPLA_2$ (Figure 2-12*C*) or $cPLA_2$ (Figure 2-12*D*) in MV producer cells did not decrease the stimulatory capacity of the MV generated, which were at least as potent as those from producer cells not pretreated with inhibitors. It should be noted that MV were obtained from producer cells treated with these inhibitors in amounts approximately equal to mock-treated producer cells, suggesting that the stimulatory phospholipid is not required for MV structural integrity or secretion from cells. Furthermore, PLD1, PLD2, $iPLA_2$, and $cPLA_2$ inhibitors were not toxic at the concentrations used since cell viability was >85% in all cases (data not shown).

I lastly considered whether lysophosphatidic acid (LPA) might be a potential stimulatory phospholipid from the MV. LPA is a product of $P2X_7$ activity (280) and it can activate macrophages to promote cytokine production (281) and cAMP synthesis (282). Pretreatment of

BMDM with Ki16425, an inhibitor selective for LPA receptors $LPAR_1$ and $LPAR_3$, did not diminish CD86 upregulation by MV (Figure 2-12*E*). This suggests that LPA does not participate in MV-induced activation of macrophages, although it does not exclude the possibility that LPA could mediate effects through other receptors.

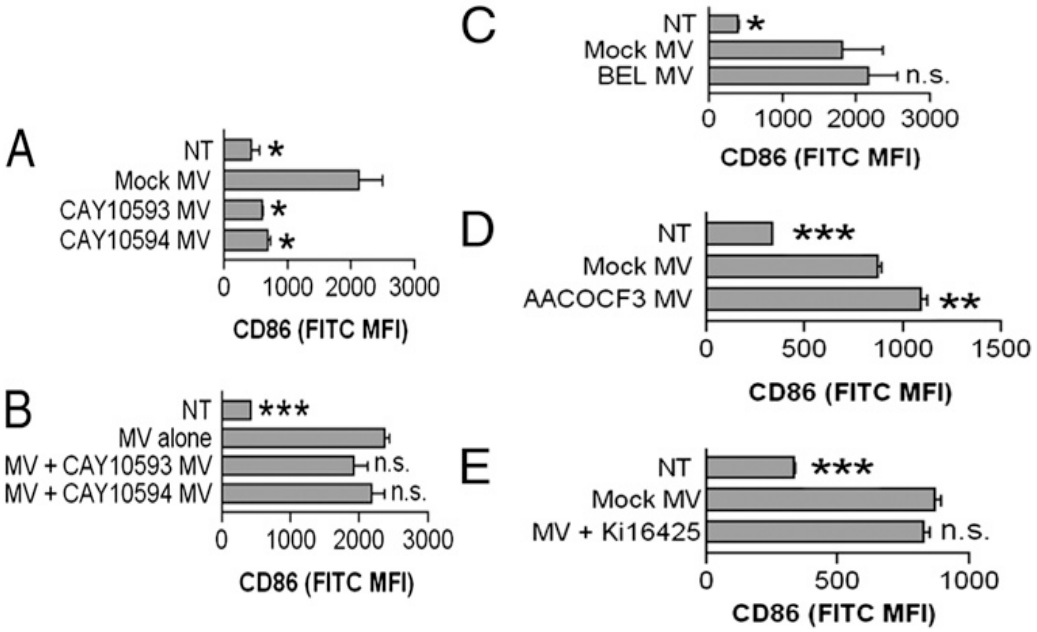

Figure 2-12: Activities of lipid-modifying enzymes PLD1 and PLD2, but not $iPLA_2$ or $cPLA_2$, are required for generating stimulatory MV that can induce CD86 expression.

J774A.1 were pretreated with 50 µM PLD1 inhibitor CAY10593 or 50 µM PLD2 inhibitor CAY10594 in A, and B, 10 µM $iPLA_2$ inhibitor BEL; in C, 10 µM AACOCF3; or in D, DMSO vehicle control for 30 min prior to and during MV generation. A total of 25 µg protein equivalents from the generated MV was incubated with BMDM for 18 h. B, 25 µg protein equivalents from MV from mock-treated J774A.1 were incubated with or without 25 µg protein equivalents from MV from PLD1- or PLD2-inhibited J774A.1. E, BMDM were treated with or without 10 µM Ki16425 prior to MV treatment. Non-treated BMDM are included as controls. Surface CD86 MFI means ± SEM of $n = 3$ are shown. The statistical comparison is made to mock MV-treated BMDM. *$p<0.05$; **$p<0.01$; ***$p<0.001$. n.s., not significant; NT, non-treated.

2.5.8 Stimulatory MV are not derived from intracellular sources

In order to better characterize the type of MV that elicit macrophage activation, I considered the source of the stimulatory MV. MV can originate from intracellular sources such as multivesicular bodies (MVB) or from the plasma membrane. In order to differentiate these origins, I first biotinylated proteins outwardly expressed on the plasma membrane prior to administration of ATP/A23187 for MV generation. Following harvest, protein equivalent amounts were incubated with streptavidin-coated magnetic beads. In this manner, extracellularly exposed protein containing MV can be removed upon magnetic selection; MV that do not contain a large surplus of extracellularly exposed proteins are negatively selected. Most of the MV are derived from the plasma membrane, as 82% of protein content from 75 µg protein equivalents of MV were apparently removed by addition of streptavidin-coated magnetic beads (data not shown) and (Figure 2-13*A*). BMDM were treated with 10 µg protein equivalents of biotinylated MV (prior to streptavidin-coated magnetic bead incubation), 10 µg protein equivalents of negatively selected MV (following streptavidin-coated magnetic bead incubation), or 10 µg protein equivalents of non-biotinylated MV. Biotinylated MV (prior to streptavidin-coated magnetic bead selection) induced CD86 upregulation of BMDM similar to non-biotinylated MV (Figure 2-13*B*). In contrast, an equal protein equivalent amount of biotinylated MV following streptavidin-coated magnetic bead selection display significantly diminished ability to activate BMDM as non-biotinylated MV (Figure 2-13*B*). The lack of retention of the biotin label at the plasma membrane of recipient BMDM from negatively selected biotinylated MV compared to biotinylated MV prior to selection was confirmed by flow cytometry (Figure 2-13*C*).

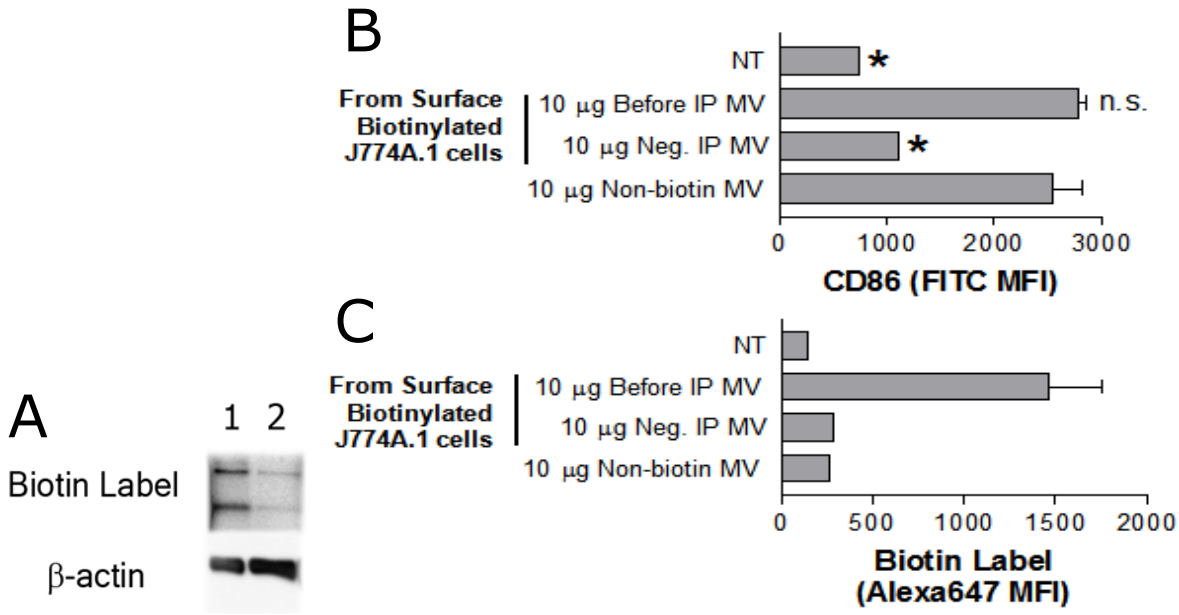

Figure 2-13: Intracellular MV are unable to activate BMDM.

A, 1 μg of protein equivalents of MV from surface biotinylated J774A.1 prior (1) to and after (2) streptavidin magnetic bead depletion are evaluate for biotin label and β-actin expression by Western blot. Data is representative of repeated experiments. B and C, 10 μg of protein equivalents of MV from surface biotinylate J774A.1 prior to and after streptavidin magnetic bead depletion or non-biotinylated J774A.1 derived MV are given to BMDM for 18 h and evaluated for surface CD86 (B) and biotin label (C) by flow cytometry. Surface CD86 MFI means ± SEM of n = 2 are shown. The statistical comparison is made to non-biotinylated MV-treated BMDM. *p<0.05;.n.s., not significant; NT, non-treated.

2.5.9 Phosphatidic acid loaded liposomes weakly stimulate CD86 expression on BMDM

Since PLD enables the generation of stimulatory MV, I considered the potential stimulatory capabilities of phosphatidic acid (PA) loaded liposomes. Liposomes were created with non-specialized lipids (Lipo Ctrl), phosphatidic acid (PA)-loaded liposomes (PA-Lipo),

lysophosphatidic acid (LPC)-loaded liposomes (LPC-Lipo), and phosphatidylcholine (POPC-Lipo) loaded liposomes (POPC-Lipo). PA-Lipo alone displayed ability to upregulate CD86 on BMDM (Figure 2-14).

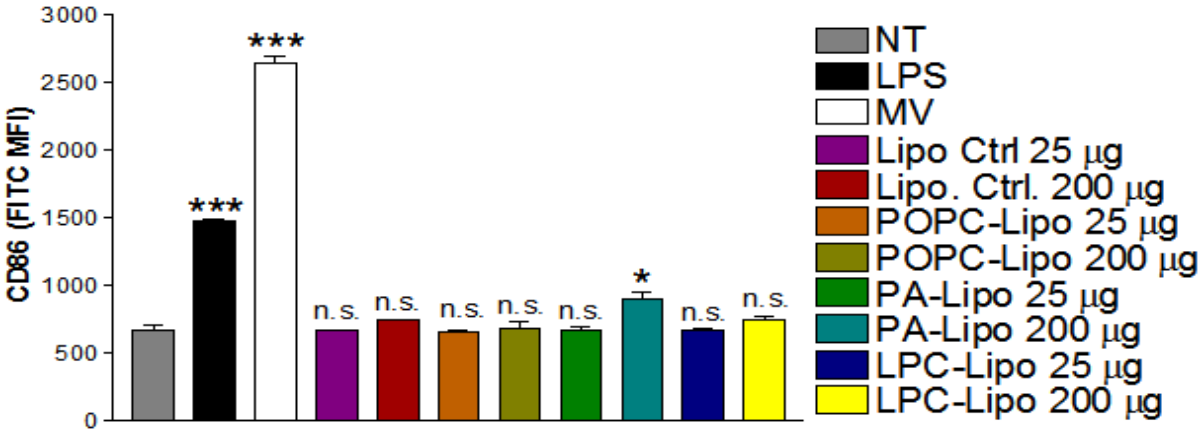

Figure 2-14: BMDM are activated by PA-loaded liposomes.

BMDM were non-treated or treated with 1 µg/ml LPS, 25 µg protein equivalents of MV, 25 µg or 200 µg lipid equivalents of indicated liposomes (components detailed in the *Materials and Methods*) for 18 h and evaluated for surface CD86 by flow cytometry. Surface CD86 MFI means ± SEM of $n = 3$ are shown. The statistical comparison is made to non-treated BMDM. *$p<0.05$; ***$p<0.001$. n.s., not significant; NT, non-treated.

2.6 DISCUSSION

MV released by cells can potently influence immune responses in a number of ways. Many cell types release exosomes constitutively and, depending on the cell of origin, may transfer antigens or other cargo to DCs that can initiate immune responses. A specialized type of MV release exists for myeloid cells that express $P2X_7$ receptors, which, when exposed to receptor agonists such as ATP, shed MV from the cell surface and release them from intracellular stores. Characterizing MV generation induced by $P2X_7$ activation on macrophages is important for understanding inflammatory processes, because tissue damage has been shown to release intracellular constituents like ATP into an environment containing large numbers of these cells (283-286).

When macrophages are primed by exposure to TLR agonists, cytokines including IL-1β and TNF-α, are synthesized and may be released from the cell following appropriate stimulation by a secondary signal (34). For IL-1β release, $P2X_7$ engagement is followed by cleavage of pro-IL-1β into the bioactive form by caspase-1 in a NLRP3-dependent process. MV have been demonstrated to contain mature IL-1β and were first characterized as surface derived vesicles (217, 245), but later as exosomes (211). TNF-α-containing exosomes have been reported to be secreted from human melanoma cells (287). I have detected TNF-α within $P2X_7$-induced MV from primed macrophages; however, TNF-α was also detected from cell culture supernatants devoid of MV (data not shown). Nevertheless, only primed macrophages would release pro-inflammatory cytokines, whose synthesis primarily depends on NF-κB activation (27), whether in MV or as soluble proteins.

My study instead focused on characterizing the biological effects of MV released by non-primed, primary macrophages, a condition that may be seen during sterile inflammation. As reported by others, MV are released following $P2X_7$ engagement on non-primed macrophages (259), yet to the best of my knowledge, have not been studied for their ability to activate macrophages. Whereas 3 mM ATP alone is sufficient for $P2X_7$ activation, I observed enhanced $P2X_7$ activity when co-administering 10 μM A23187 with 3 mM ATP. A23187 with 0.3 mM ATP was not able to induce $P2X_7$ activity; thus in this manner, A23187 is serving in some other function than for the autocrine release of endogenously stored ATP for $P2X_7$ activation. I found that $P2X_7$-induced MV from non-primed myeloid cells can induce expression of CD86, CD80, CD83, and MHC class II (Figure 2-4*A*), and also induce secretion of TNF-α from primary macrophages (Figure 2-3*A, B*). I further characterized the contents of these MV and found that phospholipids were responsible for stimulating macrophage activation in a TLR4-dependent process (Figure 2-6*B*). As separated phospholipids from MV activate macrophages, I can exclude a requirement for direct interaction of intact MV in this process. That being said, MV-mediated activation was only partially TLR4 dependent, thus MV must contain components in addition to phospholipids that activate macrophages independently of TLR4 and these activities may be contingent upon delivery of intact MV into intracellular departments.

Stimulation of primed macrophages by $P2X_7$ yields MV that are heterogeneous, consisting of exosomes (211, 259) and surface-derived vesicles (217, 245), and possibly including secreted lysosomes (256-258). The MV described in my study are predominantly 0.5-1.0 μm in diameter (Figure 2-2), distinguishing them from larger 1-4 μm apoptotic blebs (246). I observed relatively few smaller MV that would be characteristic of exosomes as analyzed by electron microscopy (data not shown), and believe that my preparations were devoid of them for

several reasons. Whereas my MV were obtained from ultracentrifugation at 100,000 x *g*, I also found that material obtained from 10,000 x *g* centrifugation exerts equivalent ability to activate macrophages (data not shown). Exosomes do not pellet at the low speed as they are only 50-100 nm in diameter. Thus, MV-induced macrophage activation seems to be exosome independent. Furthermore, the release of MHC class II-containing exosomes from macrophages requires apoptosis-associated speck-like protein containing a CARD (ASC)/NLRP3 inflammasome (259). Non-primed myeloid cells, such as I have used, typically do not express high levels of NLRP3 (288), and thus, would not be expected to release MHC class II+ exosomes efficiently. In addition, I have purified MV from D2SC-1 cells, a murine splenic DC-derived cell line that lacks ASC (data not shown), and found that these MV are potent stimulators of macrophage activation (Figure 2-3*E*). In this way, D2SC-1 cells act similarly to RAW264.7, which also lack ASC (249) yet also shed MV in response to $P2X_7$ stimulation (250). These results support the conclusion that MV distinct from previously characterized MHC class II+ exosomes are shed by myeloid cells and stimulate primary macrophages through a TLR4-dependent process involving recognition of phospholipids contained within MV.

Endogenous phospholipids can activate macrophages through TLR4. Recently, it was demonstrated that oxidized low density lipoprotein (oxLDL), which binds to the scavenger receptor B family member CD36, can promote sterile inflammation through activation of TLR4/6 heterodimer on macrophages (41). Both cell death (289, 290) and foam-cell formation (291) have also been shown to be induced by oxidized LDL through TLR4 in macrophages. Furthermore, oxidized phospholipids from minimally modified low density lipoprotein (mmLDL), which contains essentially the same phospholipids as oxLDL, stimulate macrophage ROS generation (292), ERK activation (293), membrane spreading (294), and inhibition of

phagocytic uptake of apoptotic bodies (294), through a partially TLR4-dependent pathway. Whether phospholipids in $P2X_7$-induced MV are structurally similar to those in oxLDL or mmLDL will be addressed in future studies. My study suggests that the stimulatory phospholipid is not lysophosphatidic acid (Figure 2-12*E*). Commercially available LPA, phosphatidic acid or phosphatidylserine were also unable to activate BMDM (data not shown). Phosphatidic acid loading into liposomes did however show some potential for upregulating surface CD86 (Figure 2-14). It is possible that phosphatidic acid may alter membrane topology or composition through applied negative curvature to expose novel lipids that induce macrophage activation.

Importantly, $P2X_7$-induced MV from PLD1- and PLD2-inhibited MV producer cells were unable to activate macrophages (Figure 2-12*A*), although MV yields were equivalent between drug treated and non-drug treated cells (data not shown). This dissociates MV formation from incorporation of the stimulatory phospholipid into vesicles, and suggests that *de novo* generation of a bioactive phospholipid results from $P2X_7$ activation leading to downstream PLD activation. Whereas PLD (156), $iPLA_2$, and $cPLA_2$ (155) are activated following $P2X_7$ activation (data not shown), blocking PLD activity, but not $iPLA_2$ or $cPLA_2$, impaired the MV-activating capacity (Figure 2-12). These results may explain why cell homogenates of producer cells were unable to stimulate macrophage activation (Figure 2-3*B, C*), i.e., because PLD was not activated. Activated PLD produces phosphatidic acid to coordinate ADP-ribosylation factor-6, a known regulator of exocytosis, to sites of potential exocytosis (295). Future studies will understand the specific PLD activities that enable stimulatory phospholipid loading into $P2X_7$-induced MV.

It has been suggested that host cell-derived stimulators of TLR activity might contain microbial contaminants introduced during biochemical purification, a hypothesis described in

detail recently in a thought-provoking review (22). Based on this, I considered whether MV preparations might contain endotoxin. When tested by *Limulus* amebocyte lysate assay, endotoxin was present within stimulatory MV preparations at low levels, typically ~0.25 EU/ml (data not shown). However, the same amount of endotoxin is observed in non-stimulatory MV from PLD-inhibited cells (data not shown), indicating that these low levels cannot explain the stimulation I observe. Furthermore, treatment of BMDM with equivalent amounts of LPS to that found in MV (~50 pg/ml LPS for 25 μg protein equivalents of MV) did not induce significant TNF-α release or CD86 upregulation (data not shown). It should also be noted that in addition to testing non-stimulatory MV, I observed that cell homogenates, non-surface derived MV, and ultracentrifugation supernatants were also devoid of BMDM-stimulating activity.

My study suggests that MV derived from macrophages in an environment where there is tissue damage without infection could have potent biological activities that may further drive inflammation. In tumors and other settings with significant necrosis, infiltrating macrophages expressing $P2X_7$ would be exposed to elevated levels of extracellular ATP, as previously shown in tumors (162, 296, 297). Macrophage-produced MV would then bind to adjacent cells, including macrophages and DCs, leading to their activation and resulting in secretion of TNF-α and potentially other pro-inflammatory mediators. The most novel aspect of this work, implicating phospholipids from MV as the stimulatory component, is consistent with recent work implicating phospholipids in inflammation present in atherosclerotic lesions, as discussed above. In cancer and in atherosclerosis, as well as potentially in other pathological settings, there are strong indications that sterile inflammation plays a role in disease processes through largely unknown mechanisms. Innate responses by macrophages in inflammatory diseases may in part be explained by release of stimulatory phospholipids in MV at sites of tissue damage.

3.0 ATP PROMOTES THE RELEASE OF MATURE CATHEPSIN D IN A DYNAMIN-DEPENDENT MANNER

3.1 AUTHORS AND THEIR CONTRIBUTIONS

L. Michael Thomas (Graduate Program in Immunology, University of Pittsburgh School of Medicine) designed and performed the experiments and prepared the manuscript; his funding was supported by an NIH training grant T32CA082084. Russell D. Salter (Department of Immunology, University of Pittsburgh School of Medicine) designed the scope of the study and edited the manuscript; his funding was supported by NIH funds R01AI072083 and P01CA073743. Chengqun Sun engineered the HEK293 cell line to express human $P2X_7$ and the FSDC cell line to express dynamin-GFP or dynamin (K44A)-GFP, which were used in this study. Various contributors provided reagents including murine bone marrow and cell lines, which are discussed and acknowledged within the *Materials and Methods*.

3.2 ABSTRACT

ATP engagement of purinergic receptors can promote the displacement and secretion of several intracellular inflammatory components from PAMP-primed and non-primed myeloid cells. Moreover, ATP can elicit the release of lysosomal hydrolases, which can have potent effects on the surrounding extracellular matrix that contribute to tissue structure. In this study, I sought to understand how lysosomal components such as cathepsin D are released from ATP-treated, non-primed, myeloid cells. I found that ATP-induced microvesicles contained both endosomal and lysosomal forms of cathepsin D. Prior to microvesicle generation, ATP displaced cathepsin D from within main cell bodies to the periphery of cells. The release of the mature form of cathepsin D was dependent upon $P2X_7$. The cathepsin D released in response to ATP was biologically active. Additionally, the secretion of mature cathepsin D was partially blocked by dynasore, a specific inhibitor of dynamin. Dynasore also decreased the peripheral expression of cathepsin D from the main cell body of myeloid cells. At the same time, stable expression of dynamin-2 dominant negative (K44A) did not result in decreased mature cathepsin D secretion. This work illustrates the potential for dynamin to regulate lysosomal component exocytosis, which may prove to have roles in diseases provoked by released hydrolases such as cathepsins.

3.3 INTRODUCTION

ATP can promote the modification of proteins and lipids. This includes the ability to initiate biochemical alterations of these materials (e.g., cleavage of caspase-1) (78) and the redistribution of these materials from one location of the cell to another (e.g., exocytosis of IL-1β) (248). ATP engages a set of plasma membrane expressed ATP binding receptors called purinergic receptors (130). All together, purinergic receptors can shape the functions of cells including immune cells (37).

One critical aspect of intracellular trafficking is endocytosis, which is mechanistically carried out in several different ways. Most often depicted is clathrin-mediated endocytosis although there are several other endocytotic pathways, including caveolin-mediated, CLIC/GEEC-mediated, and flotillin-mediated endocytosis processes (298). Clathrin-mediated endocytosis is characterized by clathrin-coated pits that invaginate from the plasma membrane to allow the internalization of materials from outside the cell to inside the cell. This invagination process is in part governed by dynamin, a plasma membrane localized GTPase that can constrict the plasma membrane in a turn-style fashion. Eventually, dynamin induced constriction results in the pinching off of these invaginations to form endosomes. Caveolin and flotillin act differently where invaginated membrane form caveolae. Similar to clathrin, dynamin is required for caveolin-mediated endocytosis (299). Flotillin-mediated endocytosis is dynamin-independent (300). CLIC/GEEC-mediated endocytosis through glycosylphosphatidylinositol-anchored proteins (GPI-APs) is independent of dynamin (301) . ATP engagement of purinergic receptors

have been shown to regulate clathrin-mediated endocytosis (302) and phagocytosis by macrophages (174, 303).

Secretory granule (SG) exocytosis is a coordinated process that involves aspects of intracellular trafficking and for certain SG, such as secreted lysosome related organelles (LRO), this can involve endocytosis (194). Upon outside-in signaling, conventional SG are first trafficked from the Golgi to the plasma membrane. After docking and fusing with the plasma membrane, SG release their harbored content. An immunological example of a conventional SG would be the degranulation of mast cells for the release of histamine. SG release does not necessarily require endocytosis pathways.

By contrast, LRO traffic differently. Premature components of LRO are sent from the Golgi apparatus to the plasma membrane following homeostatic cues. From the plasma membrane, immature LRO are endocytosed back into the cell, where they can eventually fuse with pre-existing multi-vesicular bodies (MVB) to form mature LRO, which are held in check until calcium-driven signals promote their movement to the plasma membrane. LRO are trafficked to the plasma membrane through calcium-independent polymerizing microtubules. At the plasma membrane, calcium-dependent fusion by SNARE proteins and synaptotagmins enables the release of LRO components into the extracellular environment.

ATP engagement of purinergic receptors found on myeloid cells have prompted the loss of cellular materials including the release of plasma membrane derived microvesicles (MV) (217, 245), exosomes from MVB (211, 259), and LRO (154). The manner in which ATP mechanistically performs these activities is not clear. Plasma membrane-derived MV shedding following ATP ligation of purinergic receptors is described to occur in a calcium-dependent

manner (217). These particular MV can be shed from either non-primed or PAMP-primed myeloid cells (249, 259). In contrast, purinergic receptor initiation for exosome exocytosis is described to require PAMP priming for the expression of the inflammasome component NLRP3, which promotes exosome exocytosis (259). The release of LRO is described from PAMP-activated myeloid cells (258); however, the group that conducted this study did not elaborate on the need for PAMP priming.

In this study, I describe a mechanism for LRO component (cathepsin D) exocytosis from non-primed myeloid cells. In response to 3 mM ATP, FSDC, a model cell line for murine immature dendritic cells, and murine bone marrow derived macrophages (BMDM) demonstrated abilities to shed 0.5-1 μm sized MV that contain both intermediate (endosomal) and mature (lysosomal) forms of cathepsin D. By 15 min, ATP promoted the displacement of lysosomal components away from the main cell bodies of cells. This displacement was dampened by inclusion of dynasore, a dynamin inhibitor. Furthermore, dynasore significantly decreased the secretion of mature, but not intermediate, cathepsin D. Dynamin itself was redistributed away from the main bodies of cells. In contrast to the effects of dynasore, however, I did not observe a significant decrease of cathepsin D secretion from FSDC that stably expressed a dominant negative form of dynamin-2. Regardless, this study suggests the possibly that dynamin may regulate the eventual secretion of ATP-induced release of LRO.

3.4 MATERIALS AND METHODS

Cell culture and reagents - FSDC, an immortalized murine immature dendritic cell line via retroviral transduction of a vector carrying an envAKR-mycMH2 fusion gene (304), (gift from P. Ricciardi-Castagnoli, Singapore Immunology Network, Singapore) was maintained in IMDM (Lonza, Basel, Switzerland) supplemented with 10% fetal bovine serum (FBS) (Gemini Bio-Products, West Sacramento, CA), 1% additional L-glutamine (Lonza), and 1% penicillin and streptomycin (Lonza). This IMDM supplemented media will hereafter be referred to as IMDM complete. Murine bone marrow derived macrophages (BMDM) were derived from bone marrow precursors (gift from L. Borghesi, University of Pittsburgh) differentiated with L-cell supplemented media as described previously (265). HEK293 cells tranduced to express human $P2X_7$ or control vector (305) are maintained in DMEM (Mediatech, Manassas, VA) complete with 10% FBS, 1% additional L-glutamine, 1% penicillin and streptomycin, and 500 μg/ml G418. For some experiments, 1 μg/ml of lipopolysacharides (LPS) from *Escherichia coli* 026:B6 (Sigma-Aldrich, St. Louis, MO) was used to prime the cells where indicated. Other regents include ATP (Thermo Fisher Scientific, Waltham, MA), A23187 (Sigma-Aldrich), latrunculin A (Invitrogen, San Diego, CA), and dynasore (EMD Chemicals, Gibbstown, NJ).

MV generation and harvest - 60 million FSDC or BMDM were plated in culture within T225 cm^2 flasks per treatment. Following 4 h to allow cells to adhere (or to also become LPS primed as described above), the cells were washed twice with 25 ml PBS. Cells were then treated with no treatment or 3 mM ATP treatment within 40 ml serum-free IMDM with no additions for 30 min at 37°C. Following the 30 min of treatment, supernatant was harvested off and

centrifuged at 309.1 x *g* for 10 min to pellet potential non-adherent cells. The supernatant following the 309.1 x *g* centrifugation was further separated with 100,000 x *g* ultracentrifugation for 1 h. The pellet fraction from the 100,000 x *g* ultracentrifugation was resuspended within 15 μl 4 x sample buffer to be subsequently run on an SDS-PAGE for western blotting.

In some instances, 800 nM latrunculin A was given in IMDM with no additions for 30 min prior to 3 mM ATP administration. 3 mM ATP was administered in the presence of 800 nM latrunculin A. MV generation and harvest proceeded as described above.

Biologically active cathepsin D studies - 2 million FSDC were plated within 6-well plates with IMDM complete then non-treated or 3 mM ATP treated for 30 min. Supernatant was collected following treatment then centrifuged at 1200 x *g* to pellet potential cells. The subsequent supernatant following the centrifugation was then stored at -80°C until utilized in the fluorimetric SensoLyte 520 Cathepsin D Assay Kit (AnaSpec, Fremont, CA). Determination of biologically active cathepsin D was performed following the manufacturer's protocol.

Western blotting - For whole supernatant experiments, 2 million cells were plated within 6-well plates with IMDM complete. Cells were washed twice with serum-free IMDM with no additions then given treatment where indicated. Some studies included a 30 min dynasore treatment prior to 3 mM ATP addition in the presence of dynasore. HEK293 studies included samples treated with 10 μM A23187 alone, 6 mM ATP alone, or 10 μM A23187 plus 6 mM ATP. Following treatment, the entire cell culture supernatant was centrifugated at 10,000 x *g* for 30 s and then the resulting centrifugation supernatant was concentrated via trichloroactetic acid and 10% cholic acid as described in (265) and loaded with 4 x sample buffer onto a 9% SDS-PAGE gel for protein electrophoresis. For HEK293 studies, cell lysates were prepared in 1% NP-

40 lysis buffer as described in (265). Protein from HEK293 cell lysates were quantified by Bradford assay and 20 µg of protein were loaded along-side concentrated supernatants on a 9% SDS-PAGE gel. Protocols for electrophoresis, subsequent protein transfer, and western blotting are described in (265). Western blot was performed using the SNAP-ID according to manufacturer's procedures (Millipore, Billerica, MA). Western blotting for cathepsin D was performed with 1/66.7 diluted goat anti-cathepsin D (Santa Cruz Biotechnology, Santa Cruz, CA) then subsequent with 1/1666.7 diluted HRP-conjugated donkey anti-goat IgG (Santa Cruz Biotechnology). In other studies, western blotting was performed with 1/1000 diluted rabbit anti-dynamin-2 (Santa Cruz Biotechnology), 1/1000 diluted mouse anti-GFP (Millipore), 1/1000 diluted mouse anti-β-actin (Sigma-Aldrich), 1/1666.7 diluted HRP-conjugated donkey anti-rabbit IgG (Biolegend, San Diego, CA), and 1/1666.7 diluted HRP-conjugated goat anti-mouse IgG (Santa Cruz Biotechnology). Signals were developed using Western blotting luminol reagent (Santa Cruz Biotechnology). Imaging and densitometry was performed with KODAK Image Station 4000MM and its accompanying KODAK MI SE Software Informer (Carestream Molecular Imaging, New Haven, CT). Densitometry readings are reported as relative percentages calculated for a band net intensity divided by the sum of the net intensities of similar molecular weight bands for all analyzed samples.

Microscopy - For confocal microscopy studies, 200,000 FSDC or BMDM were plated on poly(d-lysine)-coated coverslips within 24-well plates. Cells were allowed to adhere for at least 4 h. 4 h LPS priming (as described above) was performed for BMDM where indicated. Following the 4 h, cells were washed once with PBS then given treatments where indicated. After treatment, supernatant was discarded and the cells were washed once with PBS. 2% paraformaldehyde fixative was applied for 15 min at room temperature.

For antibody labeling experiments, after the fixation step, fixative was removed and replaced with 50 mM glycine for 5 min, then blocked and permeabilized with 1.5% BSA and 0.5% saponin in PBS for 30 min at room temperature. Coverslips were washed once with PBS then given primary antibody of 1/100 diluted rat anti-Lamp-1 (eBioscience, San Diego, CA), 1/500 diluted Alexa-488 conjugated rat anti-Lamp-1 (Biolegend, San Diego, CA), and/or 1/50 diluted rabbit anti-cathepsin D (Santa Cruz Biotechnology) where indicated at room temperature for 1 h. Coverslips were washed three times with 0.5% saponin in PBS then given 1/100 diluted Alexa-647 conjugated goat anti-rabbit IgG (Invitrogen) or 1/100 diluted Cy5 conjugated goat anti-rat IgG (Jackson Laboratories) along with 400 nM rhodamine phalloidin (Sigma-Aldrich) where indicated at room temperature for 1 h. Coverslips were washed three times with 0.5% saponin in PBS then given 1 μg/ml DAPI (Sigma-Aldrich) for 30 s. Coverslips were washed three times with PBS before mounting onto a glass slide with gelvatol (gift from CBI).

To track cathepsin D without permeabilizing cells, prior to ATP treatment, cells were given 10 μM BODIPY-pepstatin-A (Invitrogen) for 30 min. Following treatment, cells were fixed as described above, washed three times with PBS, then mounted with gelvatol on a glass slide for confocal microscopy.

Confocal microscopy images were taken with an Olympus Fluoview 1000 (Inverted) (Olympus America, Inc., Center Valley, PA). Live cell microscopy images were taken from Nikon A1 Confocal Live Cell System (Nikon Instruments Inc., Melville, N.Y.). Laser excitations were collected sequentially and background noise was minimized. Confocal microscopy included DIC microscopy. Live cell microscopy was conducted without delayed exposures; ATP was added after one minute of starting the 20 min time course. Final images were taken from

each microscope and cropped using Adobe Photoshop CS2 (Adobe, San Jose, CA). Analysis of live cell microscopy was performed with NIS Elements Viewer (Nikon Instruments Inc.)

For obtaining counts of percentage of cells with budding cathepsin D, 10 random fields of view were collected respective for each treatment. Each field of view had at least 10 cells with determinable localization of cathepsin D. Averages and SEM were obtained from 3 separate experiments. Cells were considered positive for peripheral cathepsin D if cathepsin D was observed outside of the main cell body as determined with BODIPY-pepstatin-A overlaid with DIC microscopy. An example of a cell that was counted as positive or negative is in Figure 3-5.

Dynamin-GFP and Dynamin K44A-GFP – Dynamin 2-GFP plasmid (K44K) and dynamin 2-(K44A)-GFP (dominant negative) plasmid were gifts from L. Traub (University of Pittsburgh). Rat dynamin 2-GFP (K44K) and dynamin 2-dominant negative-GFP (K44A) fragments were amplified from the plasmids containing rat dynamin 2-GFP (K44K) and dynamin 2-dominant negative-GFP (K44A) by PCR, respectively. The primers with Not I or EcoR I sites were as follows: forward primer, 5'- TTATTGCGGCCGCCTCAAGCTTGGCACCATGG -3'; reverse primer, 5'- AGTCTTAAGGAATTCATCACTTGTACAGCTCGTCCAT -3'. The Expand high fidelity PCR system (Roche Applied Science, Indianapolis, IN) was used for PCR reactions. The PCR amplicons were then cloned into the retroviral pFB/neo vector with neomycin-resistant gene using Not I and EcoR I restriction enzymes and the Rapid DNA Ligation Kit (Roche Applied Science). The corresponding sequences subcloned into vectors were verified by DNA sequencing.

For making retroviruses, retroviral packaging gp293 cells were plated in six-well plates 1 day before and co-transfected with retroviral constructs containing dynamin 2-GFP (K44K) or

dynamin 2-dominant negative-GFP (K44A) and with VSV-G vector using Lipofectamine™ LTX Reagent. 4 μg retroviral constructs, 2 μg VSV-G vector, 5 μl Plus™ reagent, and 10 μl Lipofectamine™ LTX Reagent in 500 μl of Opti-MEM® I Reduced Serum Medium were used per well with 2 ml media. Then the plates were incubated at 37°C, 5% CO_2 for 4 h, and replaced with 3 ml fresh media and continue to incubate for 2-3 d. The media which contain retroviruses were harvested and filtered. The filtered media were aliquot and stored at -80°C for transduction.

For transduction, 30,000-40,000 cells of FSDC cells were plated in 12-well plates a day before and infected by replacing their media with 1 ml retroviral preparation containing 3 μg polybrene and incubated for 1 d, then replaced with media containing with 1 mg/ml G418 for 3-5 weeks to generate stably expressing cell lines and maintained in 500 μg/ml G418.

LDL-endocytosis assays – One million native FSDC and dynamin K44A FSDC were given 10 μg/ml LDL conjugated to Alexa594 (Invitrogen) in 1 ml IMDM complete for 1 h. Flow cytometry was performed with a BD Biosciences LSR II and results analyzed using FlowJo software (Tree Star, Inc., Ashland, OR).

Statistical analyses - Unpaired Student's *t* test was performed using Graph Pad Prism (GraphPad Software, La Jolla, CA). Values of *p* were calculated where indicated, and for all statistical studies $p<0.05$ was considered as significant.

3.5 RESULTS

3.5.1 ATP promotes the release of MV that contain mature cathepsin D

Microvesicle shedding has previously been acknowledged as a function of ATP acting on the $P2X_7$ purinergic receptor (211, 217, 236, 245, 259). Given the reports of cathepsin secretion following $P2X_7$ stimulation of macrophages (186) and $P2X_7$-mediated exocytosis of LRO (154), I examined whether cathepsin D would be enriched within MV fractions. MV harvested from 3 mM ATP treated BMDM (Fig. 3-1, top panel) and FSDC (Figure 3-1, bottom panel) expressed both immature cathepsin D (46 kDa) and mature cathepsin D (33 kDa). LPS priming of BMDM was not a requirement for the expression of cathepsin D within harvested MV. Latrunculin A, an actin polymerization inhibitor, decreased the expression of cathepsin D observed within harvested MV from ATP treated FSDC (Figure 3-1, bottom panel). In agreement with ATP induced secretion of cathepsin D (as detected by western blot), ATP induced the secretion of biologically active cathepsin D secreted from FSDC (Figure 3-2).

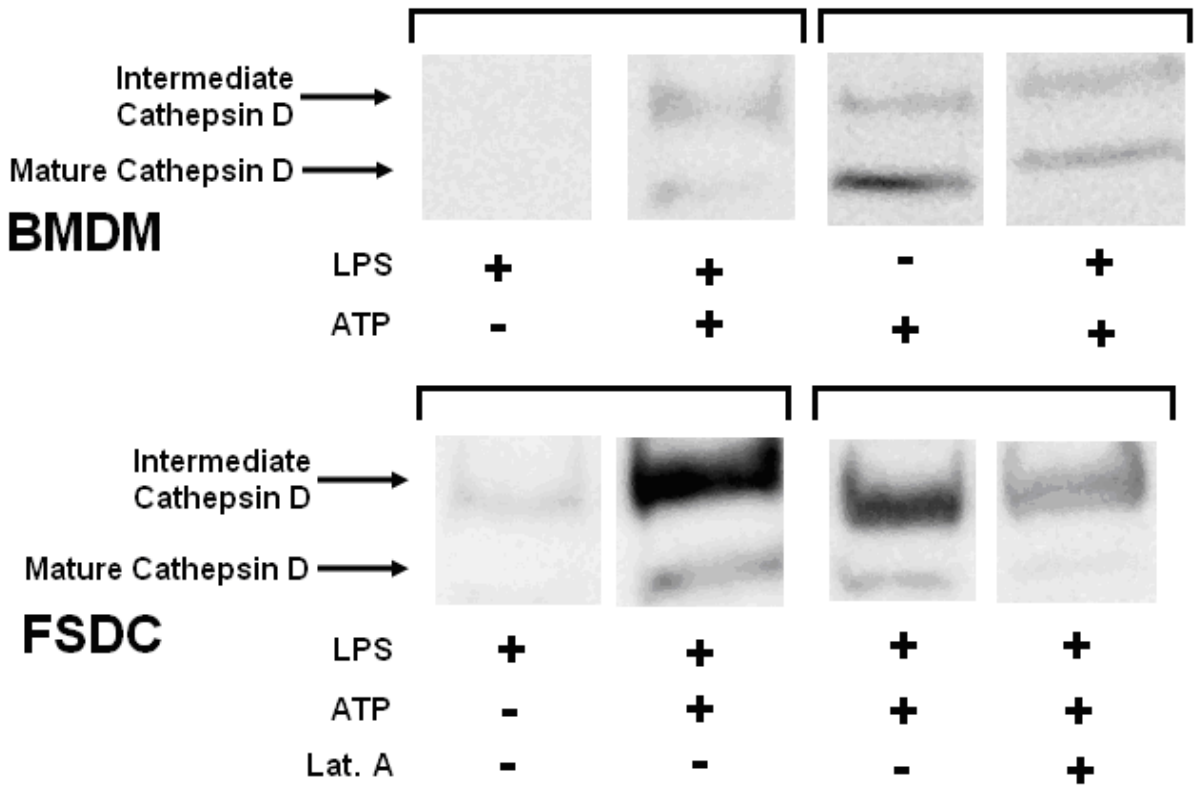

Figure 3-1: ATP-induced MV contain intermediate and mature forms of cathepsin D regardless of initial LPS priming.

BMDM (top panel) and FSDC (bottom) panel were treated with 1 µg/ml LPS or non-treated for 4 h. For FSDC, some samples were also given 800 nM latrunculin A (Lat. A) given for the final 30 min of the LPS treatment. Following the 4 h, cells were non-treated or treated with 3 mM ATP for 30 min. Supernatants were processed for MV harvest. The resulting pellet fractions following 100,000 x *g* ultracentrifugation were processed for western blot determination of intermediate cathepsin D (46 kDa) and mature cathepsin D (33 kDa). Brackets indicate individual western blots. The blots shown here are representative of repeated experiments.

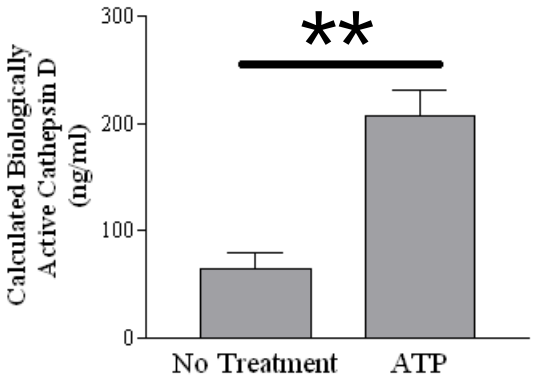

Figure 3-2: ATP promotes the release of biologically active cathepsin D.

FSDC were treated with or without 3 mM ATP for 30 min. Biologically active cathepsin D was measured and determined according to manufacturer's protocol. The histogram shows means of determined biologically active cathepsin D ± SEM of $n = 3$. $^{**}p<0.01$.

3.5.2 $P2X_7$ is an ATP-activating receptor for mature cathepsin D release

To confirm that $P2X_7$ was the activating receptor for the release of mature cathepsin D, I utilized native HEK293 cells, which do not express $P2X_7$, or HEK293 cells that express human $P2X_7$ (HEK293-$P2X_7$) (305). Only HEK293-$P2X_7$ released mature cathepsin D in response to ATP (Figure 3-3). To validate that the mechanism was specifically due to a novel function of $P2X_7$ and was not just due to an influx of calcium, I also treated cells with the calcium ionophore A23187, which alone failed to produce mature cathepsin D from either HEK293 cell type (Figure 3-3). However, A23187 in combination with 6 mM ATP though released even more mature cathepsin D than ATP alone from HEK293-$P2X_7$. This is in agreement with our previous findings that A23187 potentiates $P2X_7$ function (236).

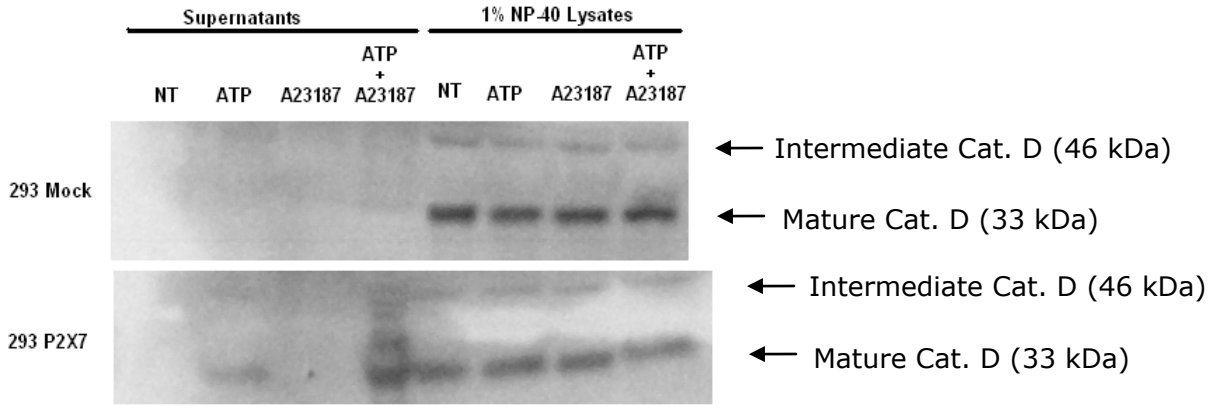

Figure 3-3: $P2X_7$ expression promotes mature cathepsin D secretion.

HEK293 (mock transduced) or HEK293 (expressing human $P2X_7$) were treated with no treatment (NT), 6 mM ATP, 10 μM A23187, or 6 mM ATP plus 10 μM A23187 for 30 min. Supernatants and lysates were evaluated for their expression of intermediate and mature forms of cathepsin D by western blot. The western blot shown is representative of repeated experiments.

3.5.3 ATP promotes the displacement of lysosomal components towards the periphery of treated cells

$P2X_7$ activity can promote LRO exocytosis (154). To characterize the potential for LRO exocytosis, localization of Lamp-1 and cathepsin D were determined between non-treated BMDM (Figure 3-4*A*) and 3 mM ATP-treated BMDM (Figure 3-4*B*). ATP treated BMDM displayed a peripheral (to the main cell body) localization of Lamp-1 and cathepsin D. Similar to direct antibody labeling of cathepsin D, BODIPY-pepstatin A signal (to label cathepsin D) was significantly localized to the periphery of 3 mM ATP treated FSDC (Figure 3-5).

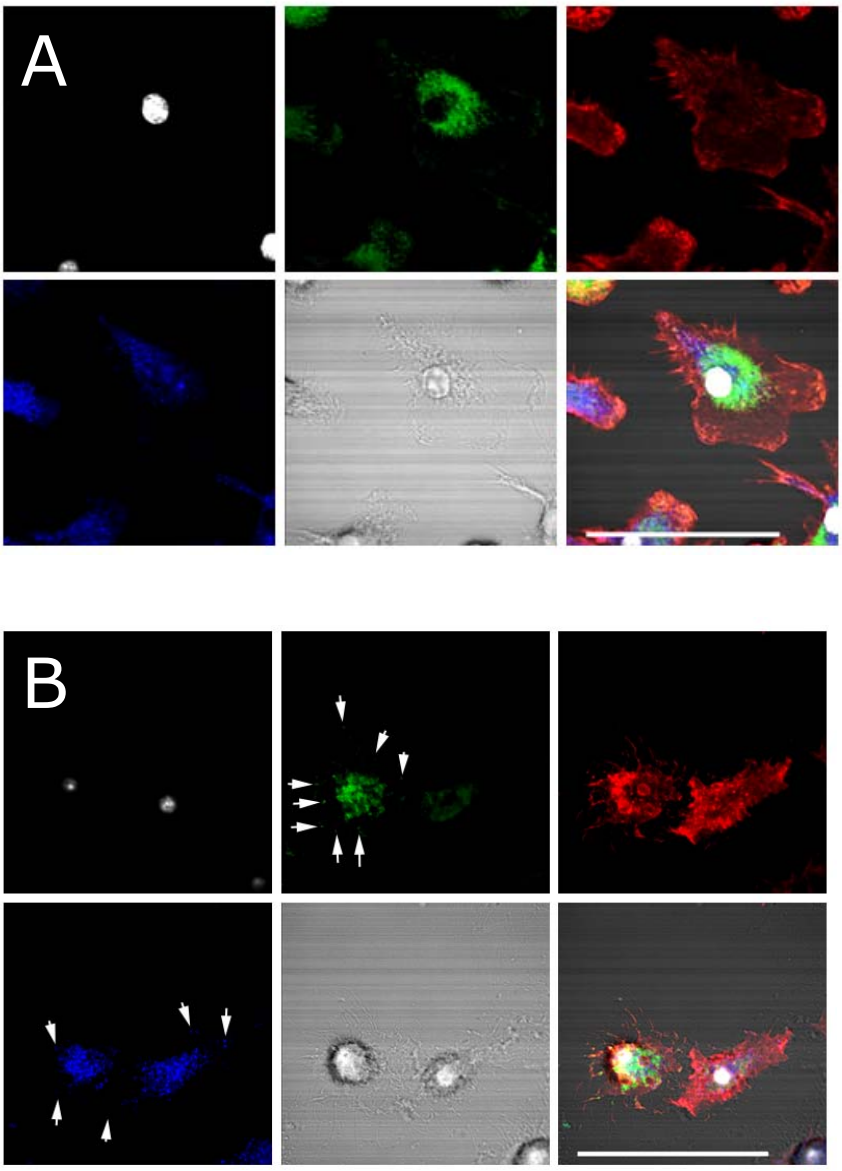

Figure 3-4: ATP promotes the displacement of cathepsin D and lamp-1 to the periphery of cells away from the main cell body of BMDM.

BMDM were left untreated (A) or treated with 3 mM ATP (B) for 15 min. Cells were stained for nuclei (gray, top left), lamp-1 (green, top middle), F-actin (red, top right), and cathepsin D (blue, bottom left). DIC microscopy (bottom middle) and overlay of all of the stains and DIC are included (bottom right). White arrows indicate peripheral expression. Images are representative of repeated experiments. Scale bar, 10 μm.

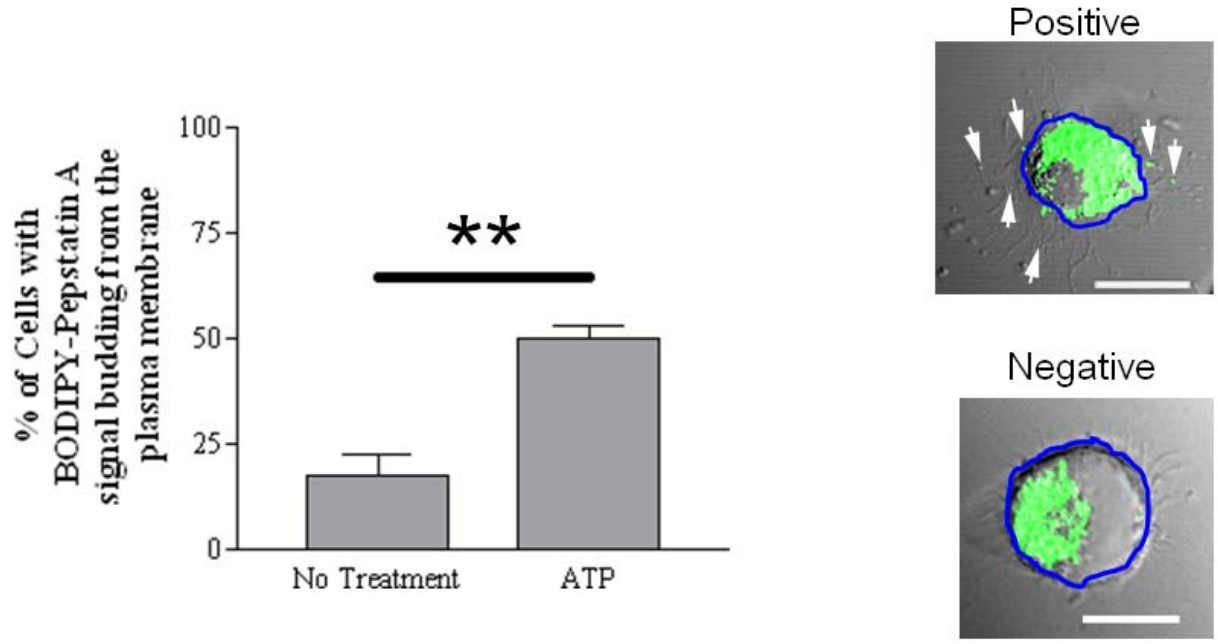

Figure 3-5: ATP promotes the displacement of cathepsin D to the periphery, away from the main cell bodies of FSDC.

FSDC were incubated with 10 µM BODIPY-pepstatin A for 30 min. Cells were cultured with or without 3 mM ATP for 15 min. BODIPY-pepstatin A signal (green) was analyzed by confocal microscopy. Individual cells were determined to be "positive" or "negative" for having BODIPY-pepstatin A signal away from their main cell bodies towards the periphery. Examples of positive and negative cells are included on the right half of the figure. The blue lines with the example images are included for clarity of the main cell bodies, which are clear with the original DIC images. White arrows indicate peripheral expression. The histogram shows the mean number of cells with displaced BODIPY-pepstatin A ± SEM of $n = 3$. Scale bar, 10 µm. $^{**}p<0.01$.

3.5.4 Dynasore inhibits mature, but not intermediate, cathepsin D secretion from ATP treated cells

Dynamin activity can be involved in the release of lytic granules (306, 307), the release of insulin granules (308), and catecholamines release from chromaffin cells (309). Furthermore, dynamin is a regulator of topological changes of the plasma membrane for exocytosis of secretory granules following their fusion with the plasma membrane (310). Given the similarity of these secreted compartments to secretory lysosomes, I then asked if dynamin was involved for cathepsin D exocytosis from myeloid cells. Pre-treatment of dynasore, an inhibitor of dynamin-1 and dynamin-2 (311), prior to ATP administration was able to significantly decrease the secretion of mature but not intermediate cathepsin D (Figure 3-6*A*-*C*). 100 µM dynasore significantly decreased mature cathepsin D expression as compared to 3 mM ATP treatment alone. Dynasore was not toxic to treated FSDC (data not shown), it does not decrease cathepsin D expression within cell lysates (data not shown), and it functioned to block LDL receptor-mediated endocytosis (data not shown), which occurs in a clathrin-dependent manner (312).

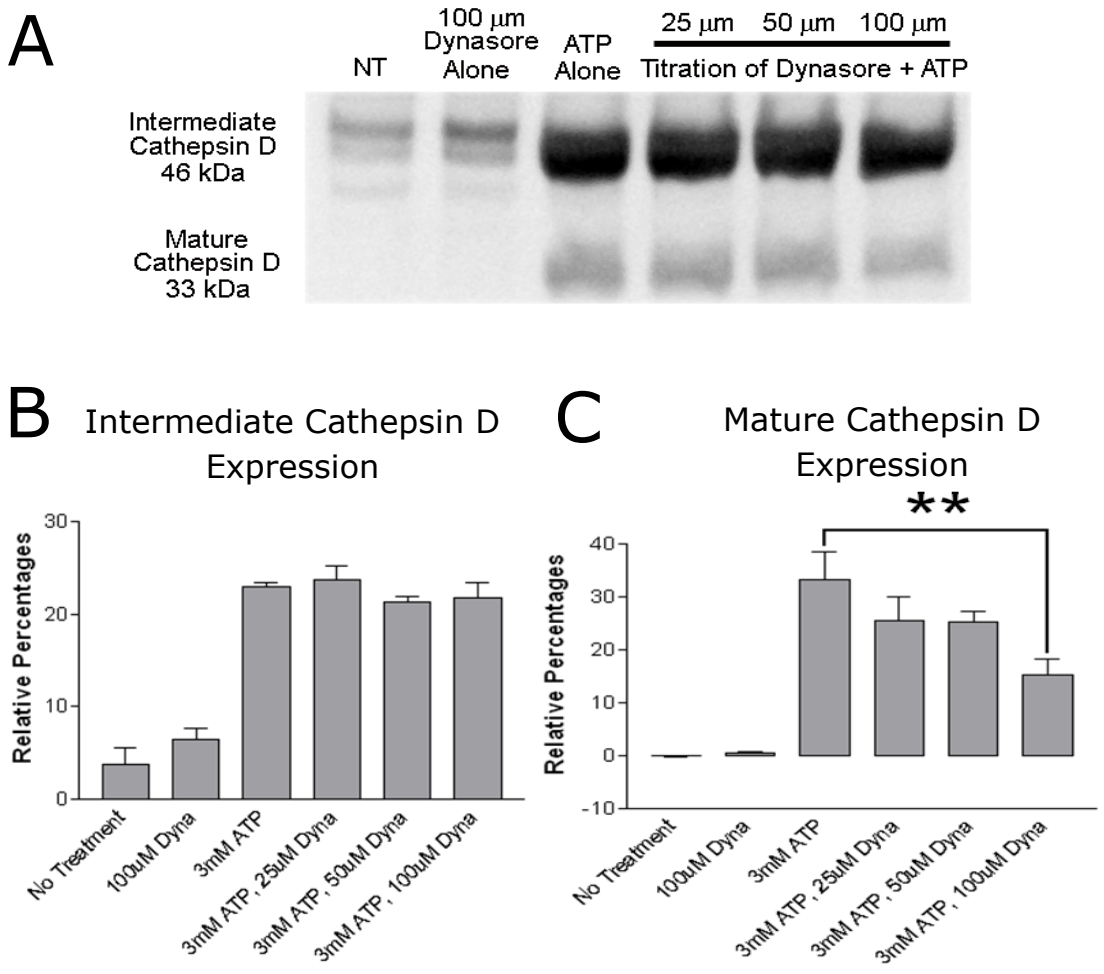

Figure 3-6: Dynasore treatment significantly decreases mature, but not intermediate, cathepsin D secretion.

FSDC were treated with various doses of dynasore (Dyna) for 30 min. Following dynasore treatment, cells were non-treated or treated with 3 mM ATP for 30 min. Supernatants were analyzed for expression of the intermediate and mature forms of cathepsin D by western blot. A representative blot is shown in A. Densitometry analysis indicates means of relative abundance of intermediate (B) and mature (C) forms of cathepsin ± SEM of $n = 3$. $^{**}p<0.01$.

To further evaluate the effects of dynasore treatment prior to ATP-mediated cathepsin D secretion, I considered that dynasore may affect the amount of cathepsin D observed at the periphery. Dynamin is primarily localized at the plasma membrane for its function in endosomal recycling, but it has been proposed to play roles in other intracellular trafficking events (298). Dynasore pretreatment resulted in decreased amounts of cathepsin D in the cell periphery, in response to 3 mM ATP (15 min); however, the decrease was not significant from three experiments (Figure 3-7).

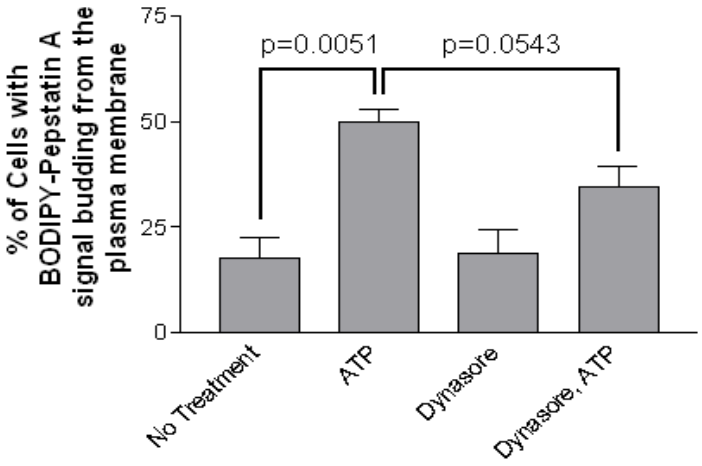

Figure 3-7: Dynasore decreases the peripheral expression of cathepsin D away from the main cell body following ATP treatment.

FSDC were were incubated with 10 µM BODIPY-pepstatin A for 30 min. Cells were non-treated or treated with 100 µM dynasore for 30 min. Cells were non-treated or treated with 3 mM ATP for 15 min. BODIPY signal and analysis was determined as described in Figure 3-5. The histogram indicates mean number of cells with displaced BODIPY-pepstatin A ± SEM of $n = 3$.

3.5.5 Over-expressed dynamin-2 localizes to the periphery upon ATP treatment

Given its involvement in potentiating mature cathepsin D secretion across the plasma membrane of ATP treated cells (Figure 3-6), I hypothesized that dynamin itself may be localized to the periphery of ATP treated cells, away from cellular main bodies. To test this hypothesis, I expressed dynamin-2 fused to GFP within FSDC. Without ATP treatment, dynamin-2-GFP signal was mainly retained within main cell bodies (Figure 3-8*A*) with strong expression at the plasma membrane. Upon 3 mM ATP treatment, dynamin-2-GFP was redistributed to the periphery with a noticeable loss from the main cell bodies within seconds (Figure 3-8*B, C, D*). This rapid loss was not observed for non-treated cells (Figure 3-8*D*); the loss over the longer course of time of non-treated and ATP-treated cells may have been due to instability of the GFP fluorochrome under the constant laser excitation employed in these experiments.

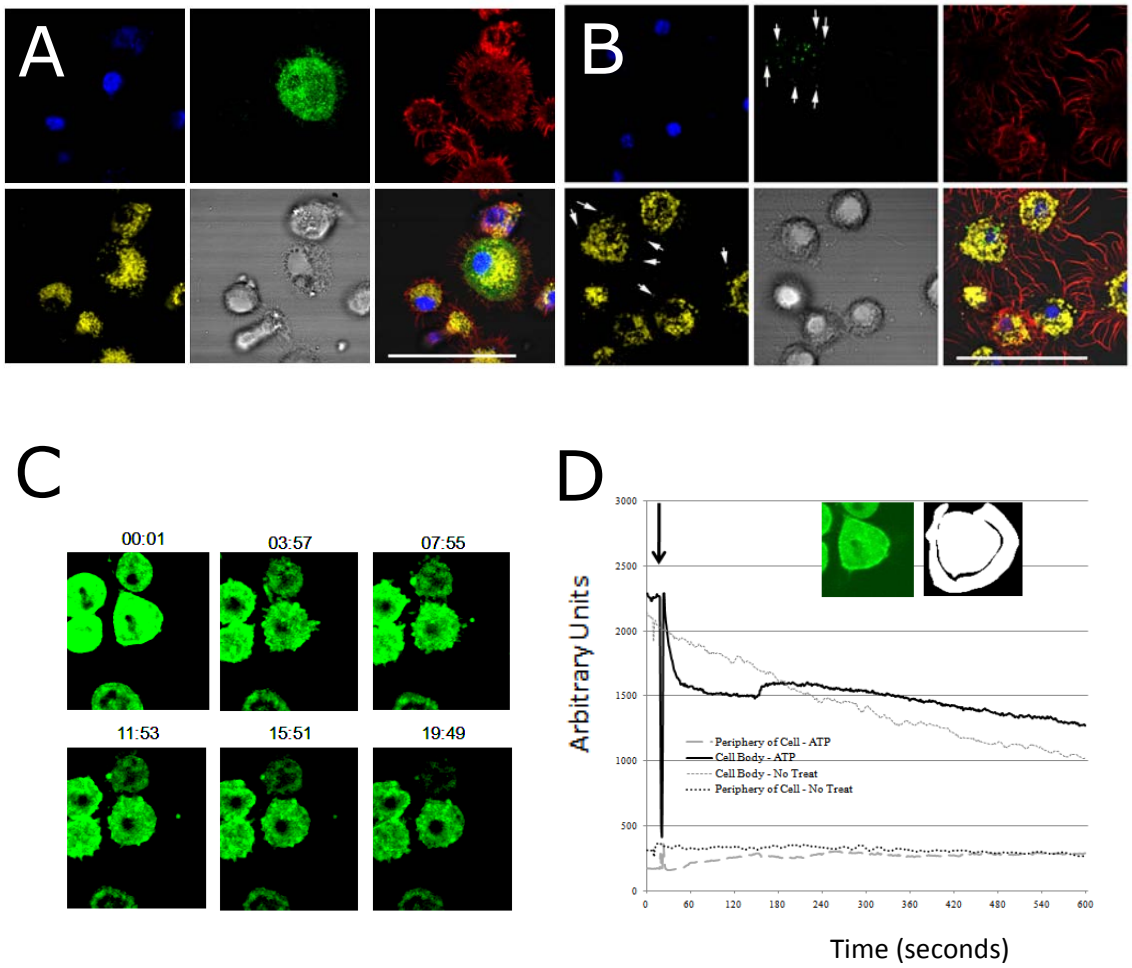

Figure 3-8: ATP promotes the displacement of dynamin to the periphery of cells away from the main cell bodies.

FSDC expressing dynamin-GFP were left untreated or treated with 3 mM ATP. In A and B, following 15 min of treatment, cells were fixed and stained for confocal microscopy. Cells were stained for nuclei (blue, top left), F-actin (red, top right), and lamp-1 (yellow, bottom left). Dynamin-GFP (green, top middle) and DIC microscopy (bottom middle) were also analyzed. Overlay of all of the signals, including the DIC, are included (bottom right). White arrows indicate peripheral expression. Images are representative of multiple experiments. Scale bar, 10 µm. In C, cells were tracked over time (min:s) following 3 mM ATP treatment. ATP was given after the first min of live cell microscopy (indicated with black arrow in D). In D, non-treated and 3 mM ATP treated cells were tracked for peripheral expression of dynamin-GFP and main cell body expression of dynamin-GFP. Examples of the gating strategy for the periphery and main cell bodies of cells in included as an inset in D.

3.5.6 Dynamin-GFP (K44A) does not decrease cathepsin D secretion from ATP treated FSDC

To evaluate dynamin other than by inhibition with dynasore, I stably expressed dynamin-2 dominant negative (K44A) within FSDC to decrease the function of endogenous dynamin-2 (313). Expression of dynamin-2 (K44A) fused to GFP was determined both by flow cytometry (analysis of GFP expression in Figure 3-9*A*) and western blot (analysis of GFP blot and dynamin-2 blot in Figure 3-9*B*). Expression of dynamin-2-GFP was assessed as well (Figure 3-9*A, B*). Functionality of the dominant negative activity of dynamin-2 (K44A)-GFP was confirmed by observing a decrease in LDL endocytosis (Figure 3-9*C, D*). Upon 3 mM ATP challenge for 30 min though, there were no detectable differences in mature cathepsin D secretion between dynamin-2 (K44A)-GFP, dynamin-2-GFP, and native FSDC (Figure 3-10). This was in contrast to dynasore-mediated inhibition of dynamin as dynasore significantly decreased mature cathepsin D secretion (Figure 3-6*A*-*C*, Figure 3-10).

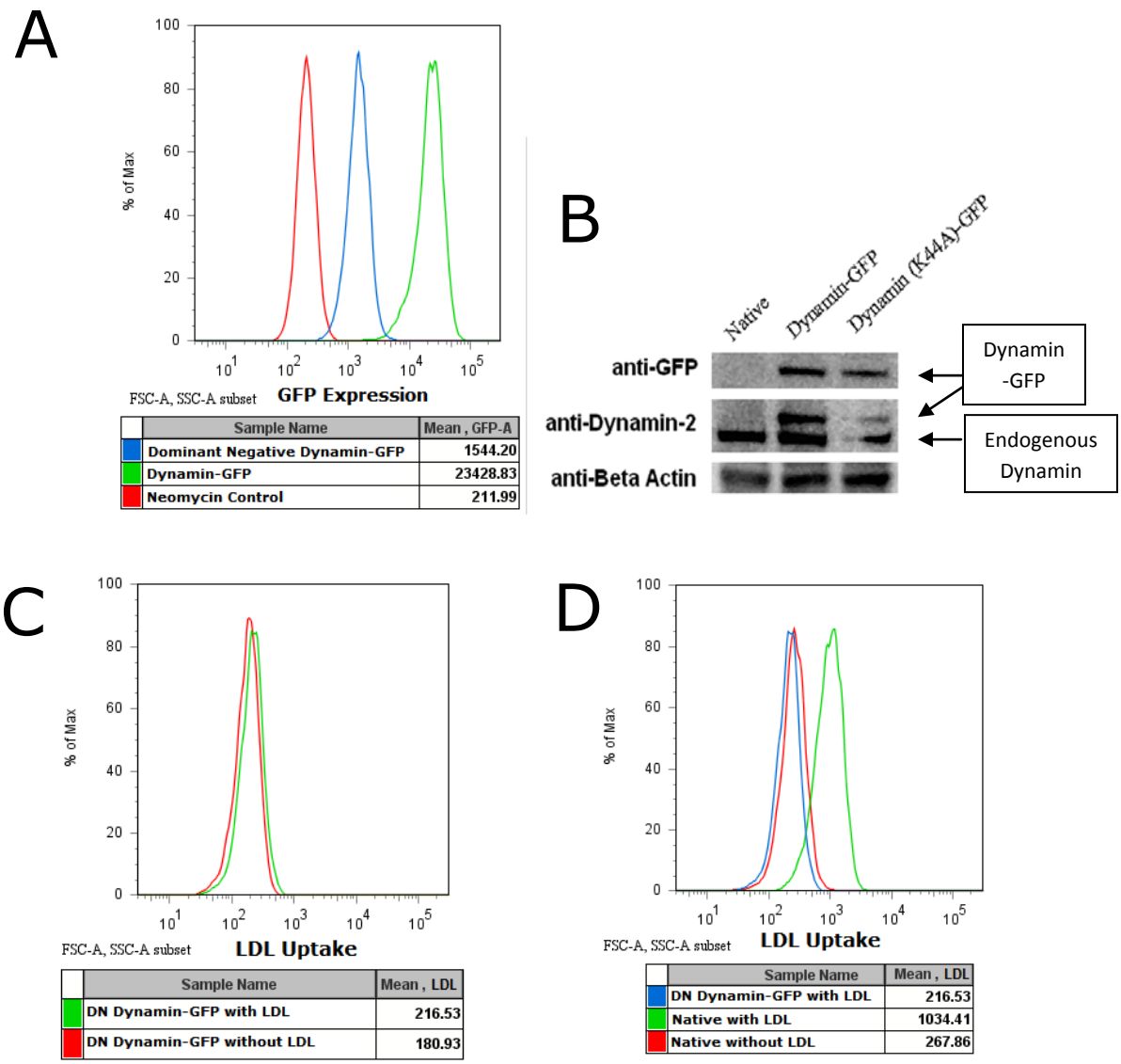

Figure 3-9: Dynamin (K44A)-GFP FSDC exhibit decreased LDL endocytosis

In A, neomycin control (red), dynamin-GFP (green), and dynamin (K44A)-GFP (blue) were evaluated for GFP expression by flow cytometry. In B, native, dynamin-GFP, and dynamin (K44A)-GFP FSDC cell lysates were evaluated for GFP and dynamin-2 expression by western blotting. In C, dynamin (K44A)-GFP FSDC were non-treated (red) or given 10 µg/ml of Alexa594-LDL (green) for 1 h. In D, native FSDC were non-treated (red) or given 10 µg/ml of Alexa594-LDL (green); dynamin (K44A)-GFP FSDC were given 10 µg/ml Alexa594-LDL (blue). C and D were conducted by flow cytometry.

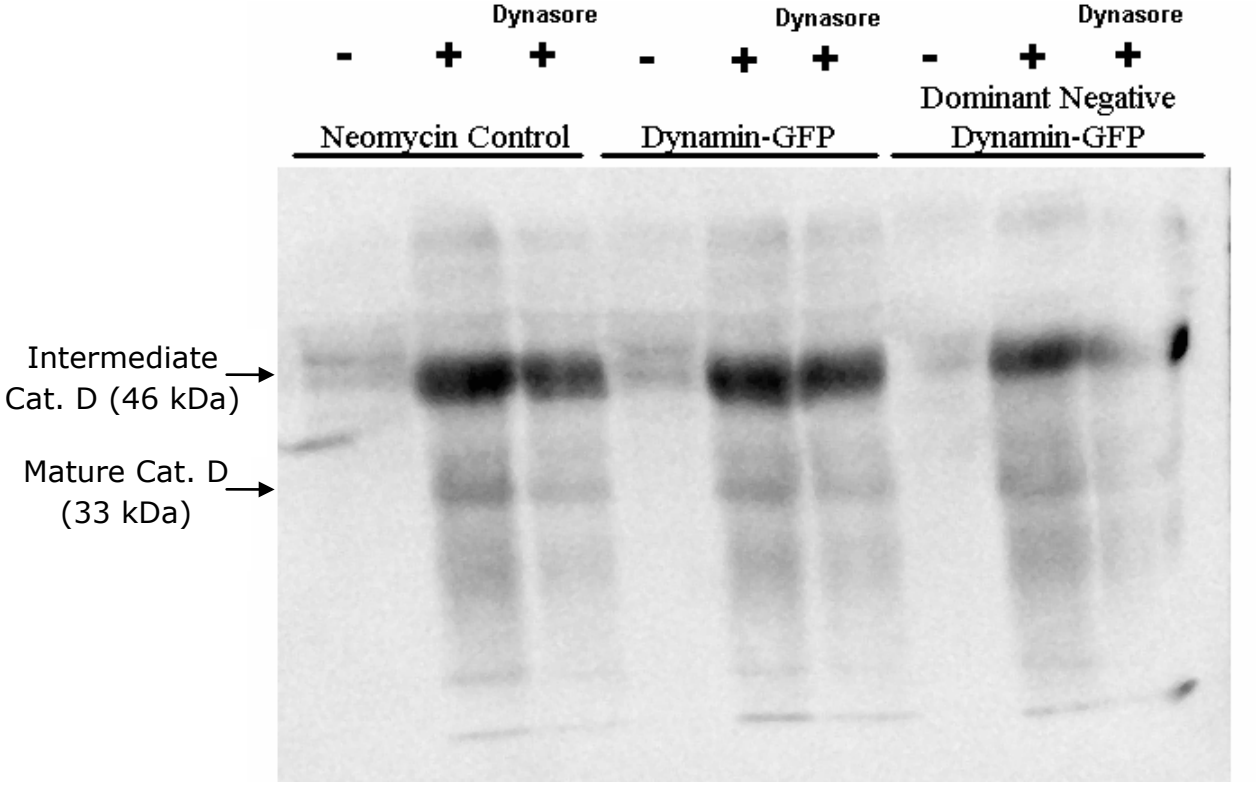

Figure 3-10: Dynamin (K44A)-GFP FSDC fail to demonstrate a decrease in mature cathepsin D secretion upon ATP treatment.

Neomycin control, dynamin-GFP, and dynamin (K44A)-GFP FSDC were non-treated or given 100 µM dynasore for 30 min. Cells were then non-treated (-) or treated with 3 mM ATP (+) for 30 min. Supernatants were analyzed for their expression of intermediate and mature forms of cathepsin D by western blot. A representative blot is shown.

3.6 DISCUSSION

ATP administration can promote the release of lysosomal components (186); however, the mechanism of how this occurs has yet to be elucidated. This study demonstrates that $P2X_7$ induces rapid lysosomal component dissemination. Membrane blebbing has consistently been observed in numerous studies and it has been implicated in the shedding of MV (217, 252); however, this is the first study to verify cathepsin D exocytosis within MV and to invoke dynamin in mature cathepsin D secretion. Intermediate (endosomal) cathepsin D and mature (lysosomal) cathepsin D forms are released following ATP-induced activation of $P2X_7$ (Figure 3-3) within MV (Figure 3-1) but they are released through distinct mechanisms (Figure 3-6) as mature cathepsin D secretion was selectively decreased in cells pretreated with the dynamin-inhibitor dynasore (Figure 3-6).

Dynamin-2 is classically described for its role with clathrin-mediated endocytosis (298); however, there have been reports suggesting its participation in exocytic processes (306, 308-310). Most of these reports have implicated its participation through dynamin inhibition but the localization of dynamin in these studies relative to secretory lysosomes had not been closely examined microscopically. With myeloid cells following ATP treatment, I observed a relocalization of dynamin to the periphery (Figure 3-8). As dynamin-2 was preferentially re-localized away from the main cell body, this would suggest its involvement in the periphery.

While dynasore treatment decreased mature cathepsin D secretion (Figure 3-6) and re-distribution to the periphery (Figure 3-7) and dynamin-2 was localized at the periphery (Figure 3-8), the dominant negative dynamin-2 (K44A)-GFP construct did not decrease mature cathepsin

D secretion (Figure 3-10). This was despite the ability of dynamin-2 (K44A)-GFP construct to inhibit LDL receptor mediated endocytosis (Figure 3-9*C, D*).

There are several reasonable explanations for the differences observed between the dynasore and dominant negative dynamin-2 (K44A) results. Dynasore and dynamin-2 (K44A) both block the GTPase function of dynamin, preventing coated vesicle formation during clathrin-mediated endocytosis (311); however, the difference is unlikely due to differences in inhibition mechanism. There are not any observed or reported discrepancies between these modes of dynamin inhibition, and both are allegedly specific for dynamin (311). One difference with how I employed them in this study is that dynasore was transiently administered whereas dynamin-2 (K44A) was stably expressed by retrovirus transduction. Stable selection favors cells that adapt survival strategies; it is very possible that these cells evolved some abnormal function to enable endocytosis of some vital materials as endocytosis is a crucial component for cellular survival. It is also possible that dynasore was more efficient at inhibiting this partial role for dynamin than the K44A dominant negative. In my study, 100 μM dynasore inhibited about 50% of the secreted mature cathepsin D in response to 3 mM ATP (Figure 3-6); if the dominant negative was not as effective, this partial inhibition may not be observed.

If dynamin is legitimately partially mediating the preferential secretion of mature but not intermediate cathepsin D from ATP treated myeloid cells, the mechanism has yet to be elaborated. A predicted outcome would an absence of peripheral cathepsin D expressed away from main cell bodies following dynasore treatment of ATP treated cells. While it is not significant, there is a trend towards a decrease of cells with cathepsin D in the periphery away from main cell bodies in the presence of dynasore (Figure 3-7); since I know that dynasore also

decreases the amount of secreted mature cathepsin D (Figure 3-6) while not decreasing the intracellular amount of cathepsin D (data not shown), cathepsin D is largely sequestered within the main cell body in response to dynasore.

How might dynamin lead to the loading of cathepsin D into MV? ATP ligation of $P2X_7$ promotes the shedding of several types of MV, including plasma membrane-derived MV (246). The topology of dynamin necessitates its function to act to invaginate vesicles into cells; however, if these various studies are correct in implicating dynamin in secretory granule exocytosis, there may be a role for vesicle excision away from the cell. Axelrod's group determined through polarized total internal reflection fluorescence microscopy (TIRFM) images of the plasma membrane–cytosol interface of chromaffin cells that dynamin plays a role in altering membrane topology during secretory granule exocytosis (310). If dynamin acts to pinch off vesicles into the periphery of ATP-treated myeloid cells, this may lead to the selective loading of materials (including lysosomal components like mature cathepsin D) into shedding MV.

4.0 $P2X_7$ ELICTS THE *DE NOVO* PRODUCTION OF F-ACTIN ENRICHED STRUCTURES FOR DISSEMINATION OF LIPIDS AND PLASMA MEMBRANE

4.1 AUTHORS AND THEIR CONTRIBUTIONS

L. Michael Thomas (Graduate Program in Immunology, University of Pittsburgh School of Medicine) designed and performed the experiments and prepared the manuscript; his funding was supported by an NIH training grant T32CA082084. Russell D. Salter (Department of Immunology, University of Pittsburgh School of Medicine) designed the scope of the study and edited the manuscript; his funding was supported by NIH funds R01AI072083 and P01CA073743. Simon C. Watkins (Department of Cell Biology and Physiology, University of Pittsburgh School of Medicine), Russell D. Salter, and L. Michael Thomas performed the described live cell biologic imaging. Various contributors provided reagents including murine bone marrow and cell lines, which are discussed and acknowledged within the *Materials and Methods*.

4.2 ABSTRACT

$P2X_7$ is capable of inducing a number of cytoskeletal modifications, including zeiotic blebbing, shedding of plasma membrane, and release of microvesicles. In this study, I discovered that $P2X_7$ initiates *de novo* actin-nucleation, leading to the production of F-actin enriched structures, resembling the morphology of filopodia. Furthermore, these extended arms displayed a twisting phenotype to the extent that they formed a beaded appearance. Calcium ionophore alone did not mimic the activities of $P2X_7$, although it did enhance $P2X_7$ activity for filopodia formation. $P2X_7$-induced filopodia required the activities of phospholipase D, calcium-dependent phospholipase A_2, N-WASP, and Rho-associated kinase. While the response has not been defined mechanistically, lipids and actin nucleation machinery were displaced to the periphery of main cell bodies within the *de novo* produced filopodia. I hypothesize that ATP induced filopodia upon fragmentation could serve as a source of materials that stimulate inflammation.

4.3 INTRODUCTION

Actin nucleation is a highly coordinated activity (314). Several stimuli can promote actin nucleation for various purposes. For example, chemotactic agents can initiate actin redistribution and the *de novo* production of actin filaments to extend out leading edge lamellipodia towards the chemotactic gradient. Actin nucleation is also important for secretory granule release; for instance, activated cytolytic immune cells promote Arp2/3-mediated actin nucleation to polarize their immunological synapases to target cells (315). Formin family actin nucleators can also coordinate microtubule processes, which are required for the exocytosis of lytic machinery (316). Arp2/3 actin nucleation results in the canonical 70° branching of actin filaments within lamellipodia (314). Formin family members such as mammalian diaphanous-2 have roles in stress fiber formation and the formation of filopodia, which, unlike the sheet-like appearance of lamellipodia, form mostly straight structures extending out from the main cell bodies of cells (314).

ATP-mediated activation of purinergic receptors can result in several morphological changes in various cells. Several purinergic receptors including A_1 (37), A_3 (131), $P2Y_2$ (131, 141, 142), $P2Y_{11}$ (37), and $P2Y_{12}$ (37, 136) can promote chemotactic movements of immune cells. Chemotaxis in this manner is largely the results of the coordinated activities of G proteins, leading to actin-based alterations in which the leading edge of lamellipodia is extended towards the chemotactic gradient (314).

$P2X_7$ is a purinergic receptor implicated in several cytoskeletal rearrangements (246). Most of these rearrangements have been described as membrane blebs. This blebbing starts

within minutes of $P2X_7$ activation in myeloid cell types and can continue over several minutes (317). Characteristically, these blebs resemble those observed during apoptosis including the externalization of phosphatidylserine (217); however, unlike apoptosis, the blebbing can subside and cells regain a healthy phenotype upon removal of the $P2X_7$ agonist (280). The exact purpose of the blebbing has been a bit elusive but some have argued that it is not involved in $P2X_7$-induced secretion of IL-1β (247) and that it is distinct from the shedding of microvesicles (252).

$P2X_7$ can modify lipids that influence the actin cytoskeleton directly or indirectly. $P2X_7$ activates several phospholipases, including phospholipase D (PLD), calcium-dependent ($cPLA_2$) and independent phospholipase A_2 ($iPLA_2$), phospholipase C (PLC), and sphingomyelinase (SMase) (183). PLD is a particularly interesting case as the PLD product phosphatidic acid (PA) can directly result in the recruitment of proteins to the plasma membrane or can be converted to other biologically active lipids (178). PA can be converted to diacylglycerol for the promotion of protein kinase C or the generation of phosphatidylinositol 4, 5-bisphosphate (PIP_2) by activating phosphatidylinositol 4-phosphate 5-kinase, which can recruit proteins that express PH domains. These recruited proteins include actin nucleators such as Arp2/3, that once recruited to the plasma membrane, are activated to induce actin polymerization (318).

In this study, I identified a new property of $P2X_7$, specifically that $P2X_7$ engages actin nucleation machinery to promote the formation of F-actin enriched structures that resemble filopodia. This activity is dependent on a $P2X_7$-driven mechanism that is not solely driven through calcium-promoted pathways. I further know that some of these pathways include PLD and $cPLA_2$. These filopodia disperse the substrate and products of PLD indicating a potential mechanism for $P2X_7$-induced spreading of pro-inflammatory mediators.

4.4 MATERIALS AND METHODS

Cell culture and reagents - FSDC, an adherent immortalized murine immature dendritic cell line via retroviral transduction of a vector carrying an envAKR-mycMH2 fusion gene (Girolomoni et al., 1995), (gift from P. Ricciardi-Castagnoli**,** Singapore Immunology Network, Singapore) was maintained in IMDM (Lonza, Basel, Switzerland) supplemented with 10% fetal bovine serum (FBS) (Gemini Bio-Products, West Sacramento, CA), 1% additional L-glutamine (Lonza), and 1% penicillin and streptomycin (Lonza). This IMDM supplemented media will hereafter be referred to as IMDM complete. Murine bone marrow derived macrophages (BMDM) were derived from bone marrow precursors (gift from L. Borghesi, University of Pittsburgh) differentiated with L-cell supplemented media as described previously (265). $P2X_7^{-/-}$ mouse bone marrow is a gift from G. Dubyak (Case Western Reserve University School of Medicine); they were on the C57BL/6 background. For some experiments, 1 μg/ml of lipopolysacharides (LPS) from *Escherichia coli* 026:B6 (Sigma-Aldrich, St. Louis, MO) was used to prime the cells where indicated.

Other regents include ATP (Thermo Fisher Scientific, Waltham, MA), BzATP (Sigma-Aldrich), KN-62 (Sigma-Aldrich), A23187 (Sigma-Aldrich), cytochalasin D (Sigma-Aldrich), latrunculin A (Invitrogen, San Diego, CA), colchicine (Sigma-Aldrich), UTP (Sigma-Aldrich), CAY10593 (Enzo Life Sciences, Farmingdale, NY), CAY10594 (Enzo Life Sciences), A 740003 (Tocris Bioscience; Ellisville, MO), 187-1 (Tocris Bioscience), HA-1077 (Enzo Life Sciences), Y-27632 (Enzo Life Sciences), AACOCF3 (Enzo Life Sciences), H-89 (Cayman Chemical, Ann Arbor, MI), Ki16425 (Cayman Chemical), SB203580 (EMD Chemicals, Gibbstown, NJ), U0126 (EMD Chemicals).

Microscopy - For filopodia quantification studies, 200,000 FSDC or BMDM were plated within 12 or 24-well plates with IMDM complete. Cells were allowed to adhere for at least 4 h. LPS priming (as described above) was performed for BMDM where indicated. Following the 4 h, cells were washed once with PBS then given treatments where indicated. Where indicated, cells were treated with inhibitor for 30 min prior to ATP administration. After treatment, supernatant was discarded and the cells were washed once with PBS. 2% paraformadehyde fixative was applied for 15 min at room temperature after which the fix was removed being replaced with Coomassie Blue (Thermo Fisher Scientific) for at least 1 h. Coomassie Blue was removed and the cells were washed three or more times with PBS. Counts were performed under a standard light microscope for at least 100 counted cells per treatment taken from at least 10 randomly chosen fields of view over 3 separate experiments.

For confocal microscopy studies, 200,000 FSDC or BMDM were plated on poly(d-lysine)-coated coverslips within 24-well plates. Cells were allowed to adhere for at least 4 h. LPS priming (as described above) was performed for BMDM where indicated. Following the 4 h, cells were washed once with PBS then given treatments where indicated. Where indicated, cells were treated with inhibitor for 30 min prior to ATP administration or treated with 10 μM BODIPY-phosphatidylcholine (Invitrogen). After treatment, supernatant was discarded and the cells were washed once with PBS. 2% paraformaldehyde fixative was applied for 15 min. After the fixation step, fixative was removed being replaced with 50 mM glycine for 5 min, then blocked and permeabilized with 1.5% BSA and 0.5% saponin in 1xPBS for 30 min at room temperature. Coverslips were then washed once with PBS then given primary antibody of 1/100 diluted anti-N-WASP (Santa Cruz Biotechnology; Santa Cruz, CA) where indicated at room temperature. Coverslips were then washed three times with 0.5% saponin in PBS then given

1/100 diluted Alexa-647 conjugated goat anti-mouse IgG (Invitrogen) along with 400 nM rhodamine phalloidin (Sigma-Aldrich) or DiI (Invitrogen) where indicated at room temperature. Coverslips were then washed 3 times with 0.5% saponin in PBS then given 1 µg/ml DAPI (Sigma-Aldrich) for 30 s. Coverslips were then washed 3 times with PBS before mounting onto a glass slide with gelvatol (gift from CBI).

Confocal microscopy images were taken with an Olympus Fluoview 1000 (Inverted) (Olympus America, Inc., Center Valley, PA). Laser excitations were collected sequentially and background noise was minimized. Confocal microscopy included DIC microscopy for observing the cellular cytoskeleton. Images were then consistently digitally enhanced (if modified at all) for signal with Adobe Photoshop CS2 (Adobe, San Jose, CA). Where necessary, counts were performed from obtained images for at least 100 counted cells per treatment taken from at least 10 randomly chosen fields of view over 3 separate experiments.

Live cell imaging was performed using a Nikon TI inverted microscope with a 60X 1.49 NA oil immersion optic, a NikonPiezo driven XYZ stage, a Prairie Sweptfield confocal head and Prairie Technology (Madison, WI) laser bench. Images were collected using a QuantEM backthinned 512B camera (Photometrics, Tucson AZ). Cells were maintained at 37^{o}C in the microscope with a Tokai Hit Environmental Stage (Tokyo Japan). Software control of the microscope was with Elements (Nikon, Melville NY).

Statistics - Student's T-test was utilized for studies invoking statistical analysis. Values of p were calculated where indicated, and for all statistical studies $p<0.05$ was considered as significant.

4.5 RESULTS

4.5.1 ATP induces *de novo* filopodial arm formation that is distinctly different from steady-state filopodia and ATP-induced membrane blebs

ATP has been known to produce several morphological changes in myeloid cells. Most often cited is the zeiotic blebbing phenomenon (246). The zeiotic blebbing appear as if the cells were boiling. This boiling ends with the cells rounding up and the loss of actin-enriched podosomes (data not shown). I also observe zeiotic blebbing within 5 min of live cell microscopy of 3 mM ATP treated FSDC (Figure 4-1); however, after the blebbing subsided, there was a progressive production of growing F-actin enriched filopodia with characteristics that differ from the resting state filopodia (Figure 4-1, 4-2). These filopodia following ATP administration had a rotating movement and were noticeably curved to form beaded structures along the filopodial arms (Figure 4-3). Kinetically, these *de novo* produced filopodia were observed from 5 min and continued to extend at 15 min (Figure 4-4). These filopodia differed morphologically and kinetically from membrane blebbing. Lower doses of ATP (0.1-0.6 mM ATP) were able to increase the percentage of FSDC with membrane blebs whereas filopodia formation required at least 1 mM ATP (Figure 4-5). Interestingly, at 1 mM ATP, whereas the production of *de novo* filopodia increased, the production of membrane blebbing actually decreased as compared to lower ATP doses.

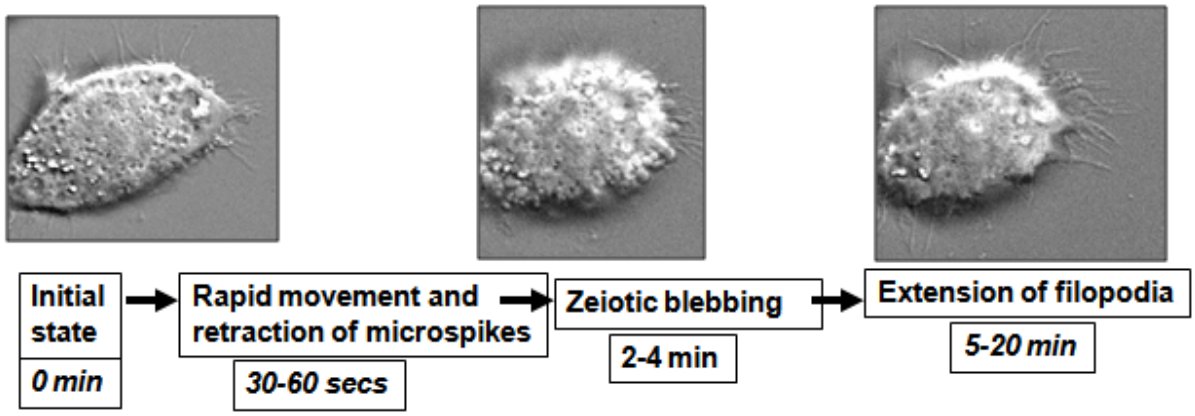

Figure 4-1: ATP induces several morphological alterations.

FSDC were treated with 3 mM ATP. Above is an illustration of some of the ensuing morphological alterations that occur over time following ATP treatment. The left image shows quiescent cells prior to ATP treatment. The middle image shows zeiotic blebbing that occurred between 2-4 min of ATP treatment. The right image shows the extension of novel filopodia that were distinctly different from filopodia of non-treated cells following 5-20 min of ATP treatment.

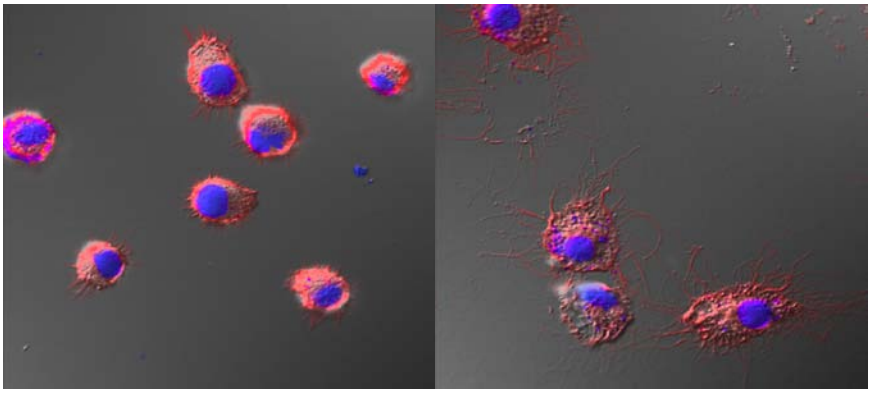

Figure 4-2: ATP treatment produces extensions enriched with F-actin.

FSDC were non-treated (left) or treated with 3 mM ATP (right) for 15 min. Cells were fixed and stained for nuclei (blue) and F-actin (red). Images were taken by confocal and overlaid with DIC microscopy. The images are representative of over 10 separate experiments.

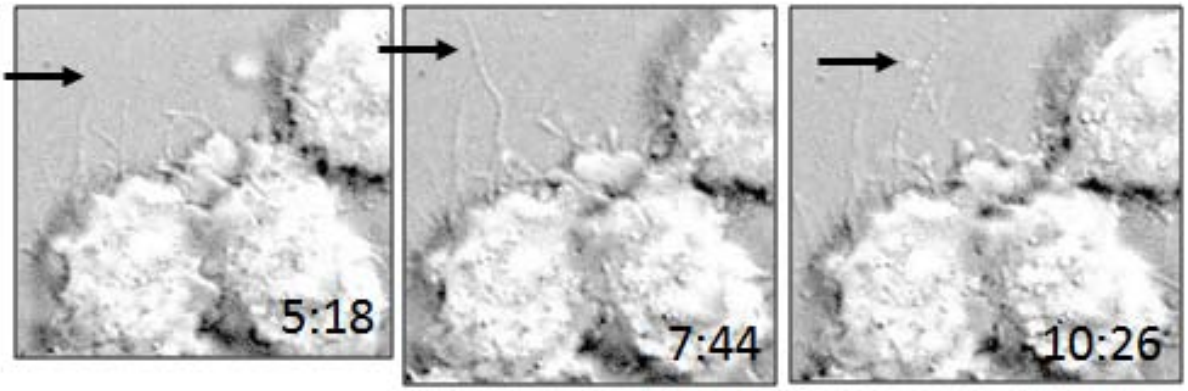

Figure 4-3: ATP treatment produces beaded filaments.

FSDC were treated with 3 mM ATP with analysis by live cell microscopy. From left to right, the arrow indicates the growth, movement, and beaded appearance of these filaments. Time is indicated in the lower right portion of each micrograph.

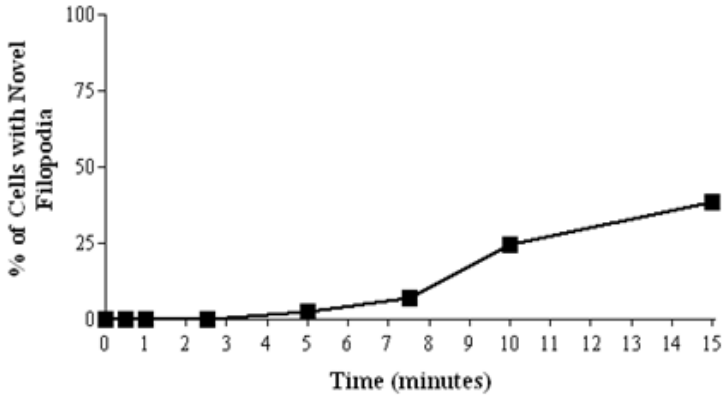

Figure 4-4: ATP induces novel filopodia development over time.

FSDC were non-treated (0), 0.5, 1, 2.5, 5, 7.5, 10, and 15 min. Cells were fixed and quantitated as being positive or negative for novel filopodia formation. The histogram is representative of repeated experiments of cells that were positive for filopodia formation.

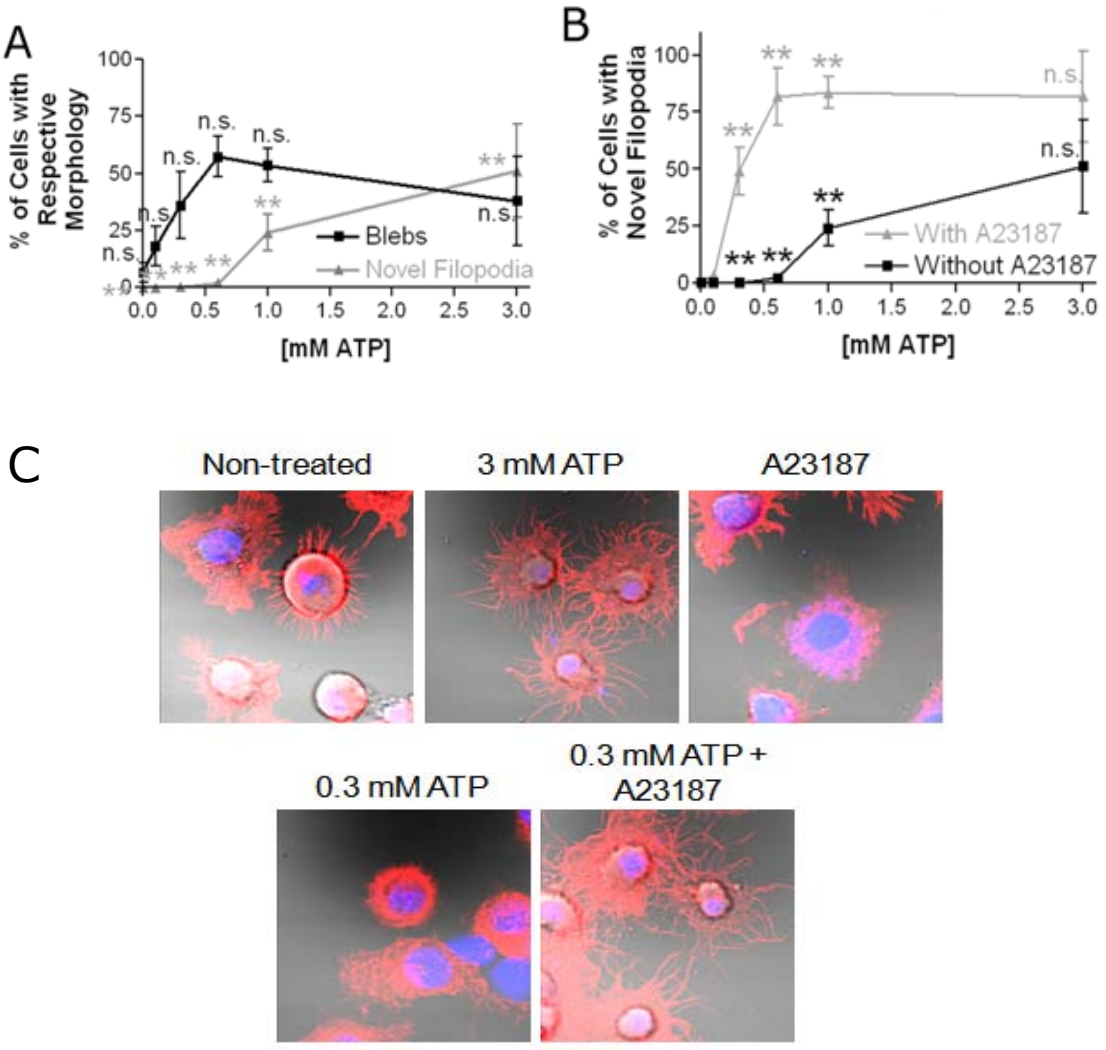

Figure 4-5: ATP concentration and calcium flux dictates blebbing and filopodia generation.

In A and B, FSDC were non-treated (0.0), 0.15, 0.3, 0.6, 1.0, and 3.0 mM ATP for 15 min. In A, cells were compared for blebbing (black) and novel filopodia (gray) generation. In B, cells were co-treated with (gray) or without (black) 10 µM A23187 along with the indicated dose of ATP then analyzed for novel filopodia formation. For A and B, the histograms indicate means of cells with the respective morphology ± SEM of $n = 3$. The statistical comparison is made to non-treated FSDC for the respective morphology. $^{**}p<0.01$; n.s., not significant. For C, FSDC were treated with indicated treatments for 15 min then fixed for confocal microscopy. Cells were stained for nuclei (blue) and F-actin (red). Images were overlaid with DIC microscopy and are representative of repeated experiments.

4.5.2 Elevated intracellular calcium potentiates ATP-induced *de novo* filopodia but it is not sufficient by itself to drive the *de novo* filopodial response

Intracellular calcium is essential for many different signal transduction pathways, and actin polymerization and cytoskeletal rearrangements can be regulated through calcium influx (314). One way to trigger a powerful calcium-driven response is to treat cells with a calcium ionophore. In order to test the role of calcium in my observed filopodial response, I tested calcium ionophore either alone or co-administered with varying amounts of ATP. Calcium ionophore A23187 in combination with at least 0.3 mM ATP, but not A23187 by itself or in combination with 0.1 mM ATP, was able to elicit the filopodial response (Figure 4-5B). In addition to potentiating the ability for lower concentrations of ATP to produce *de novo* filopodia, A23187 in combination with concentrations of ATP equal to or greater than 0.3 mM elevated the over-all percentage of cells positive for novel filopodia. This is in agreement with our previous finding that A23187 can potentiate $P2X_7$ activities of large pore formation and MV shedding (236).

4.5.3 ATP-induced *de novo* synthesis of filopodia is actin-based and does not depend on microtubule polymerizing processes

Since ATP treatment induced altered F-actin structures, I tested the possibility of *de novo* actin nucleation. Actin-based processes downstream of purinergic receptor engagement (such as $P2X_7$ activation) have been well documented for membrane blebbing. At the same time, it was possible that my observed cytoskeletal rearrangements could be mediated by microtubules. While

microtubule polymerization processes are distinct from actin polymerization processes, microtubules can influence the structure of the cytoskeleton so thus theoretically also alter the arrangement of actin. Furthermore, others have noted that ATP (through $P2X_7$) can induce microtubule polymerization in microglia cells (319). In contrast, I observed that $P2X_7$ induced altered cytoskeleton for novel filopodia was an actin polymerization phenomenon, as cytochalasin D and latrunculin A were able to inhibit the response, whereas the microtubule polymerization inhibitor colchicine was not able to significantly decrease the response (Figure 4-6*A*).

4.5.4 $P2X_7$ is the ATP activating receptor for the *de novo* filopodial response

The concentrations of ATP applied to these cells thus far are certainly high enough within the range for $P2X_7$ activation (37); however, it was possible that ATP was activating other purinergic receptor(s). To test this, I tried various purinergic receptor agonists and antagonists. BzATP, a $P2X_1$ (320), $P2X_7$ (130), and $P2Y_{11}$ (321) agonist, was able to activate the filopodial response with FSDC whereas UTP, a P2Y agonist (130), was not (Figure 4-6*B*). KN-62, a specific inhibitor of $P2X_7$ relative to inhibiting other purinergic receptors (322), was able to ablate ATP's ability to stimulate the response (Figure 4-6*C*). $P2X_7$ knock-out BMDM were unable to produce the *de novo* filopodia, as compared to the wild-type BMDM (Figure 4-6*D*). Lastly, another inhibitor of $P2X_7$, A 740003, was able to block novel filopodia generation (Figure 4-6F).

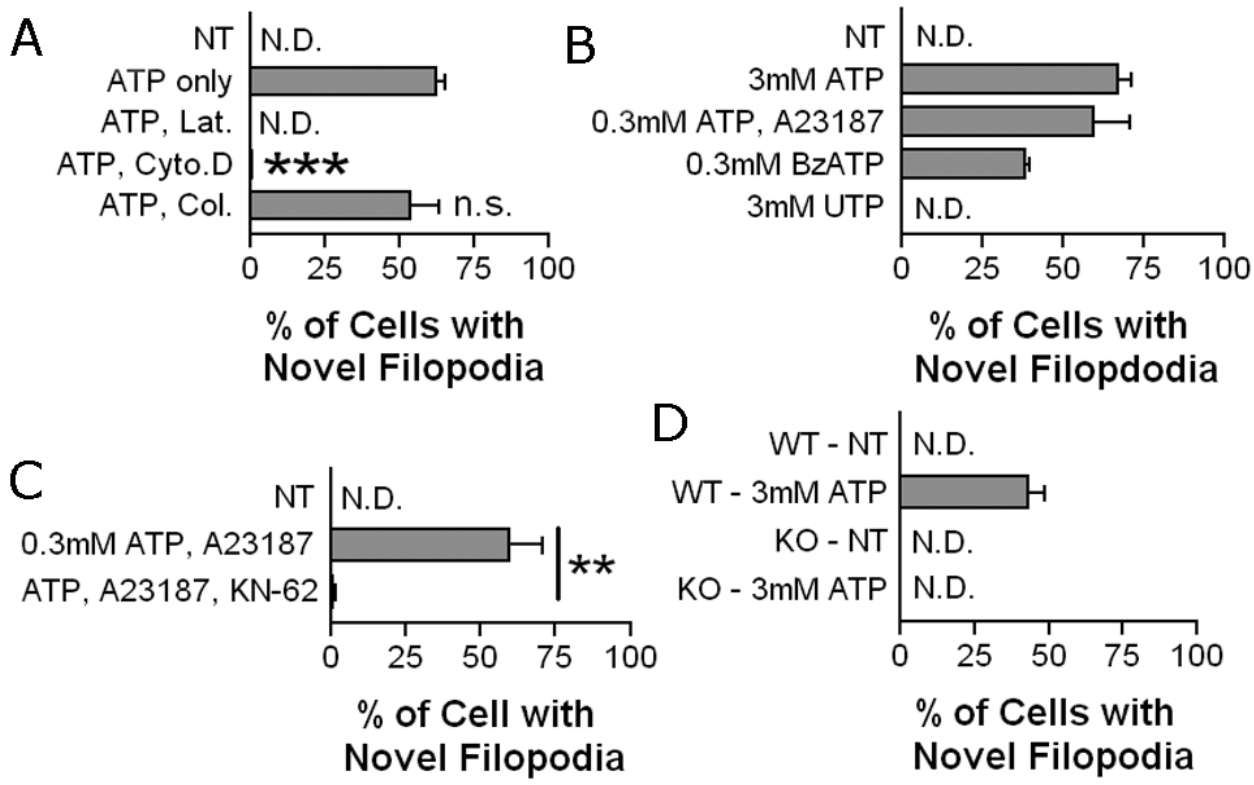

Figure 4-6: Filopodia formation is dependent on $P2X_7$ and actin polymerization.

For each panel, inhibitors are given for 30 min prior to 15 min treatment with agonists where indicated. In A, FSDC were non-treated or treated with 3 mM ATP. Where indicated, cells were pretreated with 800 nM latrunculin A (actin polymerization inhibitor), 10 µM colchicine (microtubule polymerization inhibitor), or 10 µM cytochalasin D (actin polymerization inhibitor). In B, FSDC were non-treated, 3 mM ATP, 0.3 mM ATP plus 10 µM A23187, 0.3 mM BzATP, or 3 mM UTP. In C, FSDC were non-treated or 0.3 mM ATP plus 10 µM A23187. Where indicated, cells were pretreated with 10 µM KN-62 ($P2X_7$ inhibitor). In D, wild-type (WT) or $P2X_7^{-/-}$ BMDM were non-treated or treated with 3 mM ATP. In E, FSDC were non-treated or treated with 3 mM ATP. Histogram indicates means of cells positive for novel filopodia formation ± SEM of $n = 3$. Unless indicated by brackets, statistical comparisons are made to 3 mM ATP treated cells. $^{**}p<0.01$; $^{***}p<0.001$. n.s., not significant; NT, non-treated; N.D., none detected.

4.5.5 Phospholipase D, calcium-dependent phospholipase A_2, N-WASP, and Rho-associated kinase inhibition block the *de novo* filopodial response

To understand further what might be regulating filopodia formation, I considered various pathways that have the potential to regulate actin rearrangements including phospholipases and regulators of actin nucleation such as Arp2/3 actin nucleation (e.g., through N-WASP) or formin-mediated actin nucleation (e.g., through Rho-associated kinases).

Phospholipase D (PLD) is a phospholipase that induces the cleavage of phosphatidylcholine to phosphatidic acid (PA) and choline (178). PA is incorporated in the plasma membrane as a biologically active cleavage product; choline is thought to be relatively inert. PA can promote recruitment of proteins to the plasma membrane (178), initiate phosphatidylinositol 4, 5-bisphosphate (PIP_2) synthesis pathways by activating type I phosphatidylinositol 5-kinases (323), or be modified to other biologically active materials including diacylglycerol (178). In this manner, PA can modulate the actin cytoskeleton of cells (324) including the activation of actin nucleation machinery through PIP_2 (318). PA itself can also contort the plasma membrane by incorporating negative charges within the lipid bilayer of membranes (178). PLD comes in two isoforms: PLD1 and PLD2. PLD1 is thought to act primarily at the Golgi apparatus whereas PLD2 is thought to act at the plasma membrane. However, upon activation, both of these PLD isoforms can act at the plasma membrane. Inhibition of both PLD1 and PLD2 resulted in significantly decreased amounts of cells positive for *de novo* filopodia formation (Figure 4-7*A*, Figure 4-8). Interestingly, inclusion of a stable

analog of PA (C8PA) was unable to elicit the filopodia response by itself; C8PA did however affect the cytoskeleton as C8PA was able to expand the lamellipodia of FSDC cells (data not shown).

Given the phospholipase involvement with PLD, $P2X_7$-dependence, and the potentiation observed with the inclusion of A23187 with ATP, I also considered a role for calcium-dependent phospholipase A_2 ($cPLA_2$). $P2X_7$ activates $cPLA_2$ for the secretion (but not the cleavage) of IL-1β from PAMP-stimulated human monocytes (257). PLD and $cPLA_2$ can coordinate together for the cleavage of substrates; for instance, PLD can cleave phosphatidylcholine to PA and choline, then $cPLA_2$ can cleave PA to lysophosphatidic acid (LPA). LPA is then secreted from cells, allowing it to engage LPA receptors (LPAR) in an autocrine or paracrine fashion. LPAR act as G protein coupled receptors to initiate G protein signal transduction. This is the case following $P2X_7$ activation of osteoblasts where released LPA was then able to bind to LPAR to initiate Rho-associated kinase for membrane blebbing (280). Inhibition of $cPLA_2$ through a specific $cPLA_2$ inhibitor, AACOCF3, significantly reduced the amount of cells positive for the filopodial response (Figure 4-7*B,* Figure 4-8). Blockade of $LPAR_1$ and $LPAR_3$, two LPAR expressed on myeloid cells, with Ki16425, however, did not significantly reduce the response (Figure 4-7*B*). Furthermore, exogenous administration of LPA alone did not produce *de novo* filopodia or potentiate filopodia production together with limiting amounts of ATP (data not shown).

As $P2X_7$ promotes the production of F-actin-enriched structures, actin nucleation is likely a required event for these newly formed filopodia. Actin nucleation is mediated through a couple of different actin nucleators including Arp2/3, formins, and spire proteins (314). Each type of actin nucleator can induce different types of actin-based structures. They can also coordinate

together to create various actin-based structures. For instance, Arp2/3 actin nucleation results in a predictable 70° branching of F-actin; this pattern is consistent through newly produced sheets of lamellipodia surrounding cells. This lamellipodia platform can serve as a launching pad for formin-based actin nucleation, leading to elongated actin structures such as filopodia (325). In this manner, filopodia are both a function of Arp2/3 and formin family members. Inhibition of Arp2/3 associated protein N-WASP resulted in a near complete abrogation of filopodia formation (Figure 4-7*B,* Figure 4-8). Inhibition of Rho-associated kinase with Y-27632 but not HA-1077 resulted in a significant decrease in ATP-induced filopodia (Figure 4-7*B,* Figure 4-8). Rho has also been associated with MAPK and PKA pathways. Inhibition of p38 MAPK, MEK1/2, or PKA did not result in any reduction of filopodia production (Figure 4-7*B*).

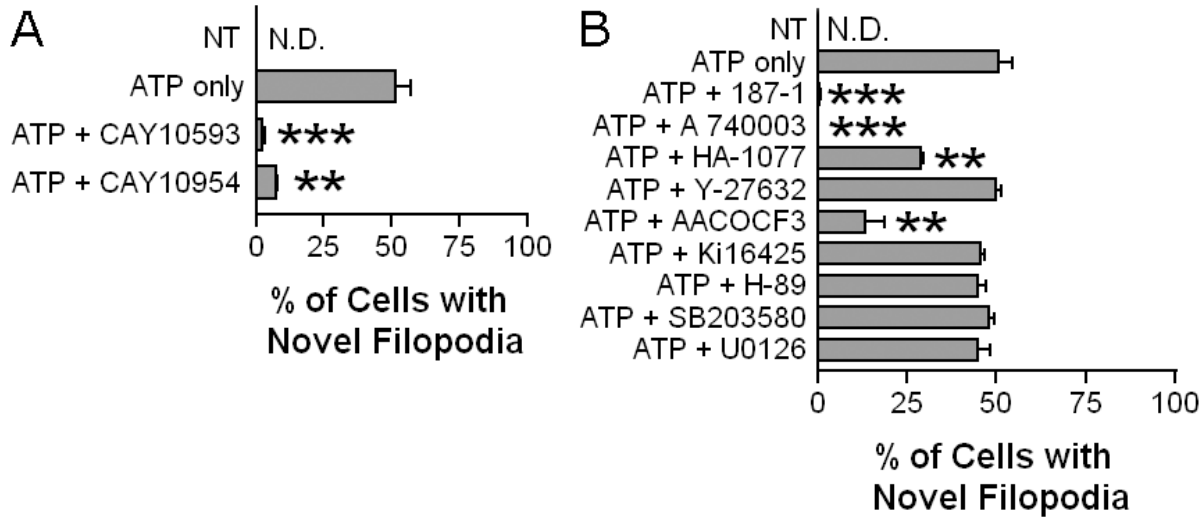

Figure 4-7: Filopodia formation is dependent on $P2X_7$, PLD, $cPLA_2$, N-WASP, and ROK.

For each panel, inhibitors are given for 30 min prior to 15 min treatment with agonists where indicated. In E, FSDC were non-treated or treated with 3 mM ATP. Where indicated, cells were pretreated with 50 µM CAY10593 (PLD1 inhibitor) or 50 µM CAY10594 (PLD2 inhibitor). In F, cells were non-treated or 3 mM ATP treated. Where indicated cells were pretreated with 50 µM 187-1 (N-WASP inhibitor), 100 µM A 740003 ($P2X_7$ inhibitor), 50 µM HA-1077 (ROK inhibitor), 50 µM Y-27632 (ROK inhibitor), 10 µM AACOCF3 ($cPLA_2$ inhibitor), 10 µM Ki16425 (lysophosphatidic acid receptor 1, 3 inhibitor), 10 µM H-89 (PKA inhibitor), 50 µM SB203580 (p38 MAPK inhibitor), or 50 µM U0126 (MEK 1/2 inhibitor). Histogram indicates means of cells positive for novel filopodia formation ± SEM of $n = 3$. Unless indicated by brackets, statistical comparisons are made to 3 mM ATP treated cells. **$p<0.01$; ***$p<0.001$. n.s., not significant; NT, non-treated; N.D., none detected.

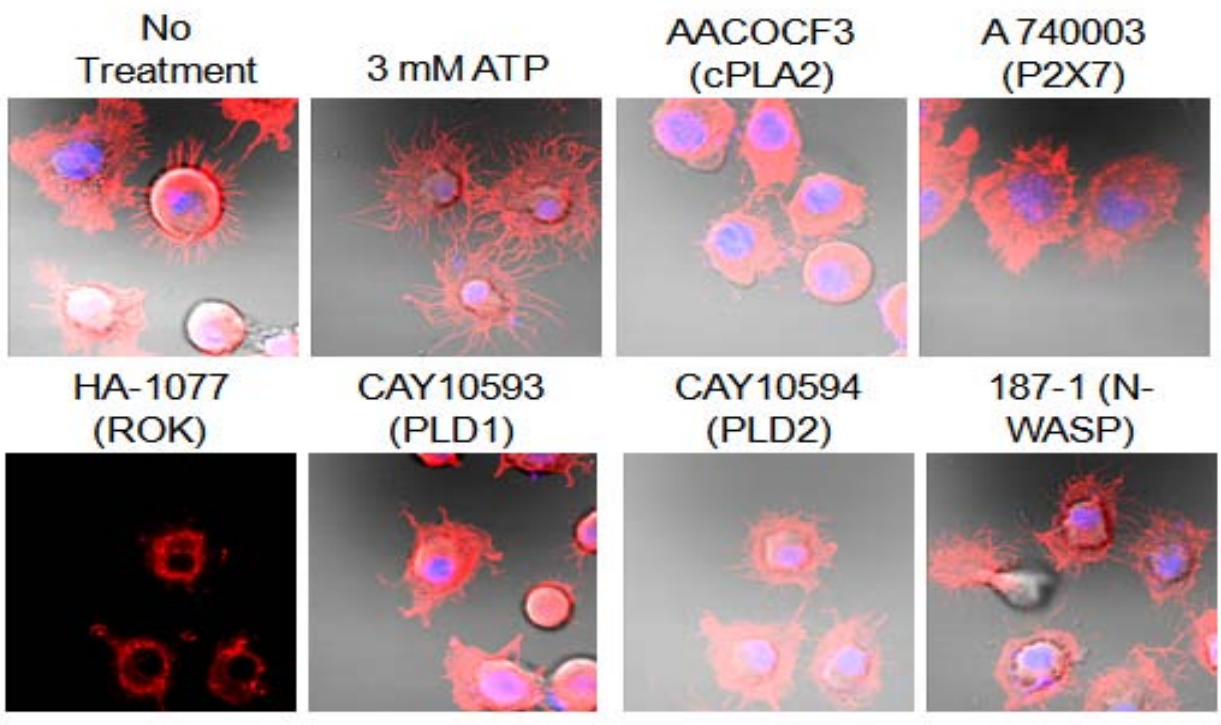

Figure 4-8: Inhibition of $P2X_7$, PLD, $cPLA_2$, N-WASP, and ROK prior to ATP treatment display an absence of filopodia.

For each panel, inhibitors are given for 30 min prior to 15 min treatment with agonists where indicated. Cells were treated similar to Figure 4-7 but were fixed and stained for nuclei (blue) and F-actin (red) for confocal microscopy. Image was overlaid with DIC microscopy (except for HA-1077 sample) and is representative of repeated experiments.

4.5.6 $P2X_7$-induced filopodia serve as locales for displaced actin nucleation components and lipids including phosphatidylcholine

Since I had identified N-WASP as a critical regulator of ATP-induced filopodia, I wanted to evaluate the localization of Arp2/3-related machinery respective to the filopodia. As these

filopodia have an oddly shaped curved morphology, N-WASP may be present within the curves of the filopodia. Alternatively, perhaps N-WASP is present at the base of the filopodia along the main cell bodies. N-WASP localized largely within the main cell body; however, N-WASP expression was found within ATP-induced filopodia (Figure 4-9*A, B*) as over 75% of the cells expressing noticeable ATP-induced filopodia had N-WASP expression within at least one of their arms of filopodia (Figure 4-9*B*).

PLD was identified as a regulator of filopodia production (Figure 4-7*A,* Figure 4-8). The main substrate is phosphatidylcholine (178). To monitor the substrates and products of PLD, BODIPY-phosphatidylcholine was incubated with cells then given ATP. At 15 min, BODIPY signal was displaced from the main cell body to the periphery, to and within the newly produced filopodia (Figure 4-9*A, B*). Over 75% of cells expressing ATP-induced filopodia had BODIPY expression within at least one of their arms of filopodia (Figure 4-9*B*). Furthermore, ATP promotes the peripheral displacement of BODIPY signal significantly away from main cell bodies as compared to non-treated cells (Figure 4-10*A, B*).

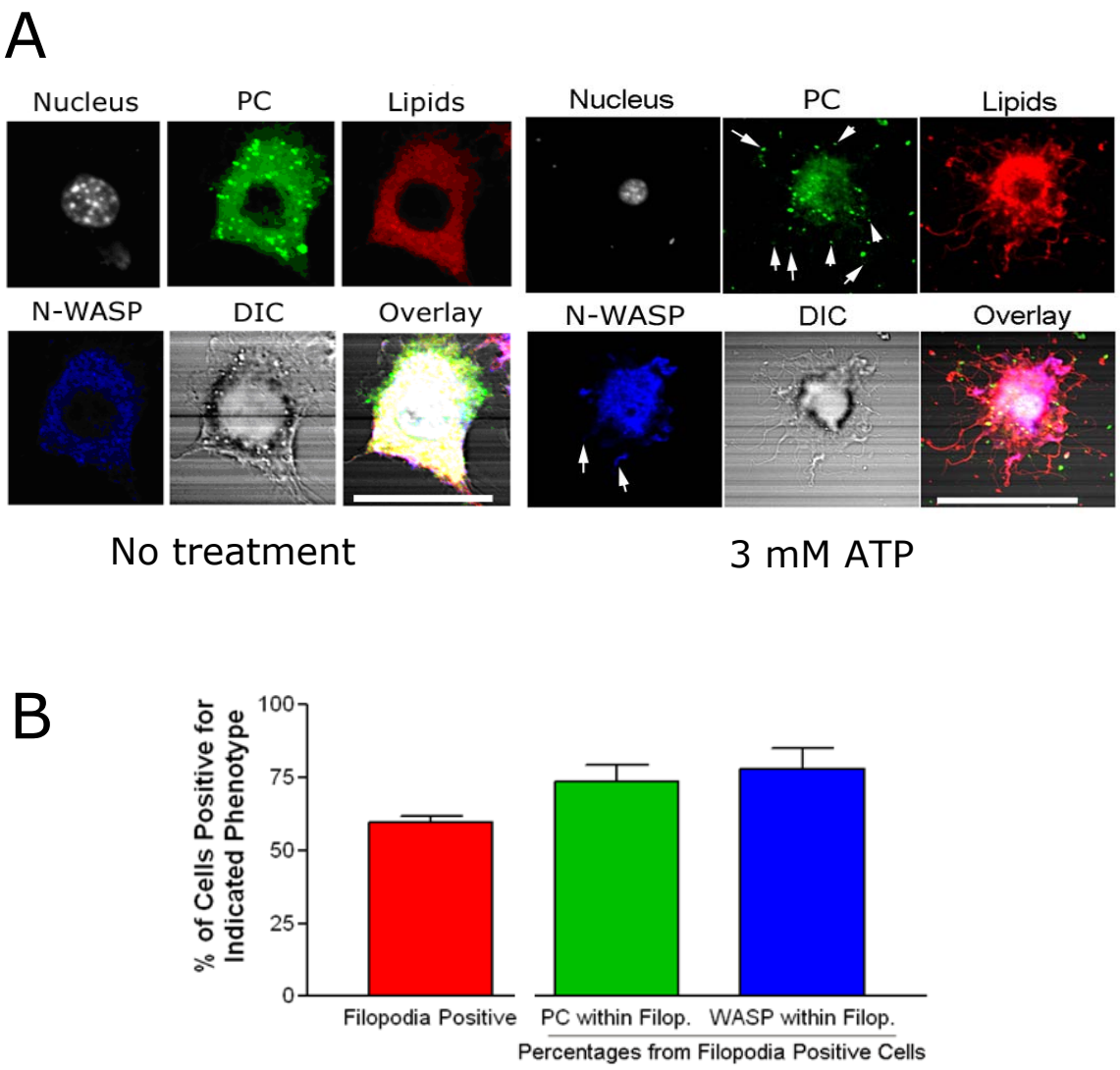

Figure 4-9: *De novo* generated filopodia contain phosphatidylcholine and N-WASP.

FSDC were given 10 µM BODIPY-phosphatidylcholine (PC) for 1 h prior to further treatment. Cells were non-treated (left in A) or treated with 3 mM ATP for 15 min (right in A) then fixed and stained for nuclei (gray), lipids (red), or N-WASP (blue) prior to confocal microscopy (A). Images were overlaid with DIC microscopy (bottom right) and are representative of repeated experiments. White arrows indicate positive expression of respective phenotype in filopodia. Scale bar, 10 µm. In B, means of cells positive for the indicated phenotype ± SEM of $n = 3$.

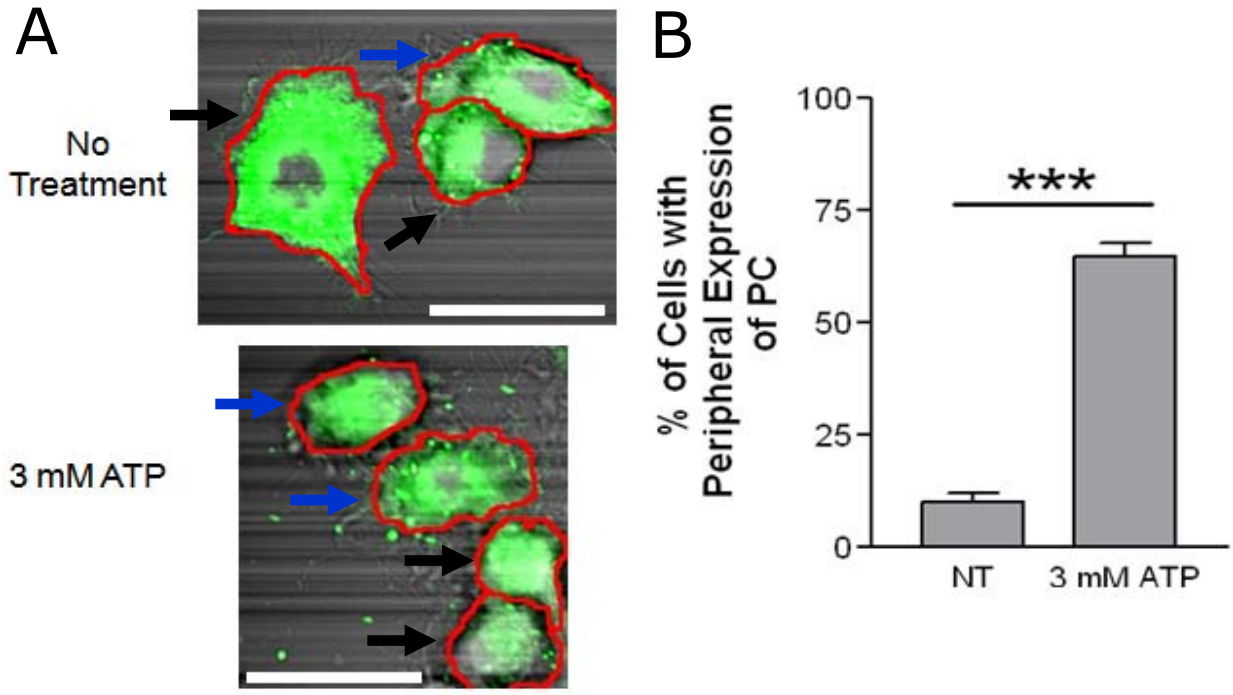

Figure 4-10: ATP promotes the peripheral displacement of BODIPY-phosphatidylcholine away from main cell bodies of FSDC.

FSDC were given 10 µM BODIPY-phosphatidylcholine for 1 h prior to further treatment. Cells were non-treated (top micrograph) or treated with 3 mM ATP for 15 min (bottom micrograph) then analyzed by confocal microscopy. In A, FSDC are shown with BODIPY (green) overlay with DIC microscopy. The red markings highlight the outline of the main cell bodies of cells, which was clearer with the original DIC micrographs. Black arrows indicate negative cells whereas blue arrows indicate positive cells for displaced BODIPY away from the main cell bodies of cells. Scale bar, 10 µm. In B, means of cells positive for the peripheral expression of BODIPY signal (PC) ± SEM of 10 fields of view that contain at least 10 cells each. ***p<0.001. NT, non-treated.

4.6 DISCUSSION

Understanding the mechanisms of how inflammatory materials are released from cells is important as these explanations ultimately come to the core of immunological processes that are relevant for inflammation and disease. As others have described, ATP administration can activate the purinergic ion channel $P2X_7$ for the induction of membrane blebbing and shedding of MV (246). Membrane blebbing has been observed in numerous studies and it was once implicated in the shedding of MV (217); however, this is the first study to identify a novel actin-based filopodia formation response following $P2X_7$-induced membrane blebbing.

This response to $P2X_7$ is a novel activity with broad cytoskeletal ramifications. $P2X_7$ induction starts with zeiotic blebbing, but after 5 min, there is a rapid extension of F-actin-based structures that we classify as filopodia. Formation of these filopodia requires activities of N-WASP, PLD, $cPLA_2$, and ROK2 (Figure 4-7, Figure 4-8). Whereas calcium ionophore alone was insufficient for inducing *de novo* filopodia, calcium ionophore synergized with minimal amounts of ATP (Figure 4-5). Given the sequence of zeiotic blebbing then filopodia formation (Figure 4-1) and the known requirements for zeiotic blebbing (including phospholipase A_2 and PLD) (280), it is possible that the blebbing primes $P2X_7$-activated cells for eventual filopodia production. The exact actin nucleation events have yet to be fully disclosed; however, given the requirement for ROK2 and N-WASP (Figure 4-7, Figure 4-8) and the structural phenotype of the F-actin structures (Figure 4-2), it is likely that this actin nucleation is at least in part mediated by formin proteins – possibly mammalian diaphanous-2 (mDia2). mDia2 induces stress fiber formation (314) for formation of elongated F-actin structures in a variety of mammalian cell types.

The exact purpose of the $P2X_7$-induced filopodia is an interesting question. $P2X_7$-induced filopodia promoted the displacement of BODIPY-phosphatidylcholine (Figure 4-9 and Figure 4-10). The BODIPY adduct would be retained with released PA (as opposed to choline) signifying that the BODIPY signal may possibly show PA localization. PA is a signaling macromolecule but it may also demonstrate how $P2X_7$ initiates the dissemination of lipid and protein mediators. $P2X_7$ promoted the twisting of *de novo* filopodia into a beaded-like appearance (Figure 4-3). Could these beads be a precursor to shed MV? Cellular requirements for filopodia formation and MV shedding were distinct, as shown in chapters 2 and 4 of this thesis. In this manner, $P2X_7$-induced filopodia may represent a subset of released MV. $P2X_7$-induced filopodia break off very readily and at later time points, the filopodia appear to be shorter; however, there is no direct evidence that filopodia and MV have a precursor-product relationship. Live cell high speed confocal microscopy is required to visualize the possibility of this relationship.

$P2X_7$ has been shown to promote inflammation in several settings; however, the cellular mechanisms have been lacking. It is noted that $P2X_7$ activation can redistribute cellular cytoskeleton into membrane blebs and MV but this is the first report for a novel actin redistribution into extending arms of filopodia. It is the goal of this study to further characterize these cytoskeletal rearrangements to reveal how inflammatory stimuli are released from $P2X_7$-activated myeloid cells. While these filopodia may not be the sole mechanism for inflammatory stimuli release, it can serve as one of the mechanisms. An intriguing possibility may exist in the physiological context of tissues *in vivo*. As these filopodia can extend over long distances (greater than the main cell body itself), it is quite possible upon ATP ligation of $P2X_7$ on myeloid cells, there is the potential for contact with multiple adjacent cells, perhaps distributing pro-inflammatory signals to cells following filopodial breakage.

5.0 OVERALL SUMMARY AND INTERPRETATIONS OF THESIS

5.1 PROPOSED MODEL AND THERAPEUTIC IMPLICATIONS

The work described within this dissertation reveals a provocative role of $P2X_7$-induced MV in modulating immunity. More specifically, these MV contain inflammatory materials. Phospholipids from MV are able to upregulate co-stimulatory molecules required for antigen presentation and induce the secretion of pro-inflammatory cytokines from macrophages. Lysosomal materials such as biologically active cathepsins are released within $P2X_7$-induced MV. Lipids and lysosomal materials are displaced from the main cell bodies of ATP-treated myeloid cells for their potential loading into MV. These studies further elucidate the role of $P2X_7$ in coordinating release of pro-inflammatory materials from myeloid cells. In a larger sense, this work describes how $P2X_7$ initiates cellular responses for release of pro-inflammatory materials in the absence of the inflammasome and moreover in the absence of infection.

Chapter 2 of this thesis provides a mechanistic understanding of how inflammatory phospholipids are associated with MV and how they mediate macrophage activation. Phospholipids and shed MV have been implicated in macrophage activation but their generation has not yet been explained. This work details a role for $P2X_7$-induced PLD in generating stimulatory MV. This may be due in part to PLD-generated PA, as PA-loaded liposomes were capable of stimulating significant macrophage activation. PLD also has a role in enabling the displacement of phospholipids into $P2X_7$-induced filopodia; I hypothesize that $P2X_7$-induced filopodia may provide material for shed MV. The phospholipids from $P2X_7$-induced MV were able to activate macrophages in a TLR4-dependent manner. More work is necessary to

understand how these phospholipids are capable of activating TLR4; however, it is hypothesized that $P2X_7$-induction results in membrane asymmetry for the exposure of several phospholipids to engage pattern recognition receptors (Figure 5-1). My thesis work has shown that $P2X_7$ greatly modifies the cellular cytoskeleton and the studies of others have established $P2X_7$ induction of PS flip (157). It is possible that this exposure reveals phospholipids to oxidative environments during diseases such as cancer, arthritis, and atherosclerosis (326, 327). $P2X_7$ itself can also generate free radicals (188, 328-331) that could oxidize phospholipids such that they can induce immune responses. Furthermore, oxidation of phospholipids, such as PC, results in oxidized-PC; oxidized-PC is capable of activating TLR4 (41, 293). Preliminary data from our lab suggest a role for oxidized phospholipids capable of macrophage activation.

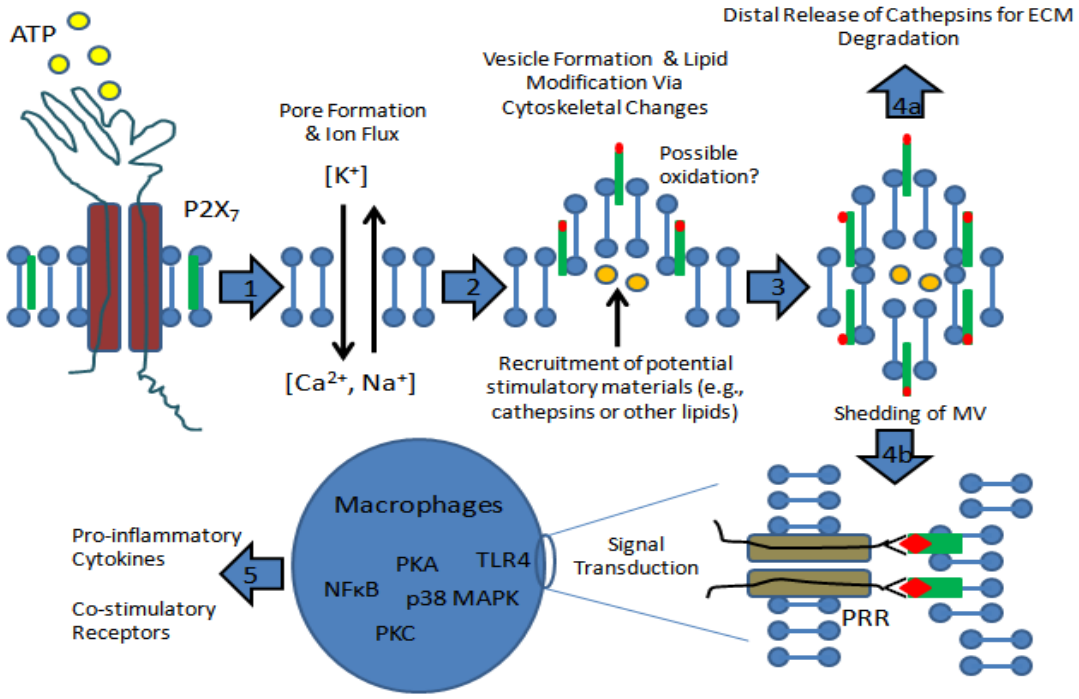

Figure 5-1: Proposed mechanism for MV-induced inflammation.

(1) ATP engages $P2X_7$ for activation of pore formation and ion flux – calcium (Ca^{2+}) and sodium (Na^{+}) influx and potassium (K^{+}) efflux. (2) Ion flux induces several changes within cells including cytoskeletal changes and recruitment of stimulatory materials (e.g., cathepsins) (orange) to the plasma membrane; this activity is modified in some instances by phospholipase D. Oxidation (red) may also modify phospholipids (green) as alterations of membrane topology are occurring at the plasma membrane. (3) The altered cytoskeleton (along with other mechanisms such as actin polymerization and calcium signaling) results in the shedding of MV. (4a) Shed MV can remobilize to distal sites for the timed release of components including cathepsins; these cathepsins can cleavage substrates such as extracellular matrix (ECM). (4b) Alternatively, shed MV could present modified phospholipids (perhaps oxidized) to macrophages that can engage a variety of pattern recognition receptors (PRR) including TLR4. Signal transduction pathways involving p38 MAPK, NF-κB, protein kinase C (PKC), and protein kinase A (PKA) enable the release of pro-inflammatory cytokines (e.g., TNF-α and IL-6) and upregulation of co-stimulatory ligands (e.g., CD80 and CD86) and MHC class II at the plasma membrane.

It is possible that $P2X_7$-induced MV also promote lipid dissemination. By nature, some lipids such as phospholipids are highly amphipathic with polar and non-polar chemical components; in this manner, phospholipids need to be associated with other lipids and/or proteins to disperse in aqueous environments. As they are comprised primarily of lipid bi-layer membranes, MV are capable of dispersing lipid mediators (210). Some novel components, including specific lipids, are trafficked into MV such as exosomes; lipids (e.g., lysobisphosphatidic acid) can be sorted through directional cues to multi-vesicular bodies (MVB), the organelle for exosome biogenesis (251). For plasma membrane-derived MV, phospholipase A_2 promotes lysophosphatidic acid formation and loading into shed MV (332). The formation of MV has been hypothesized to occur in several ways but most commonly through membrane curvature and detachment (333). Various plasma membrane components, including lipids (e.g., phosphatidic acid) and cholesterol, can impart this required membrane curvature (334). Since these components result in the membrane curvature responsible for the budding off of MV, they would thus be enriched within the MV. Formation of MV also involves membrane asymmetry. Phosphatidylserine flip outward occurs during MV formation (231). Thus MV contain not only an enrichment of novel lipids, but they can also contain unique topologies of lipids such that normally cytofacial lipids are exofacial facing outward towards the extracellular environment.

Lipid-mediated modulation of the immune system has been recognized for a long time and it is possible that $P2X_7$-induced MV participate in these processes. From my work, phospholipids from $P2X_7$-induced MV are capable of promoting macrophage activation. It is interesting to consider phospholipid-mediated immune cell activation in the setting of inflammatory diseases. $P2X_7$-induced MV themselves expose phosphatidylserine (PS) and have

thrombotic activities associated with atherosclerosis progression (190, 250). MV (described in relevant literature as microparticles) promote coagulant activities in atherosclerosis through their exposure of negatively charged phospholipids, especially PS (335). Another potential property of PS found on MV is its ability to activate the scavenger receptor CD36, which promotes atherogenesis and thrombosis (336). It is not just PS that promotes disease. In cancer, sphingomyelin from MV act with VEGF to promote angiogenesis (337, 338).

Another class of potential immune modulators described from this work are cathepsins. Cathepsins are capable of restructuring extracellular matrices (ECM) within tissue; ECM degradation following inflammatory situations can develop for diseases such as arthritis, cancer, or neurodegeneration (209). In the context of cancer, oncogenic materials including cancerous cells can be disseminated for metastasis (339). During preparation of this work, another group described that $P2X_7$ stimulated myeloid cells can release biologically active cathepsins in the absence of initial PAMP priming (186). We, however, provide a more thorough mechanistic understanding. This work describes intermediate and mature cathepsin D presence within $P2X_7$-induced MV and I reveal some of the cellular machinery for mature cathepsin D release. Cathepsin D is displaced towards the periphery of cells, where it is in close proximity to dynamin. Dynamin inhibition by dynasore resulted in significantly less mature cathepsin D secretion from ATP treated cells. Upon close evaluation, lysosomal components cathepsin D and lamp-1 were localized to the periphery within F-actin enriched filopodia. Whether or not these filopodia serve as conduits for lysosomal component release is not yet clear; however, actin polymerization inhibition did result in decreased mature cathepsin D within harvested $P2X_7$-induced MV. Given the role of dynamin for cathepsin D release from my work and a recent report of dynamin in mediating actin filament elongation (340), *de novo* produced filopodia may

serve as a release point for dynamin-mediated cathepsin D release. Much more work would be necessary to establish this potential function of dynamin and how it would coordinate with these actin structures, let alone with lysosomal compartments or machinery. However, dynamin associated exocytosis of materials is an established concept (306, 308-310). A related small GTPase to dynamin, ARF6, along with phospholipase D have also been associated with the pinching off of MV from the plasma membrane (341); these authors suggest a role for dynamin as well (333). Whether cathepsin D-loaded MV are the same as the MV that contain stimulatory phospholipids is not yet clear, but it is understood that there is a diversity of types of shed MV from $P2X_7$-stimulated myeloid cells (246).

Cathepsins within harvested MV have been documented; however, it is interesting to consider why the delivery of cathepsins within MV would be beneficial or how they could be functional. An enticing possibility is the selective delivery of cathepsins across tissues for extracellular matrix degradation; the mechanisms by which macrophages promote protease-mediated ECM degradation have not been fully characterized. MV can serve to preserve cargo; in this sense, cathepsins may act at some more distal site to be released from MV at later time points. MV also express receptors that could result in the selective targeting to preferred sites. Such receptors include integrins, which can promote the attachment of MV to certain materials, including ECM. Upon MV degradation, MV contents, including their contained cathepsins, could leak out to the local environment. Thus MV may be an effective means for cathepsin-mediated degradation of the ECM within tissue. Another interesting angle comes from the potential for MV generation following $P2X_7$-mediated filopodia production. Macrophages and dendritic cells reside primarily in selective niches within tissue. Upon $P2X_7$ induction, these newly developed filopodia could extend far into tissue where cellular passage is not generally

possible. Thus these filopodia may promote the delivery of MV across tissue barriers. Even without the need for filopodia-mediated MV shedding, the detachment of filopodia could selectively deliver cathepsins to certain ECM. This would have large implications in disease biology as cathepsin-mediated break-down of the ECM can result in angiogenesis, atherogenesis, and other diseases.

Whereas a large focus of the work described here has been to mechanistically understand what $P2X_7$-induced MV contain and how they can activate macrophages, there is potential for their therapeutic application – in particular with vaccination strategies. $P2X_7$-induced MV greatly upregulate the antigen-presenting machinery of macrophages while also promoting pro-inflammatory cytokine secretion. Since these stimulatory MV are largely derived from the plasma membrane of cells, it is certainly possible for the MV to contain a diversity of plasma membrane materials. Thus $P2X_7$-induced MV could contain antigens or intact MHC + peptides along with stimulatory activities necessary for efficient cross-priming of cytolytic CD8+ T cells, which enables effective adaptive immune responses. In some circumstances, professional antigen presenting cells (APC) can cross-present extracellular antigen epitopes on MHC class I (10). Once mature (or activated), these APC can in certain circumstances cross-prime naïve CD8+ T cells to become efficiently activated cytolytic T cells capable of killing specific antigen-cognate target cells. In this manner, it is possible to engineer myeloid cells with desired antigen expression at the plasma membrane. Upon $P2X_7$ stimulation, MV are shed with antigen and stimulatory phospholipids and possibly other stimulatory materials. These MV can be administered in a vaccination regimen. Alternatively, once enough mechanistic understanding is obtained, artificial liposomes could be generated with stimulatory phospholipids and the antigen(s) of interest.

5.2 TRANSITIONING *IN VITRO* RESULTS TO *IN VIVO* MECHANISMS

MV are not just artifacts from cell culture. MV can be harvested from *in vivo* sources including peripheral blood, urine, and ascitic fluids (333). Greater levels of MV have been harvested from the blood of cancer patients than healthy individuals. MV also have relevance in promoting diseases such as atherosclerosis (342). Given their presence and influence in disease, understanding how MV are generated *in vivo* and how they act *in vivo* are very important.

Transitioning *in vitro* cell biology observations to *in vivo* mechanisms that naturally occur is not a simple task. Observing MV shedding *in vivo* has been very circumstantial (210). In large part, this comes from the difficulties in obtaining indisputable *in vivo* imaging evidence and separating biologically shed MV from artifacts. Harvesting MV from *in vivo* sources is daunting given the potential for artifacts such as fragmented cellular components from damaged tissue.

Most of the potential for *in vivo* understanding, though, will come from modulating molecular mechanisms understood from *in vitro* studies. Such mechanisms include blockade of ATP and $P2X_7$ in addition to other molecular targets associated with stimulatory MV generation, such as PLD. Attempting to observe MV shedding should not be the primary focus for *in vivo* MV relevance. Rather, biological outcomes from molecular target blockade should be the ultimate goal in conjunction with attempts to visualize MV *in vivo*.

Our understanding of the *in vivo* function of ATP and purinergic receptors has greatly improved over the past few years. Several studies have implicated $P2X_7$ in inflammatory activities from abrogating immunosuppressive regulatory T cells (165) to promoting neutrophil recruitment (40) to promoting inflammatory disease (37, 161, 162, 189, 283, 284, 343).

Furthermore, the concept that ATP is physiologically able to promote the activation of purinergic receptors *in vivo* is now generally accepted. ATP activity through $P2X_7$ can result in graft-versus host disease (187), initiate contact hypersensitivity (161), and engage the immune response to ameliorate cancer (162) *in vivo*. Various groups have directly observed relevant amounts of physiologically released ATP from damaged cells *in vivo* and have determined ATP's role in modulating disease *in vivo*. An interesting approach utilizes implanted cells expressing an exofacial expressed luciferase protein chimera; in the presence of injected luciferin and ATP released from damaged cells, bioluminescence is produced (148, 161, 187). Individuals with hyperactive $P2X_7$ activity progressively develop inflammatory diseases such as Alzheimer's disease (189). Additionally, individuals with loss-of-function $P2X_7$ polymorphisms exhibit decreased ability to clear mycobacterial infections, which is a function of $P2X_7$ (173).

In this work, I have uncovered several cell biological phenomena that have immunological implications *in vitro*; in order to move forward *in vivo* studies are necessary. An intriguing concept presented within this summary section is the potential for $P2X_7$-induced MV to disperse their cargo to selective sites. A highly relevant model would be trauma or more generalized tissue damage. Damaged tissue can result in the release of intracellular content including ATP. MV shedding and damaged tissue fragments are currently hard to visually discriminate; a better approach would be to selectively block known mechanisms for stimulatory MV generation.

In this summary section, I discuss the potential for $P2X_7$-induced MV to complicate inflammatory diseases. As mentioned, $P2X_7$-induced MV expose PS, which has pro-coagulant properties that can exacerbate diseases such as atherosclerosis (190, 250). An important question

resides in whether $P2X_7$-induced MV can direct inflammatory disease progression. One approach would be to inhibit $P2X_7$ and stimulatory MV generation processes in an inflammatory disease model (e.g., $ApoE^{-/-}$ mouse model of atherosclerosis). Specifically evaluating MV involvement, as opposed to soluble phospholipids, may be difficult; however, *ex vivo* characterization of the relevant cell populations (e.g., macrophage foam cells developed during atherogenesis) should reveal the passive acquisition of several MV-derived materials at their cell surface. I have observed that biotinylated proteins from MV can remain on the cell surface of recipient cells for several hours. MV-derived materials are very heterogeneous and can be unique; for instance otherwise healthy cells would not express markers such as PS on their plasma membrane. While it may be difficult to make definitive conclusions, these extracted cells could also be evaluated by electron microscopy for the presence of MV on the plasma membrane or within the phagosomes of these cells.

Another practical aspect that emerges from my studies is the potential for MV to induce effective cross-priming. $P2X_7$-induced MV could deliver materials for cross-presentation or incorporate materials at the plasma membrane for semi-direct antigen presentation (antigen "cross-dressing"). Further, these MV also promote APC maturation/activation. Demonstrating cross-priming *in vivo* is important, as cross-priming is thought to be necessary for effective CD8+ T cell responses and vaccination strategies. While injection of *in vitro*-generated $P2X_7$-induced MV (loaded with a model antigen) into mice is good first step to analyze potential *in vivo* immune responses, a more physiological approach would be to initiate tissue damage along with the model antigen. Deducing $P2X_7$-induced MV relevance could partly be achieved by blocking $P2X_7$ and MV generation pathways. Following induced tissue damage, antigen-cognate CD8+ T cells could be removed from local draining lymph nodes and analyzed for activation.

Another possible extension of my studies is the possibility for MV-derived cathepsins to mediate ECM degradation. Released cathepsins have displayed abilities to degrade ECM; however, MV induced dissemination of cathepsins for ECM degradation has not been reported. $P2X_7$ activity has been linked to the release of cathepsins by the work of others (186) and from my own work. An intriguing disease model would be collagen-induced arthritis as blockade of $P2X_7$ ameliorates arthritis development (184, 185). Deducing $P2X_7$-induced MV relevance could also partly be achieved by blocking $P2X_7$ and MV generation pathways. The integrity and composition of the affected ECM could be analyzed by histochemistry. Additionally, the deposition of MV-derived materials on the localized ECM could be evaluated by histochemistry.

The task of developing *in vivo* relevance for $P2X_7$-induced MV is difficult but it could ultimately answer disputed issues in immunology. An important question deals with antigen processing, presentation, and delivery for activating naïve CD8+ T cells in lymph nodes. In mice, lymph node resident CD8α+ dendritic cells are also thought to be the best APC for cross-presenting antigen to CD8+ T cells (344). At the same time, though, in the context of presenting antigen from dying cells, migratory dendritic cells with the correct haplotype of MHC are also crucial for this priming, despite not being the primary cell type that engage CD8+ T cells (13). This sets up the hypothesis that such migratory dendritic cells are donating materials to the CD8α+ dendritic cells (12). How is this donation occurring? In order to efficiently cross-prime, the CD8α+ dendritic cells must be matured. How is this maturation occurring? Stimulatory materials from $P2X_7$-induced MV may provide some insight for not only this question but could prove to be therapeutically beneficial in future vaccination strategies.

6.0 BIBLIOGRAPHY

1. Pasparakis, M. 2009. Regulation of tissue homeostasis by NF-kappaB signalling: implications for inflammatory diseases. *Nat. Rev. Immunol.* 9:778-788.

2. Majno, G., and I. Joris. 2004. *Cells, tissues, and disease:principles of general pathology*. Oxford Univ., New York, New York.

3. Sakaguchi, S., M. Miyara, C. M. Costantino, and D. A. Hafler. 2010. FOXP3+ regulatory T cells in the human immune system. *Nat. Rev. Immunol.* 10:490-500.

4. Serhan, C. N., N. Chiang, and T. E. Van Dyke. 2008. Resolving inflammation: dual anti-inflammatory and pro-resolution lipid mediators. *Nat. Rev. Immunol.* 8:349-361.

5. Janeway, C. A. J., and R. Medzhitov. 2002. Innate immune recognition. *Annu. Rev. Immunol.* 20.

6. Soehnlein, O., and L. Lindborn. 2010. Phagocyte partnership during the onset and resolution of inflammation. *Nat. Rev. Immunol.* 10:427-439.

7. Baggiolini, M., B. Dewald, and B. Moser. 1997. Human Chemokines: An Update. *Annu. Rev. Immunol.* 15:675-705.

8. Pamer, E., and P. Cresswell. 1998. Mechanisms of MHC class I–restricted antigen processing. *Annu. Rev. Immunol.* 16:323-358.

9. Castellino, F., G. Zhong, and R. N. Germain. 1997. Antigen presentation by MHC class II molecules: invariant chain function, protein trafficking, and the molecular basis of diverse determinant capture. *Hum. Immunol.* 54:159-169.

10. Banchereau, J., F. Briere, C. Caux, J. Davoust, S. Lebecque, Y.-J. Liu, B. Pulendran, and K. Palucka. 2000. Immunobiology of dendritic cells. *Annu. Rev. Immunol.* 18:767-811.

11. Forster, R., A. C. Davalos-Misslitz, and A. Rot. 2008. CCR7 and its ligands: balancing immunity and tolerance. *Nat. Rev. Immunol.* 8:362-371.

12. Allan, R. S., J. Waithman, S. Bedoui, C. M. Jones, J. A. Villadangos, Y. Zhan, A. M. Lew, K. Shortman, W. R. Heath, and F. R. Carbone. 2006. Migratory dendritic cells transfer antigen to a lymph node-resident dendritic cell population for efficient CTL priming. *Immunity* 25:153-162.

13. Qu, C., V. A. Nguyen, M. Merad, and G. J. Randolph. 2009. MHC class I/peptide transfer between dendritic cells overcomes poor cross-presentation by monocyte-derived APCs that engulf dying cells. *J. Immunol.* 182:3650-3659.

14. Allenspach, E. J., M. P. Lemos, P. M. Porrett, L. A. Turka, and T. M. Laufer. 2008. Migratory and lymphoid-resident dendritic cells cooperate to efficiently prime naive CD4 T cells. *Immunity* 29:795-806.

15. Rot, A., and U. H. von Andrian. 2004. Chemokines in innate and adaptive host defense: basic chemokinese grammar for immune cells. *Annu. Rev. Immunol.* 22:891-928.

16. Janeway, C. A. J., C. C. Goodnow, and R. Medzhitov. 1996. Immunological tolerance: Danger – pathogen on the premises! *Curr. Biol.* 6:519-522.

17. Matzinger, P. 1994. Tolerance, danger, and the extended family. *Annu. Rev. Immunol.* 12:991-1045.

18. Kono, H., and K. L. Rock. 2008. How dying cells alert the immune system to danger. *Nat. Rev. Immunol.* 8:279-289.

19. Ravichandran, K. S. 2010. Find-me and eat-me signals in apoptotic cell clearance: progress and conundrums. *J. Exp. Med.* 207:1807-1817.

20. Ullrich, E., M. Bonmort, G. Mignot, G. Kroemer, and L. Zitvogel. 2008. Tumor stress, cell death and the ensuing immune response. *Cell Death Differ.* 15:21-28.

21. Birge, R. B., and D. S. Ucker. 2008. Innate apoptotic immunity: the calming touch of death. *Cell Death Differ.* 15:1096-1102.

22. Erridge, C. 2010. Endogenous ligands of TLR2 and TLR4: agonists or assistants? *J. Leukoc. Biol.* 87:989-999.

23. Takeda, K., T. Kaisho, and S. Akira. 2003. Toll-like receptors. *Annu. Rev. Immunol.* 2:335-376.

24. Uematsu, S., M. H. Jang, N. Chevrier, Z. Guo, Y. Kumagai, M. Yamamoto, H. Kato, N. Sougawa, H. Matsui, H. Kuwata, H. Hemmi, C. Coban, T. Kawai, K. J. Ishii, O. Takeuchi, M. Miyasaka, K. Takeda, and S. Akira. 2006. Detection of pathogenic intestinal bacteria by Toll-like receptor 5 on intestinal CD11c+ lamina propria cells. *Nat. Immunol.* 7:868-874.

25. Means, T. K., F. Hayashi, K. D. Smith, A. Aderem, and A. D. Luster. 2003. The Toll-like receptor 5 stimulus bacterial flagellin induces maturation and chemokine production in human dendritic cells. *J. Immunol.* 170:5165-5175.

26. Ghosh, S., M. J. May, and E. B. Kopp. 1998. NF-kappa B and Rel proteins: evolutionarily conserved mediators of immune responses. *Annu. Rev. Immunol.* 16:225-260.

27. Akira, S., and K. Takeda. 2004. Toll-like receptor signaling. *Nat. Rev. Immunol.* 4:499-511.

28. Jha, S., and J. P. Ting. 2009. Inflammasome-associated nucleotide-binding domain, leucine-rich repeat proteins and inflammatory diseases. *J. Immunol.* 183:7623-7629.

29. Kawai, T., and S. Akira. 2008. Toll-like receptor and RIG-I-like receptor signaling. *Ann. N. Y. Acad. Sci.* 1143:1-20.

30. Cole, J. E., E. Georgiou, and C. Monaco. 2010. The expression and functions of toll-like receptors in atherosclerosis. *Mediators Inflamm.* 2010.

31. Iwasaki, A., and R. Medzhitov. 2004. Toll-like receptor control of the adaptive immune responses. *Nat. Immunol.* 5:987-995.

32. Kawai, T., and S. Akira. 2010. The role of pattern-recognition receptors in innate immunity: update on Toll-like receptors. *Nat. Immunol.* 11:373-384.

33. Honda, K., H. Yanai, A. Takaoka, and T. Taniguchi. 2005. Regulation of the type I IFN induction: a current view. *Int. Immunol.* 17:1367-1378.

34. Martinon, F., A. Mayor, and J. Tschopp. 2009. The inflammasomes: guardians of the body. *Annu. Rev. Immunol.* 27:229-265.

35. Bianchi, M. E. 2007. DAMPs, PAMPs and alarmins: all we need to know about danger. *J. Leukoc. Biol.* 81:1-5.

36. Beigi, R., E. Kobatake, M. Aizawa, and G. R. Dubyak. 1999. Detection of local ATP release from activated platelets using cell surface-attached firefly luciferase. *Am. J. Physiol.* 276:C267-C278.

37. Bours, M. J. L., E. L. R. Swennen, F. Di Virgilio, B. N. Cronstein, and P. C. Dagneli. 2006. Adenosine 5'-triphosphate and adenosine as endogenous signaling molecules in immunity and inflammation. *Pharmacol. Ther.* 112:358-404.

38. Park, J. S., D. Svetkauskaite, Q. He, J. Y. Kim, D. Strassheim, A. Ishizaka, and E. Abraham. 2004. Involvement of toll-like receptors 2 and 4 in cellular activation by high mobility group box 1 protein. *J. Biol. Chem.* 279:7370-7377.

39. Tian, J., A. M. Avalos, S. Y. Mao, B. Chen, K. Senthil, H. Wu, P. Parroche, S. Drabic, D. Golenbock, C. Sirois, J. Hua, L. L. An, L. Audoly, G. La Rosa, A. Bierhaus, P. Naworth,

A. Marshak-Rothstein, M. K. Crow, K. A. Fitzgerald, E. Latz, P. A. Kiener, and A. J. Coyle. 2007. Toll-like receptor 9-dependent activation by DNA-containing immune complexes is mediated by HMGB1 and RAGE. *Nat. Immunol.* 8:487-496.

40. McDonald, B., K. Pittman, G. B. Menezes, S. A. Hirota, I. Slaba, C. C. Waterhouse, P. L. Beck, D. A. Muruve, and P. Kubes. 2010. Intravascular danger signals guide neutrophils to sites of sterile inflammation. *Science* 330:362-366.

41. Stewart, C. R., L. M. Stuart, K. Wilkinson, J. M. van Gils, J. Deng, A. Halle, K. J. Rayner, L. Boyer, R. Zhong, W. A. Frazier, A. Lacy-Hulbert, J. E. Khoury, D. T. Golenbock, and K. J. Moore. 2010. CD36 ligands promote sterile inflammation through assembly of a Toll-like receptor 4 and 6 heterodimer. *Nat. Immunol.* 11:155-161.

42. Schroder, K., and J. Tschopp. 2010. The inflammasomes. *Cell* 140:821-832.

43. Robinson, D. R., J. M. Dayer, and S. M. Krane. 1979. Prostaglandins and their regulation in rheumatoid inflammation. *Ann. N. Y. Acad. Sci.* 332:279-294.

44. Gutierrez, M. G., A. P. Gonzaolez, E. Anes, and G. Griffiths. 2009. Role of lipids in killing mycobacteria by macrophages: evidence for NF-kappaB-dependent and -independent killing induced by different lipids. *Cell Microbiol.* 11:406-420.

45. Cabral, G. A. 2005. Lipids as bioeffectors in the immune system. *Life Sci.* 77:1699-1710.

46. Hazen, S. L. 2008. Oxidized phospholipids as endogenous pattern recognition ligands in innate immunity. *J. Biol. Chem.* 283:15527-15531.

47. Thurnher, M. 2007. Lipids in dendritic cell biology: messengers, effectors, and antigens. *J. Leukoc. Biol.* 81:154-160.

48. Gay, N. J., M. Gangloff, and A. N. R. Weber. 2006. Toll-like receptors as molecular switches. *Nat. Rev. Immunol.* 6:693-698.

49. Jerala, R. 2007. Structural biology of the LPS recognition. *Int. J. Med. Microbiol.* 297:353-363.

50. Barton, G. M., and J. C. Kagan. 2009. A cell biological view of Toll-like receptor function: regulation through compartmentalization. *Nat. Rev. Immunol.* 9:535-542.

51. Ewald, S. E., B. L. Lee, L. Lau, K. E. Wickliffe, G. P. Shi, H. A. Chapman, and G. M. Barton. 2008. The ectodomain of Toll-like receptor 9 is cleaved to generate a functional receptor. *Nature* 456:658-662.

52. Lee, H. K., J. M. Lund, B. Ramanathan, N. Mizushima, and A. Iwasaki. 2007. Autophagy-depedent viral recognition by plasmacytoid dendritic cells. *Science* 315:1398-1401.

53. Liebmann, C. 2001. Regulation of MAP kinase activity by peptide receptor signalling pathway: paradigms of multiplicity. *Cell Signal* 13:777-785.

54. Taylor, S. S., J. Yang, J. Wu, N. M. Haste, E. Radzio-Andzelm, and G. Anand. 2004. PKA: a portrait of protein kinase dynamics. *Biochim. Biophys. Acta.* 1679:259-269.

55. Steinberg, S. F. 2008. Structural basis of protein kinase C isoform function. *Physiol. Rev.* 88:1341-1378.

56. Mailliard, R. B., A. Wankowicz-Kalinska, Q. Cai, A. Wesa, C. M. Hilkens, M. L. Kapsenberg, J. M. Kirwood, W. J. Storkus, and P. Kalinski. 2004. alpha-type-1 polarized dendritic cells: a novel immunization tool with optimized CTL-inducing activity. *Cancer Res.* 64:5934-5937.

57. Garay, J., J. A. D'Angelo, Y. Park, C. M. Summa, M. L. Aiken, E. Morales, K. Badizadegan, E. Fiebiger, and B. L. Dickinson. 2010. Crosstalk between PKA and Epac regulates the phenotypic maturation and function of human dendritic cells. *J. Immunol.* 185:3227-3238.

58. Kubo-Murai, M., K. Hazeki, N. Sukenobu, K. Yoshikawa, K. Nigorikawa, K. Inoue, T. Yamamoto, M. Matsumoto, T. Seya, N. Inoue, and O. Hazeki. 2007. Protein kinase Cdelta binds TIRAP/Mal to participate in TLR signaling. *Mol. Immunol.* 44:2257-2264.

59. Asehnoune, K., D. Strassheim, S. Mitra, J.-Y. Kim, and E. Abraham. 2005. Involvement of PKCalpha/beta in TLR4 and TLR2 dependent activation of NF-kappaB. *Cell Signal* 17:385-394.

60. McGettrick, A. F., E. K. Brint, E. M. Palsson-McDermott, D. C. Rowe, D. T. Golenbock, N. J. Gay, K. A. Fitzgerald, and L. A. O'Neill. 2006. Trif-related adapter molecule is phosphorylated by PKC{epsilon} during Toll-like receptor 4 signaling. *Proc. Natl. Acad. Sci. USA.* 103:9196-9201.

61. Cuschieri, J., K. Umanskiy, and J. Solomkin. 2004. PKC-zeta is essential for endotoxin-induced macrophage activation. *J. Surg. Res.* 121:76-83.

62. Dallot, E., C. Mehats, S. Oger, M. J. Leroy, and M. Breuiller-Fouche. 2005. A role for PKCzeta in the LPS-induced translocation NF-kappaB p65 subunit in cultured myometrial cells. *Biochimie.* 87:513-521.

63. Scheibner, K. A., M. M. Lutz, S. Boodoo, M. J. Fenton, J. D. Powell, and M. R. Horton. 2006. Hyaluronan fragments act as an endogenous danger signal by engaging TLR2. *J. Immunol.* 177:1272-1281.

64. Trushin, S. A., K. N. Pennington, E. M. Carmona, S. Asin, D. N. Savoy, D. D. Billadeau, and C. V. Paya. 2003. Protein kinase Calpha (PKCalpha) acts upstream of PKCtheta to activate IkappaB kinase and NF-kappaB in T lymphocytes. *Mol. Cell Biol.* 23:7068-7081.

65. Chen, C., C. Chou, Y. Sun, and W. Huang. 2001. Tumor necrosis factor alpha-induced activation of downstream NF-kappaB site of the promoter mediates epithelial ICAM-1 expression and monocyte adhesion. Involvement of PKCalpha, tyrosine kinase, and IKK2, but not MAPKs, pathway. *Cell Signal.* 13:543-553.

66. Cataisson, C., A. J. Pearson, S. Torgerson, S. A. Nedospasov, and S. H. Yuspa. 2005. Protein kinase C alpha-mediated chemotaxis of neutrophils requires NF-kappa B activity but is independent of TNF alpha signaling in mouse skin in vivo. *J. Immunol.* 174:1686-1692.

67. Barrat, F. J., T. Meeker, J. Gregorio, J. H. Chan, S. Uematsu, S. Akira, B. Chang, O. Duramad, and R. L. Coffman. 2005. Nucleic acids of mammalian origin can act as endogenous ligands for Toll-like receptors and may promote systemic lupus erythematosus. *J. Exp. Med.* 202:1131-1139.

68. Yanai, H., T. Ban, Z. Wang, M. K. Choi, T. Kawamura, H. Negishi, M. Nakasato, Y. Lu, S. Hangai, R. Koshiba, D. Savitsky, L. Ronfani, S. Akira, M. E. Bianchi, K. Honda, T. Tamura, T. Kodama, and T. Taniguchi. 2009. HMGB proteins function as universal sentinels for nucleic-acid-mediated innate immune responses. *Nature* 462:99-103.

69. Yang, H., H. S. Hreggvidsdottir, K. Palmblad, H. Wang, M. Ochani, J. Li, B. Lu, S. Chavan, M. Rosas-Ballina, Y. Al-Abed, S. Akira, A. Bierhaus, H. Erlandsson-Harris, U. Andersson, and K. J. Tracey. 2010. A critical cysteine is required for HMGB1 binding to Toll-like receptor 4 and activation of macrophage cytokine release. *Proc. Natl. Acad. Sci. USA.* 107:11942-11947.

70. Rosas-Ballina, M., R. S. Goldstein, M. Gallowitsch-Puerta, L. Yang, S. I. Valdes-Ferrer, N. B. Patel, S. Chavan, Y. Al-Abed, H. Yang, and K. J. Tracey. 2009. The selective alpha7 agonist GTS-21 attenuates cytokine production in human whole blood and human monocytes activated by ligands for TLR2, TLR3, TLR4, TLR9, and RAGE. *Mol. Med.* 15:195-202.

71. Jiang, D., J. Liang, J. Fan, S. Yu, S. Chen, Y. Luo, G. D. Prestwich, M. M. Mascarenhas, H. G. Garg, D. A. Quinn, R. J. Homer, D. R. Goldstein, R. Bucala, P. J. Lee, R. Medzhitov, and P. W. Noble. 2005. Regulation of lung injury and repair by Toll-like receptors and hyaluronan. *Nat. Med.* 11:1173-1179.

72. Faustin, B., L. Lartigue, J. M. Bruey, F. Luciano, E. Sergienko, B. Bailly-Maitre, N. Volkmann, D. Hanein, I. Rouiller, and J. C. Reed. 2007. Reconstituted NALP1 inflammasome reveals two-step mechanism of caspase-1 activation. *Mol. Cell.* 25:713-724.

73. Hsu, L. C., S. R. Ali, S. McGillivray, P. H. Tseng, S. Mariathasan, E. W. Humke, L. Eckmann, J. J. Powell, V. Nizet, V. M. Dixit, and M. Karin. 2008. A NOD2-NALP1 complex mediates caspase-1-dependent IL-1beta secretion in response to Bacillus anthracis infection and muramyl dipeptide. *Proc. Natl. Acad. Sci. USA.* 105:7803-7808.

74. Franchi, L., A. Amer, M. Body-Malapel, T. D. Kanneganti, N. Ozoren, R. Jagirdar, N. Inohara, P. Vandenabelle, J. Bertin, A. Coyle, E. P. Grant, and G. Nunez. 2006. Cytosolic flagellin requires Ipaf for activation of caspase-1 and interleukin 1beta in salmonella-infected macrophages. *Nat. Immunol.* 7:576-582.

75. Suzuki, T., L. Franchi, C. Toma, H. Ashida, M. Ogawa, Y. Yoshikawa, H. Mimuro, N. Inohara, C. Sasakawa, and G. Nunez. 2007. Differential regulation of caspase-1 activation, pyroptosis, and autophagy via Ipaf and ASC in Shigella-infected macrophages. *PLoS Pathog.* 3:e111.

76. Molofsky, A. B., B. G. Byrne, N. N. Whitfield, C. A. Madigan, E. T. Fuse, K. Tateda, and M. S. Swanson. 2006. Cytosolic recognition of flagellin by mouse macrophages restricts Legionella pneumophila infection. *J. Exp. Med.* 203:1093-1104.

77. Hornung, V., A. Ablasser, M. Charrel-Dennis, F. Bauernfeind, G. Horvath, D. R. Caffrey, E. Latz, and K. A. Fitzgerald. 2009. AIM2 recognizes cytosolic dsDNA and forms a caspase-1-activating inflammasome with ASC. *Nature* 458:514-518.

78. Mariathasan, S., D. S. Weiss, K. Newton, J. McBride, K. O'Rourke, M. Roose-Girma, W. P. Lee, Y. Weinrauch, D. M. Monack, and V. M. Dixit. 2006. Cryopyrin activates the inflammasome in response to toxins and ATP. *Nature* 440:228-232.

79. Martinon, F., V. Petrilli, A. Mayor, A. Tardivel, and J. Tschopp. 2006. Gout-associated uric acid crystals activate the NALP3 inflammasome. *Nature* 440:237-241.

80. Duewell, P., H. Kono, K. J. Rayner, C. M. Sirois, G. Vladimer, F. G. Bauernfeind, G. S. Abela, L. Franchi, G. Nunez, M. Schnurr, T. Espevik, E. Lien, K. A. Fitzgerald, K. L. Rock, K. J. Moore, S. D. Wright, V. Hornung, and E. Latz. 2010. NLRP3 inflammasomes are required for atherogenesis and activated by cholesterol crystals. *Nature* 464:1357-1361.

81. Hornung, V., F. Bauernfeind, A. Halle, E. O. Samstad, H. Kono, K. L. Rock, K. A. Fitzgerald, and E. Latz. 2008. Silica crystals and aluminum salts activate the NALP3 inflammasome through phagosomal destabilization. *Nat. Immunol.* 9:847-856.

82. Halle, A., V. Hornung, G. C. Petzold, C. R. Stewart, B. G. Monks, T. Reinheckel, K. A. Fitzgerald, E. Latz, K. J. Moore, and D. T. Golenbock. 2008. The NALP3 inflammasome is involved in the innate immune response to amyloid-beta. *Nat. Immunol.* 9:857-865.

83. Allen, I. C., M. A. Scull, C. B. Moore, E. K. Holl, E. McElvania-TeKippe, D. J. Taxman, E. H. Guthrie, R. J. Pickles, and J. P. Ting. 2009. The NLRP3 inflammasome mediates in vivo innate immunity to influenza A virus through recognition of viral RNA. *Immunity* 30:556-565.

84. Gross, O., H. Poeck, M. Bscheider, C. Dostert, N. Hannesschlager, S. Endres, G. Hartmann, A. Tardivel, E. Schweighoffer, V. Tybulewicz, A. Mocsai, J. Tschopp, and J. Ruland. 2009. Syk kinase signalling couples to the Nlrp3 inflammasome for anti-fungal host defence. *Nature* 459:433-436.

85. Tschopp, J., and K. Schroder. 2010. NLRP3 inflammasome activation: The convergence of multiple signalling pathways on ROS production? *Nat. Rev. Immunol.* 10:210-215.

86. Ichinohe, T., H. K. Lee, Y. Ogura, R. Flavell, and A. Iwasaki. 2009. Inflammasome recognition of influenza virus is essential for adaptive immune responses. *J. Exp. Med.* 206:79-87.

87. Thomas, P. G., P. Dash, J. R. J. Aldridge, A. H. Ellebedy, C. Reynolds, A. J. Funk, W. J. Martin, M. Lamkanfi, R. J. Webby, K. L. Boyd, P. C. Doherty, and T. D. Kanneganti. 2009. The intracellular sensor NLRP3 mediates key innate and healing responses to influenza A virus via the regulation of caspase-1. *Immunity* 30:566-575.

88. Hoffman, H. M., J. L. Mueller, D. H. Broide, A. A. Wanderer, and R. D. Kolodner. 2001. Mutation of a new gene encoding a putative pyrin-like protein causes familial cold autoinflammatory syndrome and Muckle-Wells syndrome. *Nat. Genet.* 29:301-305.

89. Agostini, L., F. Martinon, K. Burns, M. F. McDermott, P. N. Hawkins, and J. Tschopp. 2004. NALP3 forms an IL-1beta-processing inflammasome with increased activity in Muckle-Wells autoinflammatory disorder. *Immunity* 20:319-325.

90. Dostert, C., V. Petrilli, R. Van Bruggen, C. Steele, B. T. Mossman, and J. Tschopp. 2008. Innate immune activation through Nalp3 inflammasome sensing of asbestos and silica. *Science* 320:674-677.

91. Mosser, D. M., and J. P. Edwards. 2008. Exploring the full spectrum of macrophage activation. *Nat. Rev. Immunol.* 8:958-969.

92. Gordon, S. 2003. Alternative activation of macrophages. *Nat. Rev. Immunol.* 3:23-35.

93. O'Shea, J. J., and P. J. Murray. 2008. Cytokine signaling modules in inflammatory responses. *Immunity* 28:477-487.

94. Langrish, C. L., B. S. McKenzie, N. J. Wilson, R. de Waal Malefyt, R. A. Kastelein, and D. J. Cua. 2004. IL-12 and IL-23: master regulators of innate and adaptive immunity. *Immunol. Rev.* 202.

95. Trinchieri, G., S. Pflanz, and R. A. Kastelein. 2003. The IL-12 family of heterodimeric cytokines: new players in the regulation of T cell responses. *Immunity* 19:641-644.

96. Yamamoto, M., S. Sato, K. Mori, K. Hoshino, O. Takeuchi, K. Takeda, and S. Akira. 2002. Cutting edge: a novel Toll/IL-1 receptor domain-containing adapter that preferentially activates the IFN-beta promoter in the Toll-like receptor signaling. *J. Immunol.* 169:6668-6672.

97. Martinez, J., X. Huang, and Y. Yang. 2008. Direct action of type I IFN on NK cells is required for their activation in response to vaccinia viral infection in vivo. *J. Immunol.* 180:1592-1597.

98. MacMicking, J., Q. W. Xie, and C. Nathan. 1997. Nitric oxide and macrophage function. *Annu. Rev. Immunol.* 15:323-350.

99. Dale, D. C., L. Boxer, and W. C. Liles. 2008. The phagocytes: neutrophils and monocytes. *Blood* 112:935-945.

100. Szekanecz, Z., G. Kerekes, H. Der, Z. Sandor, Z. Szabo, A. Vegvari, E. Simkovics, L. Soos, A. Szentpetery, T. Besenyei, G. Szucs, S. Szanto, L. Tamasi, G. Szegedi, Y. Shoenfeld, and P. Soltesz. 2007. Accelerated atherosclerosis in rheumatoid arthritis. *Ann. N. Y. Acad. Sci.* 1108:349-358.

101. Zhang, X., and D. M. Mosser. 2008. Macrophage activation by endogenous danger signals. *J. Pathol.* 214:161-178.

102. Sarkar, S., L. A. Cooney, and D. A. Fox. 2010. The role of T helper type 17 cells in inflammatory arthritis. *Clin. Exp. Immunol.* 159:225-237.

103. van den Berg, W. B., and P. Milossec. 2009. IL-17 as a future therapeutic target for rheumatoid arthritis. *Nat. Rev. Rheumatol.* 5:549-553.

104. Martinez, F. O., L. Helming, and S. Gordon. 2009. Alternative activation of macrophages: an immunologic functional perspective. *Annu. Rev. Immunol.* 2009.

105. Stout, R. D., C. Jiang, B. Matta, I. Tietzel, S. K. Watkins, and J. Suttles. 2005. Macrophages sequentially change their functional phenotype in response to changes in microenvironmental influences. *J. Immunol.* 175:342-349.

106. Gerber, J. S., and D. M. Mosser. 2001. Reversing lipopolysaccharide toxicity by ligating the macrophage Fc gamma receptors. *J. Immunol.* 166:6861-6868.

107. Gerard, C., C. Bruyn, A. Marchant, D. Abramowicz, P. Vandenabelle, A. Delvaux, W. Fiers, M. Goldman, and T. Velu. 1993. Interleukin 10 reduces the release of tumor necrosis factor and prevents lethality in experimental endotoxemia. *J. Exp. Med.* 177:547-550.

108. Erwing, L. P., and P. M. Henson. 2007. Immunological consequences of apoptotic cell phagocytosis. *Am. J. Pathol.* 171:2-8.

109. Gold, K. N., C. M. Weyand, and J. J. Goronzy. 1994. Modulation of helper T cell function by prostaglandins. *Arthritis Rheum.* 37:925-933.

110. Hasko, G., P. Pacher, E. A. Deitch, and E. S. Vizi. 2007. Shaping of monocyte and macrophage function by adenosine receptors. *Pharmacol. Ther.* 113:264-275.

111. Hasko, G., C. Szabo, Z. H. Nemeth, and E. A. Deitch. 2002. Dopamine suppresses IL-12 p40 production by lipopolysaccharide-stimulated macrophages via a beta-adrenoceptor-mediated mechanism. *J. Neuroimmunol.* 122:34-39.

112. Sirois, J., G. Menard, A. S. Moses, and E. Y. Bissonnette. 2000. Importance of histamine in the cytokine network in the lung through H2 and H3 receptors: stimulation of IL-10 production. *J. Immunol.* 164:2964-2970.

113. Weigert, A., N. Tzieply, A. von Knethen, A. M. Johann, H. Schmidt, G. Geisslinger, and B. Brune. 2007. Tumor cell apoptosis polarizes macrophages role of sphingosine-1-phosphate. *Mol. Biol. Cell* 18:3810-3819.

114. Pollard, J. W. 2008. Macrophages define the invasive microenvironment in breast cancer. *J. Leukoc. Biol.* 84:623-630.

115. Edwards, J. P., X. Zhang, K. A. Frauwirth, and D. M. Mosser. 2006. Biochemical and functional characterization of three activated macrophage populations. *J. Leukoc. Biol.* 80:1298-1307.

116. Stein, M., S. Keshav, N. Harris, and S. Gordon. 1992. Interleukin 4 potently enhances murine macrophage mannose receptor activity: a marker of alternative immunologic macrophage activation. *J. Exp. Med.* 176:287-292.

117. Corthay, A. 2006. A three-cell model for activation of naïve T helper cells. *Scand. J. Immunol.* 64:93-96.

118. O'Brien, J., T. Lyon, J. Monks, M. S. Lucia, R. S. Wilson, L. Hines, Y. G. Man, V. Borges, and P. Schedin. 2010. Alternatively activated macrophages and collagen remodeling characterize the postpartum involuting mammary gland across species. *Am. J. Pathol.* 176:1241-1255.

119. Anthony, R. M., J. F. J. Urban, F. Alem, H. A. Hamed, C. T. Rozo, J. L. Boucher, N. Van Rooijen, and W. C. Gause. 2006. Memory T(H)2 cells induce alternatively activated macrophages to mediate protection against nematode parasites. *Nat. Med.* 12:955-960.

120. Raes, G., P. De Baestselier, W. Noel, A. Beschin, F. Brombacher, and G. G. Hassanzadeh. 2002. Differential expression of FIZZ1 and Ym1 in alternatively versus classically activated macrophages. *J. Leukoc. Biol.* 71:597-602.

121. Schreiber, T., S. Ehlers, L. Heitmann, A. Rausch, J. Mages, P. J. Murray, R. Lang, and C. Holscher. 2009. Autocrine IL-10 induces hallmarks of alternative activation in macrophages and suppresses antituberculosis effector mechanisms without compromising T cell immunity. *J. Immunol.* 183:1301-1312.

122. Swann, J. B., M. D. Vesely, A. Silva, J. Sharkey, S. Akira, R. D. Schreiber, and M. J. Smyth. 2008. Demonstration of inflammation-induced cancer and cancer immunoediting during primary tumorigenesis. *Proc. Natl. Acad. Sci. USA.* 105:652-656.

123. Lumeng, C. N., J. L. Bodzin, and A. R. Saltiel. 2007. Obesity induces a phenotypic switch in adipose tissue macrophage polarization. *J. Clin. Invest.* 117:175-184.

124. Straus, D. S., and C. K. Glass. 2007. Anti-inflammatory actions of PPAR ligands: new insights on cellular and molecular mechanisms. *Trends Immunol.* 28:551-558.

125. Zeyda, M., D. Farmer, J. Todoric, O. Aszmann, M. Speiser, G. Gyori, G. J. Zlabinger, and T. M. Stulnig. 2007. Human adipose tissue macrophages are of an anti-inflammatory phenotype but capable of excessive pro-inflammatory mediator production. *Int. J. Obes. (Lond.)* 31:1420-1428.

126. Cinti, S., G. Mitchell, G. Barbatelli, I. Murano, E. Ceresi, E. Faloia, S. Wang, M. Fortier, A. S. Greenberg, and M. S. Obin. 2005. Adipocyte death defines macrophage localization and function in adipose tissue of obese mice and humans. *J. Lipid Res.* 46:2347-2355.

127. Patel, V. A., D. J. Lee, A. Longacre-Antoni, L. Feng, W. Lieberthal, J. Rauch, D. S. Ucker, and J. S. Levine. 2009. Apoptotic and necrotic cells as sentinels of local tissue stress and inflammation: response pathways initiated in nearby viable cells. *Autoimmunity* 42:317-321.

128. Hansson, G. K., A. K. Robertson, and C. Soderberg-Naucler. 2006. Inflammation and atherosclerosis. *Annu. Rev. Pathol.* 1:297-329.

129. Martin-Fuentes, P., F. Civeira, D. Recalde, A. L. Garcia-Otin, E. Jarauta, I. Marzo, and A. Cenarro. 2007. Individual variation of scavenger receptor expression in human macrophages with oxidized low-density lipoprotein is associated with a differential inflammatory response. *J. Immunol.* 179:3242-3248.

130. Burnstock, G. 2007. Purine and pyrimidine receptors. *Cell. Mol. Life Sci.* 64:1471-1483.

131. Chen, Y., R. Corriden, Y. Inoue, L. Yip, N. Hashiguchi, A. Zinkernagel, V. Nizet, P. A. Insel, and W. G. Junger. 2006. ATP release guides neutrophil chemotaxis via P2Y2 and A3 receptors. *Science* 314:1792-1795.

132. Lecut, C., K. Frederix, D. M. Johnson, C. Deroanne, M. Thiry, C. Faccinetto, R. Maree, R. J. Evans, P. G. Volders, V. Bours, and C. Oury. 2009. P2X1 ion channels promote neutrophil chemotaxis through Rho kinase activation. *J. Immunol.* 183:2801-2809.

133. Woehrle, T., L. Yip, A. Elkhal, Y. Sumi, Y. Chen, Y. Yao, P. A. Insel, and W. G. Junger. 2010. Pannexin-1 hemichannel-mediated ATP release together with P2X1 and P2X4 receptors regulate T-cell activation at the immune synapse. *Blood* 116:3475-3484.

134. Ulmann, L., H. Hirbec, and F. Rassendren. 2010. P2X4 receptors mediate PGE2 release by tissue-resident macrophages and initiate inflammatory pain. *EMBO J.* 29:2290-2300.

135. Babelova, A., K. Moreth, W. Tsalastra-Greul, J. Zeng-Brouwers, O. Eickelberg, M. F. Young, P. Bruckner, J. Pfeilschifer, R. M. Schaefer, H. H. Grone, and L. Schaefer. 2009. Biglycan, a danger signal that activates the NLRP3 inflammasome via toll-like and P2X receptors. *J. Biol. Chem.* 284:24035-24048.

136. Ohsawa, K., Y. Irino, Y. Nakamura, C. Akazawa, K. Inoue, and S. Kohsaka. 2007. Involvement of P2X4 and P2Y12 receptors in ATP-induced microglial chemotaxis. *Glia* 55:604-616.

137. Marcet, B., M. Horckmans, F. Libert, S. Hassid, J. M. Boeynaems, and D. Communi. 2007. Extracellular nucleotides regulate CCL20 release from human primary airway epithelial cells, monocytes and monocyte-derived dendritic cells. *J. Cell. Physiol.* 211:716-727.

138. Ben Yebdri, F., F. Kukulski, A. Tremblay, and J. Sevigny. 2009. Concomitant activation of P2Y(2) and P2Y(6) receptors on monocytes is required for TLR1/2-induced neutrophil migration by regulating IL-8 secretion. *Eur. J. Immunol.* 39:2885-2894.

139. Elliott, M. R., F. B. Chekeni, P. C. Trampont, E. R. Lazarowski, A. Kadl, S. F. Walk, D. Park, R. I. Woodson, M. Ostankovich, P. Sharma, J. J. Lysiak, T. K. Harden, N. Leitinger, and K. S. Ravichandran. 2009. Nucleotides released by apoptotic cells act as a find-me signal to promote phagocytic clearance. *Nature* 461:282-286.

140. Stokes, L., and A. Surprenant. 2007. Purinergic P2Y2 receptors induce increased MCP-1/CCL2 synthesis and release from rat alveolar and peritoneal macrophages. *J. Immunol.* 179:6016-6023.

141. Kronlage, M., J. Song, L. Sorokin, K. Isfort, T. Schwerdtle, J. Leipziger, B. Robaye, P. B. Conley, H. C. Kim, S. Sargin, P. Schon, A. Schwab, and P. J. Hanley. 2010. Autocrine purinergic receptor signaling is essential for macrophage chemotaxis. *Sci. Signal.* 3:ra55.

142. Muller, T., B. Robaye, R. P. Vieira, D. Ferrari, M. Grimm, T. Jakob, S. F. Martin, F. Di Virgilio, J. M. Boeynaems, J. C. Virchow, and M. Idzko. 2010. The purinergic receptor P2Y2 receptor mediates chemotaxis of dendritic cells and eosinophils in allergic lung inflammation. *Allergy* 65:1545-1553.

143. Vanderstocken, G., B. Bondue, M. Horckmans, L. Di Pietrantonio, B. Robaye, J. M. Boeynaems, and D. Communi. 2010. P2Y2 receptor regulates VCAM-1 membrane and soluble forms and eosinophil accumulation during lung inflammation. *J. Immunol.* 185:3702-3707.

144. Kobayashi, T., H. Kouzaki, and H. Kita. 2010. Human eosinophils recognize endogenous danger signal crystalline uric acid and produce proinflammatory cytokines mediated by autocrine ATP. *J. Immunol.* 184:6350-6358.

145. Koizumi, S., Y. Shigemoto-Mogami, K. Nasu-Tada, Y. Shinozaki, K. Ohsawa, M. Tsuda, B. V. Joshi, K. A. Jacobson, S. Kohsaka, and K. Inoue. 2007. UDP acting at P2Y6 receptors is a mediator of microglial phagocytosis. *Nature* 446:1091-1095.

146. Marteau, F., N. S. Gonzalez, D. Communi, M. Goldman, J. M. Boeynaems, and D. Communi. 2005. Thrombospondin-1 and indoleamine 2,3-dioxygenase are major targets of extracellular ATP in human dendritic cells. *Blood* 106:3860-3866.

147. Vanlangenakker, N., T. Vanden Berghe, D. V. Krysko, N. Festjens, and P. Vandenabelle. 2008. Molecular mechanisms and pathophysiology of necrotic cell death. *Curr. Mol. Med.* 8:207-220.

148. Pellegatti, P., S. Falzoni, P. Pinton, R. Rizzuto, and F. Di Virgilio. 2005. A novel recombinant plasma membrane-targeted luciferase reveals a new pathway for ATP secretion. *Mol. Biol. Cell* 16:3659-3665.

149. Piccini, A., S. Carta, S. Tassi, D. Lasiglie, G. Fossati, and A. Rubartelli. 2008. ATP is released by monocytes stimulated with pathogen-sensing receptor ligands and induces IL-1beta and IL-18 secretion in an autocrine way. *Proc. Natl. Acad. Sci. USA.* 105:8067-8072.

150. Sperlagh, B., G. Hasko, Z. Nemeth, and E. S. Vizi. 1998. ATP released by LPS increases nitric oxide production in raw 264.7 macrophage cell line via P2Z/P2X7 receptors. *Neurochem. Int.* 33:209-215.

151. Dubyak, G. R. 2009. Both sides now: multiple interactions of ATP with pannexin-1 hemichannels. Focus on "A permeant regulating its permeation pore: inhibition of pannexin 1 channels by ATP". *Am. J. Physiol. Cell Physiol.* 296:C235-C241.

152. Chekeni, F. B., M. R. Elliott, J. K. Sandilos, S. F. Walk, J. M. Kinchen, E. R. Lazarowski, A. J. Armstrong, S. Penuela, D. W. Laird, G. S. Salvesen, B. E. Isakson, D. A. Bayliss, and K. S. Ravichandran. 2010. Pannexin 1 channels mediate 'find-me' signal release and membrane permeability during apoptosis. *Nature* 467:863-867.

153. Keller, M., A. Ruegg, S. Werner, and H. D. Beer. 2008. Active caspase-1 is a regulator of unconventional protein secretion. *Cell* 132:818-831.

154. Gardella, S., C. Andrei, D. Ferrera, L. V. Lotti, M. R. Torrisi, M. E. Bianchi, and A. Rubartelli. 2002. The nuclear protein HMGB1 is secreted by monocytes via a non-classical, vesicle-mediated secretory pathway. *EMBO Rep.* 3:995-1001.

155. Alzola, E., A. Pérez-Etxebarria, E. Kabré, D. J. Fogarty, M. Métioui, N. Chaïb, J. M. Macarulla, C. Matute, J. P. Dehaye, and A. Marino. 1998. Activation by P2X7 agonists of two phospholipases A2 (PLA2) in ductal cells of rat submandibular gland. Coupling of the calcium-independent PLA2 with kallikrein secretion. *J. Biol. Chem.* 273:30208-30217.

156. Humphreys, B. D., and G. R. Dubyak. 1996. Induction of the P2z/P2X7 nucleotide receptor and associated phospholipase D activity by lipopolysaccharide and IFN-gamma in the human THP-1 monocytic cell line. *J. Immunol.* 157:5627-5637.

157. Courageot, M. P., S. Lepine, M. Hours, F. Giraud, and J. C. Sulpice. 2004. Involvement of sodium in early phosphatidylserine exposure and phospholipid scrambling induced by P2X7 purinoceptor activation in thymocytes. *J. Biol. Chem.* 279:21815-21823.

158. Trautmann, A. 2009. Extracellular ATP in the immune system: more than just a "danger signal". *Sci. Signal.* 2:pe6.

159. Humphreys, B. D., and G. R. Dubyak. 1998. Modulation of P2X7 nucleotide receptor expression by pro- and anti-inflammatory stimuli in THP-1 monocytes. *J. Leukoc. Biol.* 64:265-273.

160. Solle, M., J. Labasi, D. G. Perregaux, E. Stam, N. Petrushova, B. H. Koller, R. J. Griffiths, and C. A. Gabel. 2001. Altered cytokine production in mice lacking P2X(7) receptors. *J. Biol. Chem.* 276:125-132.

161. Weber, F. C., P. R. Esser, T. Muller, J. Ganesan, P. Pellegatti, M. M. Simon, R. Zeiser, M. Idzko, T. Jakob, and S. F. Martin. 2010. Lack of the purinergic receptor P2X7 results in resistance to contact hypersensitivity. *J. Exp. Med.* 207:2609-2619.

162. Ghiringhelli, F., L. Apetoh, A. Tesniere, L. Aymeric, Y. Ma, C. Ortiz, K. Vermaelen, T. Panaretakis, G. Mignot, E. Ullrich, J. L. Perfettini, F. Schlemmer, E. Tasdemir, M. Uhl, P. Génin, A. Civas, B. Ryffel, J. Kanellopoulous, J. Tschopp, F. André, R. Lidereau, N. M. McLaughlin, N. M. Haynes, M. J. Smyth, G. Kroemer, and L. Zitvogel. 2009. Activation of the NLRP3 inflammasome in dendritic cells induces IL-1beta–dependent adaptive immunity against tumors. *Nat. Med.* 15:1170-1178.

163. van Deventer, H. W., J. E. Burgents, Q. P. Wu, R. M. Woodford, W. J. Brickey, I. C. Allen, E. McElvania-TeKippe, J. S. Serody, and J. P. Ting. 2010. The inflammasome component NLRP3 impairs antitumor vaccine by enhancing the accumulation of tumor-associated myeloid-derived suppressor cells. *Cancer Res.* 70:10161-10169.

164. Brough, D., and N. J. Rothwell. 2007. Caspase-1-dependent processing of pro-interleukin-1beta is cytosolic and precedes cell death. *J. Cell Sci.* 120:772-781.

165. Huber, S., B. Rissiek, K. Klages, J. Huehn, T. Sparwasser, F. Haag, F. Koch-Nolte, O. Boyer, M. Seman, and S. Adriouch. 2010. Extracellular NAD+ shapes the Foxp3+ regulatory T cell compartment through the ART2-P2X7 pathway. *J. Exp. Med.* 207:2561-2568.

166. Taylor, S. R., M. Gonzalez-Begne, S. Dewhurst, G. Chimini, C. F. Higgins, J. E. Melvin, and J. I. Elliott. 2008. Sequential shrinkage and swelling underlie P2X7-stimulated lymphocyte phosphatidylserine exposure and death. *J. Immunol.* 180:300-308.

167. Biswas, D., O. S. Qureshi, W. Y. Lee, J. E. Croudace, M. Mura, and D. A. Lammas. 2008. ATP-induced autophagy is associated with rapid killing of intracellular mycobacteria within human monocytes/macrophages. *BMC Immunol.* 9.

168. Galluzzi, L., J. M. Vicencio, O. Kepp, E. Tasdemir, M. C. Maiuri, and G. Kroemer. 2008. To die or not to die: that is the autophagic question. *Curr. Mol. Med.* 8:78-91.

169. Lammas, D. A., C. Stober, C. J. Harvey, N. Kendrick, S. Panchalingam, and D. S. Kumararatne. 1997. ATP-induced killing of mycobacteria by human macrophages is mediated by purinergic P2Z(P2X7) receptors. *Immunity* 7:433-444.

170. Fairbairn, I. P., C. B. Stober, D. S. Kumararatne, and D. A. Lammas. 2001. ATP-mediated killing of intracellular mycobacteria by macrophages is a P2X(7)-dependent process inducing bacterial death by phagosome-lysosome fusion. *J. Immunol.* 167:3300-3307.

171. Kusner, D. J., and J. Adams. 2000. ATP-induced killing of virulent Mycobacterium tuberculosis within human macrophages requires phospholipase D. *J. Immunol.* 164:379-388.

172. Placido, R., G. Auricchio, S. Falzoni, L. Battistini, V. Colizzi, E. Brunetti, F. Di Virgilio, and G. Mancino. 2006. P2X(7) purinergic receptors and extracellular ATP mediate apoptosis of human monocytes/macrophages infected with Mycobacterium tuberculosis reducing the intracellular bacterial viability. *Cell. Immunol.* 244:10-18.

173. Shemon, A. N., R. Sluyter, S. L. Fernando, A. L. Clarke, L. P. Dao-Ung, K. K. Skarratt, B. M. Saunders, K. S. Tan, B. J. Gu, S. J. Fuller, W. J. Britton, S. Petrou, and J. S. Wiley. 2006. A Thr357 to Ser polymorphism in homozygous and compound heterozygous subjects causes absent or reduced P2X7 function and impairs ATP-induced mycobacterial killing by macrophages. *J. Biol. Chem.* 281:2079-2086.

174. Gu, B. J., B. M. Saunders, C. Jursik, and J. S. Wiley. 2010. The P2X7-nonmuscle myosin membrane complex regulates phagocytosis of nonopsonized particles and bacteria by a pathway attenuated by extracellular ATP. *Blood* 115:1621-1631.

175. Exton, J. H. 2002. Regulation of phospholipase D. *FEBS Lett.* 531:58-61.

176. Brown, F. D., N. Thompson, K. M. Saquib, J. M. Clark, D. Powner, N. T. Thompson, R. Solari, and M. J. Wakelam. 1998. Phospholipase D1 localises to secretory granules and lysosomes and is plasma-membrane translocated on cellular stimulation. *Curr. Biol.* 8:835-838.

177. Carta, S., S. Tassi, C. Semino, G. Fossati, P. Mascagni, C. A. Dinarello, and A. Rubartelli. 2006. Histone deacetylase inhibitors prevent exocytosis of interleukin-1beta-containing secretory lysosomes: role of microtubules. *Blood* 108:1618-1626.

178. Roth, M. G. 2008. Molecular mechanisms of PLD function in membrane traffic. *Traffic* 9:1233-1239.

179. Ktistakis, N. T., C. Delon, M. Manifava, E. Wood, I. Ganley, and J. M. Sugars. 2003. Phospholipase D1 and potential targets of its hydrolysis product, phosphatidic acid. *Biochem. Soc. Trans.* 31:94-97.

180. Brindley, D. N., C. Pilquil, M. Sariahmetoglu, and K. Reue. 2009. Phosphatidate degradation: phosphatidate phosphatases (lipins) and lipid phosphate phosphatases. *Biochim. Biophys. Acta.* 1791:956-961.

181. Brindley, D. N., and C. Pilquil. 2009. Lipid phosphate phosphatases and signaling. *J. Lipid Res.* 50:S225-S230.

182. Wang, D., and R. N. Dubois. 2010. Eicosanoids and cancer. *Nat. Rev. Cancer* 10:181-193.

183. Garcia-Macros, M. P., S., A. Marino, and J. P. Dehaye. 2006. P2X7 and phospholipid signalling: the search of the "missing link" in epithelial cells. *Cell. Signal.* 18:2098-2104.

184. Al-Shukaili, A., J. Al-Kaabi, and B. Hassan. 2008. A comparative study of interleukin-1beta production and p2x7 expression after ATP stimulation by peripheral blood mononuclear cells isolated from rheumatoid arthritis patients and normal healthy controls. *Inflammation* 31:84-90.

185. Labasi, J. M., N. Petrushova, C. Donovan, S. McCurdy, P. Lira, M. M. Payette, W. Brissette, J. R. Wicks, L. Audoly, and C. A. Gabel. 2002. Absence of the P2X7 receptor alters leukocyte function and attenuates an inflammatory response. *J. Immunol.* 168:6436-6445.

186. Lopez-Castejon, G., J. Theaker, P. Pelegrin, A. D. Clifton, M. Braddock, and A. Surprenant. 2010. P2X(7) receptor-mediated release of cathepsins from macrophages is a cytokine-independent mechanism potentially involved in joint diseases. *J. Immunol.* 185:2611-2619.

187. Wilhelm, K., J. Ganesan, T. Muller, C. Durr, M. Grimm, A. Beilhack, C. D. Krempl, S. Sorichter, U. V. Gerlach, E. Juttner, A. Zerweck, F. Gartner, P. Pellegatti, F. Di Virgilio, D. Ferrari, N. Kambham, P. Fisch, J. Finke, M. Idzko, and R. Zeiser. 2010. Graft-versus-host disease is enhanced by extracellular ATP activating P2X7R. *Nat. Med.* 16:1434-1438.

188. Kim, S. Y., J. H. Moon, H. G. Lee, S. U. Kim, and Y. B. Lee. 2007. ATP released from beta-amyloid-stimulated microglia induces reactive oxygen species production in an autocrine fashion. *Exp. Mol. Med.* 39:820-827.

189. Lee, H. G., S. M. Won, B. J. Gwag, and Y. B. Lee. 2010. Microglial P2X7 receptor expression is accompanied by neuronal damage in the cerebral cortex of the APPswe/PS1dE9 mouse model of Alzheimer's disease. *Exp. Mol. Med.* [Epub ahead of print].

190. Baroni, M., C. Pizzirani, M. Pinotti, D. Ferrari, E. Adinolfi, S. Calzavarini, P. Caruso, F. Bernardi, and F. Di Virgilio. 2007. Stimulation of P2 (P2X7) receptors in human dendritic cells induces the release of tissue factor-bearing microparticles. *FASEB J.* 21:1926-1933.

191. Matute, C., I. Torre, F. Perez-Cerda, A. Perez-Samartin, E. Alberdi, E. Etxebarria, A. M. Arranz, R. Ravid, A. Rodriguez-Antiguedad, M. Sanchez-Gomez, and M. Domercq. 2007. P2X(7) receptor blockade prevents ATP excitotoxicity in oligodendrocytes and ameliorates experimental autoimmune encephalomyelitis. *J. Neurosci.* 27:9525-9533.

192. Stow, J. L., P. C. Low, C. Offenhauser, and D. Sangermani. 2009. Cytokine secretion in macrophages and other cells: pathways and mediators. *Immunobiology* 214:601-612.

193. Arvan, P., and D. Castle. 1998. Sorting and storage during secretory granule biogenesis: looking backward and looking forward. *Biochem. J.* 332:593-610.

194. Blott, E. J., and G. M. Griffiths. 2002. Secretory lysosomes. *Nat. Rev. Mol. Cell Biol.* 3:122-131.

195. Benado, A., Y. Nasagi-Atiya, and R. Sagi-Eisenberg. 2009. Protein trafficking in immune cells. *Immunobiology* 214:507-525.

196. Blott, E. J., G. Bossi, R. Clark, M. Zvelebil, and G. M. Griffiths. 2001. Fas ligand is targeted to secretory lysosomes via a proline-rich domain in its cytoplasmic tail. *J. Cell Sci.* 114:2406-2416.

197. Olszewski, M. B., D. Trzaska, E. F. Knol, V. Adamczewska, and J. Dastych. 2006. Efficient sorting of TNF-alpha to rodent mast cell granules is dependent on N-linked glycosylation. *Eur. J. Immunol.* 36:997-1008.

198. Atiya-Nasagi, Y., H. Cohen, O. Medalia, M. Fukudan, and R. Sagi-Eisenberg. 2005. O-glycosylation is essential for intracellular targeting of synaptotagmins I and II in non-neuronal specialized secretory cells. *J. Cell Sci.* 118:1363-1372.

199. Sulimenko, V., E. Draberova, T. Sulimenko, L. Macurek, V. Richterova, P. Draber, and P. Draber. 2006. Regulation of microtubule formation in activated mast cells by complexes of gamma-tubulin with Fyn and Syk kinases. *J. Immunol.* 176:7243-7253.

200. Clark, R. H., J. C. Stinchcombe, A. Day, E. Blott, S. Booth, G. Bossi, T. Hamblin, E. G. Davies, and G. M. Griffiths. 2003. Adaptor protein 3-dependent microtubule-mediated movement of lytic granules to the immunological synapse. *Nat. Immunol.* 4:1111-1120.

201. Kuroda, T. S., and M. Fukuda. 2004. Rab27A-binding protein Slp2-a is required for peripheral melanosome distribution and elongated cell shape in melanocytes. *Nat. Cell Biol.* 6:1195-1203.

202. Puri, N., and P. A. Roche. 2008. Mast cells possess distinct secretory granule subsets whose exocytosis is regulated by different SNARE isoforms. *Proc. Natl. Acad. Sci. USA.* 105:2580-2585.

203. Sander, L. E., S. P. Frank, S. Bolat, U. Blank, T. Galli, H. Bigalke, S. C. Bischoff, and A. Lorentz. 2008. Vesicle associated membrane protein (VAMP)-7 and VAMP-8, but not VAMP-2 or VAMP-3, are required for activation-induced degranulation of mature human mast cells. *Eur. J. Immunol.* 38:855-863.

204. Tapper, H., and R. Sundler. 1995. Protein kinase C and intracellular pH regulate zymosan-induced lysosomal enzyme secretion in macrophages. *J. Leukoc. Biol.* 58:485-494.

205. Tatham, P. E., N. J. Cusack, and B. D. Gomperts. 1988. Characterisation of the ATP4-receptor that mediates permeabilisation of rat mast cells. *Eur. J. Pharmacol.* 147:13-21.

206. Alzola, E., A. Perez-Etxebarria, E. Kabré, D. J. Fogarty, M. Metioui, N. Chaib, J. M. Macarulla, C. Matute, J. P. Dehaye, and A. Marino. 1998. Activation by P2X7 agonists of two phospholipases A2 (PLA2) in ductal cells of rat submandibular gland. Coupling of the calcium-independent PLA2 with kallikrein secretion. *J. Biol. Chem.* 273:30208-30217.

207. Ward, D. M., G. M. Griffiths, J. C. Stinchcombe, and J. Kaplan. 2000. Analysis of the lysosomal storage disease Chediak-Higashi syndrome. *Traffic* 1:816-822.

208. Conus, S., and H. U. Simon. 2008. Cathepsins: key modulators of cell death and inflammatory responses. *Biochem. Pharmacol.* 76:1374-1382.

209. Roycik, M. D., X. Fang, and Q. X. Sang. 2009. A fresh prospect of extracellular matrix hydrolytic enzymes and their substrates. *Curr. Pharm. Des.* 15:1295-1308.

210. Théry, C., M. Ostrowski, and E. Segura. 2009. Membrane vesicles as conveyors of immune responses. *Nat. Rev. Immunol.* 9:581-593.

211. Qu, Y., L. Franchi, G. Nunez, and G. R. Dubyak. 2007. Nonclassical IL-1 beta secretion stimulated by P2X7 receptors is dependent on inflammasome activation and correlated with exosome release in murine macrophages. *J. Immunol.* 179:1913-1925.

212. Simons, M., and G. Raposo. 2009. Exosomes--vesicular carriers for intercellular communication. *Curr. Opin. Cell Biol.* 21:575-581.

213. Geminard, C., A. De Gassart, L. Blanc, and M. Vidal. 2004. Degradation of AP2 during reticulocyte maturation enhances binding of hsc70 and Alix to a common site on TFR for sorting into exosomes. *Traffic* 5:181-193.

214. De Gassart, A., C. Geminard, B. Fevrier, G. Raposo, and M. Vidal. 2003. Lipid raft-associated protein sorting in exosomes. *Blood* 102:4336-4344.

215. Savina, A., C. M. Fader, M. T. Damiani, and M. I. Colombo. 2005. Rab11 promotes docking and fusion of multivesicular bodies in a calcium-dependent manner. *Traffic* 6:131-143.

216. Fevrier, B., and G. Raposo. 2004. Exosomes: endosomal-derived vesicles shipping extracellular messages. *Curr. Opin. Cell Biol.* 16:415-421.

217. MacKenzie, A., H. L. Wilson, E. Kiss-Toth, S. K. Dower, R. A. North, and A. Surprenant. 2001. Rapid secretion of interleukin-1beta by microvesicle shedding. *Immunity* 15:825-835.

218. Heijnen, H. F., A. E. Schiel, R. Fijnheer, H. J. Geuze, and J. J. Sixma. 1999. Activated platelets release two types of membrane vesicles: microvesicles by surface shedding and

exosomes derived from exocytosis of multivesicular bodies and alpha-granules. *Blood* 94:3791-3799.

219. Obregon, C., B. Rothen-Rutishauser, S. K. Gitahi, P. Gehr, and L. P. Nicod. 2006. Exovesicles from human activated dendritic cells fuse with resting dendritic cells, allowing them to present alloantigens. *Am. J. Pathol.* 169:2127-2136.

220. Daleke, D. L. 2008. Regulation of phospholipid asymmetry in the erythrocyte membrane. *Curr. Opin. Hematol.* 15:191-195.

221. Zwaal, R. F., and A. J. Schroit. 1997. Pathophysiologic implications of membrane phospholipid asymmetry in blood cells. *Blood* 89:1121-1132.

222. Comfurius, P., J. M. Senden, R. H. Tilly, A. J. Schroit, E. M. Bever, and R. F. Zwaal. 1990. Loss of membrane phospholipid asymmetry in platelets and red cells may be associated with calcium-induced shedding of plasma membrane and inhibition of aminophospholipid translocase. *Biochim. Biophys. Acta.* 1026:153-160.

223. Wolfs, J. L., P. Comfurius, O. Bekers, R. F. Zwaal, K. Balasubramanian, A. J. Schroit, T. Lindhout, and E. M. Bever. 2009. Direct inhibition of phospholipid scrambling activity in erythrocytes by potassium ions. *Cell. Mol. Life Sci.* 66:314-323.

224. Xie, Y., H. Zhang, W. Li, Y. Deng, M. A. Munegowda, R. Chibbar, M. Qureshi, and J. Xiang. 2010. Dendritic cells recruit T cell exosomes via exosomal LFA-1 leading to inhibition of CD8+ CTL responses through downregulation of peptide/MHC class I and Fas ligand-mediated cytotoxicity. *J. Immunol.* 185:5268-5278.

225. Miyanishi, M., K. Tada, M. Koike, Y. Uchiyama, T. Kitamura, and S. Nagata. 2007. Identification of Tim4 as a phosphatidylserine receptor. *Nature* 450:435-439.

226. Clayton, A., J. P. Mitchell, J. Court, S. Linnane, M. D. Mason, and Z. Tabi. 2008. Human tumor-derived exosomes down-modulate NKG2D expression. *J. Immunol.* 180:7249-7258.

227. Liu, C., S. Yu, K. Zinn, J. Wang, L. Zhang, Y. Jia, J. C. Kappes, S. Barnes, R. P. Kimberly, W. E. Grizzle, and H. G. Zhang. 2006. Murine mammary carcinoma exosomes promote tumor growth by suppression of NK cell function. *J. Immunol.* 176:1375-1385.

228. Skokos, D., H. G. Botros, C. Demeure, J. Morin, R. Peronet, G. Birkenmeier, S. Boudaly, and S. Mecheri. 2003. Mast cell-derived exosomes induce phenotypic and functional maturation of dendritic cells and elicit specific immune responses in vivo. *J. Immunol.* 170:3037-3045.

229. Morelli, A. E. 2006. The immune regulatory effect of apoptotic cells and exosomes on dendritic cells: its impact on transplantation. *Am. J. Transplant.* 6:254-261.

230. Morelli, A. E., A. T. Larregina, W. J. Shufesky, M. L. Sullivan, D. B. Stolz, G. D. Papworth, A. F. Zahorchak, A. J. Logar, Z. Wang, S. C. Watkins, L. D. J. Falo, and A. W. Thomson. 2004. Endocytosis, intracellular sorting, and processing of exosomes by dendritic cells. *Blood* 104:3257-3266.

231. Lima, L. G., R. Chammas, R. Q. Monteiro, M. E. Moreira, and M. A. Barcinski. 2009. Tumor-derived microvesicles modulate the establishment of metastatic melanoma in a phosphatidylserine-dependent manner. *Cancer Lett.* 283:168-175.

232. Chalmin, F., S. Ladoire, G. Mignot, J. Vincent, M. Bruchard, J. P. Remy-Martin, W. Boireau, A. Rouleau, B. Simon, D. Lanneau, A. De Thonel, G. Multhoff, A. Hamman, F. Martin, B. Chauffert, E. Solary, L. Zitvogel, C. Garrido, B. Ryffel, C. Borg, L. Apethoh, C. Rebe, and F. Ghiringhelli. 2010. Membrane-associated Hsp72 from tumor-derived exosomes mediates STAT3-dependent immunosuppressive function of mouse and human myeloid-derived suppressor cells. *J. Clin. Invest.* 120:457-471.

233. Obregon, C., B. Rothen-Rutishauser, P. Gerber, P. Gehr, and L. P. Nichod. 2009. Active uptake of dendritic cell-derived exovesicles by epithelial cells induces the release of inflammatory mediators through a TNF-alpha-mediated pathway. *Am. J. Pathol.* 175:696-705.

234. Xie, Y., H. Zheng, W. Li, Y. Deng, M. A. Munegowda, R. Chibbar, M. Qureshi, and J. Xiang. 2010. Dendritic cells recruit T cell exosomes via exosomal LFA-1 leading to inhibition of CD8+ CTL responses through downregulation of peptide/MHC class I and Fas ligand-mediated cytotoxicity. *J. Immunol.* 185:5268-5278.

235. Lenassi, M., G. Cagney, M. Liao, T. Vaupotic, K. Bartholomeeusen, Y. Cheng, N. J. Krogan, A. Plemenitas, and B. M. Peterlin. 2010. HIV Nef is secreted in exosomes and triggers apoptosis in bystander CD4+ T cells. *Traffic* 11:110-122.

236. Thomas, L. M., and R. D. Salter. 2010. Activation of macrophages by P2X7-induced microvesicles from myeloid cells is mediated by phospholipids and is partially dependent on TLR4. *J. Immunol.* 185:3740-3749.

237. Ramachandra, L., Y. Qu, Y. Wang, C. J. Lewis, B. A. Cobb, K. Takatsu, W. H. Boom, G. R. Dubyak, and C. V. Harding. 2010. Mycobacterium tuberculosis synergizes with ATP to induce release of microvesicles and exosomes containing major histocompatibility complex class II molecules capable of antigen presentation. *Infect. Immun.* 78:5116-5125.

238. Barres, C., L. Blanc, P. Bette-Bobillo, S. Andre, R. Mamoun, H. J. Gabius, and M. Vidal. 2010. Galectin-5 is bound onto the surface of rat reticulocyte exosomes and modulates vesicle uptake by macrophages. *Blood* 115:696-705.

239. Silverman, J. M., J. Clos, E. Horakova, A. Y. Wang, M. Wiesgigl, I. Kelly, M. A. Lynn, W. R. McMaster, L. J. Foster, M. K. Levings, and N. E. Reiner. 2010. Leishmania

exosomes modulate innate and adaptive immune responses through effects on monocytes and dendritic cells. *J. Immunol.* 185:5011-5022.

240. Andreola, G., L. Rivoltini, C. Castelli, V. Huber, P. Perego, P. Deho, P. Squarcina, P. Accornero, F. Lozupone, L. Lugini, A. Stringaro, A. Molinari, G. Arancia, M. Gentile, G. Parmiani, and S. Fais. 2002. Induction of lymphocyte apoptosis by tumor cell secretion of FasL-bearing microvesicles. *J. Exp. Med.* 195:1303-1316.

241. Zhang, H. G., C. Liu, K. Su, S. Yu, L. Zhang, S. Zhang, J. Wang, X. Cao, W. Grizzle, and R. P. Kimberly. 2006. A membrane form of TNF-alpha presented by exosomes delays T cell activation-induced cell death. *J. Immunol.* 176:7385-7393.

242. Admyre, C., S. M. Johansson, S. Paulie, and S. Gabrielsson. 2006. Direct exosome stimulation of peripheral human T cells detected by ELISPOT. *Eur. J. Immunol.* 36:1772-1781.

243. Dolan, B. P., K. D. J. Gibbs, and S. Ostrand-Rosenberg. 2006. Tumor-specific CD4+ T cells are activated by "cross-dressed" dendritic cells presenting peptide-MHC class II complexes acquired from cell-based cancer vaccines. *J. Immunol.* 176:1447-1455.

244. Segura, E., C. Guerin, N. Hogg, S. Amigorena, and C. Thery. 2007. CD8+ dendritic cells use LFA-1 to capture MHC-peptide complexes from exosomes in vivo. *J. Immunol.* 179:1489-1496.

245. Pizzirani, C., D. Ferrari, P. Chiozzi, E. Adinolfi, D. Sandonà, E. Savaglio, and F. Di Virgilio. 2007. Stimulation of P2 receptors causes release of IL-1beta–loaded microvesicles from human dendritic cells. *Blood* 109:3856-3864.

246. Qu, Y., and G. R. Dubyak. 2009. P2X7 receptors regulate multiple types of membrane trafficking responses and non-classical secretion pathways. *Purinergic Signal.* 5:163-173.

247. Verhoef, P., M. Estacion, W. Schilling, and G. R. Dubyak. 2003. P2X7 receptor-dependent blebbing and the activation of Rho-effector kinases, caspases, and IL-1 β release. *J. Immunol.* 170:5728-5738.

248. Ferrari, D., C. Pizzirani, E. Adinolfi, R. M. Lemoli, A. Curti, M. Idzko, E. Panther, and F. Di Virgilio. 2006. The P2X7 receptor: a key player in IL-1 processing and release. *J. Immunol.* 176:3877-3883.

249. Pelegrin, P., C. Barroso-Gutierrez, and A. Surprenant. 2008. P2X7 receptor differentially couples to distinct release pathways for IL-1beta in mouse macrophage. *J. Immunol.* 180:7147 -7157.

250. Moore, S. F., and A. B. MacKenzie. 2007. Murine macrophage P2X7 receptors support rapid prothrombotic responses. *Cell Signal.* 19:855-866.

251. Cocucci, E., G. Racchetti, and J. Meldolesi. 2009. Shedding microvesicles: artefacts no more. *Trends Cell Biol.* 19:43-51.

252. Bianco, F., E. Pravettoni, A. Colombo, U. Schenk, T. Möller, M. Matteoli, and C. Verderio. 2005. Astrocyte-derived ATP induces vesicle shedding and IL-1 beta release from microglia. *J. Immunol.* 174:7268-7277.

253. Baj-Krzyworzeka, M., R. Szatanek, K. Weglarczyk, J. Baran, B. Urbanowicz, P. Brański, M. Z. Ratajczak, and M. Zembala. 2006. Tumour-derived microvesicles carry several surface determinants and mRNA of tumour cells and transfer some of these determinants to monocytes. *Cancer Immunol. Immunother.* 55:808-818.

254. Pilzer, D., and Z. Fishelson. 2005. Mortalin/GRP75 promotes release of membrane vesicles from immune attacked cells and protection from complement-mediated lysis. *Int. Immunol.* 17:1239-1248.

255. Sidhu, S. S., A. T. Mengistab, A. N. Tauscher, J. LaVail, and C. Basbaum. 2004. The microvesicle as a vehicle for EMMPRIN in tumor–stromal interactions. *Oncogene* 23:956-963.

256. Andrei, C., C. Dazzi, L. Lotti, M. R. Torrisi, G. Chimini, and A. Rubartelli. 1999. The secretory route of the leaderless protein interleukin 1beta involves exocytosis of endolysosome-related vesicles. *Mol. Biol. Cell* 10:1463-1475.

257. Andrei, C., P. Margiocco, A. Poggi, L. V. Lotti, M. R. Torrisi, and A. Rubartelli. 2004. Phospholipases C and A2 control lysosome-mediated IL-1 β secretion: Implications for inflammatory processes. *Proc. Natl. Acad. Sci. USA.* 101:9745-9750.

258. Gardella, S., C. Andrei, L. V. Lotti, A. Poggi, M. R. Torrisi, M. R. Zocchi, and A. Rubartelli. 2001. CD8(+) T lymphocytes induce polarized exocytosis of secretory lysosomes by dendritic cells with release of interleukin-1beta and cathepsin D. *Blood* 98:2152-2159.

259. Qu, Y., L. Ramachandra, S. Mohr, L. Franchi, C. V. Harding, G. Nunez, and G. R. Dubyak. 2009. P2X7 receptor-stimulated secretion of MHC class II-containing exosomes requires the ASC/NLRP3 inflammasome but is independent of caspase-1. *J. Immunol.* 182:5052-5062.

260. Wilson, H. L., S. E. Francis, S. K. Dower, and D. C. Crossman. 2004. Secretion of intracellular IL-1 receptor antagonist (type 1) is dependent on P2X7 receptor activation. *J. Immunol.* 173:1202-1208.

261. Hogquist, K. A., E. R. Unanue, and D. D. Chaplin. 1991. Release of IL-1 from mononuclear phagocytes. *J. Immunol.* 147:2181-2186.

262. Singer, I. I., S. Scott, J. Chin, E. K. Bayne, G. Limjuco, J. Wiedner, D. K. Miller, K. Chapman, and M. J. Kostura. 1995. The interleukin-1 beta-converting enzyme (ICE) is localized on the external cell surface membranes and in the cytoplasmic ground substance of human monocytes by immuno-electron microscopy. *J. Exp. Med.* 182:1447-1459.

263. Baj-Krzyworzeka, M., R. Szatanek, K. Weglarczyk, J. Baran, and M. Zembala. 2007. Tumour-derived microvesicles modulate biological activity of human monocytes. *Immunol. Lett.* 113:76-82.

264. Valenti, R., V. Huber, P. Filipazzi, L. Pilla, G. Sovena, A. Villa, A. Corbelli, S. Fais, G. Parmiani, and L. Rivoltini. 2006. Human tumor-released microvesicles promote the differentiation of myeloid cells with transforming growth factor-beta-mediated suppressive activity on T lymphocytes. *Cancer Res.* 66:9290-9298.

265. Chu, J., L. M. Thomas, S. C. Watkins, L. Franchi, G. Núñez, and R. D. Salter. 2009. Cholersterol-dependent cytolysins induce rapid release of mature IL-1beta from murine macrophages in a NLRP3 inflammasome and cathepsin B-dependent manner. *J. Leukoc. Biol.* 86:1227-1238.

266. Radin, M. S., S. Sinha, B. A. Bhatt, N. Dedousis, and R. M. O'Doherty. 2008. Inhibition or deletion of the lipopolysaccharide receptor Toll-like receptor-4 confers partial protection against lipid-induced insulin resistance in rodent skeletal muscle. *Diabetologia* 51:336-346.

267. Englert, J. M., L. E. Hanford, N. Kaminski, J. M. Tobolewski, R. J. Tan, C. L. Fattman, L. Ramsgaard, T. J. Richards, I. Loutaev, P. P. Nawroth, M. Kasper, A. Bierhaus, and T. D. Oury. 2008. A role for the receptor for advanced glycation end products in idiopathic pulmonary fibrosis. *Am. J. Pathol.* 172:583-591.

268. Bligh, E. G., and W. J. Dyer. 1959. A rapid method of total lipid extraction and purification. *Can. J. Biochem. Physiol.* 37:911-917.

269. Christie, W. W. 1982. A simple procedure for rapid transmethylation of glycerolipids and cholesteryl esters. *J. Lipid Res.* 23:1072-1075.

270. Donnelly-Roberts, D., M. Namovic, P. Han, and M. Jarvis. 2009. Mammalian P2X7 receptor pharmacology: comparison of recombinant mouse, rat and human P2X7 receptors. *Br. J. Pharmacol.* 157:1203-1214.

271. Termeer, C., F. Benedix, J. Sleeman, C. Fieber, U. Voith, T. Ahrens, K. Miyake, M. Freudenberg, C. Galanos, and J. C. Simon. 2002. Oligosaccharides of Hyaluronan activate dendritic cells via toll-like receptor 4. *J. Exp. Med.* 195:99-111.

272. Vogl, T., K. Tenbrock, S. Ludwig, N. Leukert, C. Ehrhardt, M. A. van Zoelen, W. Nacken, D. Foell, T. van der Poll, C. Sorg, and J. Roth. 2007. Mrp8 and Mrp14 are

endogenous activators of Toll-like receptor 4, promoting lethal, endotoxin-induced shock. *Nat. Med.* 13:1042-1049.

273. Andersson, U., H. Wang, K. Palmblad, A. C. Aveberger, O. Bloom, H. Erlandsson-Harris, A. Janson, R. Kokkola, M. Zhang, H. Yang, and K. J. Tracey. 2000. High mobility group 1 protein (HMG-1) stimulates proinflammatory cytokine synthesis in human monocytes. *J. Exp. Med.* 192:565-570.

274. Wang, H., O. Bloom, M. Zhang, J. M. Vishnubhakat, M. Ombrellino, J. Che, A. Frazier, H. Yang, S. Ivanova, L. Borovikova, K. R. Manogue, E. Faist, E. Abraham, J. Andersson, U. Andersson, P. E. Molina, N. N. Abumrad, A. Sama, and K. J. Tracey. 1999. HMG-1 as a late mediator of endotoxin lethality in mice. *Science* 285:248-251.

275. Scaffidi, P., T. Misteli, and M. E. Bianchi. 2002. Release of chromatin protein HMGB1 by necrotic cells triggers inflammation. *Nature* 418:191-195.

276. Hu, S. P., C. Harrison, K. Xu, C. J. Cornish, and C. L. Geczy. 1996. Induction of the chemotactic S100 protein, CP-10, in monocyte/macrophages by lipopolysaccharide. *Blood* 87:3919-3928.

277. Xu, K., and C. L. Geczy. 2000. IFN-gamma and TNF regulate macrophage expression of the chemotactic S100 protein S100A8. *J. Immunol.* 164:4916-4923.

278. Zheng, L., T. E. Riehl, and W. F. Stenson. 2009. Regulation of colonic epithelial repair in mice by Toll-like receptors and hyaluronic acid. *Gastroenterology* 137:2041-2051.

279. Lotze, M. T., and K. J. Tracey. 2005. High-mobility group box 1 protein (HMGB1): nuclear weapon in the immune arsenal. *Nat. Rev. Immunol.* 5:331-342.

280. Panupinthu, N., L. Zhao, F. Possmayer, H. Z. Ke, S. M. Sims, and S. J. Dixon. 2007. P2X7 nucleotide receptors mediate blebbing in osteoblasts through a pathway involving lysophosphatidic acid. *J. Biol. Chem.* 282:3403-3412.

281. Lee, H., J. J. Liao, M. Graeler, M. C. Huang, and E. J. Goetzl. 2002. Lysophospholipid regulation of mononuclear phagocytes. *Biochim. Biophys. Acta.* 1582:175-177.

282. Lin, W. W., S. H. Chang, and S. M. Wang. 1999. Roles of atypical protein kinase C in lysophosphatidic acid-induced type II adenylyl cyclase activation in RAW 264.7 macrophages. *Br. J. Pharmacol.* 128:1189-1198.

283. Domercq, M., A. Perez-Samartin, D. Aparicio, E. Alberdi, O. Pampliega, and C. Matute. 2010. P2X7 receptors mediate ischemic damage to oligodendrocytes. *Glia* 58:730-740.

284. Idzko, M., H. Hammad, M. van Nimwegen, M. Kool, M. A. Willart, F. Muskens, H. C. Hoogsteden, W. Luttmann, D. Ferrari, F. Di Virgilio, J. C. Virchow, Jr, and B. N.

Lambrecht. 2007. Extracellular ATP triggers and maintains asthmatic airway inflammation by activating dendritic cells. *Nat. Med.* 13:913-919.

285. Mortaz, E., S. Braber, M. Nazary, M. E. Givi, F. P. Nijkamp, and G. Folkerts. 2009. ATP in the pathogenesis of lung emphysema. *Eur. J. Pharmacol.* 619:92-96.

286. Peng, W., M. L. Cotrina, X. Han, H. Yu, L. Bekar, L. Blum, T. Takano, G. F. Tian, S. A. Goldman, and M. Nedergaard. 2009. Systemic administration of an antagonist of the ATP-sensitive receptor P2X7 improves recovery after spinal cord injury. *Proc. Natl. Acad. Sci. USA.* 106:12489-12493.

287. Söderberg, A., A. M. Barral, M. Söderström, B. Sander, and A. Rosén. 2007. Redox-signaling transmitted in trans to neighboring cells by melanoma-derived TNF-containing exosomes. *Free Radic. Biol. Med.* 43:90-99.

288. Bauernfeind, F. G., G. Horvath, A. Stutz, E. S. Alnemri, K. MacDonald, D. Speert, T. Fernandes-Alnemri, J. Wu, B. G. Monks, K. A. Fitzgerald, V. Hornung, and E. Latz. 2009. Cutting edge: NF-kappaB activating pattern recognition and cytokine receptors license NLRP3 inflammasome activation by regulating NLRP3 expression. *J. Immunol.* 183:787-791.

289. Nowicki, M., K. Müller, H. Serke, J. Kosacka, C. Vilser, A. Ricken, and K. Spanel-Borowski. 2010. Oxidized low-density lipoprotein (oxLDL)-induced cell death in dorsal root ganglion cell cultures depends not on the lectin-like oxLDL receptor-1 but on the toll-like receptor-4. *J. Neurosci. Res.* 88:403-412.

290. Serke, H., C. Vilser, M. Nowicki, F. A. Hmeidan, V. Blumenauer, K. Hummitzsch, A. Lösche, and K. Spanel-Borowski. 2009. Granulosa cell subtypes respond by autophagy or cell death to oxLDL-dependent activation of the oxidized lipoprotein receptor 1 and toll-like 4 receptor. *Autophagy* 5:991-1003.

291. Chen, S., R. Sorrentino, K. Shimada, Y. Bulut, T. M. Doherty, T. R. Crother, and M. Arditi. 2008. Chlamydia pneumoniae-induced foam cell formation requires MyD88-dependent and -independent signaling and is reciprocally modulated by liver X receptor activation. *J. Immunol.* 181:7186-7193.

292. Bae, Y. S., J. H. Lee, S. H. Choi, S. Kim, F. Almazan, J. L. Witztum, and Y. I. Miller. 2009. Macrophages generate reactive oxygen species in response to minimally oxidized low-density lipoprotein: toll-like receptor 4- and spleen tyrosine kinase-dependent activation of NADPH oxidase 2. *Circ. Res.* 104:210-218.

293. Miller, Y. I., S. Viriyakosol, D. S. Worrall, A. Boullier, S. Butler, and J. L. Witztum. 2005. Toll-like receptor 4-dependent and -independent cytokine secretion induced by minimally oxidized low-density lipoprotein in macrophages. *Arterioscler. Thromb. Vasc. Biol.* 25:1213-1219.

294. Miller, Y. I., S. Viriyakosol, C. J. Binder, J. R. Feramisco, T. N. Kirkland, and J. L. Witztum. 2003. Minimally modified LDL binds to CD14, induces macrophage spreading via TLR4/MD-2, and inhibits phagocytosis of apoptotic cells. *J. Biol. Chem.* 278:1561-1568.

295. Zeniou-Meyer, M., N. Zabari, U. Ashery, S. Chasserot-Golaz, A. M. Haeberlé, V. Demais, Y. Bailly, I. Gottfried, H. Nakanishi, A. M. Neiman, G. Du, M. A. Frohman, M. F. Bader, and N. Vitale. 2007. Phospholipase D1 production of phosphatidic acid at the plasma membrane promotes exocytosis of large dense-core granules at a late stage. *J. Biol. Chem.* 282:21746-21757.

296. Aymeric, L., L. Apetoh, F. Ghiringhelli, A. Tesniere, I. Martins, G. Kroemer, M. J. Smyth, and L. Zitvogel. 2010. Tumor cell death and ATP release prime dendritic cells and efficient anticancer immunity. *Cancer Res.* 70:855-858.

297. Martins, I., A. Tesniere, O. Kepp, M. Michaud, F. Schlemmer, L. Senovilla, C. Séror, D. Métivier, J. L. Perfettini, L. Zitvogel, and G. Kroemer. 2009. Chemotherapy induces ATP release from tumor cells. *Cell Cycle* 8:3723-3728.

298. Doherty, G. J., and H. T. McMahon. 2009. Mechanisms of endocytosis. *Annu. Rev. Biochem.* 78:857-902.

299. Sverdlov, M., A. N. Shajahan, and R. D. Minshall. 2007. Tyrosine phosphorylation-dependence of caveolae-mediated endocytosis. *J. Cell. Mol. Med.* 11:1239-1250.

300. Glebov, O. O., N. A. Bright, and B. J. Nichols. 2006. Flotillin-1 defines a clathrin-independent endocytic pathway in mammalian cells. *Nat. Cell Biol.* 8:46-54.

301. Sabharanjak, S., P. Sharma, R. G. Parton, and S. Mayor. 2002. GPI-anchored proteins are delivered to recycling endosomes via a distinct cdc42-regulated, clathrin-independent pinocytic pathway. *Dev. Cell* 2:411-423.

302. Malaval, C., M. Laffargue, R. Barbaras, C. Rolland, C. Peres, E. Champagne, B. Perret, F. Terce, X. Collet, and L. O. Martinez. 2009. RhoA/ROCK I signalling downstream of the P2Y13 ADP-receptor controls HDL endocytosis in human hepatocytes. *Cell. Signal.* 21:120-127.

303. Marques-da-Silva, C., G. Burnstock, D. M. Ojcius, and R. Coutinho-Silva. 2011. Purinergic receptor agonists modulate phagocytosis and clearance of apoptotic cells in macrophages. *Immunobiology* 216:1-11.

304. Girolomoni, G., M. B. Lutz, S. Pastore, C. U. Assmann, A. Cavani, and P. Ricciardi-Castagnoli. 1995. Establishment of a cell line with features of early dendritic cell precursors from fetal mouse skin. *Eur. J. Immunol.* 25:2163-2169.

305. Sun, C., J. Chu, S. Singh, and R. D. Salter. 2010. Identification and characterization of a novel variant of the human P2X(7) receptor resulting in gain of function. *Purinergic Signal.* 6:31-45.

306. Arneson, L. N., C. M. Segovis, T. S. Gomez, R. A. Schoon, C. J. Dick, Z. Lou, D. D. Billadeau, and P. J. Leibson. 2008. Dynamin 2 regulates granule exocytosis during NK cell-mediated cytotoxicity. *J. Immunol.* 181:6995-7001.

307. Veugelers, K., B. Motyka, C. Frantz, I. Shostak, T. Sawchuk, and R. C. Bleackley. 2004. The granzyme B-serglycin complex from cytotoxic granules requires dynamin for endocytosis. *Blood* 103:3845-3853.

308. Min, L., Y. M. Leung, A. Tomas, R. T. Watson, H. Y. Gaisano, P. A. Halban, J. E. Pessin, and J. C. Hou. 2007. Dynamin is functionally coupled to insulin granule exocytosis. *J. Biol. Chem.* 282:33530-33536.

309. Gonzalez-Jamett, A. M., X. Baez-Matus, M. A. Hevia, M. J. Guerra, M. J. Olivares, A. D. Martinez, A. Neely, and A. M. Cardenas. 2010. The association of dynamin with synaptophysin regulates quantal size and duration of exocytotic events in chromaffin cells. *J. Neurosci.* 30:10683-10691.

310. Anantharam, A., B. Onoa, R. H. Edwards, R. W. Holz, and D. Axelrod. 2010. Localized topological changes of the plasma membrane upon exocytosis visualized by polarized TIRFM. *J. Cell Biol.* 188:415-428.

311. Macia, E., M. Ehrlich, R. Massol, E. Boucrot, C. Brunner, and T. Kirchausen. 2006. Dynasore, a cell-permeable inhibitor of dynamin. *Dev. Cell* 10:839-850.

312. Anderson, R. G., M. S. Brown, and J. L. Goldstein. 1977. Role of the coated endocytic vesicle in the uptake of receptor-bound low density lipoprotein in human fibroblasts. *Cell* 10:351-364.

313. Damke, H., T. Baba, D. E. Warnock, and S. L. Schmid. 1994. Induction of mutant dynamin specifically blocks endocytic coated vesicle formation. *J. Cell Biol.* 127:915-934.

314. Campellone, K. G., and M. D. Welch. 2010. A nucleator arms race: cellular control of actin assembly. *Nat. Rev. Mol. Cell Biol.* 11:237-251.

315. Billadeau, D. D., and J. K. Burkhardt. 2006. Regulation of cytoskeletal dynamics at the immune synapse: new stars join the actin troupe. *Traffic* 7:1451-1460.

316. Gomez, T. S., K. Kumar, R. B. Medeiros, Y. Shimizu, P. J. Leibson, and D. D. Billadeau. 2007. Formins regulate the actin-related protein 2/3 complex-independent polarization of the centrosome to the immunological synapse. *Immunity* 26:177-190.

317. Pfeiffer, Z. A., M. Aga, U. Prabhu, J. J. Watters, D. J. Hall, and P. J. Bertics. 2004. The nucleotide receptor P2X7 mediates actin reorganization and membrane blebbing in RAW 264.7 macrophages via p38 MAP kinase and Rho. *J. Leukoc. Biol.* 75:1173-1182.

318. Higgs, H. N., and T. D. Pollard. 2000. Activation by Cdc42 and PIP(2) of Wiskott-Aldrich syndrome protein (WASp) stimulates actin nucleation by Arp2/3 complex. *J. Cell Biol.* 150:1311-1320.

319. Takenouchi, T., Y. Iwamaru, S. Sugama, M. Sato, M. Hashimoto, and H. Kitani. 2008. Lysophospholipids and ATP mutually suppress maturation and release of IL-1 beta in mouse microglial cells using a Rho-dependent pathway. *J. Immunol.* 180:7827-7839.

320. Khakh, B. S., G. Burnstock, C. Kennedy, B. F. King, R. A. North, P. Seguela, M. Voigt, and P. P. Humphrey. 2001. International union of pharmacology. XXIV. Current status of the nomenclature and properties of P2X receptors and their subunits. *Pharmacol. Rev.* 53:107-118.

321. Communi, D., B. Robaye, and J. M. Boeynaems. 1999. Pharmacological characterization of the human P2Y11 receptor. *Br. J. Pharmacol.* 128:1199-1206.

322. Chessell, I. P., A. D. Michel, and P. P. Humphrey. 1998. Effects of antagonists at the human recombinant P2X7 receptor. *Br. J. Pharmacol.* 124:1314-1320.

323. Jenkins, G. H., P. L. Fisette, and R. A. Anderson. 1994. Type I phosphatidylinositol 4-phosphate 5-kinase isoforms are specifically stimulated by phosphatidic acid. *J. Biol. Chem.* 269:11547-11554.

324. Ha, K. S., and J. H. Exton. 1993. Activation of actin polymerization by phosphatidic acid derived from phosphatidylcholine in IIC9 fibroblasts. *J. Cell Biol.* 123:1789-1796.

325. Yang, C., L. Czech, S. Gerboth, S. Kojima, G. Scita, and T. Svitkina. 2007. Novel roles of formin mDia2 in lamellipodia and filopodia formation in motile cells. *PLoS Biol.* 5:e317.

326. Hitchon, C. A., and H. S. El-Gabalawy. 2004. Oxidation in rheumatoid arthritis. *Arthritis Res. Ther.* 6:265-278.

327. Negre-Salvayre, A., N. Auge, V. Ayala, H. Basaga, J. Boada, R. Brenke, S. Chapple, G. Cohen, J. Feher, T. Grune, G. Lengyel, G. E. Mann, R. Pamplona, G. Poli, M. Portero-Otin, Y. Riahi, R. Salvayre, S. Sasson, J. Serrano, O. Shamni, W. Siems, R. C. Siow, I. Wiswedel, K. Zarkovic, and N. Zarkovic. 2010. Pathological aspects of lipid peroxidation. *Free Radic. Res.* 44:1125-1171.

328. Hewinson, J., S. F. Moore, C. Glover, A. G. Watts, and A. B. MacKenzie. 2008. A key role for redox signaling in rapid P2X7 receptor-induced IL-1 beta processing in human monocytes. *J. Immunol.* 180:8410-8420.

329. Parvathenani, L. K., S. Tertyshnikova, C. R. Greco, S. B. Roberts, B. Robertson, and R. Posmantur. 2003. P2X7 mediates superoxide production in primary microglia and is up-regulated in a transgenic mouse model of Alzheimer's disease. *J. Biol. Chem.* 278:13309-13317.

330. Pfeiffer, Z. A., A. N. Guerra, L. M. Hill, M. L. Gavala, U. Prabhu, M. Aga, D. J. Hall, and P. J. Bertics. 2007. Nucleotide receptor signaling in murine macrophages is linked to reactive oxygen species generation. *Free Radic. Biol. Med.* 42:1506-1516.

331. Suh, B. C., J. S. Kim, U. Namgung, H. Ha, and K. T. Kim. 2001. P2X7 nucleotide receptor mediation of membrane pore formation and superoxide generation in human promyelocytes and neutrophils. *J. Immunol.* 166:6754-6763.

332. Fourcade, O., M. F. Simon, C. Viode, N. Rugani, F. Leballe, A. Ragab, B. Fournie, L. Sarda, and H. Chap. 1995. Secretory phospholipase A2 generates the novel lipid mediator lysophosphatidic acid in membrane microvesicles shed from activated cells. *Cell* 80:919-927.

333. Muralidharan-Chari, V., J. W. Clancy, A. Sedgwick, and C. D'Souza-Schorey. 2010. Microvesicles: mediators of extracellular communication during cancer progression. *J. Cell Sci.* 123:1603-1611.

334. Huttner, W. B., and J. Zimmerberg. 2001. Implications of lipid microdomains for membrane curvature, budding and fission: Commentary. *Curr. Opin. Cell Biol.* 13:478-484.

335. Martinez, M. C., A. Tesse, F. Zobairi, and R. Andriantsitohaina. 2005. Shed membrane microparticles from circulating and vascular cells in regulating vascular function. *Am. J. Physiol. Heart Circ. Physiol.* 288:H1004-H1009.

336. Silverstein, R. L. 2009. Inflammation, atherosclerosis, and arterial thrombosis: role of the scavenger receptor CD36. *Cleve. Clin. J. Med.* 76:S27-S30.

337. Kim, C. W., H. M. Lee, T. H. Lee, C. Kang, H. K. Kleinmn, and Y. S. Gho. 2002. Extracellular membrane vesicles from tumor cells promote angiogenesis via sphingomyelin. *Cancer Res.* 62:6312-6317.

338. Wysoczynski, M., and M. Z. Ratajczak. 2009. Lung cancer secreted microvesicles: underappreciated modulators of microenvironment in expanding tumors. *Int. J. Cancer* 125:1595-1603.

339. Brooks, S. A., H. J. Lomax-Browne, T. M. Carter, C. E. Kinch, and D. M. Hall. 2010. Molecular interactions in cancer cell metastasis. *Acta. Histochem.* 112:3-25.

340. Gu, C., S. Yaddanapudi, A. Weins, T. Osborn, J. Reiser, M. Pollak, J. Hartwig, and S. Sever. 2010. Direct dynamin-actin interactions regulate the actin cytoskeleton. *EMBO J.* 29:3593-3606.

341. Muralidharan-Chari, V., J. Clancy, C. Plou, M. Romao, P. Chavrier, G. Raposo, and C. D'Souza-Schorey. 2009. ARF6-regulated shedding of tumor cell-derived plasma membrane microvesicles. *Curr. Biol.* 19:1875-1885.

342. Kim, H. K., K. S. Song, Y. S. Park, Y. H. Kang, Y. J. Lee, K. R. Lee, H. K. Kim, K. W. Ryu, J. M. Bae, and S. Kim. 2003. Elevated levels of circulating platelet microparticles, VEGF, IL-6 and RANTES in patients with gastric cancer: possible role of a metastasis predictor. *Eur. J. Cancer* 39:184-191.

343. Atarashi, K., J. Nishimura, T. Shima, Y. Umesaki, M. Yamamoto, M. Onoue, H. Yagita, N. Ishii, R. Evan, K. Honda, and K. Takeda. 2008. ATP drives lamina propria T(H)17 cell differentiation. *Nature* 455:808-812.

344. den Haan, J. M., S. M. Lehar, and M. J. Bevan. 2000. CD8(+) but not CD8(-) dendritic cells cross-prime cytotoxic T cells in vivo. *J. Exp. Med.* 192:1685-1696.